MCDONNELL DOUGLAS CORPORATION

Copy number /

CR 151916
Report number MDC A4571

MATHEMATICAL MODEL FOR LIFT/CRUISE FAN V/STOL AIRCRAFT SIMULATOR PROGRAMMING DATA

Revision date

Revision letter

Issue date 6 December 1976

Contract number NAS2-9144

Prepared by M. P. Bland, B. Fajfar, R. K. Konsewicz

MCDONNELL AIRCRAFT COMPANY

Box 516, Saint Louis, Missouri 63166 – Tel. (314)232-0232

MCDONNELL DOUGLAS CORPORATION

INTRODUCTION

This is a simulation data report prepared for the purpose of programming the Flight Simulator for Advanced Aircraft (FSAA) for tests of the Lift/Cruise Fan V/STOL Research Technology Aircraft (RTA). These simulation tests are intended to provide insight into problem areas which may be encountered in operational use of this aircraft.

The flight control system simulated is a mix of direct mechanical and electrical controls with a dual control augmentation system (CAS), which is a lower cost alternate approach to the MCAIR recommended baseline system. The MCAIR recommended baseline system for the RTA is a triplex digital/analog implementation of control law solution which can also meet the design goals of the Navy mission operational aircraft.

The mathematical model of the aircraft is defined here in sufficient detail to represent all the necessary pertinent aircraft and system characteristics. The model includes the capability to simulate two basic versions of aircraft propulsion system: (1) the gas-coupled configuration which uses insulated air ducts to transmit power between gas generators and fans in the form of high energy engine exhaust and (2) the mechanically coupled power system which uses shafts, clutches, and gearboxes for power transmittal. Both configurations are modeled such that the simulation can include vertical as well as rolling takeoff and landing, hover, powered-lift flight, aerodynamic flight, and the transition between powered-lift and aerodynamic flight.

TABLE OF CONTENTS

LIST OF FIGURES

LIST OF FIGURES (continued)

LIST OF FIGURES (continued)

LIST OF FIGURES (continued)

LIST OF FIGURES (continued)

LIST OF FIGURES (continued)

LIST OF SYMBOLS

Symbol	
a_{NG}, a_{LMG}, a_{RMG}	Landing gear strut compression in nose gear, left and right main gears (ft)
A_E	Coefficient of second order term in expression for engine lag (sec^2)
A_J	Effective exhaust jet area (ft^2)
b	Wing span (ft)
b_{NG}, b_{MG}	Landing gear oleo damping coefficient for nose gear and main gear (lb sec/ft)
B_E	Coefficient of first order term in expression for engine lag (sec)
$BIAS_{\beta 1}, BIAS_{\beta 2}, BIAS_{\beta 3}$	Fan blade pitch bias signal. Shaft-coupled fans (degrees)
B_{1E}, B_{2E}	Engine transfer function denominator coefficients. Shaft coupled system (sec and sec^2 respectively)
$\bar{c}$	Wing mean aerodynamic chord (ft)
C_{DWB}	Drag coefficient of wing-body configuration alone (nondimensional)
C_{Dt}	Drag coefficient for the horizontal tail (nondimensional)
C_{ℓ_p}	Rolling moment coefficient due to roll rate (nondimensional)
C_{ℓ_r}	Rolling moment coefficient due to yaw rate (nondimensional)
C_{ℓ_β}	Rolling moment coefficient due to sideslip (nondimensional)
C_{L_t}	Lift coefficient for the horizontal tail (nondimensional)
$C_{L_{WB}}$	Lift coefficient of wing-body configuration alone (nondimensional)
$C_{L_{\dot{\alpha}}}$	Lift coefficient due to $\dot{\alpha}$ (nondimensional)
$C_{L_{\dot{\theta}}}$	Lift coefficient due to pitch rate (nondimensional)
$C_{m_{WB}}$	Pitching moment coefficient of wing-body configuration alone (nondimensional)

LIST OF SYMBOLS (Continued)

Symbol	
$C_{m_{\dot{\alpha}}}$	Pitching moment coefficient due to $\dot{\alpha}$ (nondimensional)
$C_{m_{\dot{\theta}}}$	Pitching moment coefficient due to pitch rate (nondimensional)
C_{n_p}	Yawing moment coefficient due to roll rate (nondimensional)
C_{n_r}	Yawing moment coefficient due to yaw rate (nondimensional)
C_{n_β}	Yawing moment coefficient due to sideslip (nondimensional)
C_{y_p}	Sideforce coefficient due to roll rate (nondimensional)
C_{y_r}	Sideforce coefficient due to yaw rate (nondimensional)
C_{y_β}	Sideforce coefficient due to sideslip (nondimensional)
D	Total aerodynamic drag in stability axes (pounds)
DB_θ	Pitch stick deadband (inches)
DB_ϕ	Lateral stick deadband (inches)
DB_ψ	Rudder pedal deadband (inches)
D_e	Effective fan exhaust jet diameter (feet)
F_{F1}, F_{F2}, F_{F3}	Fan stream thrust of fan 1, 2, and 3 respectively. Gas-coupled fans only (pounds)
$F_{GO1}, F_{GO2}, F_{GO3}$	Total fan thrust at zero airspeed for fans 1, 2, and 3 respectively. Gas-coupled fans only (pounds)
F_G/F_{GO}	Ratio of fan gross thrust to fan gross thrust at zero airspeed (nondimensional)
$F_{GU1}, F_{GU2}, F_{GU3}$	Gross uninstalled thrust on fans 1, 2, and 3 respectively (pounds)
F_{G1}	Gross thrust of left fan (pounds)
F_{G2}	Gross thrust of right fan (pounds)
F_{G3}	Gross thrust of forward fan (pounds)
F_{T1}, F_{T2}, F_{T3}	Tip turbine residual thrust developed by fans 1, 2, and 3 respectively. Gas-coupled fans only (pounds)

LIST OF SYMBOLS (Continued)

Symbol	
F_{X1}, F_{Y1}, F_{Z1}	Resultant x, y, and z components respectively of left fan gross thrust F_{G1} (pounds)
F_{X2}, F_{Y2}, F_{Z2}	Resultant x, y, and z components respectively of right fan gross thrust F_{G2} (pounds)
F_{X3}, F_{Y3}, F_{Z3}	Resultant x, y, and z components respectively of forward fan gross thrust F_{G3} (pounds)
F_{α}, F_{θ}	Functions of angle of attack and pitch attitude used to define α_F - fuselage angle of attack used in aerodynamic table lookup (nondimensional)
g	Acceleration due to gravity (32.174 feet/second^2)
$G_{\phi}, G_{\theta}, G_{\psi}$	Force gradients for roll stick, pitch stick, and rudder pedals respectively (pounds/inch)
h	Altitude of airplane CG (feet)
HP_E	Total horsepower generated by engines. Shaft-coupled system (horsepower)
$HP_{E1}, HP_{E2}, HP_{E3}$	Engine horsepower for numbers 1, 2, and 3. Shaft-coupled system (horsepower)
$HP_{F1}, HP_{F2}, HP_{F3}$	Fan horsepower for numbers 1, 2, and 3. Shaft-coupled system (horsepower)
HP_1, HP_2, HP_3	Tip turbine gas horsepower supplied to fans 1, 2, and 3 respectively. Gas-coupled fans only (horsepower)
I_{ATT}	Attitude command discrete. Attitude command mode = 1, rate command mode = 0 (nondimensional)
$IAUTO_3$	Discrete for automatic shutdown of number 3 engine during conversion. $IAUTO_3$ = 1 causes number 3 engine power to be reduced continuously as a function of thrust vector angle during conversion. $IAUTO_3 \neq 1$ causes a discrete shutdown of number 3 fan at a specific vector angle (nondimensional)
$ICAS_Y$	Yaw CAS and Yaw Vane Control switch discrete. If $ICAS_Y$ = 1 then n_Y and v_B feedbacks are not used in Yaw CAS, but v_B feedback is used in Yaw Vane Control. If $ICAS_Y \neq 1$ then n_Y and v_B feedbacks in Yaw CAS are used and the v_B feedback in Yaw Vane Control is open (nondimensional).

LIST OF SYMBOLS (Continued)

Symbol	
$ICAS_\theta$	Pitch control augmentation switch discrete. CAS engaged = 1, CAS disengaged = 0 (nondimensional)
$ICAS_\phi$	Roll control augmentation switch discrete. CAS engaged = 1, CAS disengaged = 0 (nondimensional)
$ICAS_\psi$	Yaw control augmentation switch discrete. CAS engaged = 1, CAS disengaged = 0 (nondimensional)
ICON	Conversion discrete for automatic shutdown of number 3 engine. Gas-coupled fans: ICON = -1 for interconnect valves closed, ICON = 0 for interconnect valves open, ICON = 1 for automatic cycling of interconnect values for number 3 shutdown Shaft-coupled fans: ICON ≠ 1 for discrete declutching of number 3 fan ICON = 1 for automatic number 3 engine shutdown. (nondimensional)
I_{DAMP}	Pilot's height damper switch discrete. Nominal value = 1 Height damper disengaged = 0 (nondimensional)
I_{DOORC}	Cockpit indicator discrete for fan doors closed (nondimensional)
I_{DOORO}	Cockpit indicator discrete for fan doors open (nondimensional)
IE_1, IE_2, IE_3	Engine failure discretes. Causes failure of engines 1, 2, and 3 respectively (nondimensional)
I_{FLAP}	Pilot's flap switch discrete. $I_{FLAP} = 0$, flaps stationary; $I_{FLAP} = -1$, maximum rate up; $I_{FLAP} = +1$, maximum rate down (nondimensional)
I_{FUEL}	Fuel usage discrete. Nominal value = 1. $I_{FUEL} = 0$ stops fuel flow and holds airplane weight constant (nondimensional)
I_{GEAR}	Pilot's landing gear switch discrete. Gear up value = -1. Gear down = 1 (nondimensional)
I_{GEARD}	Cockpit indicator discrete for gear down (nondimensional)
I_{GEARU}	Cockpit indicator discrete for gear up (nondimensional)

LIST OF SYMBOLS (Continued)

Symbol	
I_P	Fan rotor polar moment of inertia. Gas-coupled fan only (slug ft^2)
$ITRIM_\theta$	Pitch trim discrete. Nominal value = 0, pitch up = 1, pitch down = -1 (nondimensional)
$ITRIM_\phi$	Lateral trim discrete. Nominal value = 0, roll right = 1, roll left = -1 (nondimensional)
$ITRIM_\psi$	Yaw trim discrete. Nominal value = 0, yaw right = 1, yaw left = -1 (nondimensional)
I_{WOW}	Weight-on-wheels discrete. Nose wheel strut extended = 0, nose wheel strut compressed = 1 (nondimensional)
I_x, I_y, I_z	Vehicle inertias about x, y and z body axes (slug ft^2)
I_{xz}	Product of inertia with respect to x and z body axes (slug ft^2)
I_1, I_2, I_3, I_4	Inertia terms used in equations of motion (slug^2 ft^4)
$I\theta_{DMP}$	Pilot's dump valve switch discrete. Nominal value = 0. $I\theta_{DMP}$ = 1 exhausts number 3 engine flow out overboard dump. All fans and engines number 1 and number 2 remain interconnected. Gas-coupled fans only (nondimensional)
$I\theta_{DUMP}$	Dump valve discrete for conversion. $I\theta_{DUMP}$ = 1 for dump valve closed and number 3 fan operating. $I\theta_{DUMP}$ = 0 for dump valve open and number 3 fan shutdown. Gas coupled fans only (nondimensional)
$I\theta_{DUMPI}$	Cockpit indicator discrete for dump valve. Gas-coupled fan only (nondimensional)
$I\theta_{IV}$	Interconnect valve discrete. $I\theta_{IV}$ = 0 for interconnect valves open to permit gas transfer. $I\theta_{IV}$ = 1 for interconnect valves closed and no gas transfer. Gas-coupled fans only (nondimensional)
$I\boldsymbol{\Omega}$	Total angular momentum of fans and engines ((slug ft^2)/sec)
$I\Omega_z$	$I\Omega$ component along body z axis (slug ft^2/sec)
$I\Omega_x$	$I\Omega$ component along body x axis (slug ft^2/sec)
J	Polar moment of inertia of the two L/C fans. Shaft coupled system (slug ft^2)

LIST OF SYMBOLS (Continued)

Symbol	
J_E	Engine rotor moment of inertia for gyroscopic coupling (slug ft^2)
J_F	Fan rotor moment of inertia for gyroscopic coupling (slug ft^2)
J_3	Polar moment of inertia of the lift fan. Shaft coupled system (slug ft^2)
k_{NG}, k_{MG}	Landing gear strut spring rates for nose gear and main gear, respectively (lb/ft)
K	Conversion of units constant in fan dynamics model. Shaft coupled system (dimensionless)
K_A	Aileron roll input gain (degrees/volt)
K_{BIAS}	Path gain for fan speed dependent bias signal. Shaft-coupled system (nondimensional)
K_c	Conversion constant from fan speed in rad/sec to fan speed in percent (percent sec/rad)
K_{CLTH}	Gain of fan number 3 clutch signal. Shaft-coupled system (volts/deg)
K_{C_θ}	Pitch axis CAS stick transducer gain (volts/inch)
K_{C_ϕ}	Lateral axis CAS stick transducer gain (volts/inch)
K_{C_ψ}	CAS rudder pedal transducer gain (volts/inch)
K_{DERATE}	Fan thrust multiplication factor. Shaft-coupled system (nondimensional)
K_{DROOP}	Flap to aileron interconnect gain for drooped ailerons (nondimensional)
K_{ET}	Fuel flow forward path gain. Shaft-coupled system (lb/(volt hour))
K_{E1}, K_{E2}, K_{E3}	Fuel flow forward path gains for engines 1, 2, and 3 respectively. Shaft-coupled system (nondimensional)
K_F	Altitude rate forward loop gain. Shaft-coupled system (nondimensional)
K_{F_N}	Fan speed forward loop gain. Shaft-coupled system (nondimensional)

LIST OF SYMBOLS (Continued)

Symbol	
K_{FLAP}	Variable aileron gain due to drooped ailerons. Function of flap deflection (nondimensional)
$K_{G\dot{h}}$	Altitude rate feedback gain. Shaft-coupled system (nondimensional)
$K_{\dot{h}}$	Height damper feedback gain (% RPM - sec/ft)
K_H	Stabilator pitch input gain (degrees/volt)
$K_{HP1}, K_{HP2}, K_{HP3}$	Tip turbine gas horsepower failure gains for fans 1, 2, and 3 respectively. Nominal value = 1. $K_{HP} < 1$ for engine failure. Gas-coupled fan only (nondimensional)
K_{I_θ}	Integral gain in pitch axis proportional plus integral controller (1/seconds)
K_{I_ϕ}	Integral gain in lateral axis proportional plus integral controller (1/seconds)
K_{I_ψ}	Integral gain in directional axis proportional plus integral controller (1/seconds)
K_{M_θ}	Manual stick transducer gain in pitch axis (volts/inch)
K_{M_ϕ}	Manual stick transducer gain in roll axis (volts/inch)
K_{M_ψ}	Manual rudder pedal transducer gain (volts/inch)
$K_{MC\theta}, K_{MC\phi}, K_{MC\psi}$	Gains in pilot input branch into pitch, roll, and yaw CAS, respectively (volts/inch)
K_{n_y}	Lateral acceleration feedback gain in yaw axis (volts/g)
K_{n_z}	Normal acceleration feedback gain in pitch axis (volts/g)
K_N	Conversion constant from engine fuel flow to engine speed in percent - shaft coupled system (% RPM/hp)
K_{NO}	Normal acceleration and angle of attack feedback phase-out gain (nondimensional)
K_{Nf}	Fan speed feedback gain. Shaft-coupled system (volts/percent)
K_p	Roll rate feedback gain (volt seconds/radian)
K_{pA}, K_{pV}	Roll rate feedback gain value for aerodynamic flight and powered-lift flight respectively (volt seconds/radian)

LIST OF SYMBOLS (Continued)

Symbol	
K_{PO}	Powered-lift control phase-out gain. Used in pitch, roll, yaw, vertical, and lateral axes (nondimensional)
K_{p_θ}	Proportional gain in pitch axis proportional plus integral controller (nondimensional)
K_{p_ϕ}	Proportional gain in lateral axis proportional plus integral controller (nondimensional)
K_{p_ψ}	Proportional gain in directional axis proportional plus integral controller (nondimensional)
K_q	Pitch rate feedback gain (volt-seconds/radian)
K_{qA}, K_{qV}	Pitch rate feedback gain value for aerodynamic flight and powered-lift flight respectively (volt seconds/radian)
K_r	Yaw rate feedback gain when not in attitude command mode (volt seconds/radian)
K_{ro}	Yaw rate feedback gain in attitude command mode (volt seconds/radian)
K_R	Rudder yaw input gain (degrees/volt)
K_S	Pilot input stall prevention gain (nondimensional)
K_{SS}	Value of stall prevention gain K_S at high angle of attack (nondimensional)
$K_{TC\theta}$	Pitch axis CAS trim rate gain (volts/second)
$K_{TC\phi}$	Lateral axis CAS trim rate gain (volts/second)
$K_{TC\psi}$	Yaw axis CAS trim rate gain (volts/second)
$K_{TM\theta}$	Pitch axis manual trim rate gain (volts/second)
$K_{TM\phi}$	Roll axis manual trim rate gain (volts/second)
$K_{TM\psi}$	Yaw axis manual trim rate gain (volts/second)
K_{TRAN}	Forward path gain for shutdown signal to number 3 fan blade actuator. Shaft-coupled system (degrees/volt)
K_{TT1}, K_{TT2}, K_{TT3}	Tip turbine residual thrust failure gains for fans 1, 2, and 3 respectively. Nominal value = 1. $K_{TT} < 1$ for engine failure. Gas-coupled fans only (nondimensional)

LIST OF SYMBOLS (Continued)

Symbol	
K_{T1}	Left fan TRM actuator gain (degrees/percent thrust reduction)
K_{T2}	Right fan TRM actuator gain (degrees/percent thrust reduction)
K_{T3}	Forward fan TRM actuator gain (degrees/percent thrust modulation)
K_v	Side velocity feedback gain in yaw axis (volt seconds/foot)
K_{Y_L}	Lift fan yaw vane gain for sideforce input (degrees/volt)
K_α	Angle of attack feedback gain for stall prevention (volts/degree)
K_{α_q}	Pitch rate gain for angle of attack anticipation in stall prevention (degree seconds/radian)
K_{β_N}	Fan blade pitch loop gain. Shaft-coupled system (nondimensional)
$K_{\beta\theta 1}, K_{\beta\theta 2}, K_{\beta\theta 3}$	Forward path gain for pitch command signal to fan blade actuators 1, 2, and 3. Shaft-coupled system (degrees/volt)
K_{β_ϕ}	Forward path gain for roll command signal to fan blade actuators. Shaft-coupled system (degs/volt)
$K_{\beta_1}, K_{\beta_2}, K_{\beta_3}$	Forward path gain for fan blade actuators 1, 2, and 3. Shaft-coupled system (degs/volt)
$K_{Y_{L/C}}$	Lift/cruise fan yaw vane gain for sideforce input (degrees/volt)
$K_{\delta T1}$	Power lever command gain/CAS loop. Shaft-coupled system (nondimensional)
$K_{\delta T2}$	Power lever command gain. Shaft-coupled system (nondimensional)
K_θ	Pitch attitude feedback gain (volts/radian)
$K\theta_L$	Vector rate on lift fan during conversion (degree/second)
$K\theta_{L/C}$	Vector rate on lift/cruise fans during conversion (degrees/second)
K_ϕ	Roll attitude feedback gain in roll channel (volts/radian)
$K_{\phi\psi}$	Roll-to-yaw interconnect gain. Function of θ_J (nondimensional)

LIST OF SYMBOLS (Continued)

Symbol	
K_{ψ_L}	Lift fan yaw vane gain for yaw input (degrees/volt)
$K_{\psi_{L/C}}$	Lift/cruise fan yaw vane gain for yaw input (degrees/volt)
K_ω	Conversion constant from engine fuel flow to engine speed in rad/sec. Shaft-coupled system((rad/sec)/hp)
ℓ_1,ℓ_2,ℓ_3 m_1,m_2,m_3 n_1,n_2,n_3	Direction cosines corresponding to transformation between body and earth-fixed coordinate systems (nondimensional)
ℓ_t	Horizontal tail moment arm (FS_{CG} to $FS_{.25\bar{c}_{H.T.}}$)/12 (ft)
L	Total aerodynamic lift in stability axis (pounds)
L_A,M_A,N_A	Aerodynamic moments (excluding ram drag effects) about body x, y, and z axes, respectively (ft lb)
L_B,M_B,N_B	Total external moments exerted on the vehicle about body x, y, and z axes (ft lb)
L_F,M_F,N_F	Moments produced by fan forces about x, y and z body axes (ft lb)
LIM_h	Limit on altitude rate feedback signal (volts)
LIM_{WF1}, LIM_{WF2}, LIM_{WF3}	Limits on fuel flow to engines No. 1, 2, and 3, respectively (pounds/hour)
$LIM_{\beta N}$	Limit on height control command to fan blade angles (volts)
L_{LG},M_{LG},N_{LG}	Moments produced by landing gear ground reaction forces about x, y, and z body axes, respectively (ft lb)
$LM_{C\theta}$	Pitch axis CAS stick transducer limit (inches)
$LM_{C\phi}$	Lateral axis CAS stick transducer limit (inches)
$LM_{C\psi}$	CAS rudder pedal transducer limit (inches)
LM_{DAMP}	Height damper authority limit (percent engine RPM)
$LM_{I\theta}$	Integrator limit in pitch axis proportional plus integral controller (volts)
$LM_{I\phi}$	Integration limit in lateral axis proportional plus integral controller (volts)
$LM_{I\psi}$	Integrator limit in directional axis proportional plus integral controller (volts)

LIST OF SYMBOLS (Continued)

Symbol	
$LM_{M\theta}$	Manual stick transducer limit in pitch axis (inches)
$LM_{M\phi}$	Manual stick transducer limit in roll axis (inches
$LM_{M\psi}$	Manual rudder pedal transducer limit (inches)
LMN_G	Maximum commanded engine speed limit. Gas-coupled fan only (percent engine RPM)
$LM_{TC\theta}$	Pitch axis CAS trim limit (volts)
$LM_{TC\phi}$	Lateral axis CAS trim limit (volts)
$LM_{TC\psi}$	Yaw axis CAS trim limit (volts)
$LM_{TM\theta}$	Pitch axis manual trim authority limit (volts)
$LM_{TM\phi}$	Roll axis manual trim authority limit (volts)
$LM_{TM\psi}$	Yaw axis manual trim authority limit (volts)
$LM_{\theta H}$	Pitch attitude hold pitch angle limit (radians)
$LM_{\theta L}$	Thrust vector angle limit on lift fan. Most horizontal angle over which thrust vector angle is continuously variable (degrees)
$LM\theta_{L/C}$	Thrust vector angle limit on lift/cruise fans. Most horizontal angle over which thrust vector angle is continuously variable (degrees)
$LM_{\phi H}$	Roll attitude hold bank angle limit (radians)
L_p, L_r	Ram drag roll moment derivatives due to roll and yaw rates (ft lb sec)
$L_{RAM}, M_{RAM}, N_{RAM}$	Moments produced by ram drag forces about x, y, and z body axes (ft lb)
L_u, L_v, L_w	Dimensional scale lengths used in continuous random turbulence model (ft)
L_v	Ram drag roll moment derivative due to side velocity ((ft lb sec)/ft)
m	Mass of the aircraft (slugs)
$\dot{m}_{E1}, \dot{m}_{E2}, \dot{m}_{E3}$	Engine airflow through engines 1, 2, and 3 respectively (slugs/sec)
$\dot{m}_{F1}, \dot{m}_{F2}, \dot{m}_{F3}$	Fan airflow (slug/second)

LIST OF SYMBOLS (Continued)

Symbol	
M_q	Pitch ram drag moment derivative due to pitch rate ((ft lb sec)/rad)
M_u, M_w	Pitch ram drag moment derivatives due to x and z velocity components, respectively ((ft lb sec)/ft)
N_x, N_y, N_z	Accelerations sensed at aircraft CG along the x, y, z body axes (g's)
n_X, n_Y, n_Z	Aircraft load factor components along *x*, *y*, and *z* body axes, respectively (g's)
n_{XP}, n_{YP}, n_{ZP}	Acceleration components sensed at pilot's station along x, y and z body axes (g's)
N	Fan speed - shaft coupled system (rad/sec)
N_{ED}	Engine design speed. Gas-coupled fan only (RPM)
N_{FD}	Fan design speed (RPM)
N_{F1}, N_{F2}, N_{F3}	Rotational speed of fan 1, 2, and 3 respectively (percent fan design speed)
N_G	Engine speed commanded by master power lever and height damper. Gas-coupled fans only (percent)
N_{GDAMP}	Height damper engine RPM input (percent engine RPM)
N_{GI}	Sum of N_G and N_{GDAMP} signals (percent)
N_p, N_r	Ram drag yaw moment derivatives due to roll and yaw rates (ft lb sec)
N_v	Ram drag yaw moment derivative due to side velocity ((ft lb sec)/ft)
N_1, N_2, N_3	Speed of engines 1, 2 and 3 (percent)
$N_\%$	Fan speed. Shaft coupled system (percent)
p	Airplane roll rate. Inertial velocity about x body axis (radians/second)
$\hat{p}$	Nondimensional roll rate (nondimensional)
p_N, q_N, r_N	Disturbance increments in p, q, r (radians/sec)

LIST OF SYMBOLS (Continued)

Symbol	
P_{ST}, q_{ST}, r_{ST}	Total effective airplane rotation rates, including disturbances, about stability x, y, z axes (radians/sec)
P_T, q_T, r_T	Total effective airplane rotation rates, including disturbances, about body x, y, z axes (radians/sec)
PLM_A	Aileron actuator position limit (degrees)
PLM_F	Flap extension limit (degrees)
PLM_H	Stabilator actuator position limit (degrees)
PLM_R	Rudder actuator position limit (degrees)
PLM_T	TRM actuator position limit (degrees)
PLM_V	ETaC valve actuator position limit (degrees)
PLM_Y	Yaw vane actuator position limit (degrees)
$PLM_{\beta+}, PLM_{\beta-}$	Upper and lower fan blade pitch angle limits. Shaft coupled system (degrees)
PM	Total aerodynamic pitching moment in stability axes (ft-lb)
q	Airplane pitch rate. Inertial velocity about y body axis (radians/second)
$\bar{q}$	Dynamic pressure, $\bar{q} = 1/2\ \rho\ V^2$ (lb/ft^2)
r	Airplane yaw rate. Inertial velocity about z body axis (radians/second)
$\hat{r}$	Nondimensional yaw rate (nondimensional)
R	Horizontal component of the distance between the aircraft and the glide slope transmitter (feet)

LIST OF SYMBOLS (Continued)

Symbol	
R_{FLAP}	Flap extension rate (degrees/second)
RLM_A	Aileron actuator rate limit (degrees/second)
RLM_H	Stabilator actuator rate limit (degrees/second)
RLM_L	Maximum thrust vectoring rate on lift fan lowers (degrees/second)
$RLM_{L/C}$	Maximum thrust vectoring rate on lift/cruise nozzle (degrees/second)
RLM_N	Fan acceleration limit. Shaft-coupled system (rad/sec^2)
RLM_R	Rudder actuator rate limit (degrees/second)
RLM_T	TRM actuator rate limit (degrees/second)
RLM_V	ETaC valve actuator rate limit (degrees/second)
RLM_Y	Yaw vane actuator rate limit (degrees/second)
RLM_β	Fan blade pitch angle rate limit. Shaft-coupled system (deg/sec)
RM	Total aerodynamic roll moment in stability axes (ft lbs)
S	Laplace transform operator (1/sec)
SF	Total aerodynamic sideforce in stability axes (lb)
S_t	Horizontal tail area (ft^2)
S_W	Wing area (ft^2)
t	Time (sec)
T	Total gross thrust (lb)
T_{DOORL}	Time required to open lift fan doors (seconds)
$T_{DOORL/C}$	Time required to open lift/cruise fan doors (seconds)
T_{F1}, T_{F2}, T_{F3}	Fan thrust for fans 1, 2, and 3. Shaft-coupled system (lbs)

LIST OF SYMBOLS (Continued)

Symbol	
T_{GEAR}	Time required for gear extension (seconds)
T_{R1}, T_{R2}	Thrust of engine cores for numbers 1 and 2. Shaft coupled system (lbs)
$TQ_{F1}, TQ_{F2}, TQ_{F3}$	Fan torque required for fans 1, 2, and 3 respectively. Gas-coupled fans only (foot-pounds)
$TQ_{T1}, TQ_{T2}, TQ_{T3}$	Tip turbine torque of fan 1, 2, and 3 respectively. Gas coupled fans only (foot-pounds)
TRM_{BIAS}	TRM bias signal. Function of power setting (percent thrust reduction)
T_1	Left lift/cruise fan thrust reduction (percent)
T_2	Right lift/cruise fan thrust reduction (percent)
T_3	Lift fan thrust reduction (percent)
u_B, v_B, w_B	Components of V along x, y, z body axes, respectively (ft/sec)
u_{BN}, v_{BN}, w_{BN}	Disturbance increments in u_B, v_B, and w_B (ft/sec)
u_E, v_E, w_E	Airplane CG velocity components with respect to the earth-fixed coordinate system (ft/sec)
u_{IB}, v_{IB}, w_{IB}	Inertial velocity components in the x, y, and z airplane body axes (ft/sec)
v_B	Airspeed component along y body axes (feet/second)
V	Airplane velocity with respect to air (ft/sec)
$V_{BIAS\beta}$	Fan blade pitch bias signal. Shaft-coupled system (volts)
V_{CLUTCH}	Fan number 3 clutch signal. Shaft-coupled system (volts)
V_{J3}	Signal representing the inertia of the lift fan. Shaft-coupled system (slug ft^2)
$(V/V_J)_{LCLEFT}$, $(V/V_J)_{LCRIGHT}$, $(V/V_J)_{NL}$	Jet velocity ratios at left, right, and forward fans respectively (nondimensional)
V_{TRANS}	Shutdown signal to number 3 fan blade actuator from effective nozzle angle. Shaft-coupled system (volts)
V_{WIND}	Total mean wind velocity (ft/sec)

LIST OF SYMBOLS (Continued)

Symbol	
V_1	Power lever schedule output. Shaft-coupled systems (volts)
V_2	Power lever schedule output/CAS loop. Shaft-coupled system (volts)
w_x, w_y, w_z	Wind velocity components along the x, y, and z axes (ft/sec)
W	Airplane weight (pounds)
W_{EMPTY}	Airplane operating weights with no usable fuel (pounds)
$\dot{W}_F$	Total fuel flow rate (pounds/hour)
W_{FUEL}	Total useable fuel remaining in aircraft (pounds)
$W_{F_{MAX}}$	Maximum useable fuel carried or aircraft (pounds)
$\dot{W}_{F_1}$	Fuel flow rate to number 1 engine (pounds/hour)
$\dot{W}_{F_2}$	Fuel flow rate to number 2 engine (pounds/hour)
$\dot{W}_{F_3}$	Fuel flow rate to number 3 engine (pounds/hour)
x,y,h	Aircraft CG position with respect to earth-fixed coordinate system (ft)
$x_{EL}, x_{EL/C}$	x body axis coordinate of lift engine and lift/cruise engine inlets respectively (feet)
$x_{FL}, x_{FL/C}$	x body axis coordinate of lift fan and lift/cruise fan inlets respectively (feet)
x_{LGS}, y_{LGS}	x and y earth axis coordinates respectively of glide slope transmitter (feet)
x_{LLOC}, y_{LLOC}	Location of localizer transmitter in earth-fixed coordinate system (ft)
x_{LMRK}, y_{LMRK}	Location of compass location in earth-fixed coordinates (ft)
x_{NG}, x_{MG}	x body axis location of nose wheel and main wheel respectively (feet)
x_o, y_o, h_o	Initial location of aircraft CG in earth-fixed coordinate system (ft)
x_p, y_p, z_p	Location of pilot in body axis coordinate system (ft)
x_{PE}, y_{PE}, h_{PE}	Location of pilot in earth-fixed coordinate system (ft)

LIST OF SYMBOLS (Continued)

Symbol	
$x_{TL}, x_{TL/C}$	x body axis coordinate of thrust application point on lift fan and lift/cruise fan respectively (feet)
x_A, y_A, z_A	Aerodynamic forces (excluding ram drag effects) along body x, y, z axes (lb)
X_B, Y_B, Z_B	Total forces exerted on the airplane along the x, y, z body axes (lb)
X_E, Y_E, Z_E	Total forces exerted on the airplane and measured along reference inertial x, y, z axes (lb)
X_F, Y_F, Z_F	Total fan and nozzle thrust forces in body coordinate system (lb)
X_{LG}, Y_{LG}, Z_{LG}	Total forces produced by landing gear reactions in x, y, z body axes (lb)
X_{NG}, X_{LMG}, X_{RMG}	Landing gear rolling friction forces (lb)
X_q	Ram drag x axis force due to pitch rate (lb sec)
$X_{RAM}, Y_{RAM}, Z_{RAM}$	Ram drag force components in the direction of the x, y, z body axes (lb)
X_u	Axial ram drag force due to x axis velocity (lb sec/ft)
Xl_{NG}, Yl_{NG}, Xl_{MG}, Yl_{MG}	Landing gear reaction forces in body x and y directions for nose and main gear (lb)
$y_{EL/C}$	y body axis coordinate of right lift/cruise engine inlet (feet)
$y_{FL/C}$	y body axis coordinate of right lift/cruise fan inlet (feet)
y_{MG}	y body axis location of right main wheel (feet)
$y_{TL/C}$	y body axis coordinate of right fan thrust application point (feet)
YM	Total aerodynamic yawing moment in stability axes (ft-lb)
Y_{NG}, Y_{LMG}, Y_{RMG}	Sliding friction forces on nose and left and right main landing gears (lb)
Y_p	Ram drag side force due to roll rate (lb/sec)
Y_r	Ram drag side force due to yaw rate (lb/sec)

LIST OF SYMBOLS (Continued)

Symbol	
$z_{EL}, z_{EL/C}$	z body axes coordinate of lift engine and lift/cruise engine inlets respectively (feet)
$z_{FL}, z_{FL/C}$	z body axis coordinate of lift fan and lift/cruise fan inlets respectively (feet)
z_{NG}, z_{MG}	z body axis location of nose wheel and main wheel respectively (feet)
$z_{TL}, z_{TL/C}$	z body axis coordinate of thrust application point on lift fan and lift/cruise fan respectively (feet)
Z_{NG}, Z_{LMG}, Z_{RMG}	z axis oleo forces on nose, left and right main landing gear (lb)
Z_q	Ram drag z axis force due to pitch rate (lb/sec)
Z_w	Ram drag force due to y axis velocity (lb sec/ft)
Z_t	Horizontal tail moment arm (WL_{CG} to $WL_{H.T.PIVOT}$)/12 (ft)
α	Airplane angle of attack (degrees)
$\hat{\dot{\alpha}}$	Nondimensional rate of change of angle of attack (nondimensional)
α_F	Fuselage angle of attack. Depends on both true angle of attack and pitch attitude for table lookup at low airspeed (degrees)
α_R	Reference angle of attack used in stall prevention feedbacks. Blend of angle of attack and pitch rate (degrees)
α_{BIAS}	Angle of attack bias. Angle of attack at which angle of attack feedback signal begins to reduce angle of attack (degrees)
α_t	Angle of attack of horizontal tail (degrees)
α_1	Effective sideward thrust deflection angle on left fan (degrees)
α_2	Effective sideward thrust deflection angle on right fan (degrees)
α_3	Effective sideward thrust deflection angle on forward fan (degrees)

LIST OF SYMBOLS (Continued)

Symbol	
α_{R1}, α_{R2}	Reference angle of attack values used to define stall prevention gain K_S (degrees)
β	Airplane sideslip angle (degrees)
$\beta_1, \beta_2, \beta_3$	Fan blade pitch angle. Shaft coupled system (deg)
γ_{GS}	Nominal glide slope angle (deg)
γ_{3C}	Forward fan yaw vane command. Vane actuator input (degrees)
γ_{2C}	Right fan yaw vane command. Vane actuator input (degrees)
γ_{1C}	Left fan yaw vane command. Vane actuator input (degrees)
γ_3	Forward fan yaw vane angle (degrees)
γ_2	Right fan yaw vane angle (degrees)
γ_1	Left fan yaw vane angle (degrees)
δ_{AI}	Aileron roll input (degrees)
δ_{AL}	Left aileron deflection (degrees)
δ_{ALC}	Left aileron command. Input to aileron actuator (degrees)
δ_{AR}	Right aileron deflection (degrees)
δ_{ARC}	Right aileron command. Input to aileron actuator (degrees)
$\delta_{CAS\theta}$	Pitch CAS input to pitch axis (volts)
$\delta_{CAS\phi}$	Roll CAS input to roll axis (volts)
$\delta_{CAS\psi}$	Yaw CAS input to yaw axis (volts)
δ_{DOORL}	Lift fan door position. Full close = 0. Full open = 1 (nondimensional)
$\delta_{DOORL/C}$	Lift/cruise fan door position. Full close = 0. Full open = 1 (nondimensional)
δ_{FLAP}	Flap deflection angle (deg)
δ_{GEAR}	Landing gear position. Full up = 0. Full down = 1 (nondimensional)
δ_H	Stabilator deflection (degrees)

LIST OF SYMBOLS (Continued)

Symbol	
δ_{HC}	Commanded stabilator deflection. Input to stabilator actuator (degrees)
δ_{HI}	Stabilator pitch input (degrees)
δ_{IY}	Pilot's input generating side velocity, v_B (inches)
$\delta_{I\theta}$	Pitch stick input (inches)
$\delta_{I\phi}$	Lateral stick input (inches)
$\delta_{I\psi}$	Rudder pedal input (inches)
δ_{LIFT}	Fan exit airflow correction factor, lift unit. Shaft-coupled system (nondimensional)
$\delta_{L/C}$	Fan exit airflow correction factor, lift/cruise unit. Shaft-coupled system (nondimensional)
δ_R	Rudder deflection angle (degrees)
δ_{RC}	Commanded rudder deflection (degrees)
δ_{RI}	Rudder yaw input (degrees)
δ_T	Power lever position (%)
δV_f	Fuel flow signal to engines. Shaft-coupled system (volts)
δV_β	Fan blade pitch forward loop signal. Shaft-coupled system (volts)
$\delta V_1, \delta V_2, \delta V_3$	Engine shutdown signals for numbers 1, 2 and 3 engines. Shaft-coupled system (volts)
δ_Y	Sideforce command input (volts)
δ_1	Position of number 1 engine throttle lever (percent full input)
δ_2	Position of number 2 engine throttle lever (percent full input)
δ_3	Position of number 3 engine throttle lever (percent full input)

LIST OF SYMBOLS (Continued)

Symbol	
δ_θ	Powered-lift pitch command (volts)
δ_ϕ	Powered-lift roll command (volts)
δ_{ϕ_ψ}	Roll input to yaw axis (volts)
δ_ψ	Powered-lift yaw command (volts)
ΔHP	Difference between total engine horsepower and total fan horsepower. Shaft-coupled system (horsepower)
$\Delta HP_1, \Delta HP_2, \Delta HP_3$	Horsepower increments used in gas-coupled fan tip-turbine math models 1, 2, and 3 (horsepower)
$\Delta C_{D_{AILERON}}$	Change in drag coefficient due to aileron deflection (nondimensional)
$\Delta C_{D_{DOORS}}$	Drag coefficient change due to opening fan door (nondimensional)
$\Delta C_{D_{FLAP}}$	Change in drag coefficient due to flap deflection (nondimensional)
$\Delta C_{D_{GE}}$	Change in drag coefficient due to ground effects (nondimensional)
$\Delta C_{D_{GEAR}}$	Drag coefficient change due to landing gear (nondimensional)
$\Delta C_{\ell_{AILERON}}$	Change in roll moment coefficient due to aileron deflection (nondimensional)
$\Delta C_{\ell_{RUDDER}}$	Change in roll moment coefficient due to rudder deflection (nondimensional)
$\Delta C_{\ell\beta_{AILERON}}$	Change in $C_{\ell\beta}$ due to drooped ailerons (nondimensional)
$\Delta C_{\ell\beta_{DOORS}}$	Change in $C_{\ell\beta}$ due to opening fan closure doors (nondimensional)
$\Delta C_{\ell\beta_{FLAP}}$	Change in $C_{\ell\beta}$ due to flap deflection (nondimensional)
$\Delta C_{\ell\beta_{GE}}$	Change in $C_{\ell\beta}$ due to ground effects (nondimensional)
$\Delta C_{L_{AILERON}}$	Change in lift coefficient due to aileron deflection (nondimensional)
$\Delta C_{L_{DOORS}}$	Lift coefficient change due to opening fan doors (nondimensional)

LIST OF SYMBOLS (Continued)

Symbol	
$\Delta C_{L_{FLAP}}$	Change in lift coefficient due to flap deflection (nondimensional)
$\Delta C_{L_{GE}}$	Change in lift coefficient due to ground effects (nondimensional)
$\Delta C_{L_{GEAR}}$	Lift coefficient change due to landing gear (nondimensional)
$\Delta C_{m_{AILERON}}$	Change in pitching moment coefficient due to aileron deflection (nondimensional)
$\Delta C_{m_{DOORS}}$	Pitching moment coefficient change due to opening fan doors (nondimensional)
$\Delta C_{m_{FLAP}}$	Change in pitching moment coefficient due to flap deflection (nondimensional)
$\Delta C_{m_{GE}}$	Change in pitching moment coefficient due to ground effects (nondimensional)
$\Delta C_{m_{GEAR}}$	Pitching moment coefficient change due to landing gear (nondimensional)
$\Delta C_{n_{AILERON}}$	Change in yaw moment coefficient due to aileron deflection (nondimensional)
$\Delta C_{n_{RUDDER}}$	Change in yaw moment coefficient due to rudder deflection (nondimensional)
$\Delta C_{n_{\beta AILERON}}$	Change in C_{n_β} due to drooped ailerons (nondimensional)
$\Delta C_{n_{\beta DOORS}}$	Change in C_{n_β} due to opening fan closure doors (nondimensional)
$\Delta C_{n_{\beta FLAP}}$	Change in C_{n_β} due to flap deflection (nondimensional)
$\Delta C_{n_{\beta GE}}$	Change in C_{n_β} due to ground effects (nondimensional)
$\Delta C_{Y_{AILERON}}$	Change in sideforce coefficient due to aileron deflection (nondimensional)
$\Delta C_{Y_{RUDDER}}$	Change in sideforce coefficient due to rudder deflection (nondimensional)
$\Delta C_{Y_{\beta AILERON}}$	Change in C_{Y_β} due to drooped ailerons (nondimensional)
$\Delta C_{Y_{\beta DOORS}}$	Change in C_{Y_β} due to opening fan closure doors (nondimensional)

LIST OF SYMBOLS (Continued)

Symbol	
$\Delta Cy_{\beta_{FLAP}}$	Change in Cy_{β} due to flap deflection (nondimensional)
$\Delta Cy_{\beta_{GE}}$	Change in Cy_{β} due to ground effects (nondimensional)
Δx_1	Variation in left fan x thrust application point with thrust vector angle (feet)
Δx_2	Variation in right fan x thrust application point with thrust vector angle (feet)
Δx_3	Variation in forward fan x thrust application point with thrust vector angle (feet)
Δz_1	Variation in left fan z thrust application point with thrust vector angle (feet)
Δz_2	Variation in right fan z thrust application point with thrust vector angle (feet)
$\left(\frac{\Delta D}{T}\right)_{POWER}$	Nondimensional power induced drag (nondimensional)
$\left(\frac{\Delta L}{T}\right)_{POWER}$	Nondimensional power induced lift (nondimensional)
$\left(\frac{\Delta PM}{TD_e}\right)_{POWER}$	Nondimensional power induced pitching moment (nondimensional)
$\left(\frac{\Delta RM}{TD_e}\right)_{POWER}$	Nondimensional power induced rolling moment (nondimensional)
$\left(\frac{\Delta SF}{T}\right)_{POWER}$	Nondimensional power induced sideforce (nondimensional)
$\left(\frac{\Delta YM}{TD_e}\right)_{POWER}$	Nondimensional power induced yaw moment (nondimensional)
$\Delta\left(\frac{\Delta D}{T}\right)_{POWER\ GE}$	Change in power induced drag due to ground effects (nondimensional)
$\left[\Delta\left(\frac{\Delta D}{T}\right)_{POWER}\right]_{\phi}$	Change in power induced drag due to bank angle in ground proximity (nondimensional)
$\left[\Delta\left(\frac{\Delta L}{T}\right)_{POWER}\right]_{GE}$	Change in power induced lift due to ground effects (nondimensional)
$\left[\Delta\left(\frac{\Delta L}{T}\right)_{POWER}\right]_{\phi}$	Change in power induced lift due to bank angle in ground proximity (nondimensional)

LIST OF SYMBOLS (Continued)

Symbol	
$\left[\Delta\left(\frac{\Delta PM}{TD_e}\right)_{POWER}\right]_{GE}$	Change in power induced pitching moment due to ground effects (nondimensional)
$\left[\Delta\left(\frac{\Delta PM}{TD_e}\right)_{POWER}\right]_{\phi}$	Change in power induced pitching moment due to bank angle in ground proximity (nondimensional)
$\left[\Delta\left(\frac{\Delta RM}{TD_e}\right)_{POWER}\right]_{GE}$	Change in power induced rolling moment due to ground effects (nondimensional)
$\left[\Delta\left(\frac{\Delta RM}{TD_e}\right)_{POWER}\right]_{\phi}$	Change in power induced rolling moment due to bank angle in ground proximity (nondimensional)
$\left[\Delta\left(\frac{\Delta SF}{T}\right)_{POWER}\right]_{GE}$	Change in power induced sideforce due to ground effects (nondimensional)
$\left[\Delta\left(\frac{\Delta SF}{T}\right)_{POWER}\right]_{\phi}$	Change in power induced sideforce due to bank angle in ground proximity (nondimensional)
$\left[\Delta\left(\frac{\Delta YM}{TD_e}\right)_{POWER}\right]_{GE}$	Change in power induced yawing moment due to ground effects (nondimensional)
$\left[\Delta\left(\frac{\Delta YM}{TD_e}\right)_{POWER}\right]_{\phi}$	Change in power induced yawing moment due to bank angle in ground proximity (nondimensional)
$\Delta\epsilon_{AILERON}$	Change in downwash angle due to drooped ailerons (nondimensional)
$\Delta\epsilon_{FLAP}$	Change in downwash angle due to flap deflection (degrees)
$\Delta\epsilon_{GE}$	Change in downwash angle due to ground effects (nondimensional)
$\Delta\epsilon_{POWER}$	Power induced change in tail downwash angle (degrees)
$\Delta\eta_{AILERON}$	Change in tail efficiency factor due to drooped ailerons (nondimensional)
$\Delta\eta t_{FLAP}$	Change in tail efficiency factor due to flap deflection (nondimensional)
$\Delta\eta t_{GE}$	Change in tail efficiency factor due to ground effects (nondimensional)
$\Delta\eta t_{POWER}$	Power induced change in tail efficiency factor (nondimensional)

LIST OF SYMBOLS (Continued)

Symbol	
ε	Total downwash angle (deg)
ε_{GS}	Glide slope error (deg)
ε_{LOC}	Localizer error (deg)
ε_{WB}	Downwash angle of wing-body configuration alone (nondimensional)
ζ_{TL}	Transition lever position (%)
η_t	Total tail efficiency factor (nondimensional)
$\eta_{t_{WB}}$	Tail efficiency factor of wing-body configuration alone (nondimensional)
θ	Airplane pitch angle (radians)
$\hat{\dot{\theta}}$	Nondimensional pitch rate (nondimensional)
θ_J	Command thrust vector angle (degrees)
θ_{JC}	Thrust vector angle at which conversion process begins (degrees)
θ_{LC}	Lift/cruise fan thrust vector angle; designates either left or right fan vector angle (degrees)
$\theta_{LC_{LEFT}}$	Left fan thrust vector angle. Equal to $\boldsymbol{\theta}_1$ (degree)
$\theta_{LC_{RIGHT}}$	Right fan thrust vector angle. Equal to $\boldsymbol{\theta}_2$ (degree)
θ_{NL}	Forward fan thrust vector angle. Equal to $\boldsymbol{\theta}_3$ (degree)
θ_{V1}	ETaC valve angle on left lift/cruise fan (degrees)
θ_{V2}	ETaC valve angle on right lift/cruise fan (degrees)
θ_{V3}	ETaC valve angle on lift fan (degrees)
θ_{V1C}	Commanded ETaC valve angle on left lift/cruise fan. Input to valve actuator (degrees)
θ_{V2C}	Commanded ETaC valve angle on right lift/cruise fan. Input to valve actuator (degrees)
θ_{V3C}	Commanded ETaC valve angle on lift fan. Input to valve actuator (degrees)
θ_1	Left fan thrust vector angle (degrees)

LIST OF SYMBOLS (Continued)

Symbol	
θ_2	Right fan thrust vector angle (degrees)
θ_3	Forward fan thrust vector angle (degrees)
θ_{1C}	Commanded thrust vector angle on left fan nozzle. Nozzle actuator input (degrees)
θ_{2C}	Command thrust vector angle on right fan nozzle. Nozzle actuator input (degrees)
θ_{3C}	Commanded thrust vector angle on lift fan louvers. Louver actuator input (degree)
$\sqrt{\theta}$	Temperature correction factor for fan exit airflow. Shaft-coupled system (nondimensional)
μ_S, μ_R	Coefficients of rolling and sliding friction (nondimensional)
ρ	Atmosphere density (slugs/ft^3)
$\rho_1, \rho_2, \rho_3, \rho_4$	Independent, zero mean, unit variance, normally distributed random variables used in continuous random turbulence model (nondimensional)
$\sigma_u, \sigma_v, \sigma_w$	Turbulence intensities used in continuous random turbulence model (ft/sec)
σ_1	TRM port opening on left fan (degrees)
σ_2	TRM port opening on right fan (degrees)
σ_3	TRM louver angle on forward fan (degrees)
σ_{1C}	Commanded TRM port opening on left fan. Input to TRM actuator (degrees)
σ_{2C}	Commanded TRM port opening on right fan. Input to TRM actuator (degrees)
σ_{3C}	Commanded TRM louver angle on forward fan. Input to TRM actuator (degrees)
τ_{DCT}	Duct lag time constant (sec)
τ_E	Time constant - engine transfer function numerator. Shaft-coupled system (sec)
τ_L	Low pass filter time constant in fuel flow loop. Shaft-coupled system (sec)

LIST OF SYMBOLS (Continued)

Symbol	
τ_{NE}	First order time constant in engine lag (seconds)
τ_{n_Y}	Lateral acceleration feedback filter time constant (seconds)
τ_{n_Z}	Normal acceleration feedback filter time constant (seconds)
$\tau_{N\beta}$	Time constant of fan speed to blade bias signal. Shaft coupled system (sec)
$\tau_{N\theta}, \tau_{D\theta}$	Pitch axis CAS compensation filter time constants in numerator and denominator respectively (seconds)
$\tau_{N\phi}, \tau_{D\phi}$	Lateral axis CAS compensation filter time constants in numerator and denominator respectively (seconds)
τ_r	Yaw rate washout filter time constant (seconds)
τ_T	TRM washout time constant (seconds)
τ_{TS}	Time constant effective nozzle angle to fan blade number 3 command signal. Shaft coupled system (sec)
τ_v	Side velocity feedback filter time constant (seconds)
τ_{VC}	Time constant of fan number clutch signal. Shaft fan system (seconds)
τ_α	Angle of attack feedback filter time constant (seconds)
ϕ	Airplane roll angle (radians)
ψ	Airplane heading angle (degrees)
ψ_{ADF}	Automatic direction finder heading (degrees)
ψ_{WIND}	Direction from which mean wind is coming (degree)
$\omega_1, \omega_2, \omega_3$	Rotational speed of engine cores 1, 2, and 3, respectively (radians/second)
$\omega_{F1}, \omega_{F2}, \omega_{F3}$	Rotational speed of fans 1, 2, and 3 respectively (radians/second)

ACRONYMS

ADI	attitude director indicator
CG	center of gravity
CAS	control augmentation system
ETaC	Energy Transfer and Control
FS	fuselage station
FSAA	Flight Simulator for Advanced Aircraft
GE	ground effect
HSI	horizontal situation indicator
HT	horizontal tail
IFR	instrument flight rules
OGE	out of ground effect
RPM	revolutions per minute
RTA	Research Technology Aircraft
TED	trailing edge down
TEL	trailing edge left
TER	trailing edge right
TEU	trailing edge up
TRM	Thrust Reduction Modulation
V/STOL	vertical and/or short takeoff and landing
VFR	visual flight rules
VTO	vertical takeoff
WL	waterline

LIST OF PAGES

1. GENERAL ARRANGEMENT

The simulated aircraft is a Lift/Cruise Fan V/STOL Research Technology Aircraft (RTA). The aircraft is powered by three turbojet engines which drive three fans. One of the fans is located in the forward fuselage and is used only during powered-lift flight. During the aerodynamic portion of flight the forward fan, called the lift fan or fan No. 3, is shut down and its air duct is closed to reduce aerodynamic drag. The other two fans are installed at the wing root and are used during powered-lift and aerodynamic flight. These two lift/cruise fans are numbered respectively fan No. 1 (left) and fan No. 2 (right). Their exhaust nozzles can be deflected such that their thrust can be directed either horizontally, vertically, or at any angle in-between. In addition, all three fans have the capability to have their thrust deflected sideward for sideforce control.

The simulation math model is set up to represent two configurations of the aircraft. In one configuration the power between power plants and fans is transferred by mean of air ducts which supply high energy heated air to drive the "tip turbines" on the periphery of each fan. This configuration is referred to as the gas-coupled configuration. The overall simulation block diagram for this configuration is presented in Figure 1-1.

In the other configuration gas generator power is transferred mechanically between fans by interconnecting shafts which force all fans to operate at the same speed. This shaft-coupled configuration is represented in a general form by the block diagram of Figure 1-2. In several parts the second diagram is the same as the corresponding gas-coupled configuration, indicating basic similarity between the two versions.

More detailed descriptions of all blocks shown in Figure 1-1 and 1-2 is presented in subsequent sections of this report.

FIGURE 1-1
SIMULATION MATH MODEL - GAS COUPLED FANS

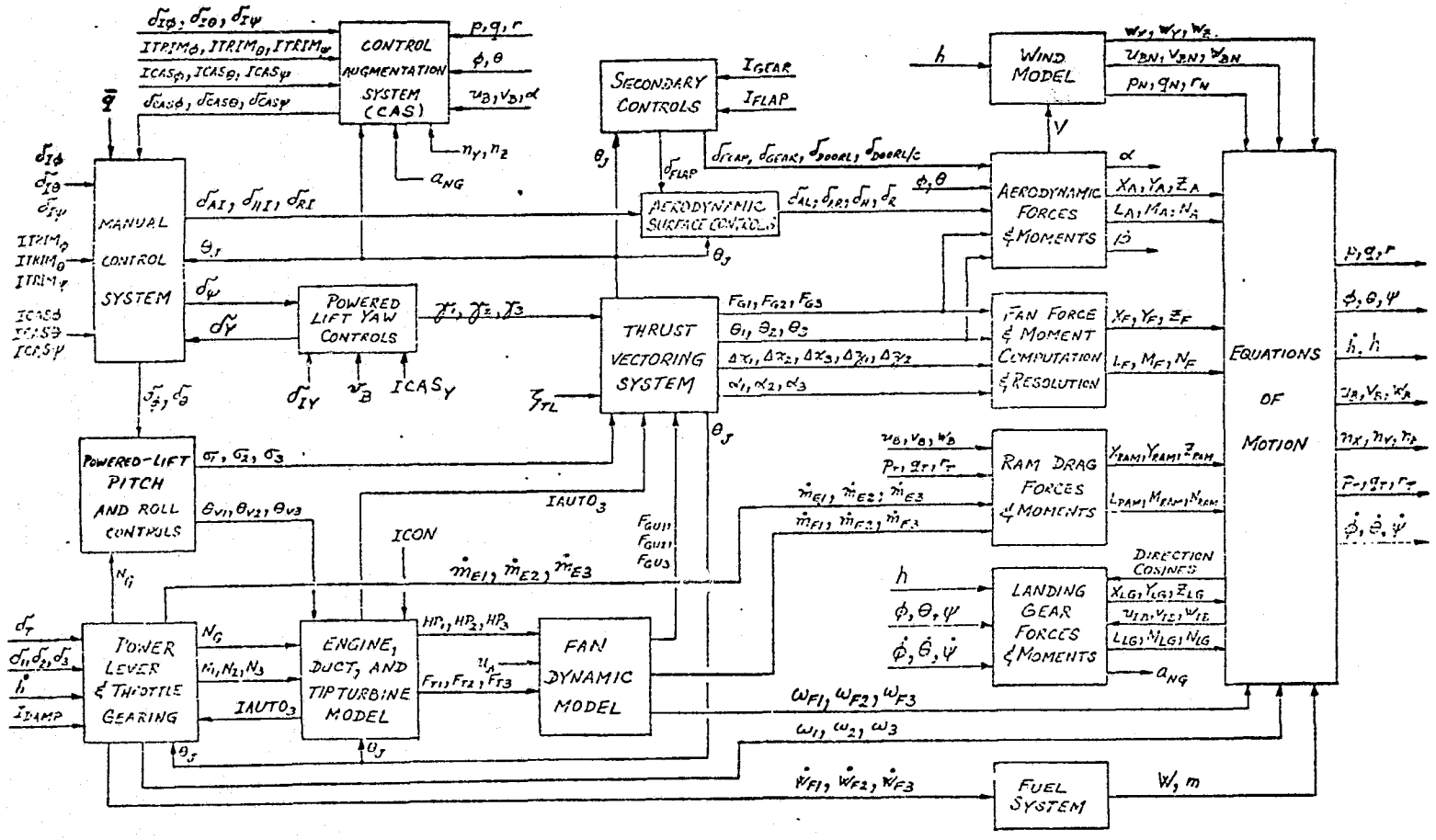

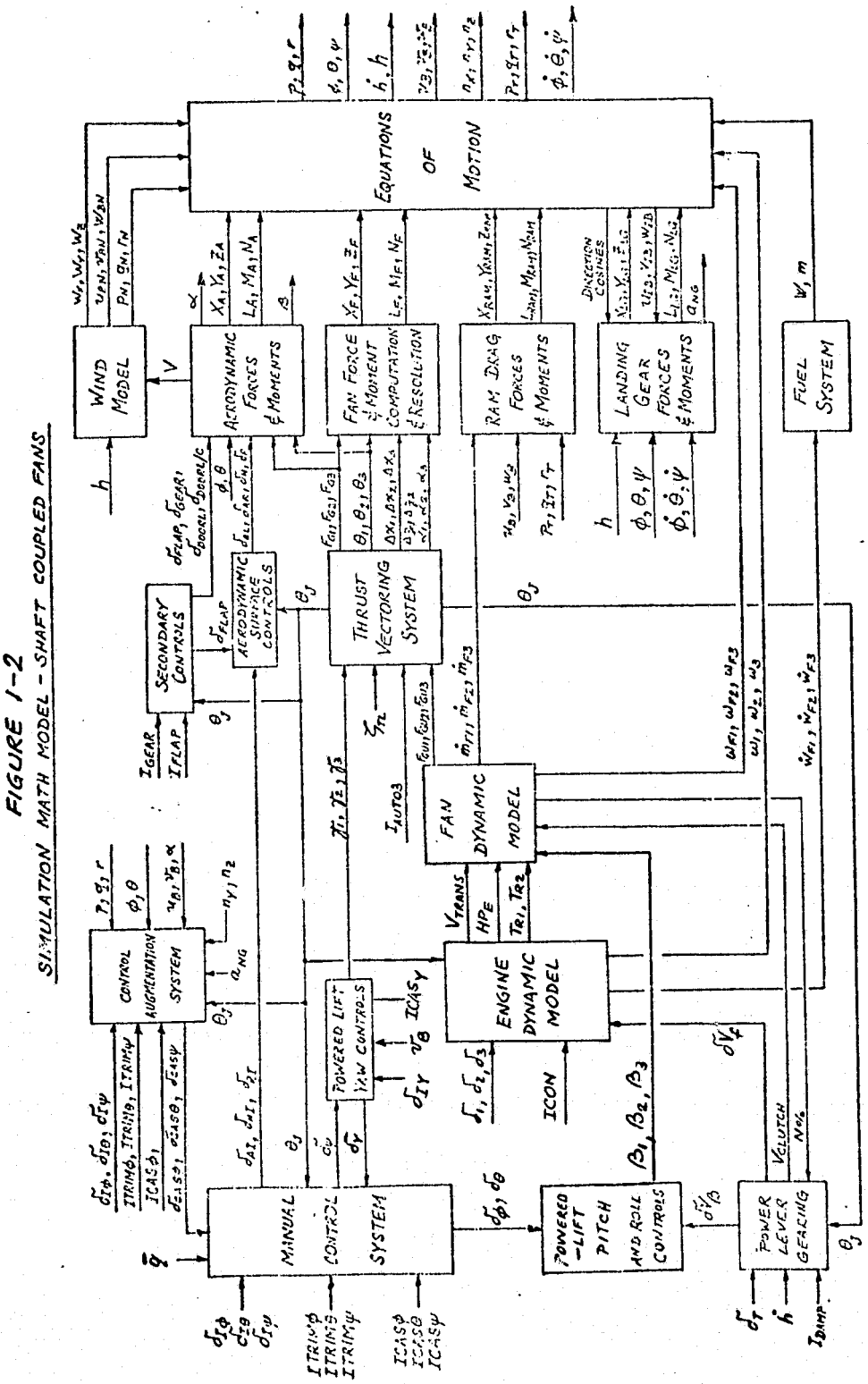

FIGURE 1-2

SIMULATION MATH MODEL - SHAFT COUPLED FANS

2. MANUAL CONTROL SYSTEM

The manual control system provides the pilot with a capability to control the airplane in all flight phases without the Control Augmentation System (CAS). It activates aerodynamic as well as power lift controls. The Manual Control System Diagram, Figure 2-1, shows how the pilot's stick, pedal, and trim inputs are used to generate the aerodynamic (δ_{HI}, δ_{AI}, δ_{RI}) and power lift control signals (δ_{θ}, δ_{ϕ}, δ_{ψ}). The three pilot trim inputs ($ITRIM_{\theta}$, $ITRIM_{\phi}$, $ITRIM_{\psi}$) are usable in the manual control system only when the corresponding trim inputs into CAS are deactivated. The discretes selected by the pilot, $ICAS_{\theta}$, $ICAS_{\phi}$, and $ICAS_{\psi}$, are used to channel the trim inputs either into manual or into CAS control system.

The roll and pitch inputs, $\delta_{I\phi}$ and $\delta_{I\theta}$, are generated by the pilot with the corresponding stick deflections, while $\delta_{CAS\phi}$, $\delta_{CAS\theta}$, and $\delta_{CAS\psi}$ signals are the inputs into the manual control system from the CAS system which is described in the next section.

The roll-to-yaw cross-feed signal passes through a first order lag circuit with a 0.1 second time constant to generate the yaw loop input, $\delta_{\phi\psi}$. The cross-feed gain, $K_{\phi\psi}$, and the phase-out gain, K_{PO}, are scheduled as function of commanded thrust vector angle (θ_J). The phase-out gain (K_{PO}) schedule is shown on the same page with the diagram (Figure 2-1), but the cross-feed gain schedule is plotted separately (Figure 2-2). The pitch forward loop gain, $K_{M\theta}$, is scheduled as function of dynamic pressure, plotted in Figure 2-3. All other manual control system gains, deadbands, and limits are constants tabulated in Figure 2-4.

The integrator output limits are represented in this report by block diagram schematics of the type shown in Figure 2-5. Either of the two schematics shown in Figure 2-5 represents the same form of integrator limit: whenever the associated integrator output reaches one of the preset limit values, it remains constant until the integrator input changes sign. At the instant the integrator input changes

sign the integrator resumes integrating and its output backs away from the limiting value.

Any other limits shown in block diagrams - specifically those which are not shown in the same block with an integrator or have no feedback going to an intergrator - have no direct effect on integrator output. These other limits just limit the signal in the specific branch where the limit is located.

FIGURE 2-1
MANUAL CONTROL SYSTEM

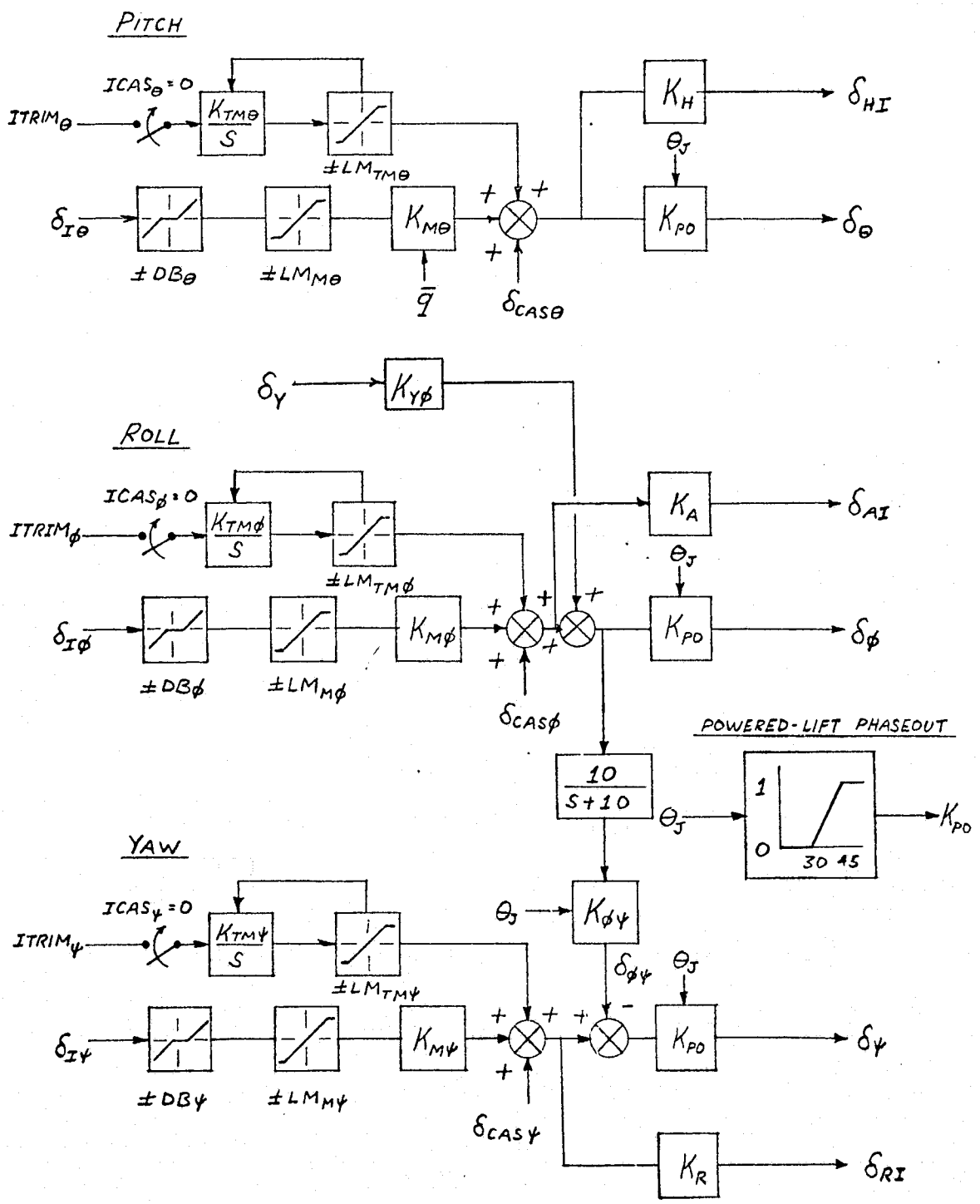

FIGURE 2-2

ROLL / YAW INTERCONNECT GAIN

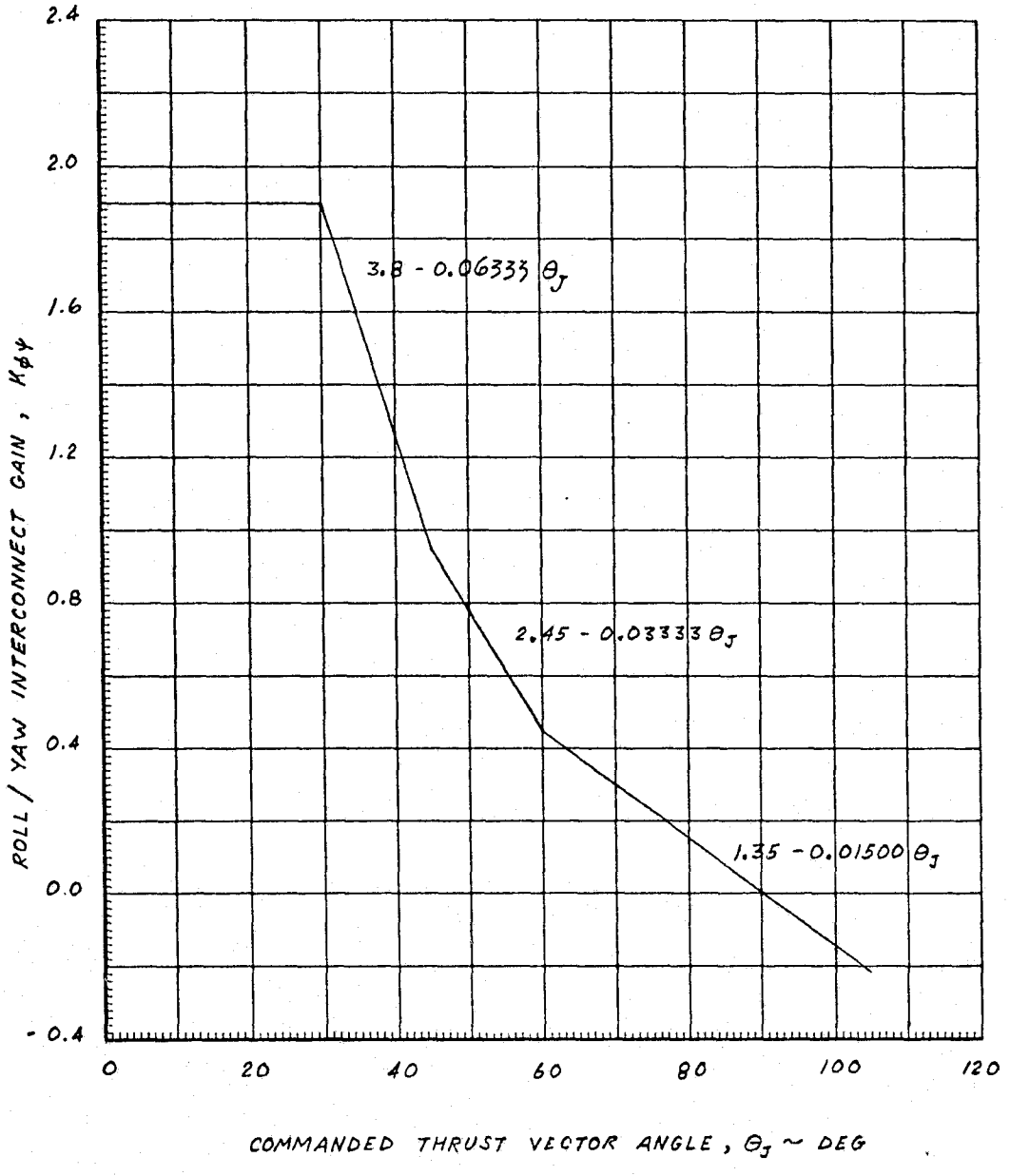

FIGURE 2-3
MANUAL STICK RATIO CHANGER GAIN

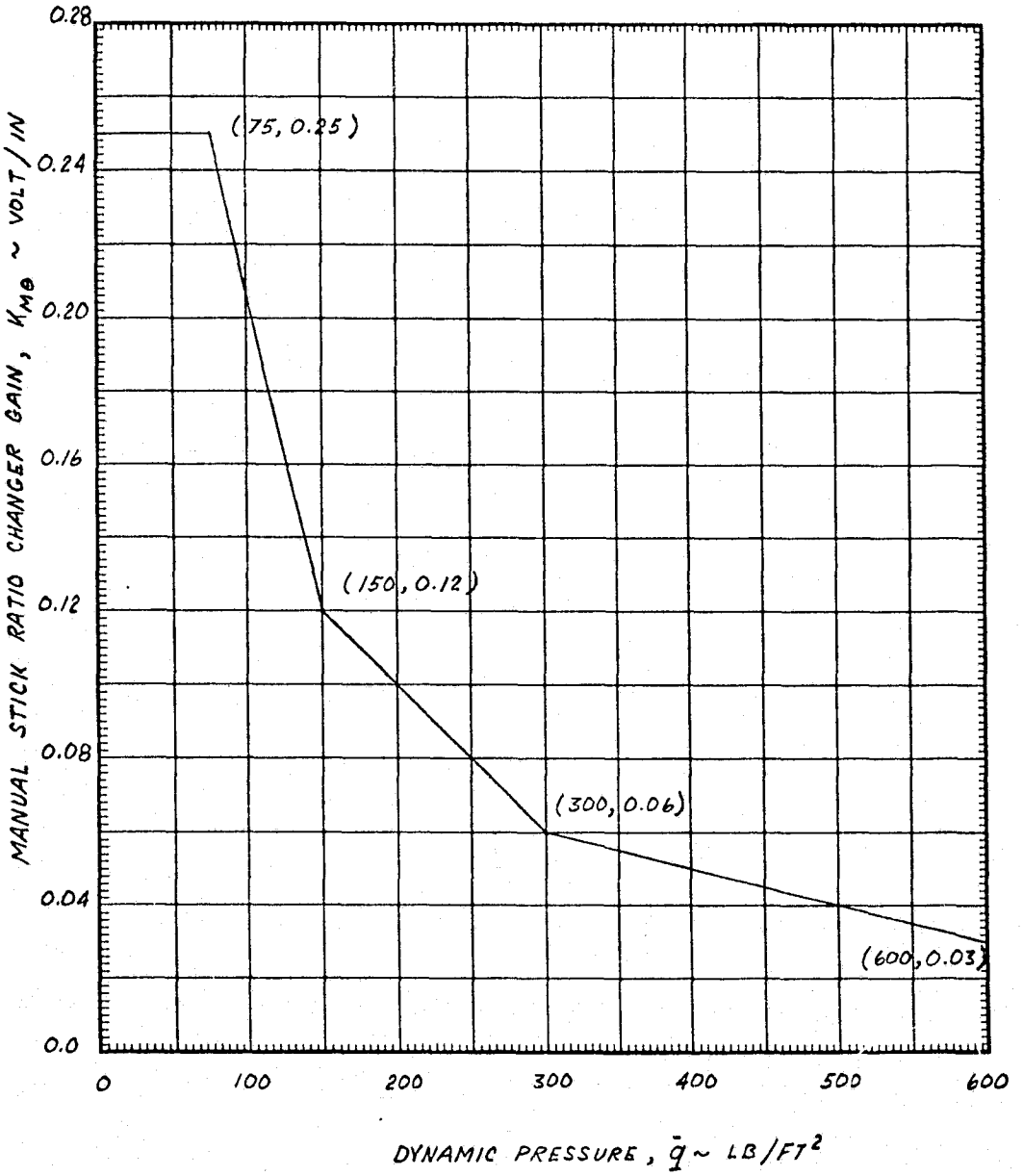

FIGURE 2-4

MANUAL CONTROL SYSTEM PARAMETERS

K_H	Stabilator Gain	20.0 deg/volt
K_A	Aileron Gain	15.0 deg/volt
K_R	Rudder Gain	15.0 deg/volt
DB_θ	Pitch Stick Deadband	0.05 in.
DB_ϕ	Roll Stick Deadband	0.05 in.
DB_ψ	Pedal Deadband	0.05 in.
$LM_{M\theta}$	Manual Stick Transducer Limit	4.0 in.
$LM_{M\phi}$	Manual Roll Stick Transducer Limit	3.5 in.
$LM_{M\psi}$	Manual Pedal Transducer Limit	2.5 in.
$K_{M\theta}$	Manual Pitch Stick Gain	Schedule
$K_{M\phi}$	Manual Roll Stick Gain	0.2857 volts/in.
$K_{M\psi}$	Manual Pedal Gain	0.40 volts/in.
$LM_{TM\theta}$	Pitch Manual Trim Limit	0.5 volts
$LM_{TM\phi}$	Roll Manual Trim Limit	0.5 volts
$LM_{TM\psi}$	Yaw Manual Trim Limit	0.5 volts
$K_{TM\theta}$	Manual Pitch Trim Gain	0.1 volts/sec
$K_{TM\phi}$	Manual Roll Trim Gain	0.1 volts/sec
$K_{TM\psi}$	Manual Yaw Trim Gain	0.1 volts/sec
$K_{Y\phi}$	Sideforce/Roll Interconnect	0.21

FIGURE 2-5

BLOCK DIAGRAM REPRESENTATION

OF TYPICAL INTEGRATOR OUTPUT LIMIT

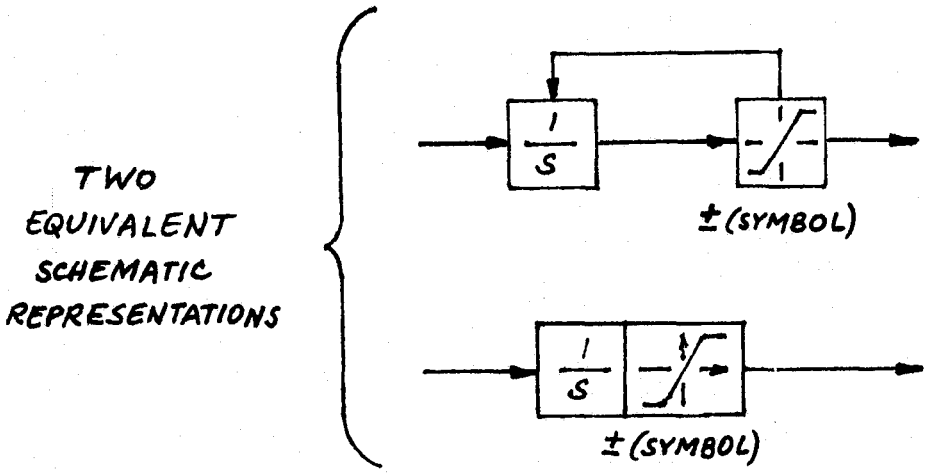

3. CONTROL AUGMENTATION SYSTEM

The Control Augmentation System (CAS) uses stabilization networks, controllers, and feedback elements. They are all integrated to enhance the aircraft's flying qualities and to minimize the pilot's work load. In this report each of the three CAS control axes is described separately, with separate diagrams, parameter definitions, and scheduled gains.

The CAS roll axis control diagram is presented in Figure 3-1. Two of the gains, the forward loop gain ($K_{c\phi}$) and the rate feedback gain (K_p), are scheduled as function of commanded thrust vector angle (θ_J). The two schedules are plotted in Figures 3-2 and 3-3. All other gains, deadbands, and limits are constants, tabulated in Figure 3-4.

Parameter $\delta_{I\phi}$ is the pilot's stick input parameter for roll and $ITRIM_\phi$ is the trim signal. The roll feedback rate and angle are p and ϕ. The output signal $\delta_{CAS\phi}$ is sent to the manual control system, Figure 2-1. The attitude command discrete, I_{ATT}, is set automatically as function of forward airspeed, u_B, as shown in Figure 3-1. At low airspeeds, below 30 knots, I_{ATT} is set to unity and this switches the appropriate CAS functions to attitude command mode. At higher airspeeds, above 40 knots, I_{ATT} is set to zero and consequently CAS is switched to rate command mode.

Pitch CAS, Figure 3-5, accepts pilot's stick input, $\delta_{I\theta}$, and pilot's switch signals $ITRIM_\theta$ and $ICAS_\theta$. $ITRIM_\theta$ controls the pitch trim and $ICAS_\theta$ engages or disengages the CAS functions in pitch.

In addition to pilot's inputs, the pitch CAS accepts the pitch rate (q), pitch angle (θ), normal load factor (n_z), and airplane angle of attack (α) feedback signals. Also, the commanded thrust vector angle input (θ_J) is used to schedule one forward branch gain ($K_{C\theta}$) and two feedback gains (K_q and K_{NO}). The schedule for one of the feedback gains (K_{NO}) is defined on the same page with pitch CAS diagram (Figure 3-5), the other two schedules are presented in Figures 3-6 and 3-7. Forward branch gain K_S is scheduled as function of feedback "reference angle of attack" (α_R)

FIGURE 3-1
ROLL CAS

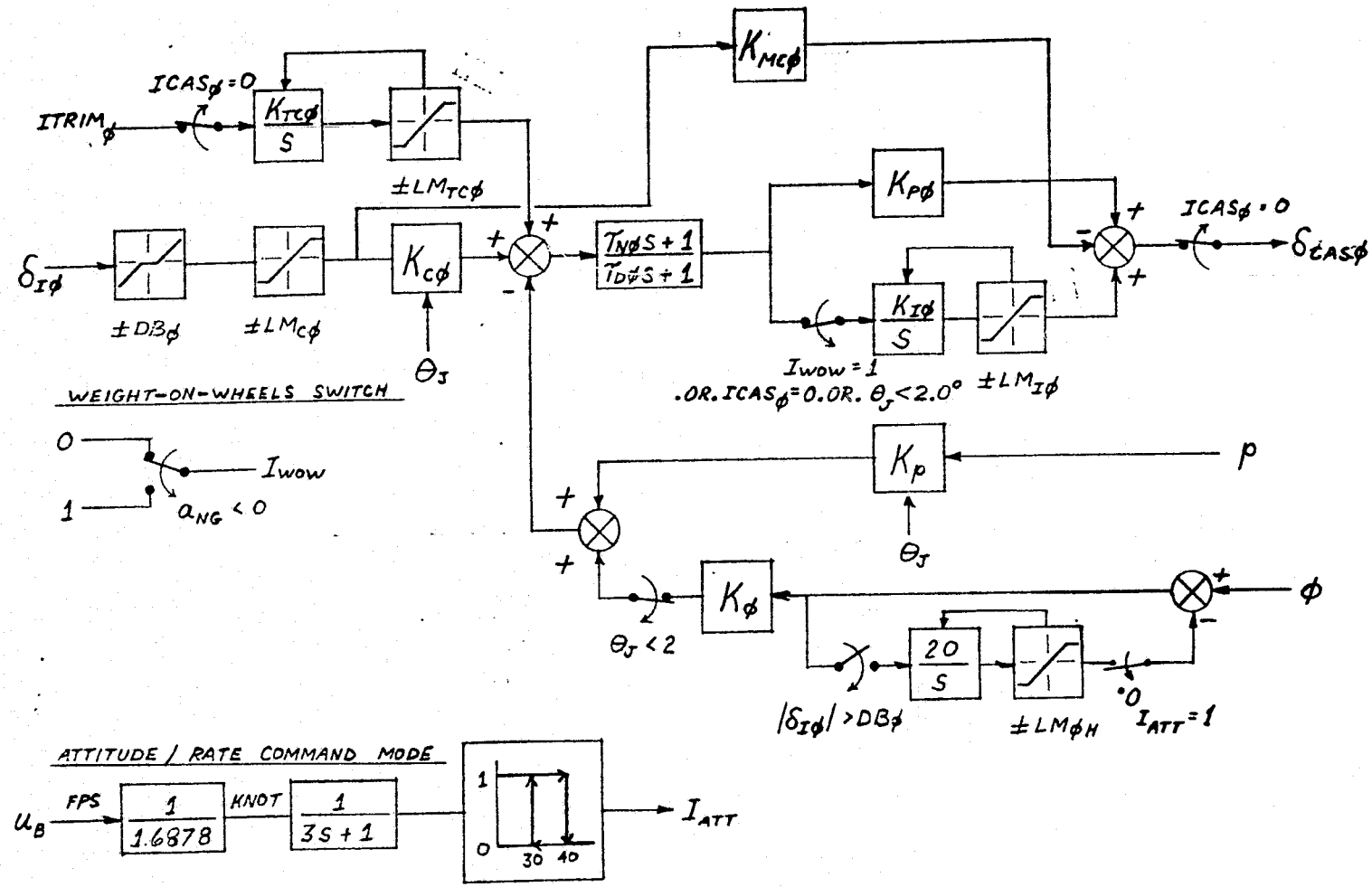

FIGURE 3-2

ROLL CAS FORWARD LOOP GAIN

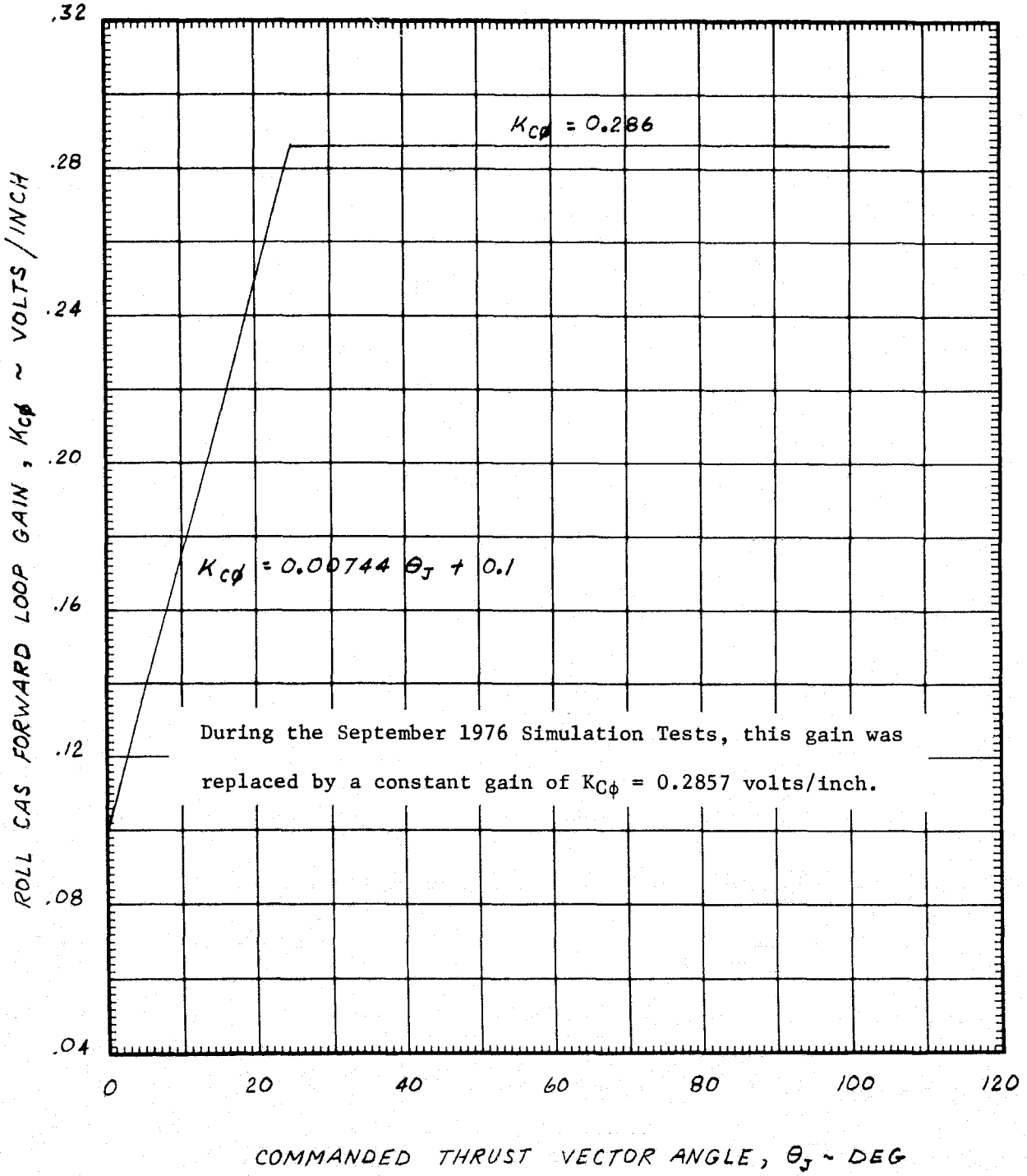

FIGURE 3-3

ROLL RATE FEEDBACK GAIN

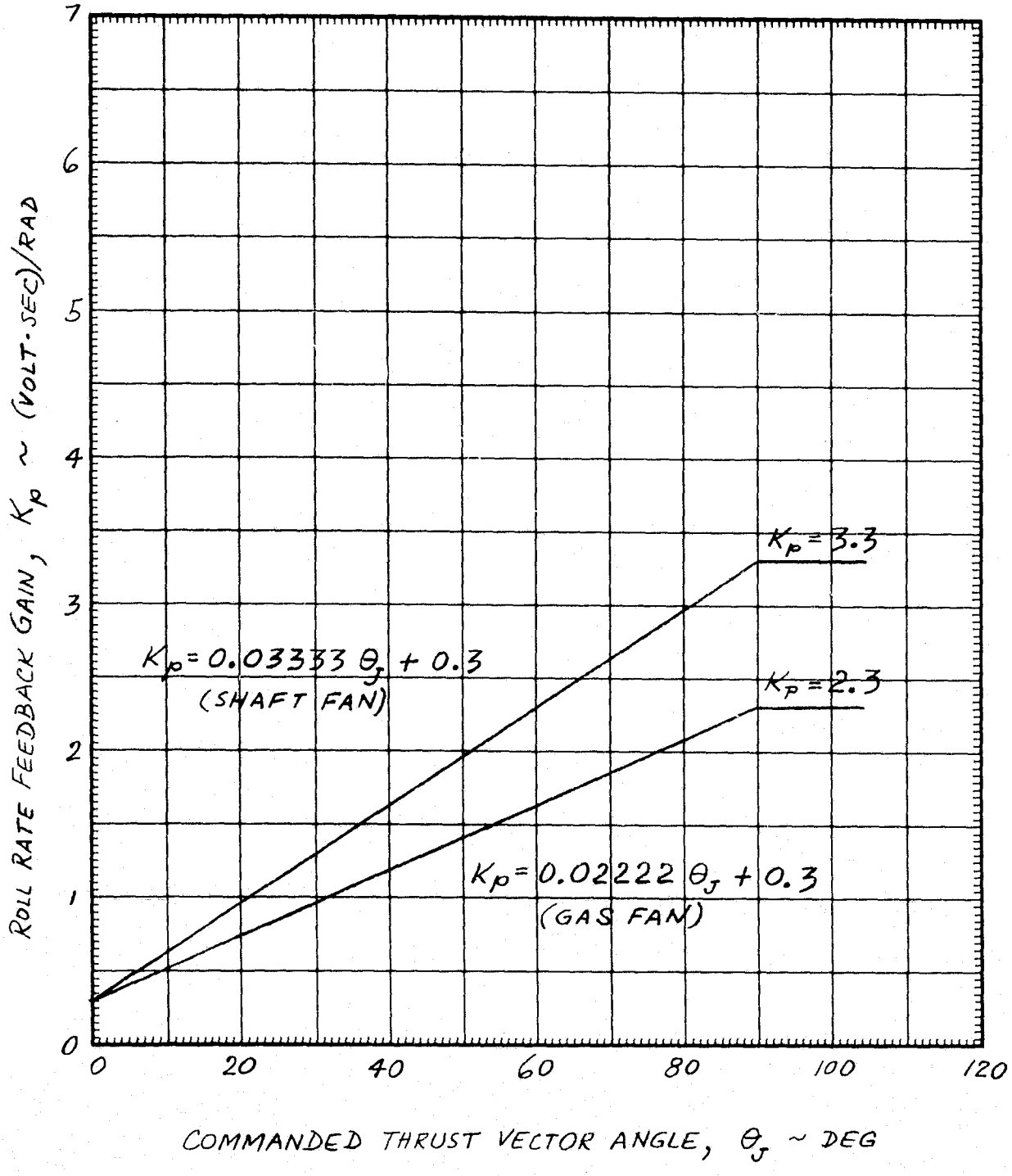

FIGURE 3-4

ROLL CAS PARAMETERS

DB_ϕ	Lateral Stick Deadband	0.05 in.
$LM_{c\phi}$	Lateral Stick CAS Transducer Limit	3.5 in.
$K_{c\phi}$	Transducer Forward Loop Gain	Schedule
K_p	Roll Rate Feedback Gain	Schedule
K_ϕ	Bank Angle Feedback Gain (Shaft) (Gas)	2.9 Volt/Rad 2.0 Volt/Rad
$LM_{\phi H}$	Roll Attitude Hold Limit	0.7854 Rad
$K_{TC\phi}$	CAS Trim Rate Gain	0.1 Volt/sec
$LM_{TC\phi}$	CAS Trim Limit	0.5 Volt
$\tau_{N\phi}$	Compensation Filter Numerator	0.0
$\tau_{D\phi}$	Compensation Filter Denominator	0.0
$K_{P\phi}$	Controller Proportional Gain	1.0
$K_{I\phi}$	Controller Integrator Gain	1.0 sec^{-1}
$LM_{I\phi}$	Integrator Limit	2.0 Volts
$K_{MC\phi}$	Manual Roll Stick Gain	0.2857 volt/inch

FIGURE 3-5
PITCH CAS

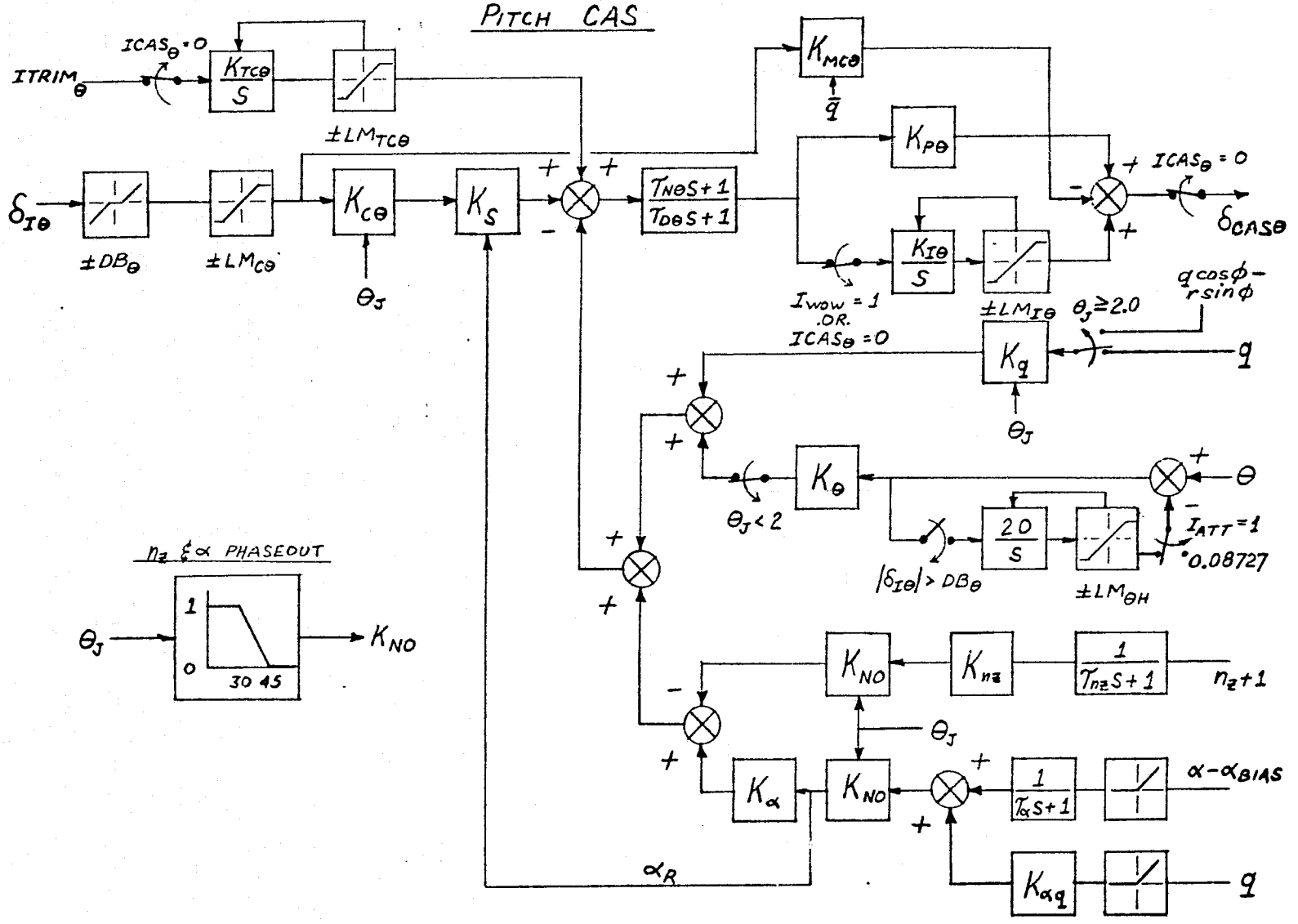

FIGURE 3-6

PITCH CAS FORWARD LOOP GAIN

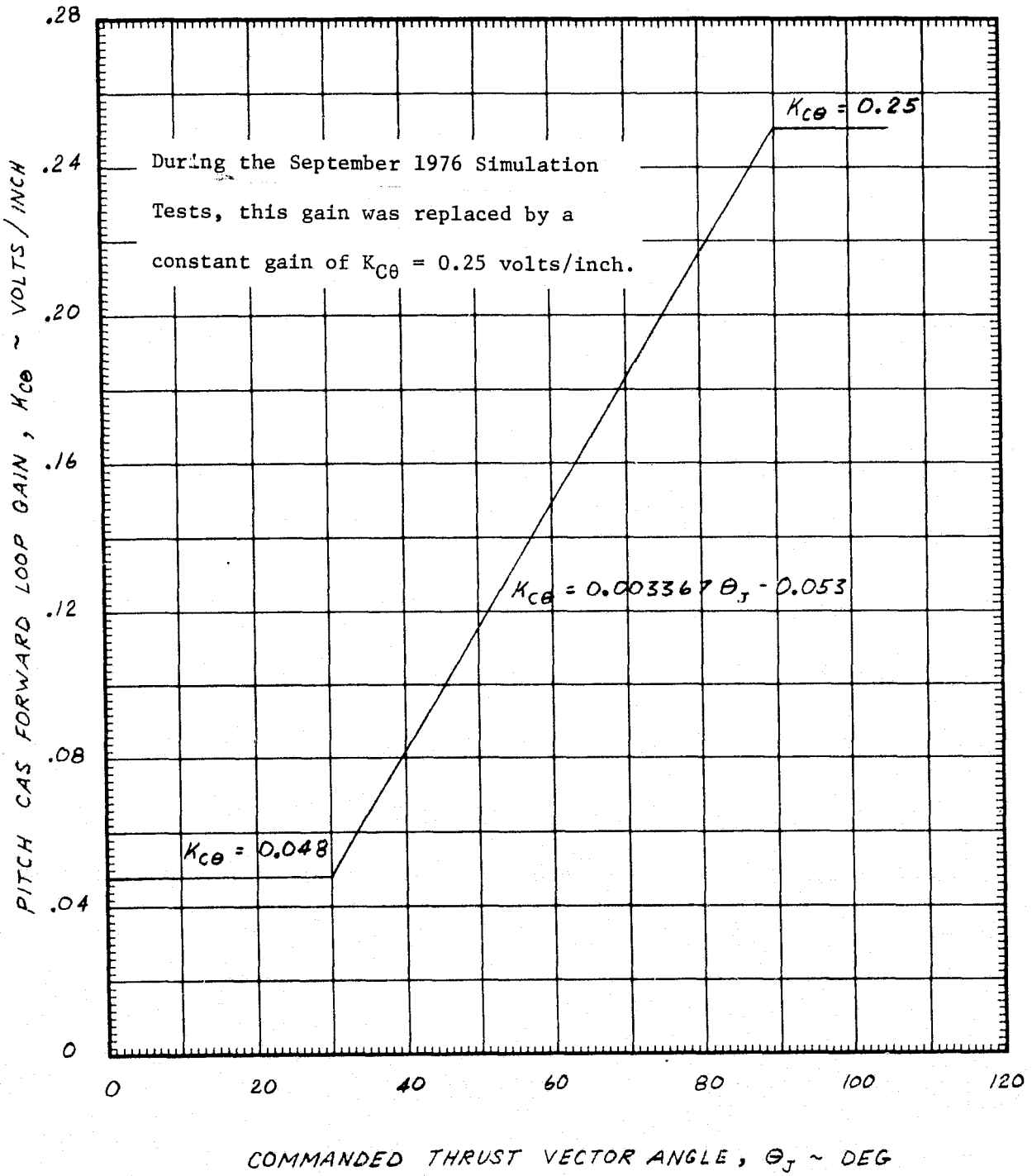

FIGURE 3-7

PITCH RATE FEEDBACK GAIN

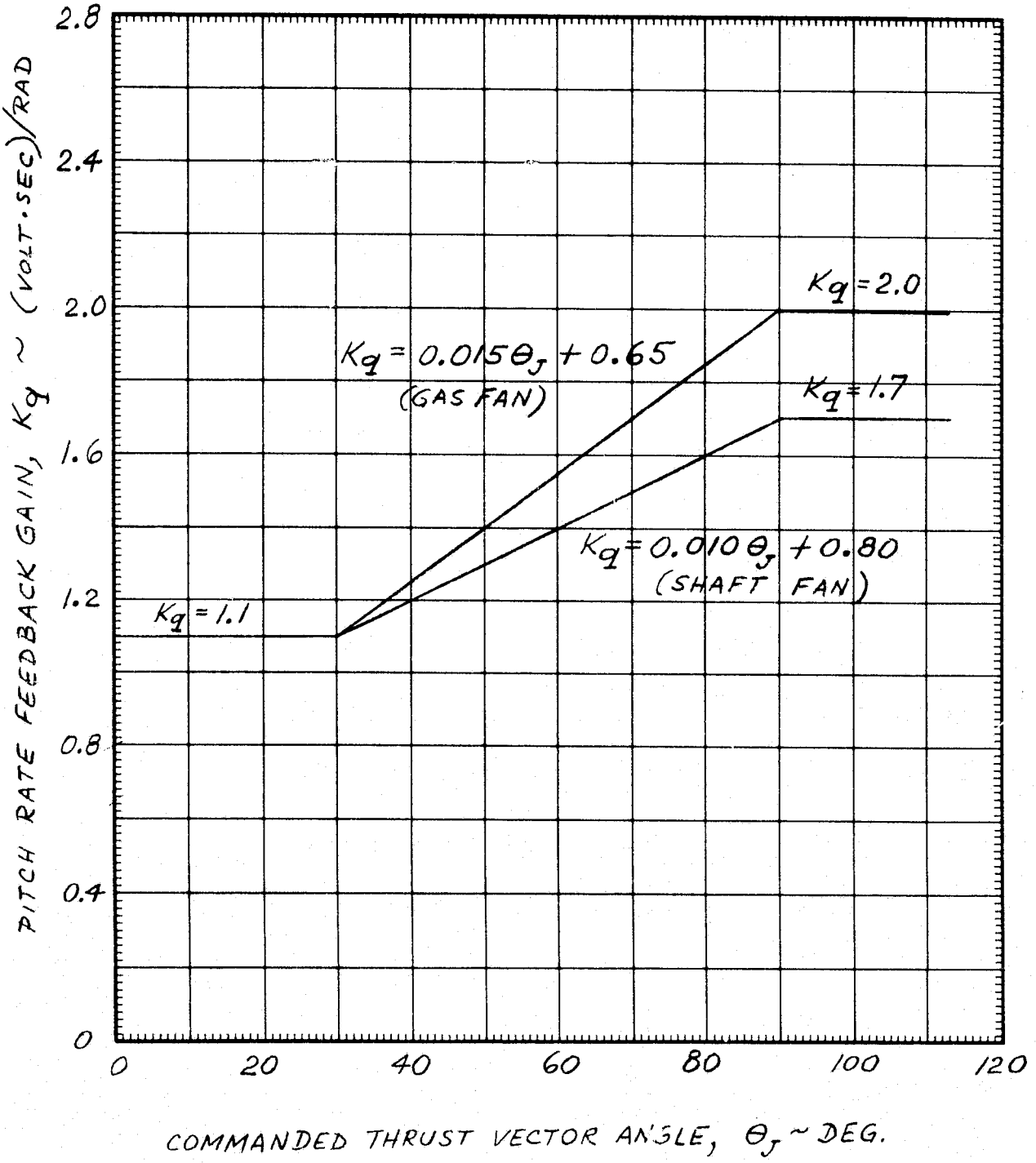

as depicted in Figure 3-8. Gain $K_{MC\theta}$ is scheduled as function of dynamic pressure ($\bar{q}$), using the same schedule as gain $K_{M\theta}$ in Section 2. All other pitch CAS parameters are constants tabulated in Figure 3-9.

The pitch CAS serves to augment the aircraft's pitch flying qualities and, through scheduled gain K_S, to reduce the chance of inadvertently developing excessive airplane angle of attack. The output, $\delta_{CAS\theta}$, generated by pitch CAS is utilized as one of the inputs into the manual control system presented in Figure 2-1.

The yaw augmentation part of CAS is depicted in block diagram form in Figure 3-10. Similarly to roll and pitch channels, the yaw CAS inputs from the pilot are the pedal deflection, $\delta_{I\psi}$, and the switch signals $ITRIM_{\psi}$ and $ICAS_Y$. The discrete inputs I_{ATT} and I_{WOW} are generated as shown in Figure 3-1. I_{ATT} selects either rate command mode or attitude command mode, depending on aircraft forward velocity. I_{WOW} is unity when aircraft's weight is supported by its wheels and zero when aircraft is flying. The forward loop gain $K_{c\psi}$, is plotted as function of θ_J in Figure 3-11. The feedback gains K_r amd K_v are also scheduled as function of commanded thrust vector angle, θ_J, using the schedules plotted in Figures 3-12 and 3-13, respectively. All other yaw CAS gains, deadbands, and limits have constant values tabulated in Figure 3-14.

The parameters used as yaw CAS feedbacks are the yaw rate, r, the lateral load factor, n_y, and side velocity, v_B. The yaw CAS output signal is $\delta_{CAS\psi}$; it is used as one of the inputs into the manual control system, shown in Figure 2-1.

FIGURE 3-8

STALL PREVENTER GAIN

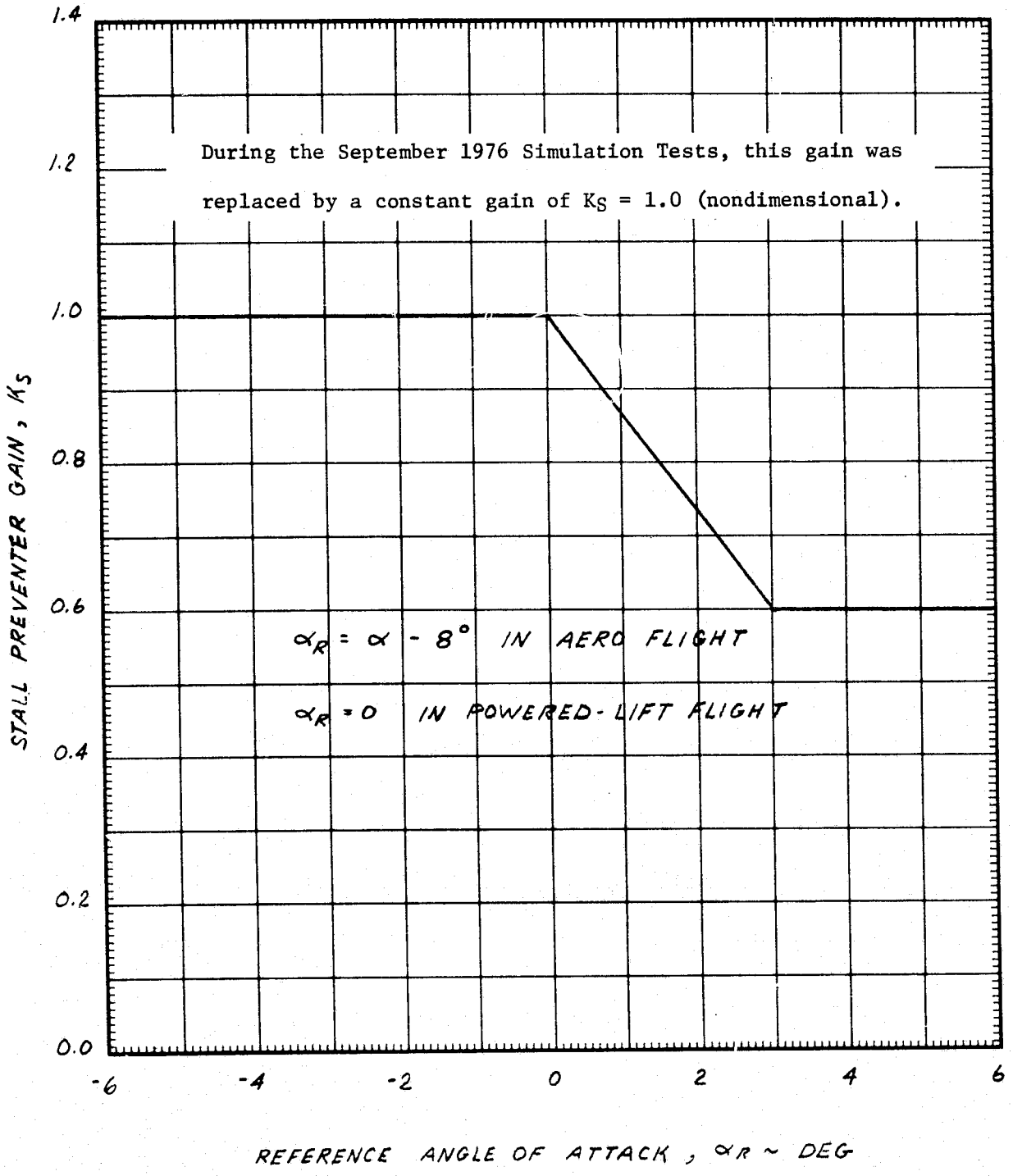

FIGURE 3-9

PITCH CAS PARAMETERS

DB_θ	Longitudinal Stick Deadband	0.05 in.
$LM_{c\theta}$	Longitudinal Stick CAS Transducer Limit	4.0 in.
$K_{c\theta}$	Transducer Forward Loop Gain	Schedule
K_q	Pitch Rate Feedback Gain	Schedule
K_θ	Pitch Attitude Feedback Gain (Shaft)	1.7 volt/rad
	(Gas)	2.0 volt/rad
$LM_{\theta H}$	Pitch Attitude Hold Limit	0.7854 rad
K_{nz}	Normal Acceleration Feedback Gain	0.09 volt/g
τ_{nz}	Normal Acceleration Filter Constant	0.0
K_α	Angle of Attack Feedback Gain	0.0
τ_α	Angle of Attack Filter Constant	0.0
$K_{\alpha q}$	Pitch Rate Anticipation Gain	0.0
K_S	Stall Preventor Gain	Schedule
α_{BIAS}	Stall Preventor α Bias	8.0 Deg
$K_{TC\theta}$	CAS Trim Rate Gain	0.1 volt/sec
$LM_{TC\theta}$	CAS Trim Limit	0.5 volt
$K_{MC\theta}$	Manual Pitch Stick Gain	Schedule
$\tau_{N\theta}$	Compensation Filter Numerator	0.0
$\tau_{D\theta}$	Compensation Filter Denominator	0.0
$K_{P\theta}$	Controller Proportional Gain	1.0
$K_{I\theta}$	Controller Integrator Gain	1.0 sec^{-1}
$LM_{I\theta}$	Integrator Limit	2.0 volts

FIGURE 3-10
YAW CAS

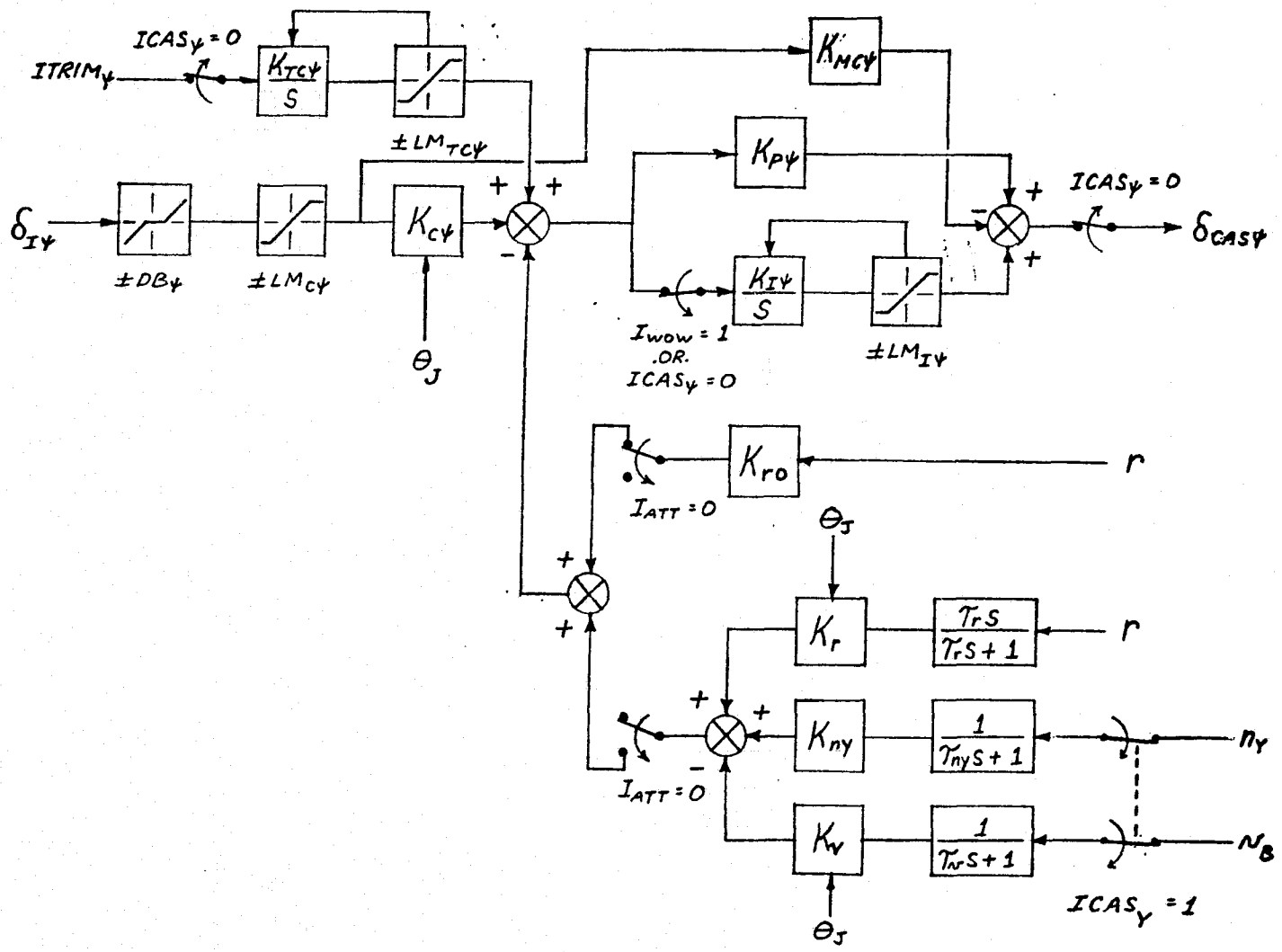

FIGURE 3-11

YAW CAS FORWARD LOOP GAIN

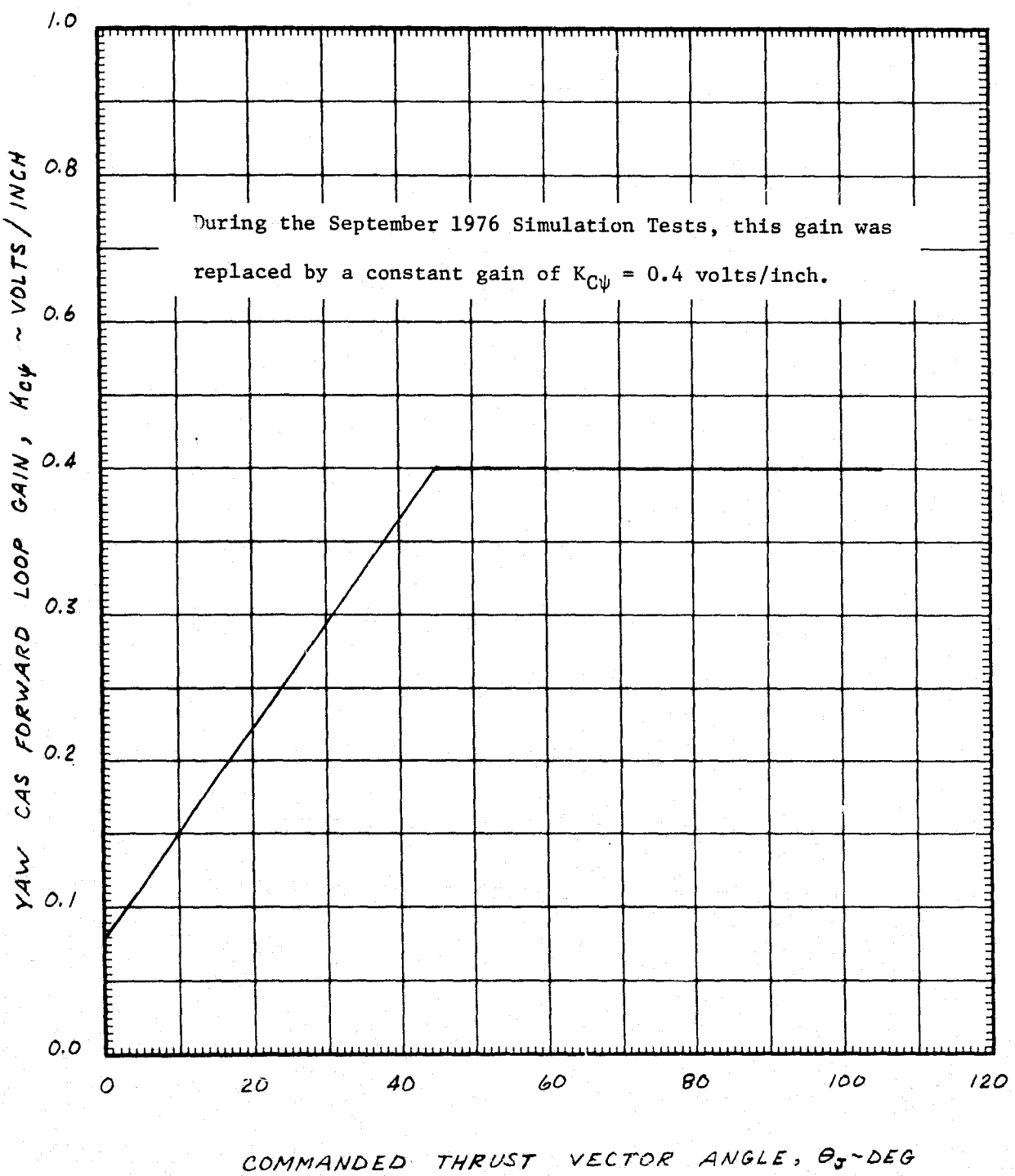

FIGURE 3-12

YAW RATE FEEDBACK GAIN

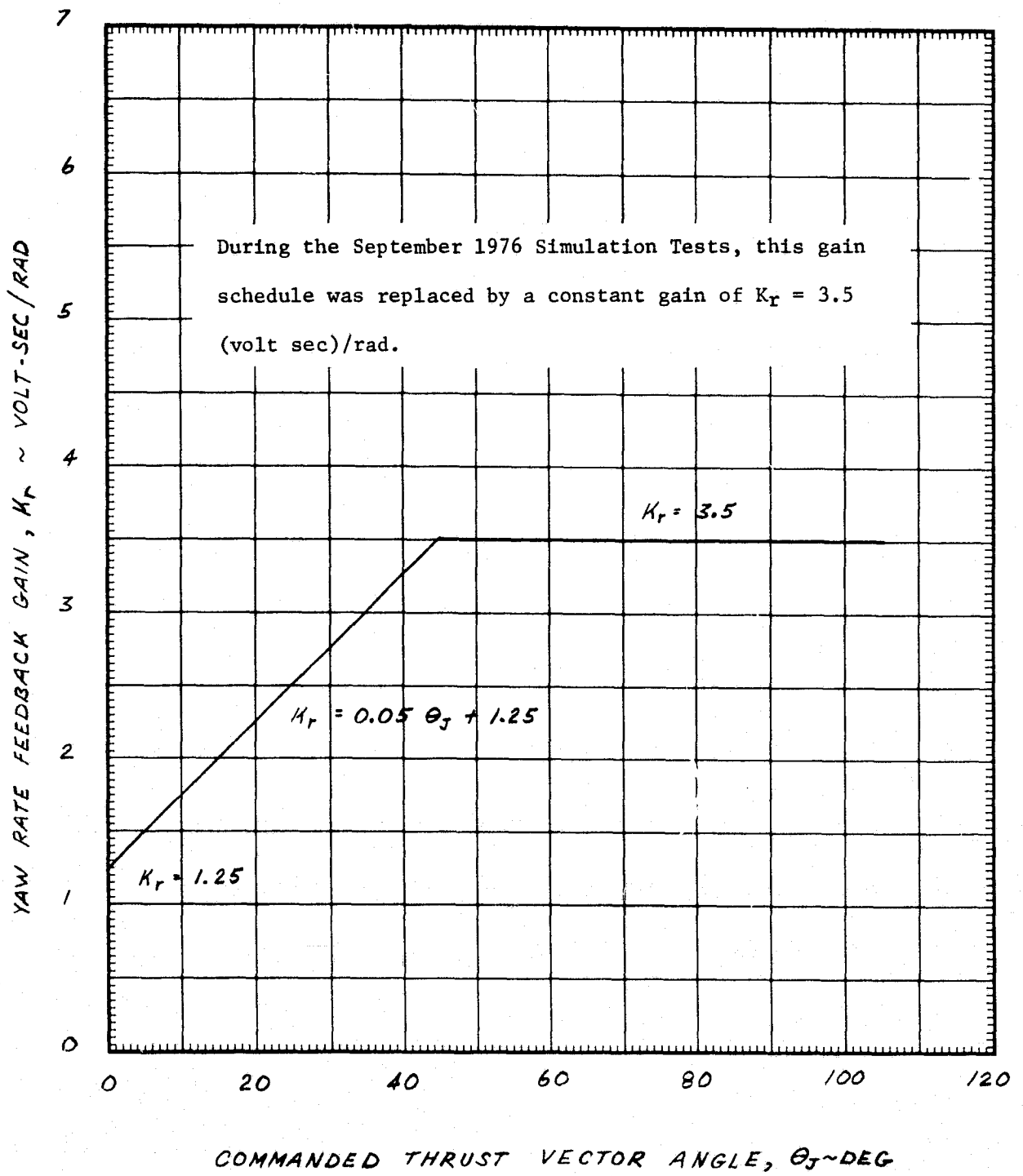

FIGURE 3-13

SIDE VELOCITY FEEDBACK GAIN

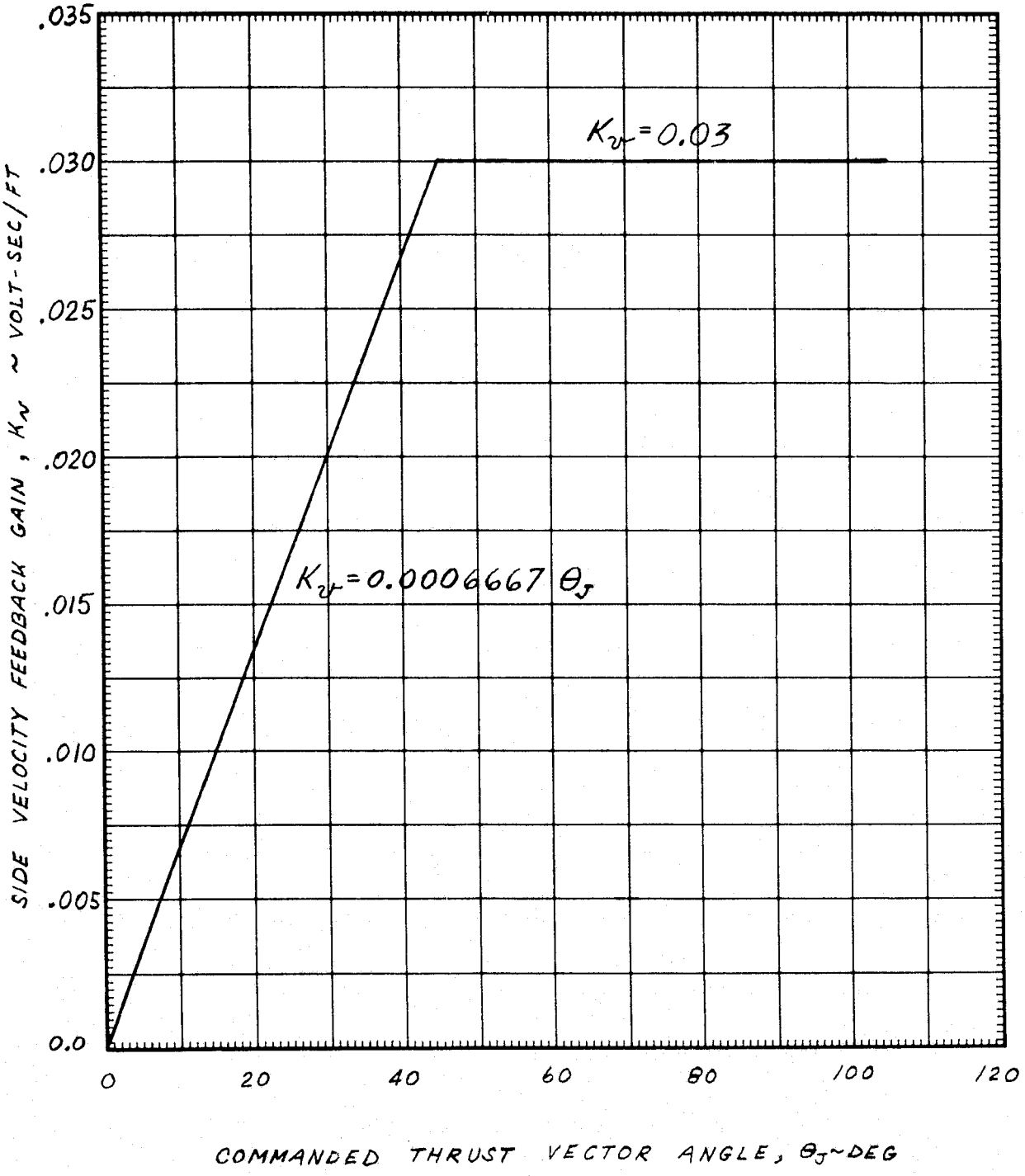

FIGURE 3-14

YAW CAS PARAMETERS

DB_ψ	Rudder Pedal Deadband	0.05 in.
$LM_{c\psi}$	Rudder Pedal CAS Transducer Limit	2.5 in.
$K_{c\psi}$	Transducer Forward Loop Gain	Schedule
K_{ro}	Hover Yaw Rate Gain	1.25 volt-sec/rad
K_r	Yaw Rate Feedback Gain	Schedule
τ_r	Yaw Rate Washout Time Constant	2.0 sec.
K_{ny}	Lateral Acceleration Feedback Gain	0.6 volt/g
K_v	Side Velocity Feedback Gain	Schedule
τ_{ny}	Lateral Acceleration Filter Constant	0.0
τ_v	Side Velocity Filter Constant	0.0
$K_{TC\psi}$	CAS Trim Rate Gain	0.1 volt/sec
$LM_{TC\psi}$	CAS Trim Limit	0.5 volt
$K_{P\psi}$	Controller Proportional Gain	1.0
$K_{I\psi}$	Controller Integrator Gain	1.0 sec^{-1}
$LM_{I\psi}$	Integrator Limit	2.0 volts
$K_{MC\psi}$	Manual Pedal Gain	0.4 volts/inch

4. SECONDARY CONTROLS

Secondary flight controls are used by the pilot less frequently than the primary flight controls. The secondary controls control the flaps, landing gear and fan doors. The actual aircraft will use a separate fan door actuator for each of the two lift cruise fans, however, in the simulation one lift/cruise door actuator math model is considered sufficient. The block diagrams of all secondary control actuators are presented in Figure 4-1 and the associated constants are tabulated in Figure 4-2.

The inputs to flap and landing gear actuators are switch positions set by the pilot. The input to fan door actuators is also provided by a switch, but this switch is activated by the thrust vector command signal (θ_J). In vertical takeoff and in hover the fan doors are fully open, with δ_{DOORL} and $\delta_{DOORL/C}$ both at unity values. When the commanded thrust vector angle decreases below 2.0 degrees the door actuator switch reverses its position and all three fan doors start closing at a maximum rate. Conversely, if the lift/cruise fan doors are initially closed they start opening at the maximum rate when the commanded thrust vector angle exceeds 2.0 degrees.

FIGURE 4-1
SECONDARY CONTROLS

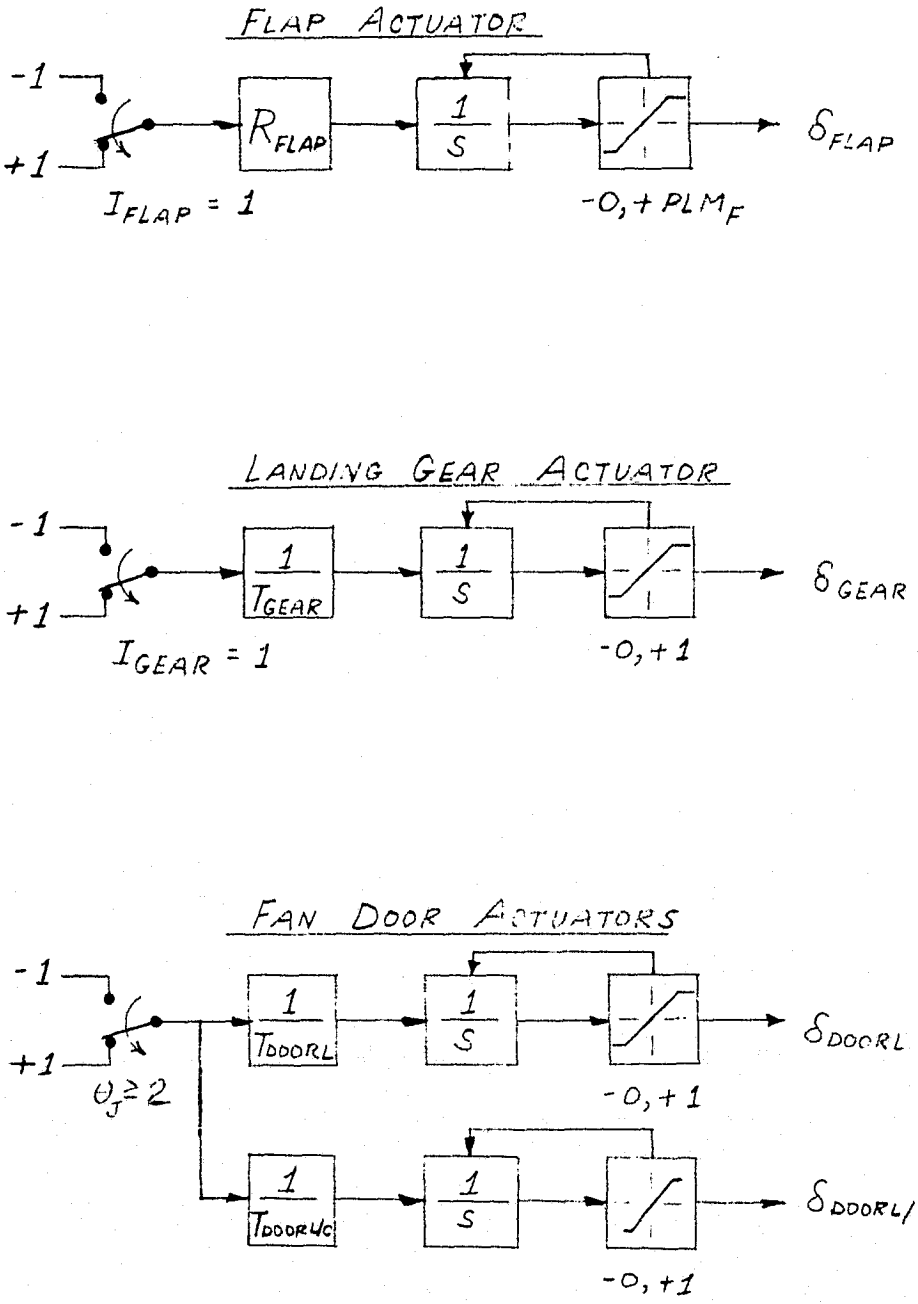

FIGURE 4-2

SECONDARY CONTROL SYSTEM PARAMETERS

PLM_F	Flap Extension Limit	25.0 deg
R_{FLAP}	Flap Extension Rate	2.5 deg/sec.
T_{GEAR}	Time Req'd for Gear Extension	4.0 sec.
T_{DOORL}	Lift Fan Door Open/Close Time	1.0 sec.
$T_{DOORL/C}$	Lift/Cruise Fan Door Open/Close Time	1.0 sec.

5. AERODYNAMIC SURFACE CONTROLS

The block diagrams for aerodynamic control surface actuators are presented in Figure 5-1. The roll, pitch, and yaw control inputs to the actuators (δ_{AI}, δ_{HI}, δ_{RI}) are generated as shown in the manual control system block diagram of Figure 2-1.

The aerodynamic roll control is achieved with left and right aileron actuators shown at top of Figure 5-1. The two aileron actuators are shown connected such that they can also be used as drooped ailerons, thus adding to the lifting power generated by the flaps.

The diagram of the stabilator actuator shows two inputs: (1) a regular command signal, δ_{HI}, from the manual control system, and (2) an input which is scheduled as a function of the commanded thrust vector angle, θ_J. Again, for the current simulation math model, the input scheduled as function of θ_J is set to zero. However, the capability for non-zero scheduled input is shown in Figure 5-1 and is intended to be used, if necessary, to compensate for any potential force disturbances which may be acting on the horizontal tail and vary as function of thrust vector angle. No such force or moment disturbances are included in the current simulation model.

Other gains and limits used in the aerodynamic controls diagram are constant and are tabulated in Figure 5-2.

FIGURE 5-1

AERODYNAMIC CONTROL SURFACES

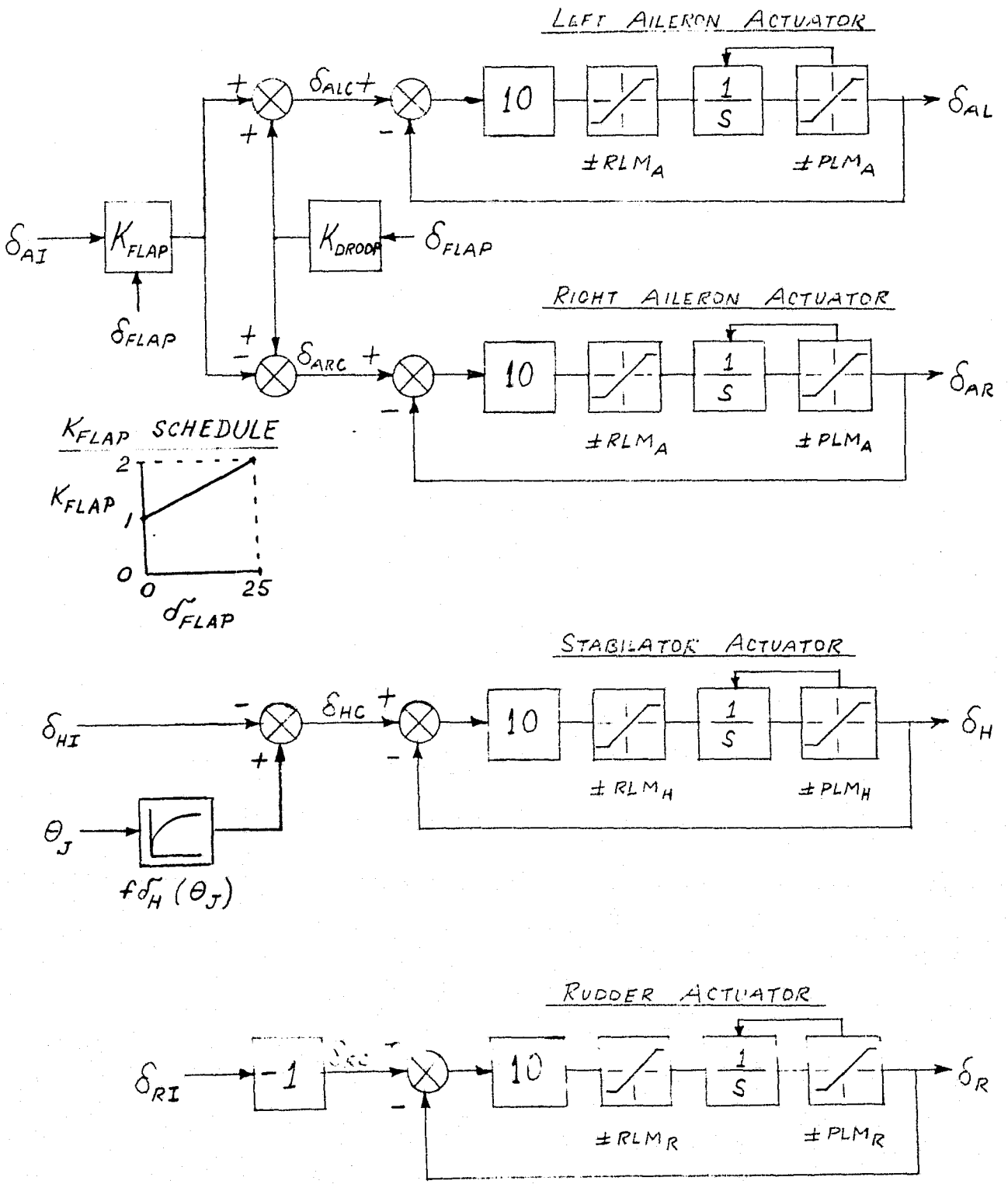

FIGURE 5-2

AERODYNAMIC CONTROL SURFACE PARAMETERS

PLM_A	Aileron Actuator Position Limit	30.0 deg
PLM_H	Stabilator Actuator Position Limit	30.0 deg
PLM_R	Rudder Actuator Position Limit	30.0 deg
RLM_A	Aileron Actuator Rate Limit	150.0 deg/sec
RLM_H	Stabilator Actuator Rate Limit	25.0 deg/sec
RLM_R	Rudder Actuator Rate Limit	100.0 deg/sec
K_{DROOP}	Flap-Aileron Interconnect Gain	0.6 (nondimensional)
K_{FLAP}	Aileron Gain	Schedule
$f_{\delta_H}(\theta_J)$	Stabilator Bias Vs. Vector Angle	0.0 deg

6. POWERED-LIFT YAW CONTROL SYSTEM

In powered-lift flight the yaw moments on the aircraft are produced by lateral deflections of fan thrust. The lateral thrust deflections are generated by yaw vanes which are located under each of the three fans. After transition to aerodynamic flight, the yaw vanes are used to close or partially close the fan exhaust nozzles in order to provide a streamlined configuration for aerodynamic flight. A diagram of yaw vane controls is presented in Figure 6-1.

The inputs to the powered-lift yaw control system are the pilot's side force switch position signal (δ_{IY}) and the yaw signal (δ_{ψ}) from the manual control system. The aircraft side velocity, v_B, is used as the feedback to the system. The main outputs are the three yaw vane deflections: γ_1 and γ_2 represent respectively the left and right lift-cruise fan vane deflections, and γ_3 is the forward fan yaw vane angle. In addition, the system generates the side force command signal, δ_Y, which produces an additional yaw vane deflection increment, for side force, and δ_Y is also fed back into the roll loop of the manual control system (Figure 2-1).

The constants used in the yaw vane control diagram are tabulated in Figure 6-2.

FIGURE 6-1
YAW VANE CONTROLS

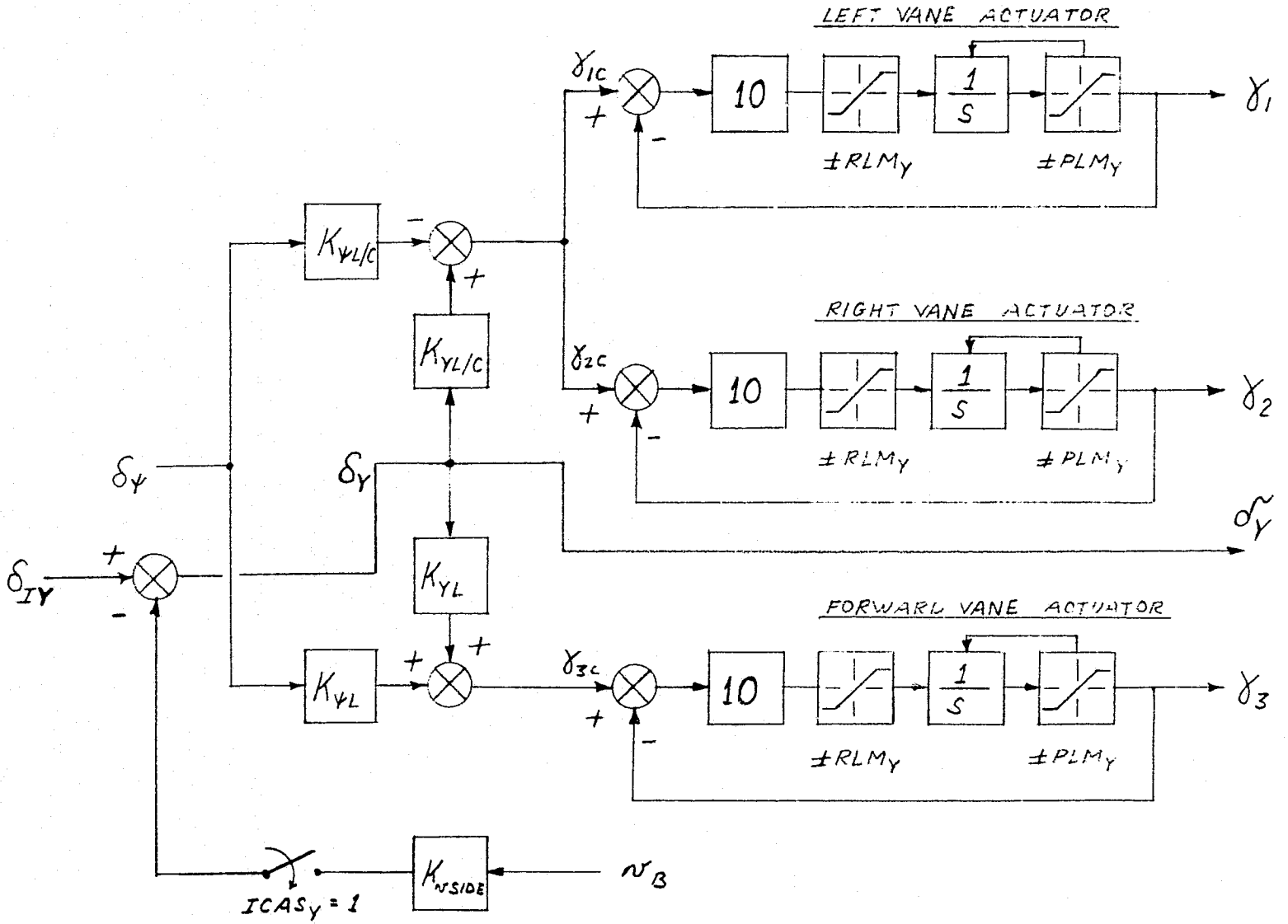

FIGURE 6-2

YAW VANE CONTROL PARAMETERS

PLM_Y	Yaw Vane Actuator Position Limit	10.0 deg
RLM_Y	Yaw Vane Actuator Rate Limit	100.0 deg/sec
$K_{\psi_{L/C}}$	L/C Yaw Vane Yaw Input Gain	5.0 deg/volt
K_{ψ_L}	Lift Fan Yaw Vane Yaw Input Gain	10.0 deg/volt
$K_{Y_{L/C}}$	L/C Yaw Vane Sideforce Gain	6.0 deg/volt
K_{Y_L}	Lift Fan Yaw Vane Sideforce Gain	6.0 deg/volt
$K_{v_{SIDE}}$	Sideforce CAS Velocity Feedback	0.012 volt-sec/ft

7. POWERED-LIFT PITCH AND ROLL CONTROL SYSTEM

In powered-lift flight all the main pitch and roll control moments are generated by incremental variations in total fan thrust. In gas-coupled fan configuration the thrust of individual fans is varied by changing the angles of ETaC valves and by changing the Thrust Reduction Modulation (TRM) with louver angles or port openings. In shaft-coupled configuration the fan thrust modulation is achieved by changing the pitch angle of the fan blades.

The diagrams and data for gas-coupled configuration are presented first. The diagram in Figure 7-1 shows how the pitch control (δ_ϕ) and roll control (δ_θ) signals (from Manual Control System) are used to modulate the three ETaC valves: θ_{V1}, θ_{V2}, and θ_{V3}. The next diagram, Figure 7-2, depicts schematically the Thrust Reduction Modulation Controls. In this diagram the lift/cruise fan signals, σ_1 and σ_2, represent the size of the thrust reduction port openings located near the top of the lift/cruise nozzle. By varying the size of the lift/cruise TRM port openings the corresponding fan thrust is varied, thus providing the necessary modulation for roll and pitch control. This is the only fan thrust modulation required for roll control; however, for pitch control the forward fan thrust also has to be modulated.

The forward fan TRM signal, σ_3 in Figure 7-2, physically represents an incremental change in forward fan louver angles which in turn modulate the forward fan thrust. The combined thrust variations of the forward fan and of the two lift/cruise fans provide the necessary control moments for aircraft pitch control.

The constants used in the above two diagrams are listed in Figure 7-3. Figures 7-4 through 7-15 present the remaining functions needed to define all computations in pitch and roll control diagrams for powered-lift flight. In some cases the graphical representation of applicable functions can not be plotted with sufficient accuracy desired for digital simulation. In these cases each plot is followed by figures which list the numerical values of the coordinates used to prepare the plot.

FIGURE 7-1

ENERGY TRANSFER AND CONTROL (ETaC) CONTROLS

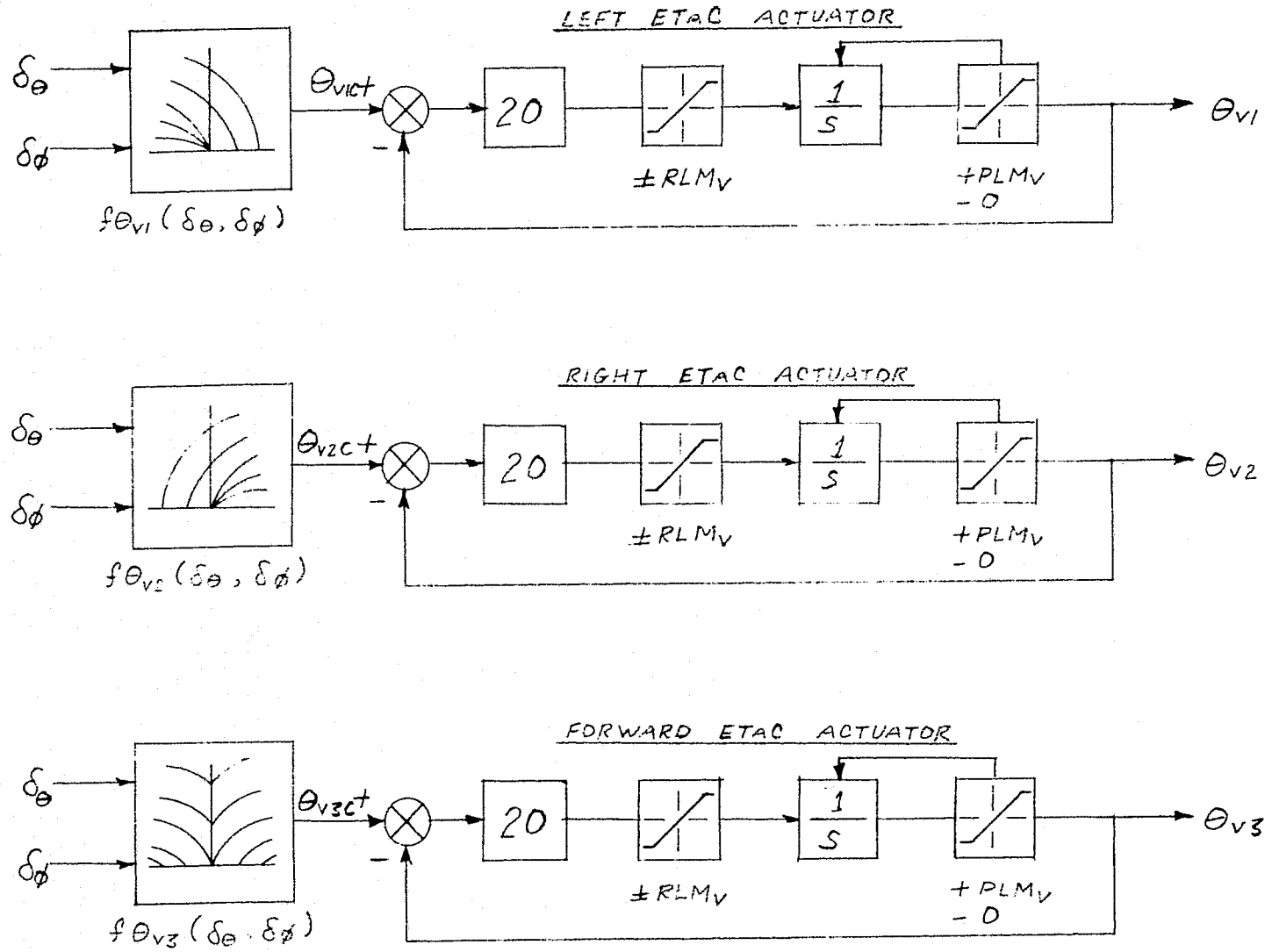

FIGURE 7-2
THRUST REDUCTION MODULATION (TRM) CONTROLS

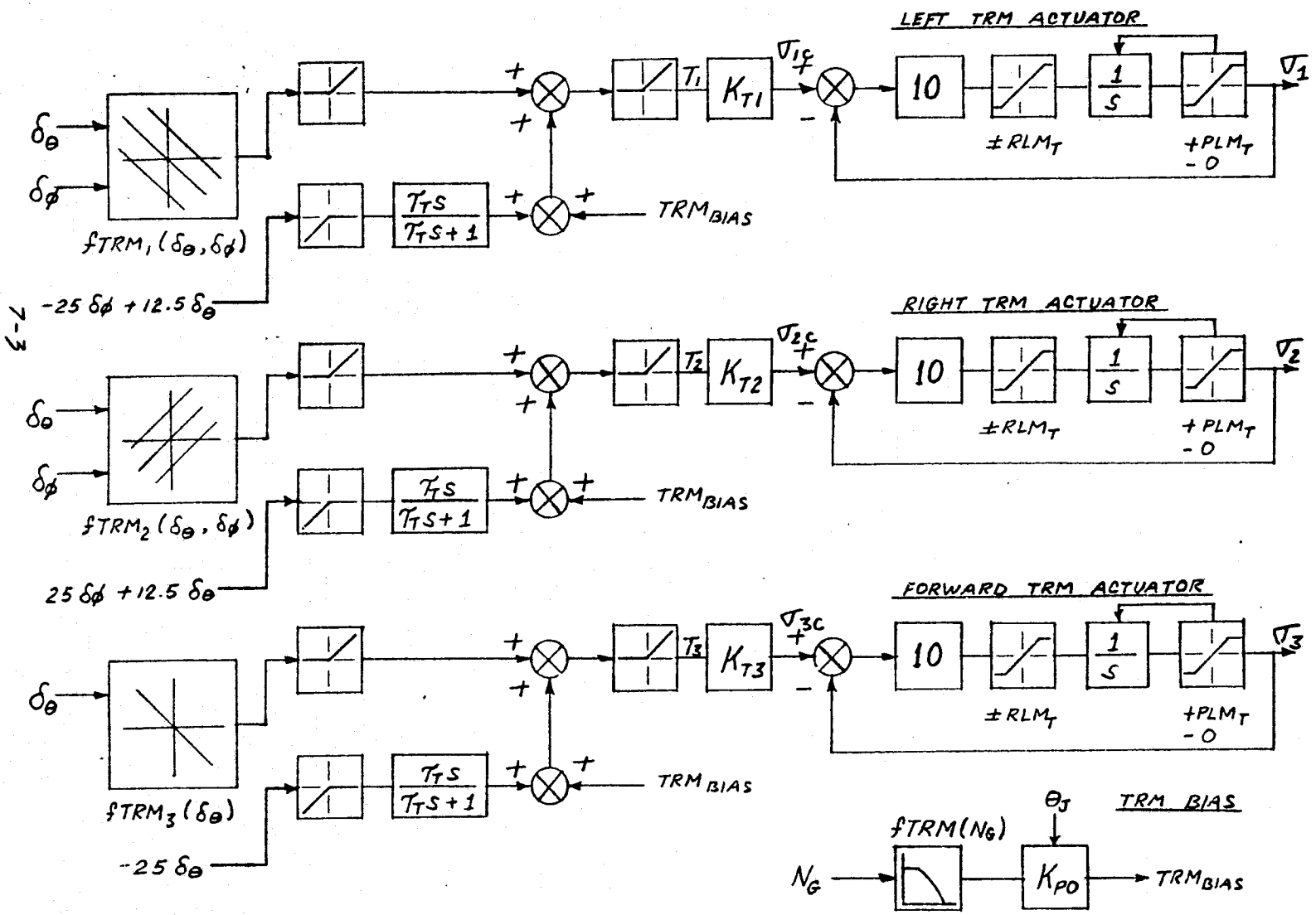

FIGURE 7-3

ETaC AND TRM PARAMETERS

PLM_V	ETaC Valve Actuator Position Limit	40.0 deg
RLM_V	ETaC Valve Actuator Rate Limit	400.0 deg/sec
PLM_T	TRM Actuator Position Limit	35.0 deg
RLM_T	TRM Actuator Rate Limit	350.0 deg/sec
K_{T1}	Left Fan TRM Gain	1.0 deg/percent
K_{T2}	Right Fan TRM Gain	1.0 deg/percent
K_{T3}	Forward Fan TRM Gain	1.0 deg/percent
τ_T	TRM Washout Time Constant	0.3 sec

FIGURE 7-4

#1 FAN ETAC VALVE SCHEDULE

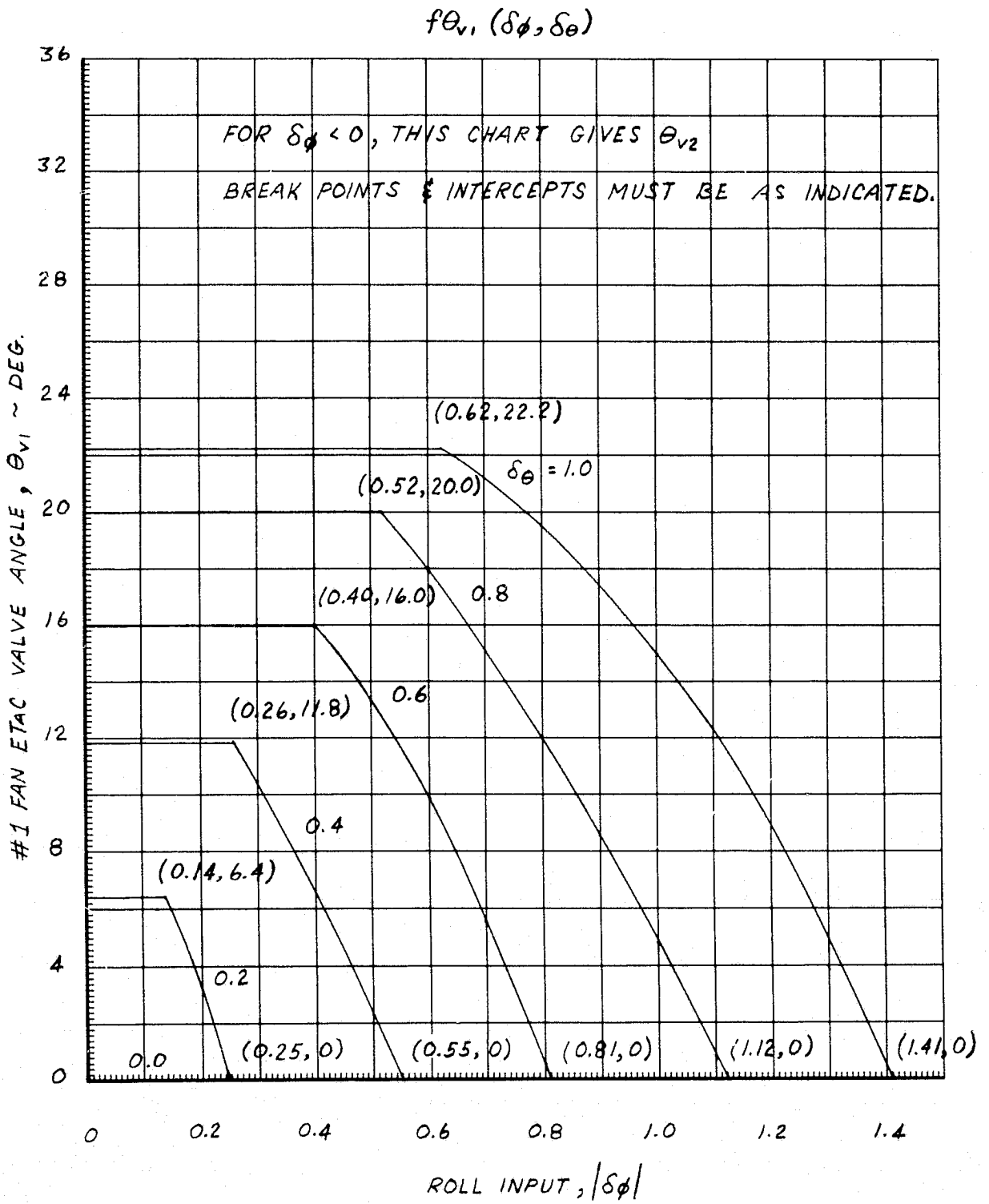

FIGURE 7-5

#1 FAN ETAC VALVE SCHEDULE DATA POINTS

θ_{V1} ~ DEGREES — $f\theta_{V1}(\delta\phi, \delta\theta)$

$\delta\theta$ \ $\lvert\delta\phi\rvert$	0.0	0.2	0.4	0.6	0.8	1.0	1.2	1.4
0.0	0.0	0.0	0.0	0.0	0.0	0.0	0.0	0.0
0.2	6.4	3.2	0.0	0.0	0.0	0.0	0.0	0.0
0.4	11.8	11.8	6.5	0.0	0.0	0.0	0.0	0.0
0.6	16.0	16.0	16.0	9.8	0.6	0.0	0.0	0.0
0.8	20.0	20.0	20.0	17.5	12.0	4.9	0.0	0.0
1.0	22.2	22.2	22.2	22.2	19.5	15.0	8.9	0.6

FOR $\delta\phi < 0$, THIS TABLE GIVES θ_{V2}.

BREAK POINTS & INTERCEPTS INDICATED IN FIGURE.

FIGURE 7-6

#2 FAN ETAC VALVE SCHEDULE

$f\theta_{V2}(\delta\phi, \delta\theta)$

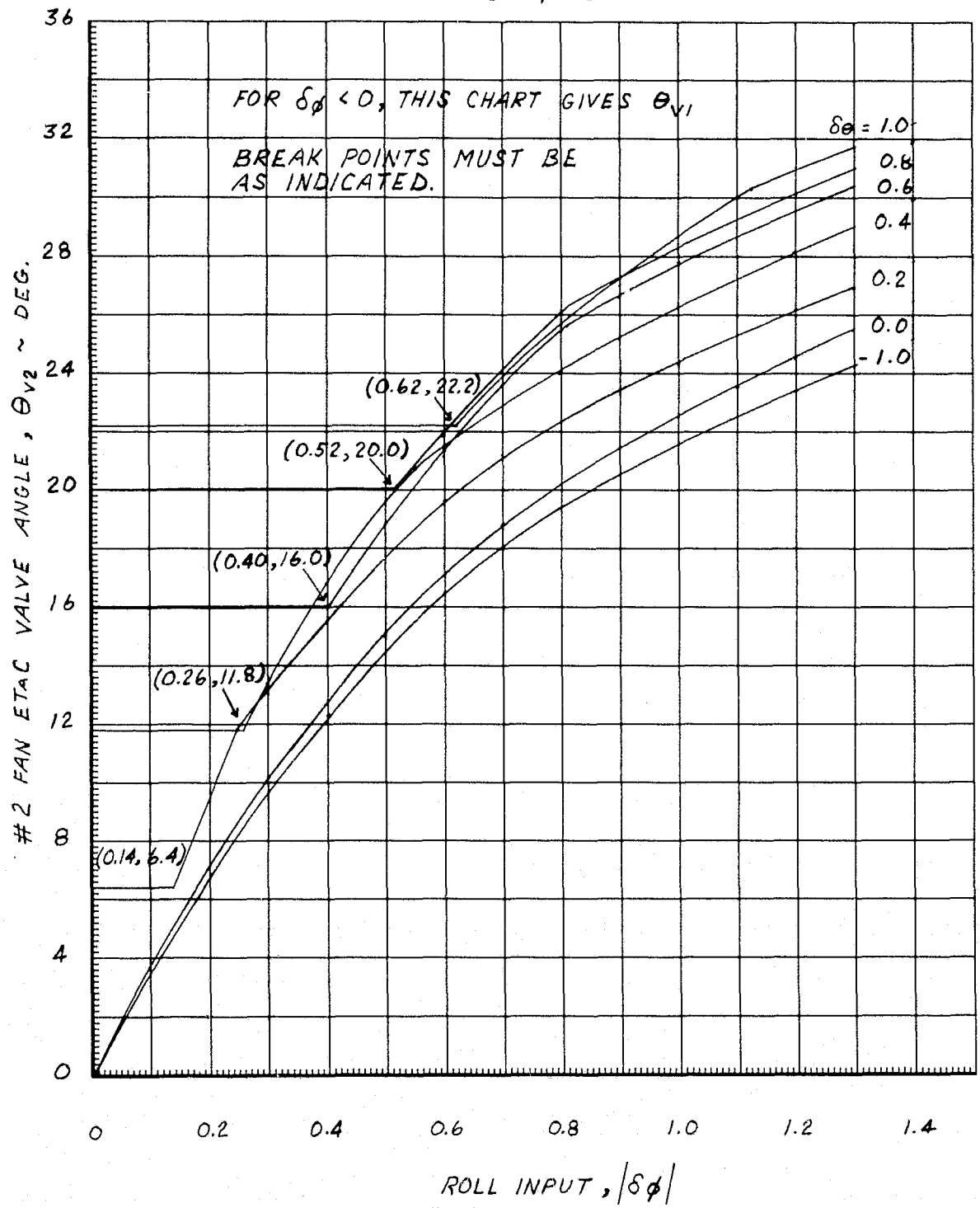

FIGURE 7-7

#2 FAN ETAC VALVE SCHEDULE DATA POINTS

θ_{V2} ~ DEGREES — $f\theta_{V2}(\delta\phi, \delta\theta)$

$\delta\theta$ \ $\delta\phi$	0.0	0.2	0.4	0.6	0.8	1.0	1.2	1.4
-1.0	0.0	6.7	12.1	16.4	19.4	21.6	23.4	25.2
0.0	0.0	7.1	12.7	17.1	20.2	22.5	24.6	26.5
0.2	6.4	9.5	15.5	19.5	22.3	24.4	26.2	27.8
0.4	11.8	11.8	16.8	21.4	24.1	26.2	28.2	30.0
0.6	16.0	16.0	16.0	21.3	25.5	27.7	29.5	30.4
0.8	20.0	20.0	20.0	22.0	26.1	28.3	30.2	31.9
1.0	22.2	22.2	22.2	22.2	25.6	28.7	30.9	32.5

FOR $\delta\phi < 0$, THIS TABLE GIVES θ_{V1}.

BREAK POINTS MUST BE AS INDICATED IN FIGURE.

FIGURE 7-8

#3 FAN ETAC VALVE SCHEDULE

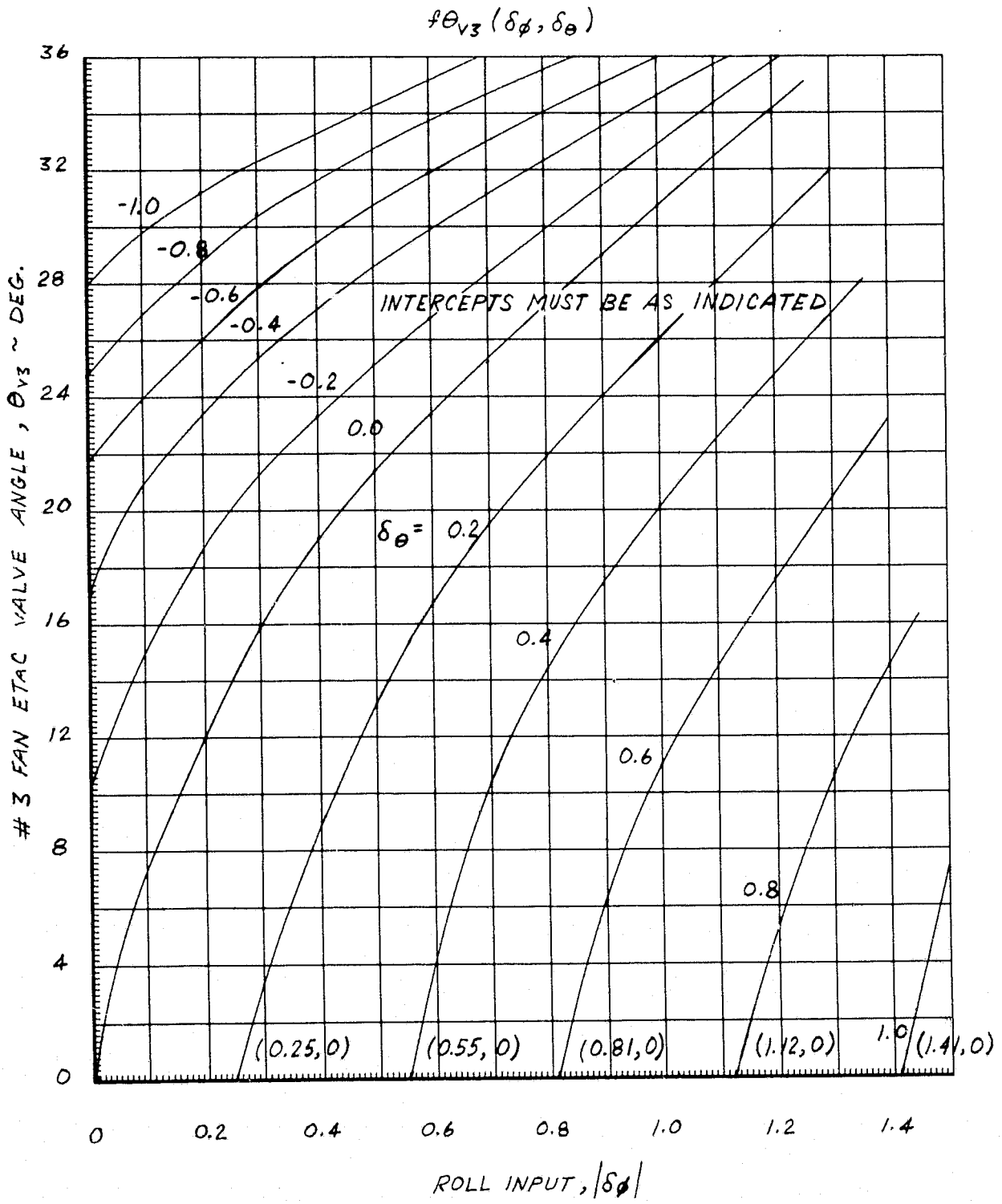

FIGURE 7-9

#3 FAN ETAC VALVE SCHEDULE DATA POINTS

θ_{V3} ~ DEGREES — $f\theta_{V3}(\delta\phi, \delta\theta)$

$\delta\theta$ \ $\delta\phi$	0.0	0.2	0.4	0.6	0.8	1.0	1.2	1.4
-1.0	28.0	31.2	33.2	35.1	37.0	38.9	40.8	42.7
-0.8	24.9	28.7	31.6	33.7	35.5	37.3	39.1	40.9
-0.6	21.8	26.0	29.4	31.9	34.0	36.0	38.0	40.0
-0.4	17.1	23.4	27.0	29.9	32.3	34.6	36.9	39.2
-0.2	10.5	18.6	23.3	26.7	29.9	32.8	35.8	38.8
0.0	0.0	12.0	19.0	23.4	27.2	30.7	34.2	37.7
0.2	0.0	0.0	8.8	16.7	21.8	26.0	30.0	34.0
0.4	0.0	0.0	0.0	4.2	14.4	20.1	24.7	29.3
0.6	0.0	0.0	0.0	0.0	0.0	11.0	17.5	23.2
0.8	0.0	0.0	0.0	0.0	0.0	0.0	5.3	10.6
1.0	0.0	0.0	0.0	0.0	0.0	0.0	0.0	0.0

INTERCEPTS MUST BE AS INDICATED IN FIGURE.

FIGURE 7-10

#1 FAN TRM SCHEDULE

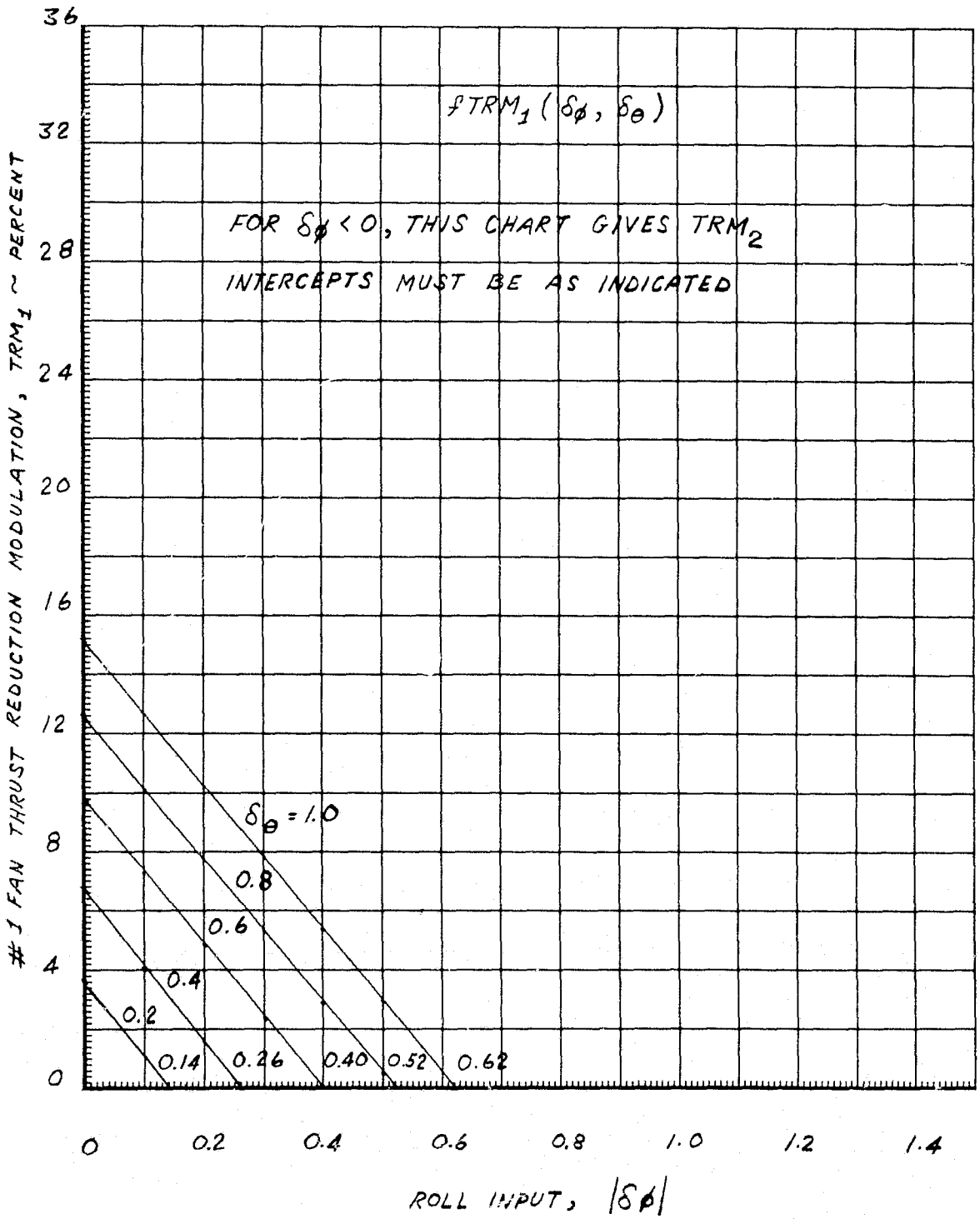

FIGURE 7-11

#1 FAN TRM SCHEDULE DATA POINTS

	TRM_1 ~ PERCENT					$fTRM_1(\delta\phi, \delta\theta)$		
$\delta\theta$ \ $\delta\phi$	0.0	0.2	0.4	0.6	0.8	1.0	1.2	1.4
0.0	0.0	0.0	0.0	0.0	0.0	0.0	0.0	0.0
0.2	3.5	0.0	0.0	0.0	0.0	0.0	0.0	0.0
0.4	6.6	1.6	0.0	0.0	0.0	0.0	0.0	0.0
0.6	9.8	4.9	0.0	0.0	0.0	0.0	0.0	0.0
0.8	12.5	7.8	3.0	0.0	0.0	0.0	0.0	0.0
1.0	15.1	10.2	5.5	0.6	0.0	0.0	0.0	0.0

FOR $\delta\phi < 0$, THIS TABLE GIVES θ_{V2}.

INTERCEPTS MUST BE AS SHOWN IN FIGURE.

FIGURE 7-12

2 FAN TRM SCHEDULE

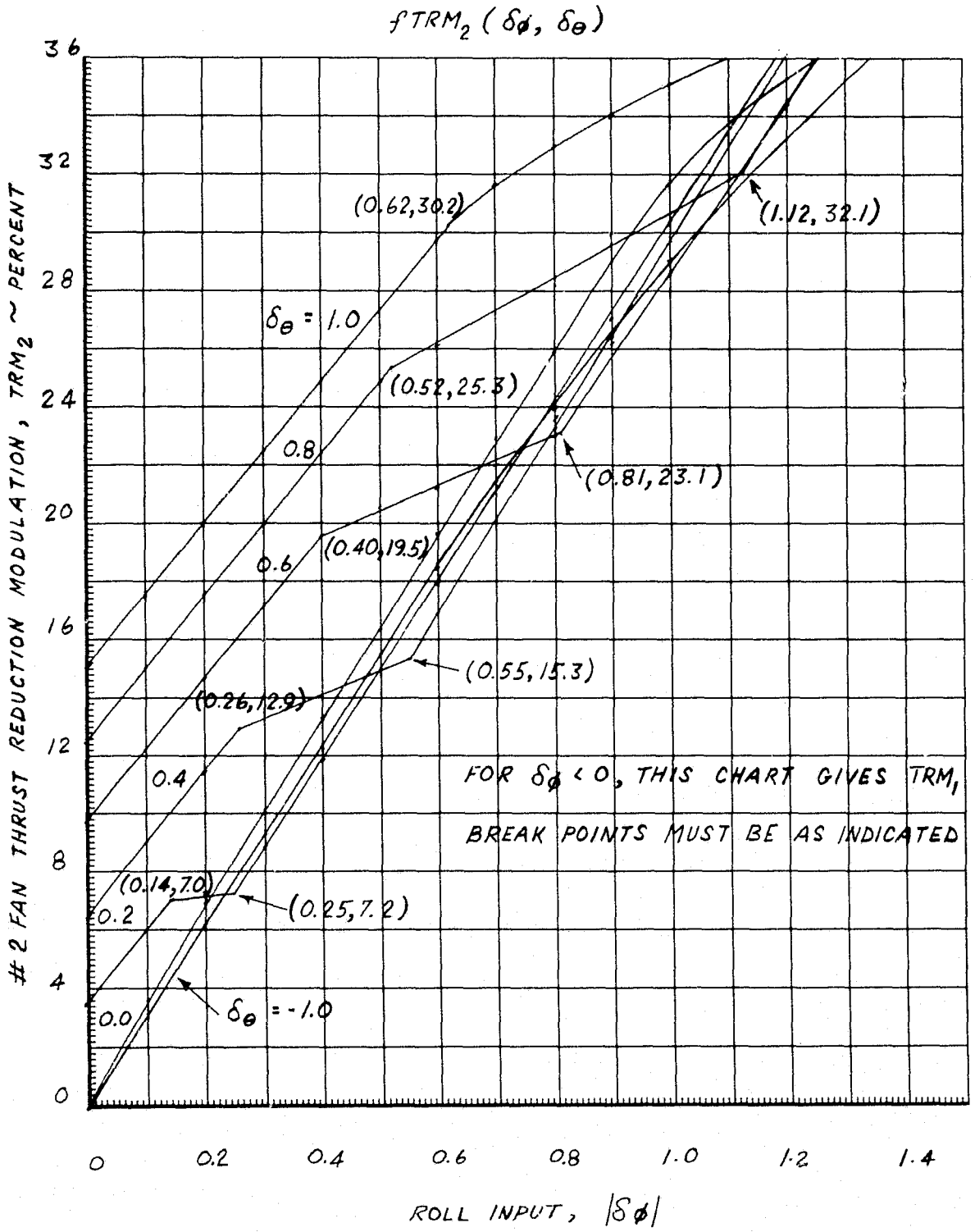

FIGURE 7-13

#2 FAN TRM SCHEDULE DATA POINTS

	TRM_2 ~ PERCENT					$fTRM_2(\delta\phi, \delta\theta)$		
$\delta\theta$ \ $\delta\phi$	0.0	0.2	0.4	0.6	0.8	1.0	1.2	1.4
-1.0	0.0	6.2	12.3	18.6	24.1	29.0	33.2	37.2
0.0	0.0	6.8	13.2	19.5	25.9	31.7	35.2	38.0
0.2	3.5	7.2	11.9	18.1	24.2	30.4	36.9	38.9
0.4	6.6	11.5	14.1	16.9	23.3	29.7	36.1	42.5
0.6	9.8	14.6	19.5	21.3	23.0	28.6	34.4	40.2
0.8	12.5	17.5	22.4	26.2	28.4	30.6	34.5	40.4
1.0	15.1	20.0	24.8	29.7	32.9	35.1	37.0	38.7

FOR $\delta\phi < 0$, THIS TABLE GIVES θ_{VI}.

BREAK POINTS MUST BE AS SHOWN IN FIGURE.

FIGURE 7-14

3 FAN TRM SCHEDULE

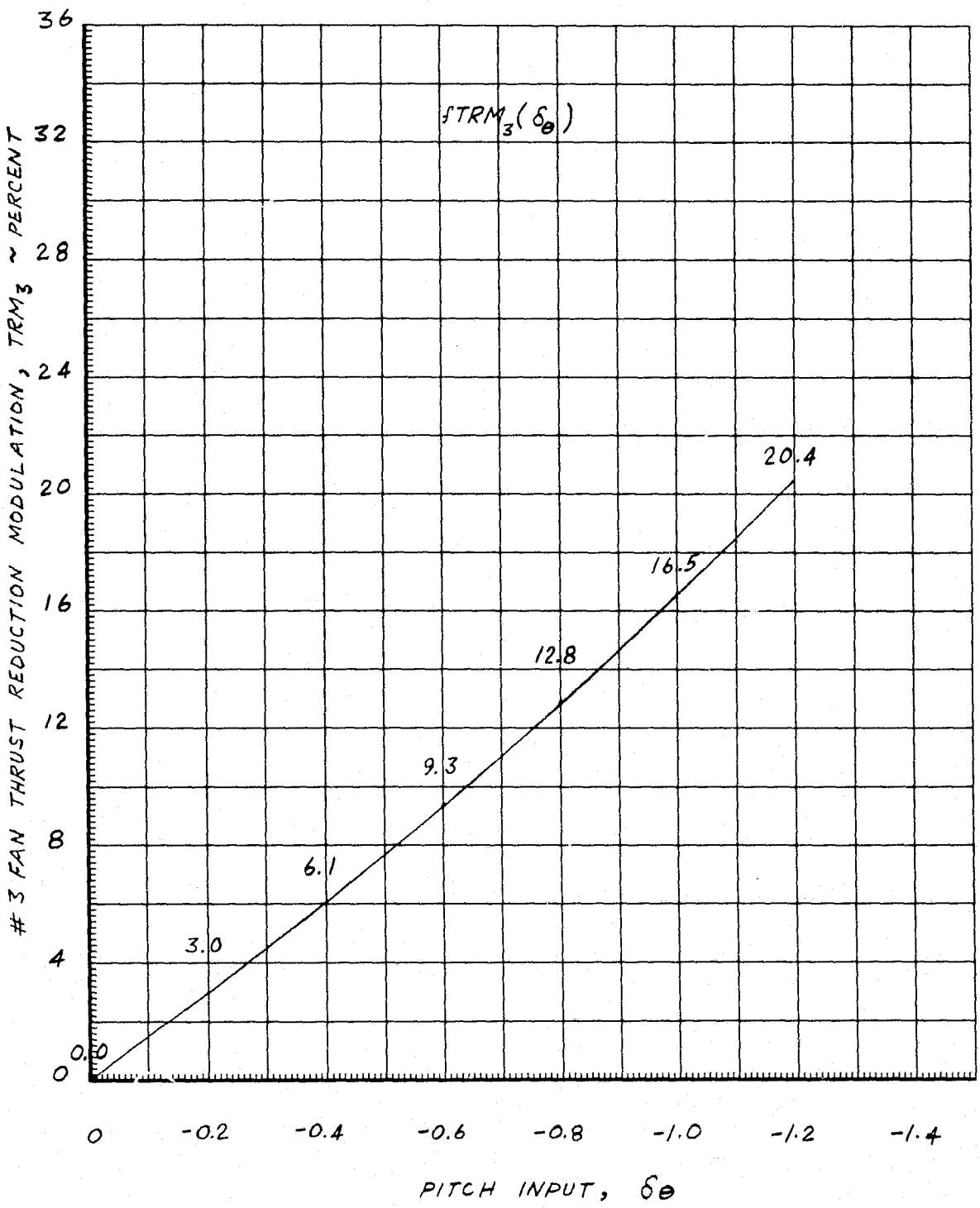

FIGURE 7-15

TRM PRESET

GAS FAN RTA

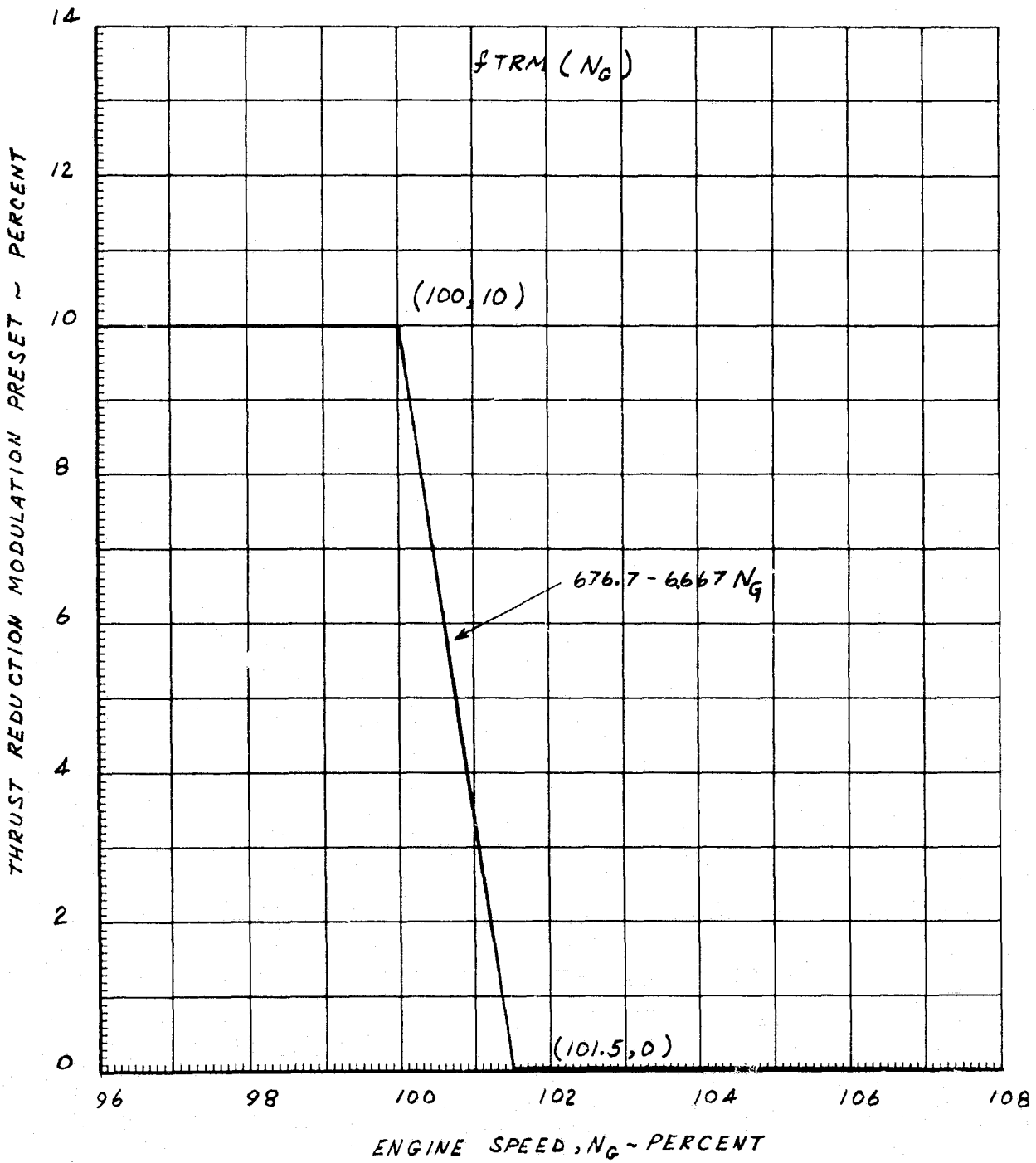

The pitch and roll control fan thrust modulation for shaft-coupled configuration is represented by the block diagram in Figure 7-16. The pitch and roll control input signals, δ_θ and δ_ϕ, are obtained from the Manual Control System, while inputs δV_β and V_{TRANS} come from Power Lever System and Engine Dynamics models, respectively. The constants used in the diagram are tabulated in Figure 7-17.

The system outputs, β_1, β_2, and β_3, are the fan blade pitch angles which are used as inputs into Fan Dynamics Model of the shaft-coupled configuration (Figure 10-4).

FIGURE 7-16

FAN BLADE PITCH ACTUATORS AND CONTROL SIGNAL MIXING

(SHAFT FAN SYSTEM)

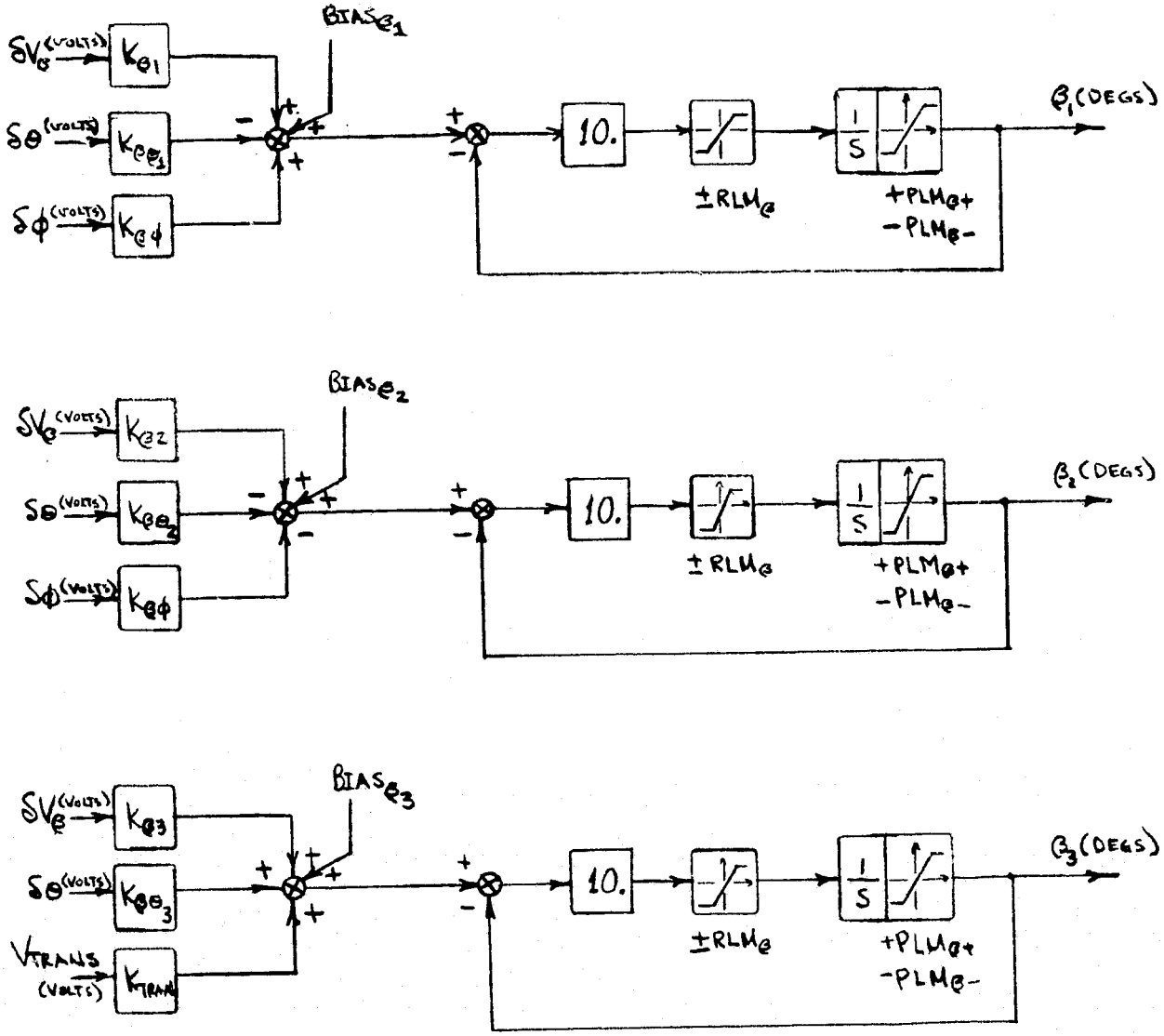

FIGURE 7-17

PITCH AND ROLL CONTROL SYSTEM PARAMETERS

(SHAFT-COUPLED FANS)

$BIAS_{\beta 1}$	Fan Blade No. 1 Bias Signal	+1.5 deg
$BIAS_{\beta 2}$	Fan Blade No. 2 Bias Signal	+1.5 deg
$BIAS_{\beta 3}$	Fan Blade No. 3 Bias Signal	+1.5 deg
$K_{\beta 1}$	Forward Path Gain for Fan Blade Actuator 1	1.0 deg/volt
$K_{\beta 2}$	Forward Path Gain for Fan Blade Actuator 2	1.0 deg/volt
$K_{\beta 3}$	Forward Path Gain for Fan Blade Actuator 3	1.0 deg/volt
$K_{\beta\theta 1}$	Pitch Signal Gain for Fan Blade No. 1	4.4 deg/volt
$K_{\beta\theta 2}$	Pitch Signal Gain for Fan Blade No. 2	4.4 deg/volt
$K_{\beta\theta 3}$	Pitch Signal Gain for Fan Blade No. 3	8.8 deg/volt
$K_{\beta\theta}$	Roll Signal Gain for Fan Blades 1 and 2	8.8 deg/volt
KTRAN	Shutdown Signal Gain for Fan Blade 3	-35.7 deg/volt
$PLM_{\beta+}$	Upper Fan Blade Pitch Limit	7.3 deg
$PLM_{\beta-}$	Lower Fan Blade Pitch Limit	-30.0 deg
RLM_{β}	Blade Pitch Rate Limit	100.0 deg/sec

8. POWER LEVER AND THROTTLE GEARING

The power lever and throttle gearing is used by the pilot to control the total fan thrust by adjusting the engine speed (N_G) and engine power output. The pilot positions the master power lever, δ_T, and he can also separately adjust the individual engine power levers (δ_1, δ_2, and δ_3). Individual power lever adjustments are necessary primarily for special conditions, such as transitions between powered-lift and aerodynamic flight or in engine startups and shutdowns.

The block diagram of power lever gearing arrangement for gas-coupled configuration is presented in Figure 8-1. The inputs are the pilot's master power lever (δ_T), aircraft altitude rate ($\dot{h}$), and the commanded thrust vector angle (θ_J); the output (N_G) is the commanded engine speed.

The effect of individual power lever settings is depicted in Figure 8-2. When all three individual levers are at their maximum setting, then the effective commanded engine speed is N_G, which is set by the master power lever (Figure 8-1). However, if the pilot reduces an individual power lever setting, then the corresponding engine speed is reduced accordingly.

The individual parameter functions and tabular data used in the above two block diagrams are presented in Figures 8-3 through 8-7. Figures 8-1 through 8-7 apply to gas-coupled configuration and the remaining diagrams and data apply to shaft-coupled power system.

FIGURE 8-1

POWER LEVER GEARING

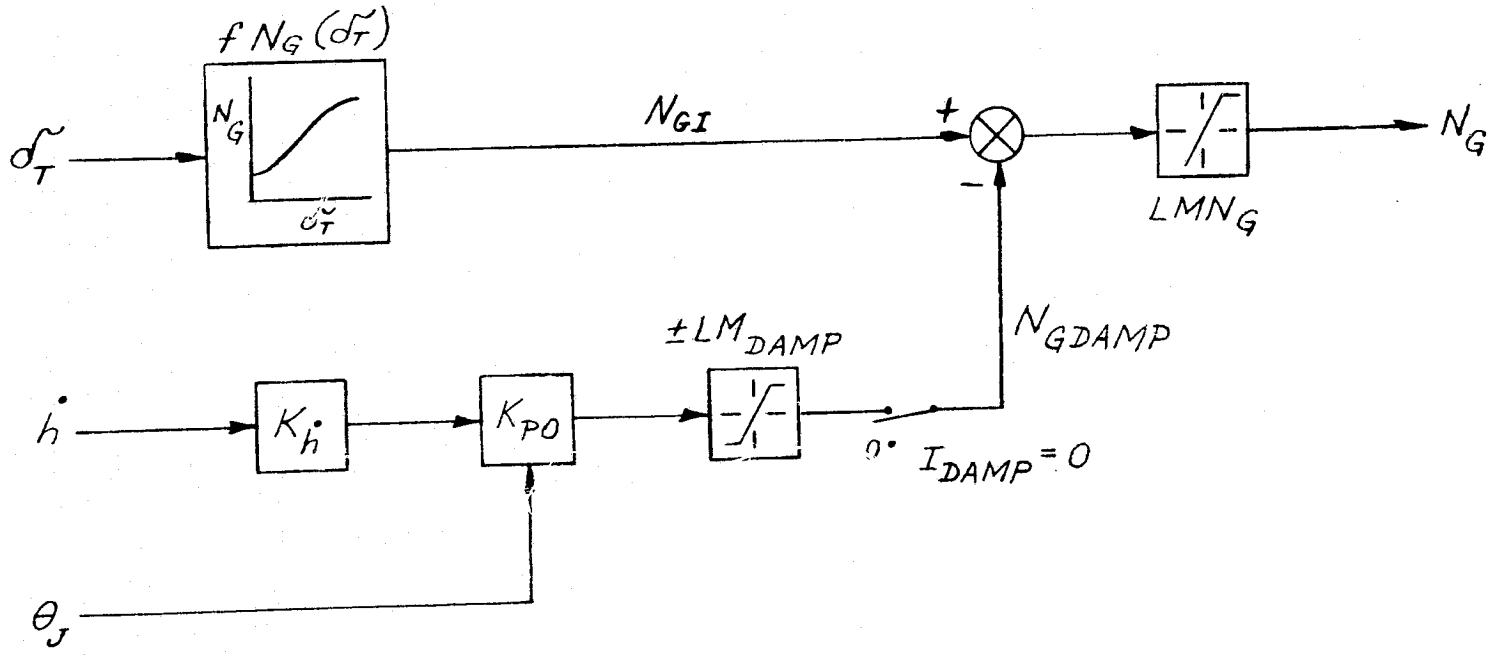

FIGURE 8-2
THROTTLE LEVER GEARING

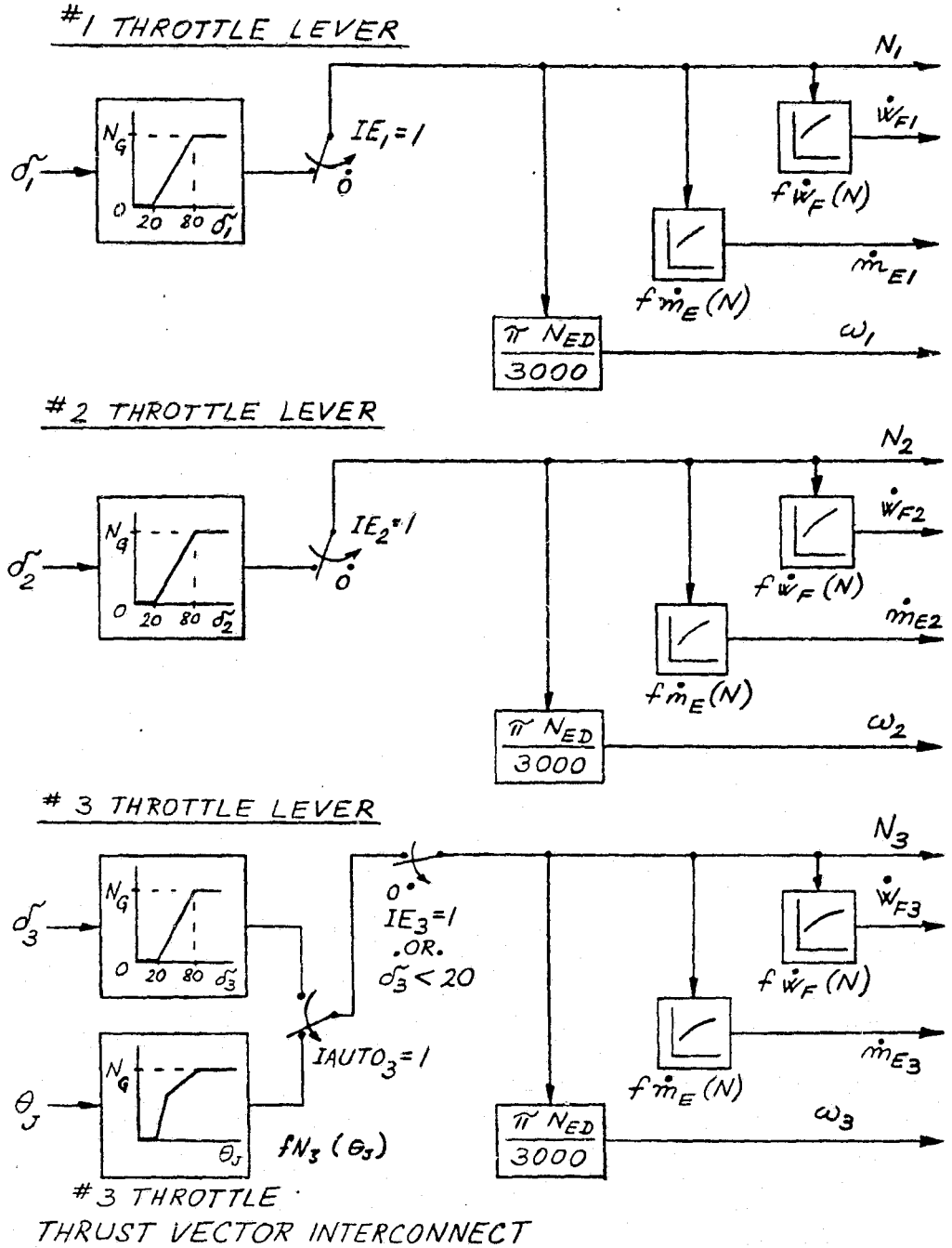

FIGURE 8-3

LIFT ENGINE SHUT-DOWN SCHEDULE

(GAS - COUPLED FAN)

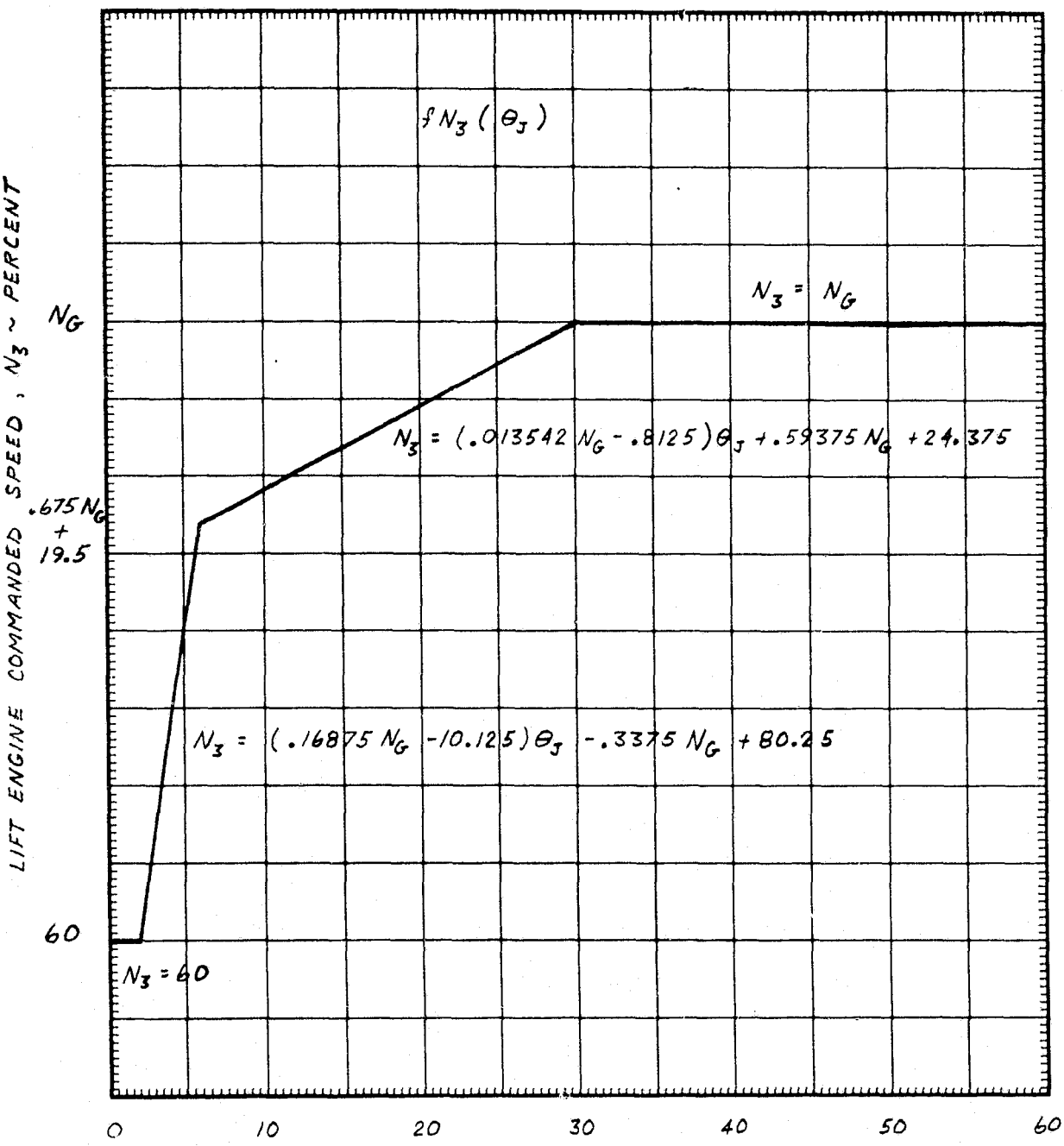

FIGURE 8-4

POWER LEVER AND THROTTLE GEARING PARAMETERS

LMN_G	Maximum Engine Speed Command	107.6 %
LM_{DAMP}	Height Damper Authority Limit	1.0 %
$K_{\dot{h}}$	Height Damper Feedback Gain	0.23 %/FPS
N_{ED}	Engine Design Speed	13,650 RPM

FIGURE 8-5

POWER LEVER GEARING

GAS FAN RTA

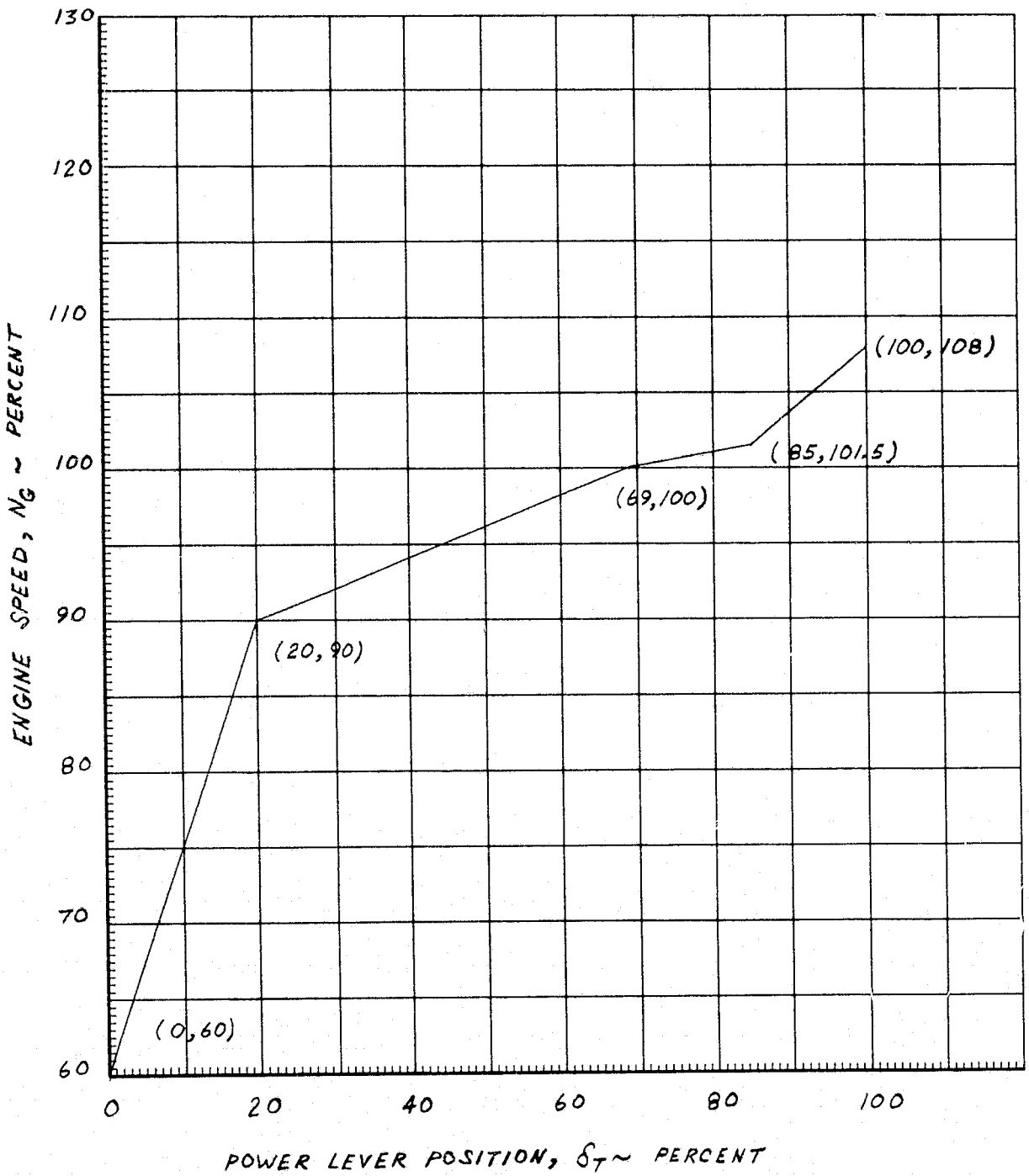

FIGURE 8-6

ENGINE FUEL FLOW
(GAS-COUPLED FANS)

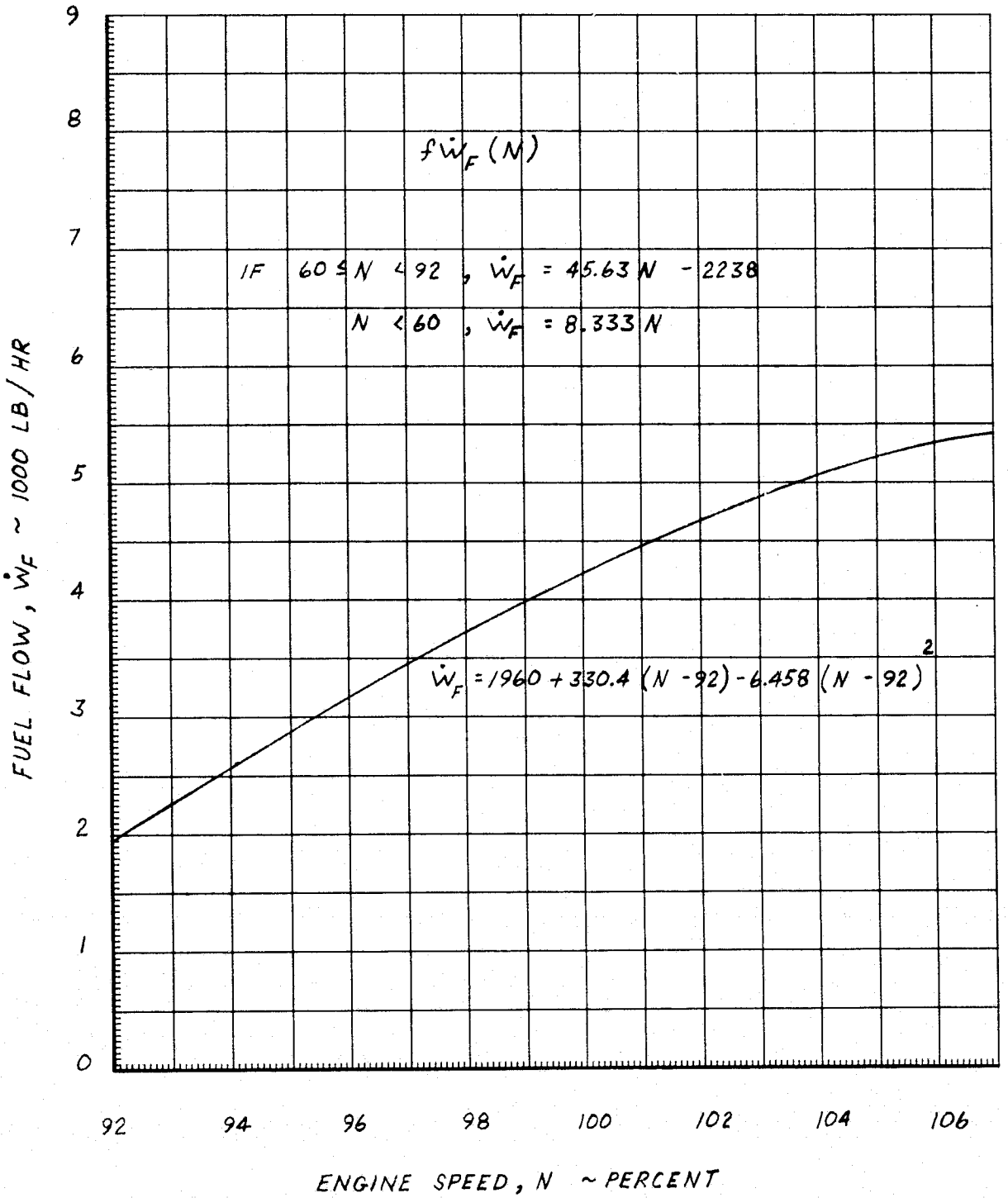

FIGURE 8-7
ENGINE AIR FLOW
(GAS-COUPLED FANS)

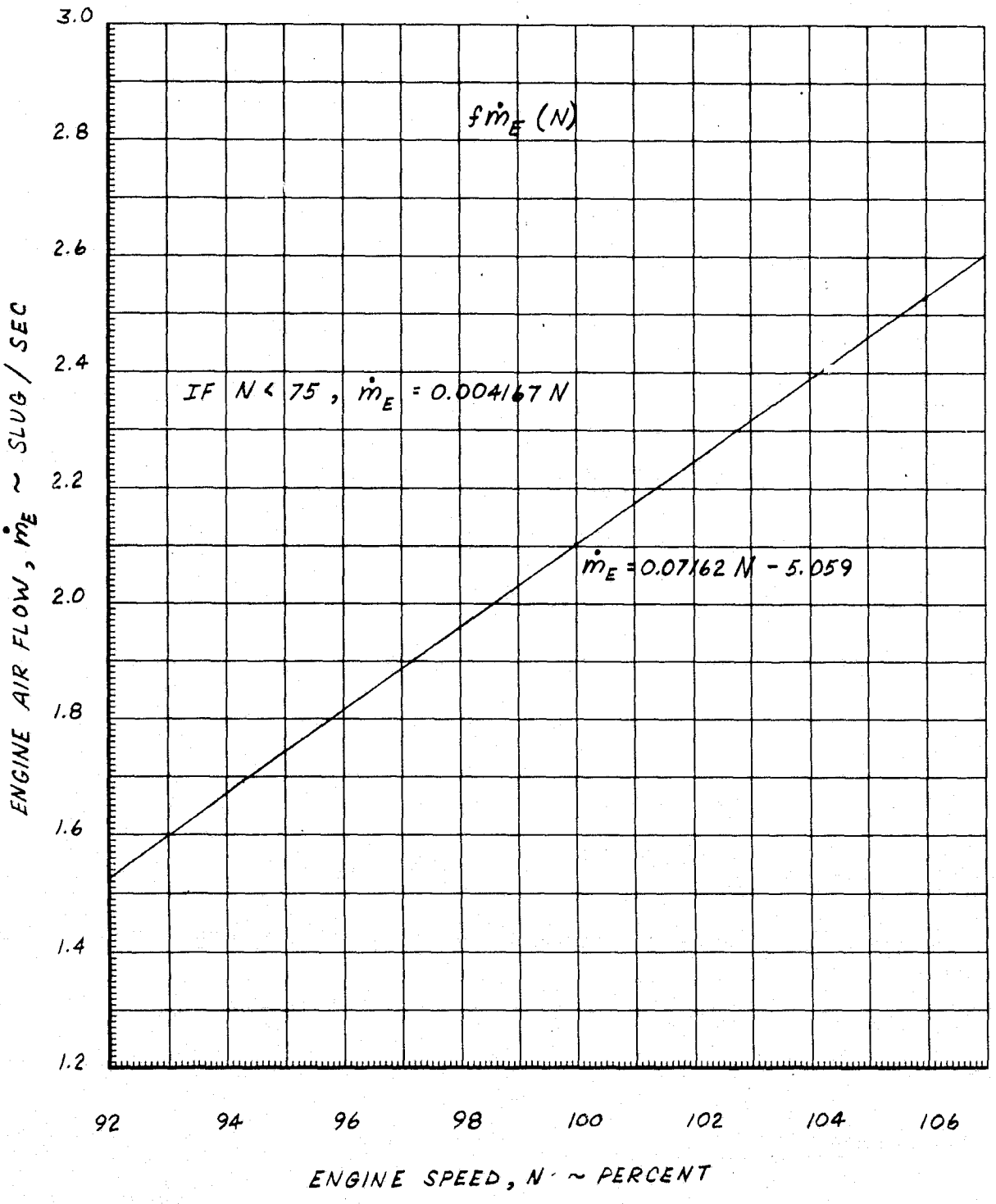

The power lever system for the shaft-coupled fans is presented in block diagram form in Figure 8-8. This power lever system uses the same main inputs as the gas-coupled configuration: the master power lever (δ_T), the aircraft altitude rate ($\dot{h}$), and the commanded thrust vector angle (θ_J). In addition to the three main inputs this power lever system also uses the fan speed feedback ($N_\%$). In shaft-coupled configuration the fan speed is the same for all fans in normal operating condition. The outputs of the power lever system are the engine fuel flow command signal (δV_f), the fan blade pitch signal (δV_β), and the forward fan clutch signal (V_{CLUTCH}) which is used to declutch the forward fan for aerodynamic flight.

The tabulated and plotted data for the shaft-coupled power lever block diagram are presented in Figures 8-9 through 8-11.

FIGURE 8-8

POWER LEVER SYSTEM MODEL

(SHAFT-COUPLED FAN SYSTEM)

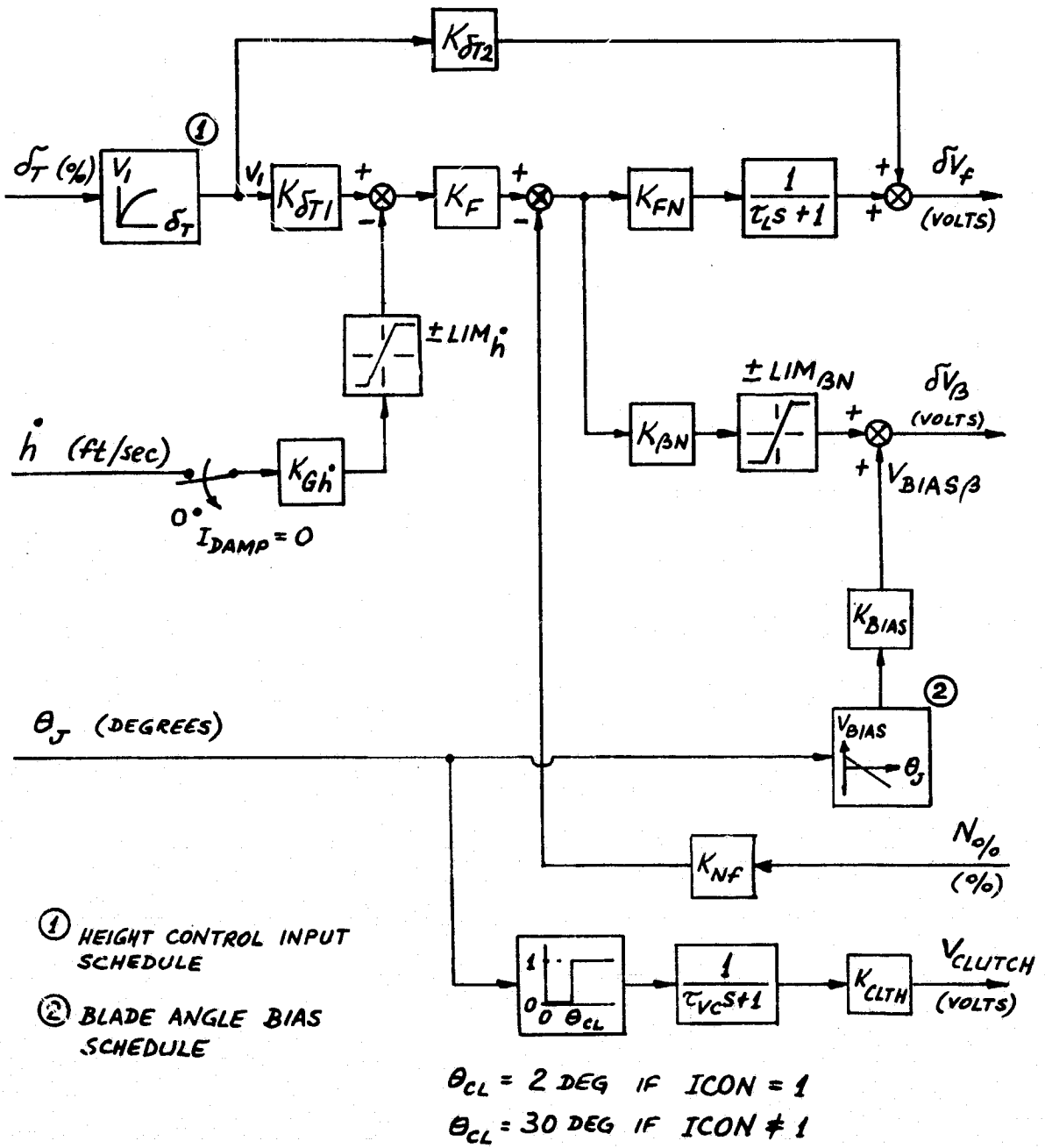

FIGURE 8-9

POWER LEVER SYSTEM PARAMETERS

(SHAFT-COUPLED FANS)

K_{BIAS}	Path Gain for Speed Dependent Bias Signal	1.0 volt/volt
K_{β_N}	Fan Blade Pitch Path Gain	50. volts/volt
K_{CLTH}	Gain of Fan No. 3 Clutch Signal	1.0 volts/volt
K_F	Altitude Rate Forward Loop Gain	1.0 volts/volt
K_{F_N}	Fan Speed Forward Loop Gain	.60 volts/volt
$K_{G_{\dot{h}}}$	Altitude Rate Feedback Gain	.06 volts/ft/sec
K_{N_f}	Fan Speed Loop Feedback Gain	.00766 volts/%
$K_{\delta T1}$	Power Lever Command Gain	1.0 volt/volt
$K_{\delta T2}$	Power Lever Command Gain (D.E.L. Path)	1.0 volt/volt
$LIM_{\dot{h}}$	Limit on Altitude Rate Feedback	.035 volt
LIM_{β_N}	Limit on Fan Blade Height Control Signal	3.7 volts
τ_L	Low Pass Filter Time Constant	.25 sec
τ_{vc}	Fan No. 3 Clutch Signal Time Constant	.1 sec

FIGURE 8-10

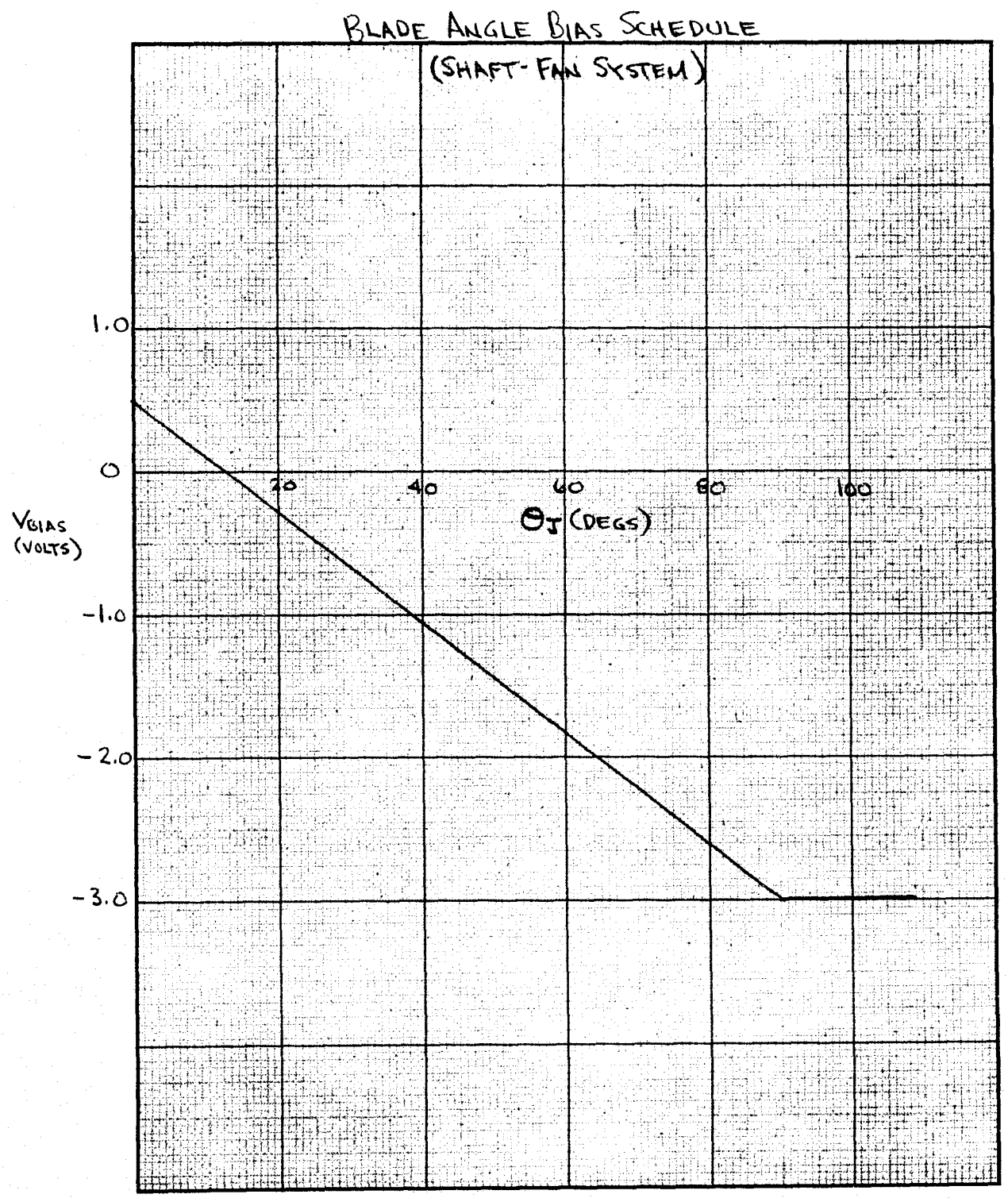
BLADE ANGLE BIAS SCHEDULE
(SHAFT-FAN SYSTEM)
1.0
0
-1.0
-2.0
-3.0
20
40
60
80
100
V_{BIAS} (VOLTS)
θ_J (DEGS)

FIGURE 8-11

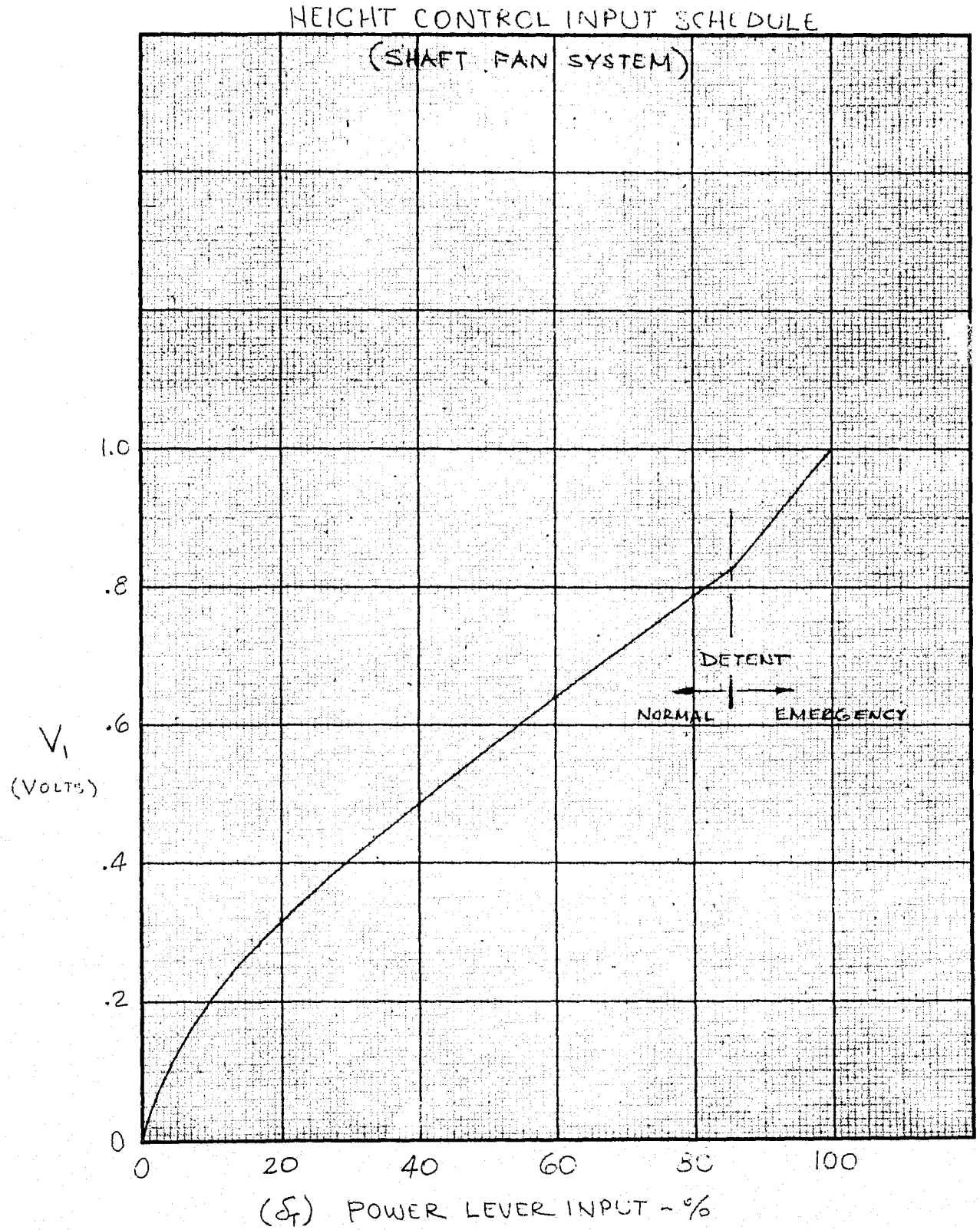
HEIGHT CONTROL INPUT SCHEDULE
(SHAFT FAN SYSTEM)
1.0
.8
.6
.4
.2
0
V_1
(VOLTS)
DETENT
NORMAL
EMERGENCY
0
20
40
60
80
100
(δ) POWER LEVER INPUT - %

9. ENGINE MODEL

The engine simulation math model provides a relatively complex representation of individual engines and the interconnect logic. This degree of detail is considered important because the aircraft's propulsion system is the most essential system on the aircraft providing lift and aircraft control. The simulation model includes the capability to represent the gas-coupled fans as well as shaft-coupled fans. In addition the simulation includes the capability to model normal aircraft operation as well as several failure modes. The overall simulation model was arranged such that in most cases configuration change-overs can be accomplished without major interruption in conducting the simulation. Each of the above capabilities requires some increase in the simulation model complexity.

The gas-coupled configuration is described in first part of this section. Here Figure 9-1 is a schematic representation of the interconnect valve and dump valve logic. The controlling parameter, ICON, is set externally by the operator of the simulation study; it determines whether the forward (No. 3) engine is shut down manually or automatically and it determines whether the interconnect valve is open or closed. Figure 9-2 contains a brief list of associated constants.

Figures 9-3 through 9-5 are block diagrams of the three engine and tip turbine models. The main inputs in the diagrams are the engine speeds (N_G, N_1, N_2, N_3), derived in Section 8, and the ETaC valve angles (θ_{V1}, θ_{V2}, θ_{V3}) derived in Section 7. The outputs are the tip turbine horsepower supplied to the fans (HP_1, HP_2, and HP_3) and the tip turbine residual thrust developed by each of the three fans (F_{T1}, F_{T2}, and F_{T3}). The related data in graphical or, when necessary, in tabular form is supplied in Figures 9-6 through 9-19.

FIGURE 9-1

INTERCONNECT VALVE AND DUMP VALVE LOGIC

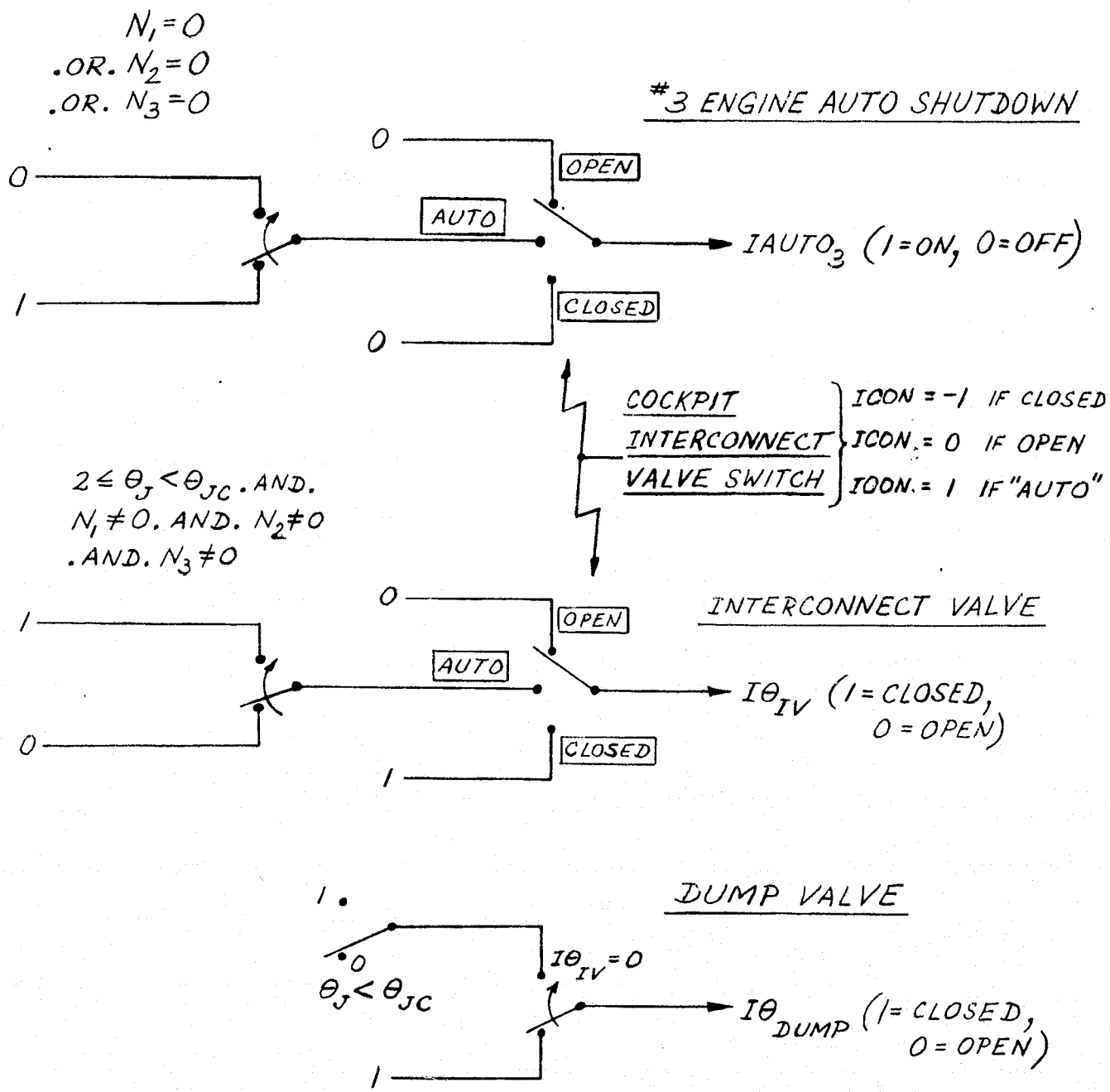

FIGURE 9-2

INTERCONNECT VALVE AND DUMP VALVE PARAMETERS

(GAS-COUPLED FANS)

ICON	Conversion Discrete Nominal Value	1
θ_{JC}	Conversion Thrust Vector Angle	30.0 deg

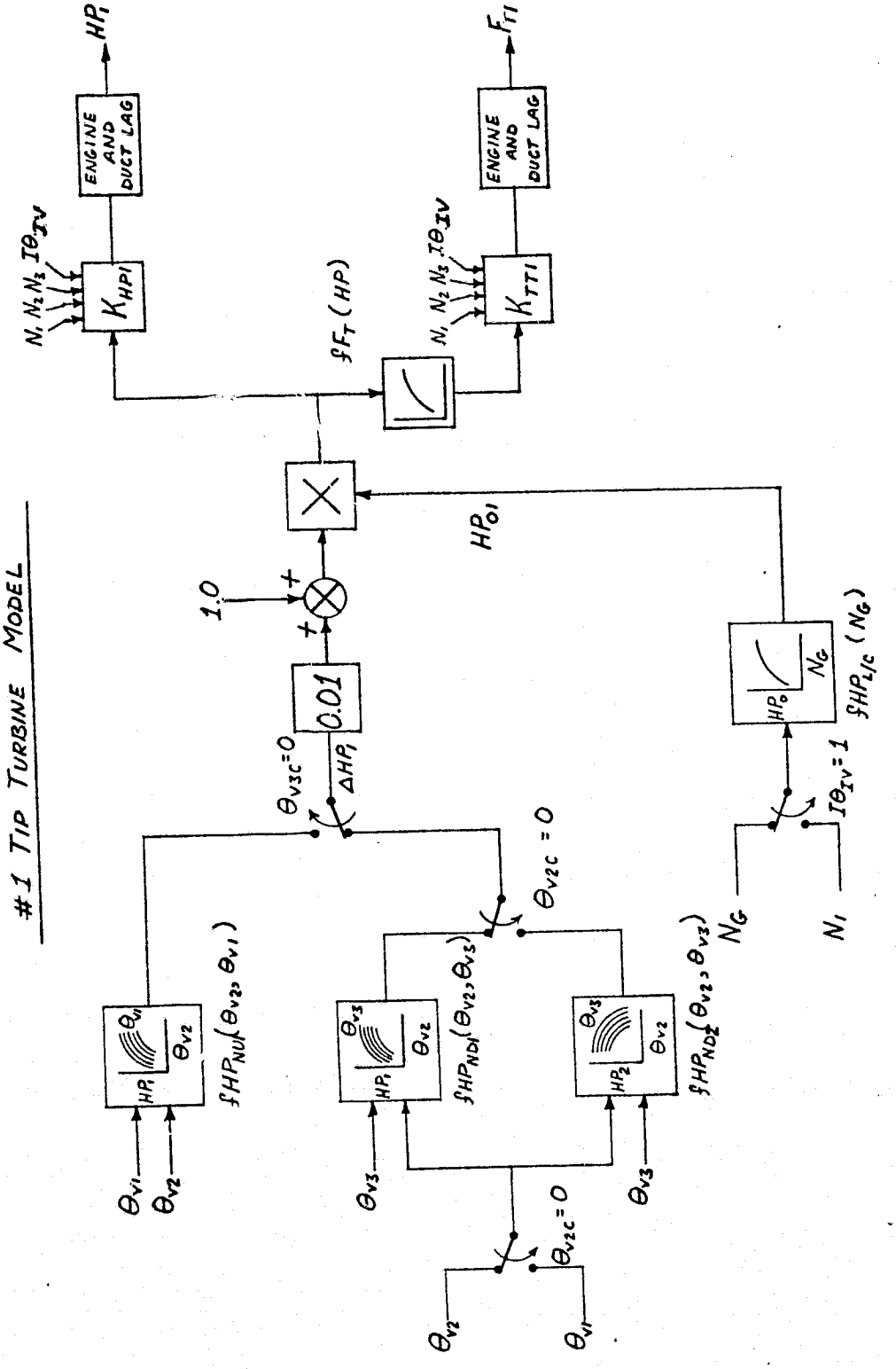

FIGURE 9-3

#1 TIP TURBINE MODEL

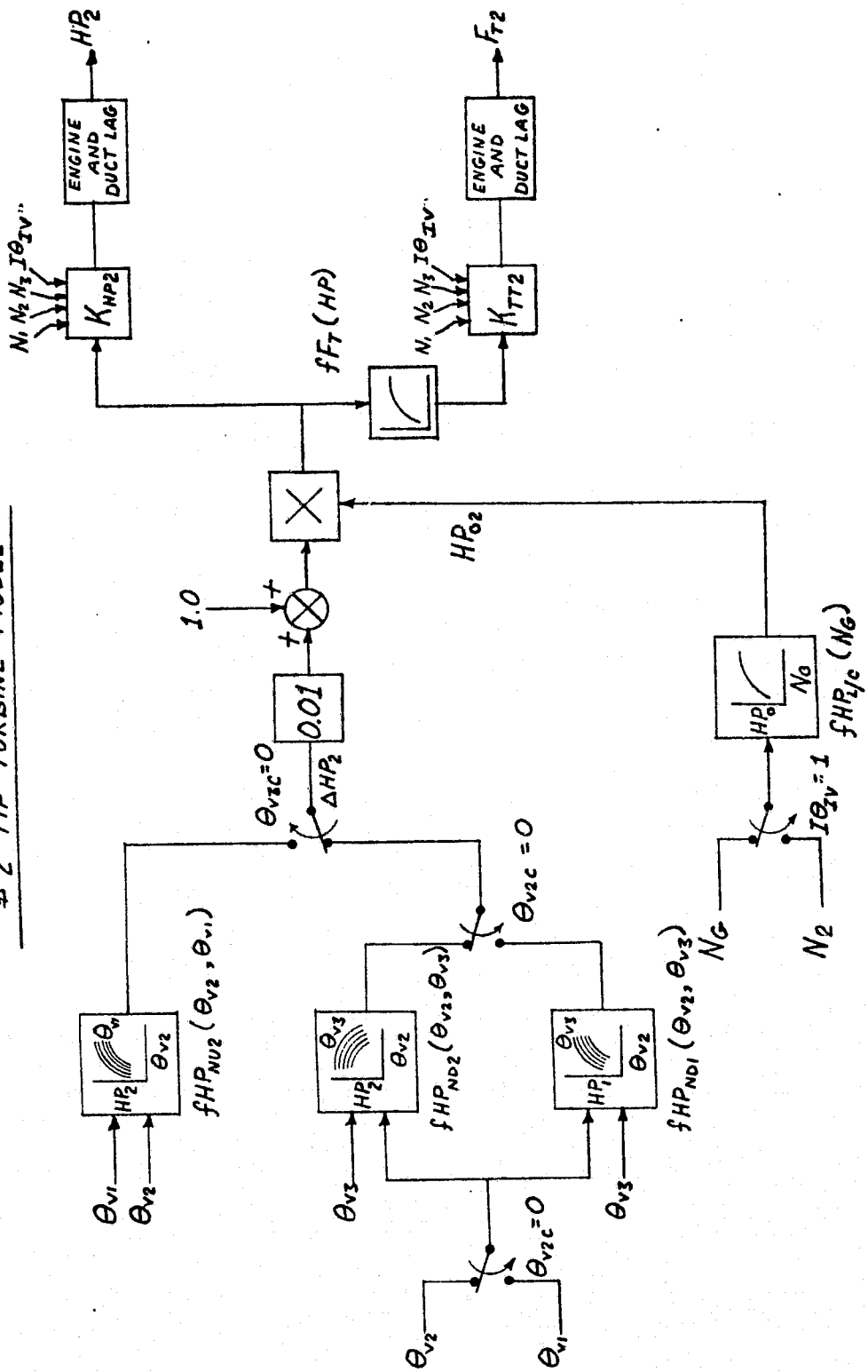

FIGURE 9-4
#2 TIP TURBINE MODEL

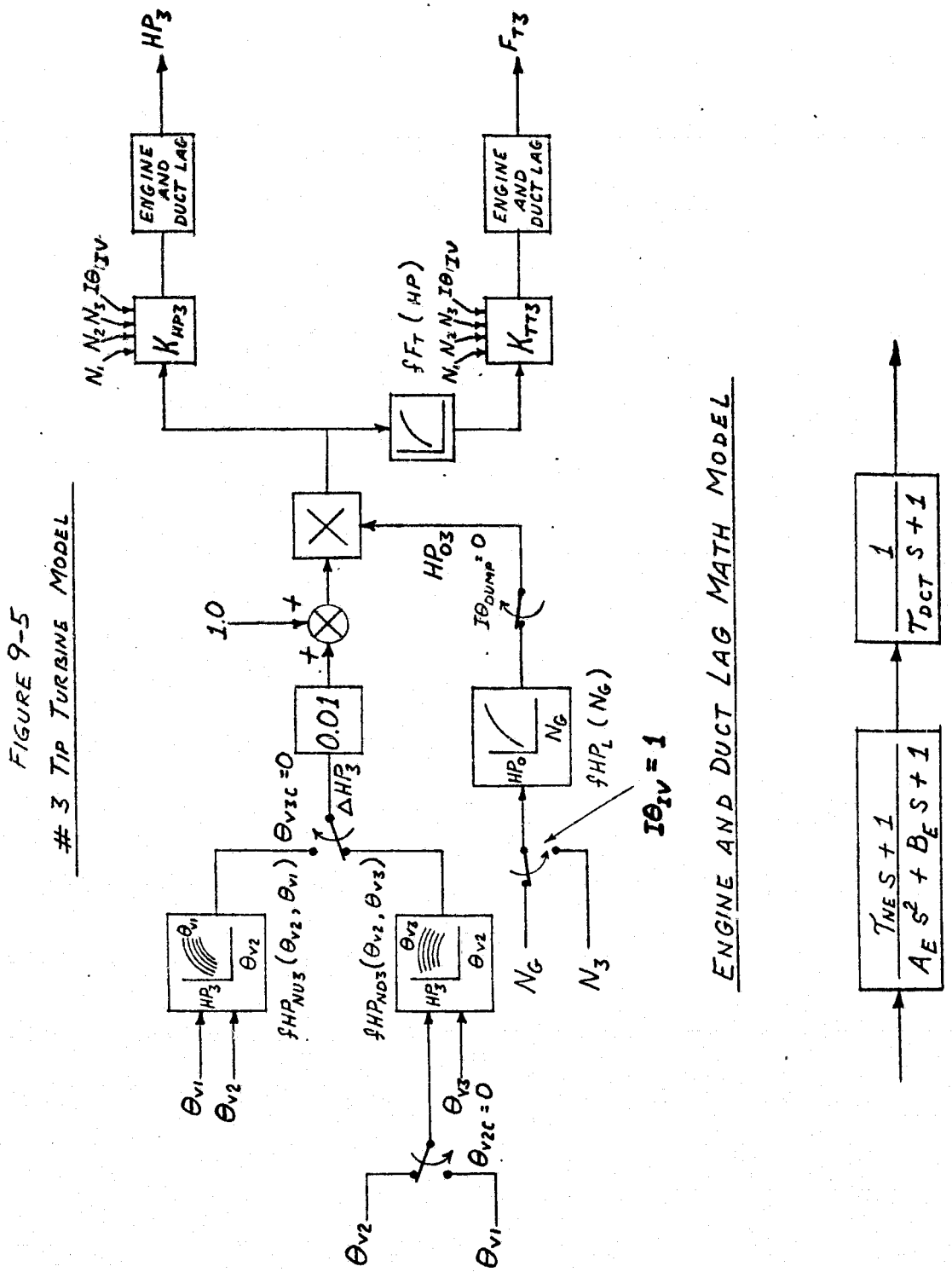

FIGURE 9-5

3 TIP TURBINE MODEL

ENGINE AND DUCT LAG MATH MODEL

FIGURE 9-6

ENGINE MODEL DATA

A_E	Engine Lag Coefficient	0.00694	sec^2
B_E	Engine Lag Coefficient	0.0833	sec
τ_{NE}	First Order Engine Lead	0.0	sec
τ_{DCT}	Duct Lag Time Constant	0.045	sec

FIGURE 9-7

LIFT / CRUISE FAN HORSEPOWER AT ZERO VALVE ANGLE

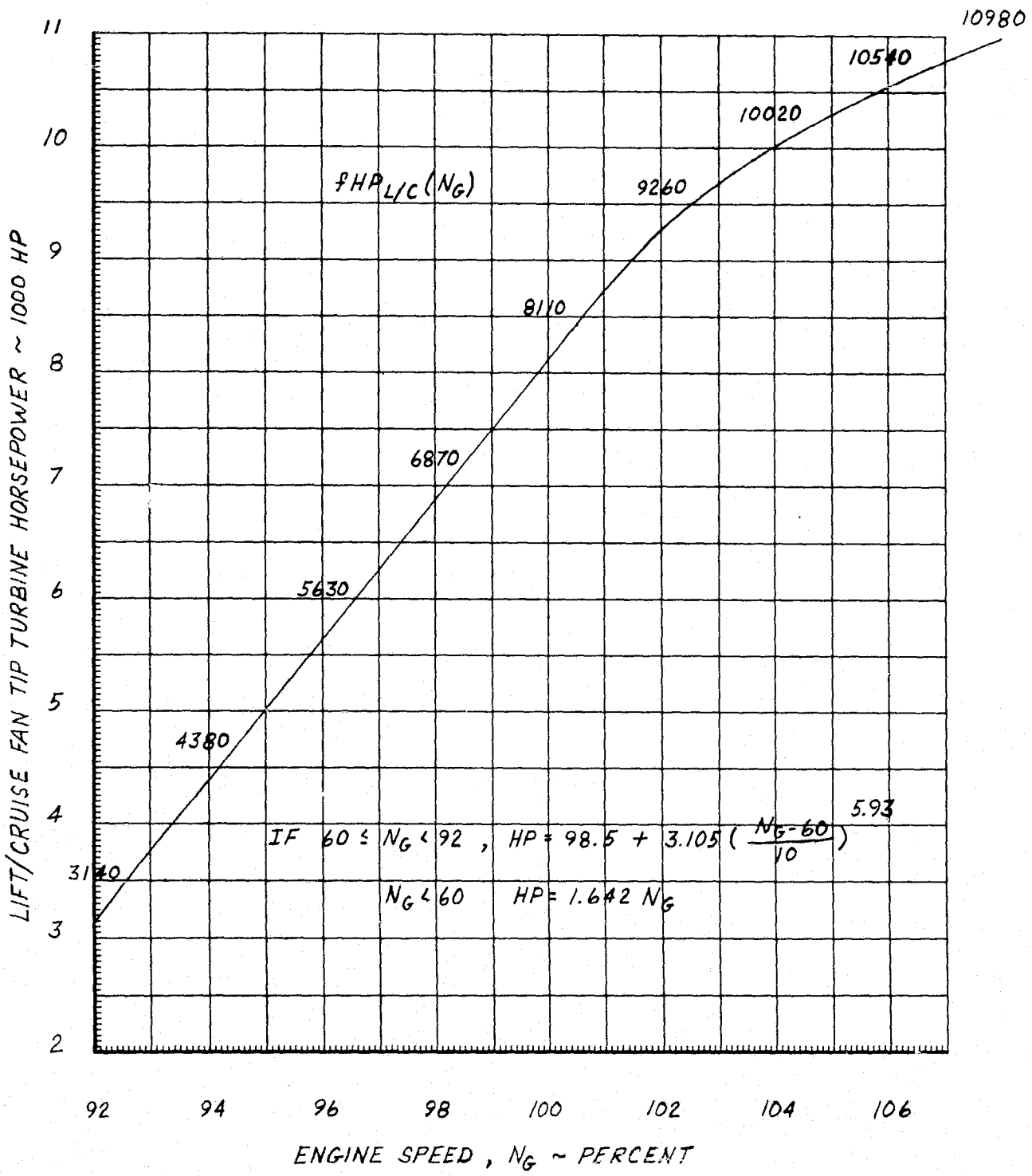

FIGURE 9-8

LIFT FAN HORSEPOWER AT ZERO VALVE ANGLE

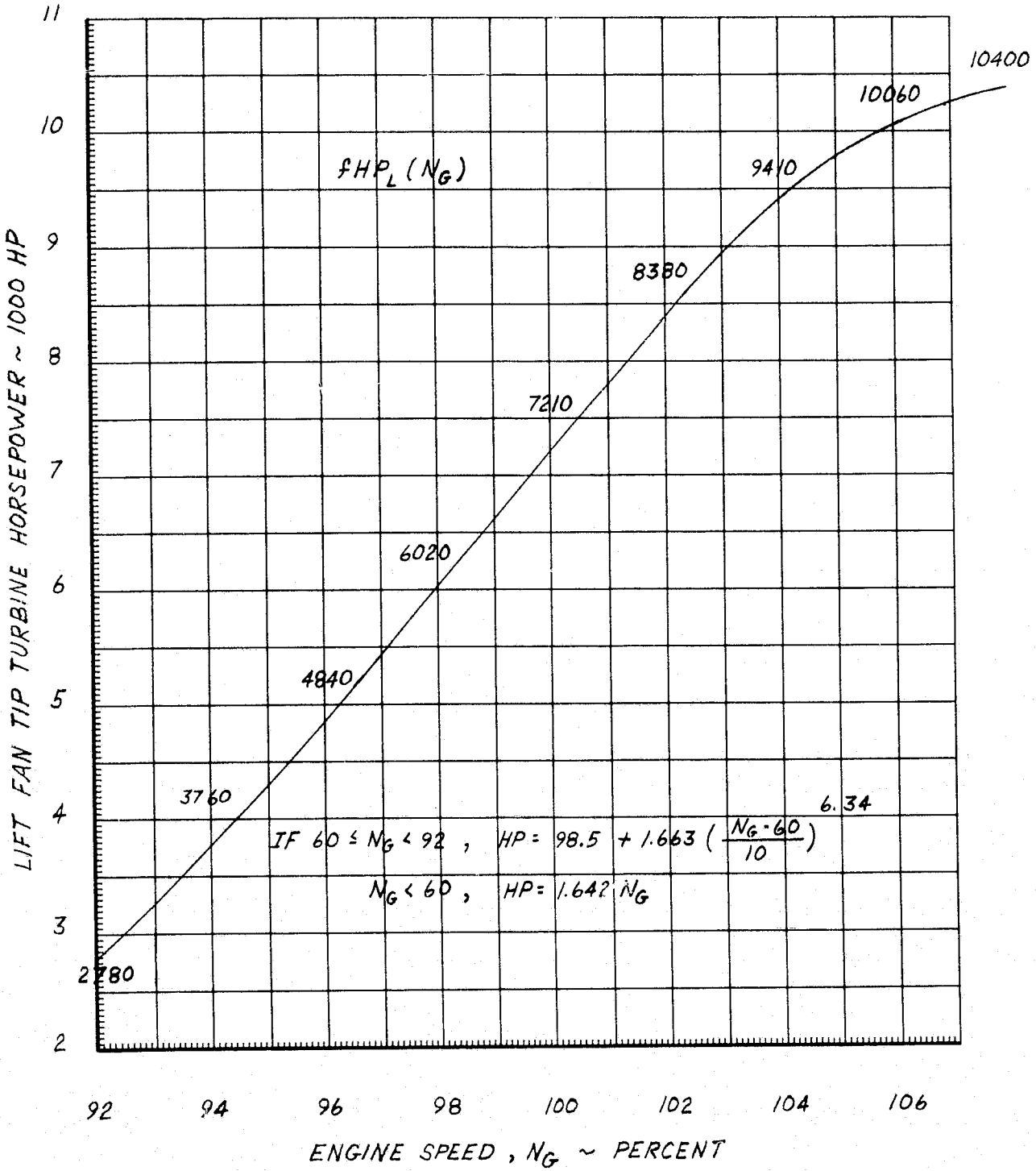

FIGURE 9-9

#1 TIP TURBINE HORSEPOWER MODULATION
NOSE UP PITCH & RIGHT ROLL

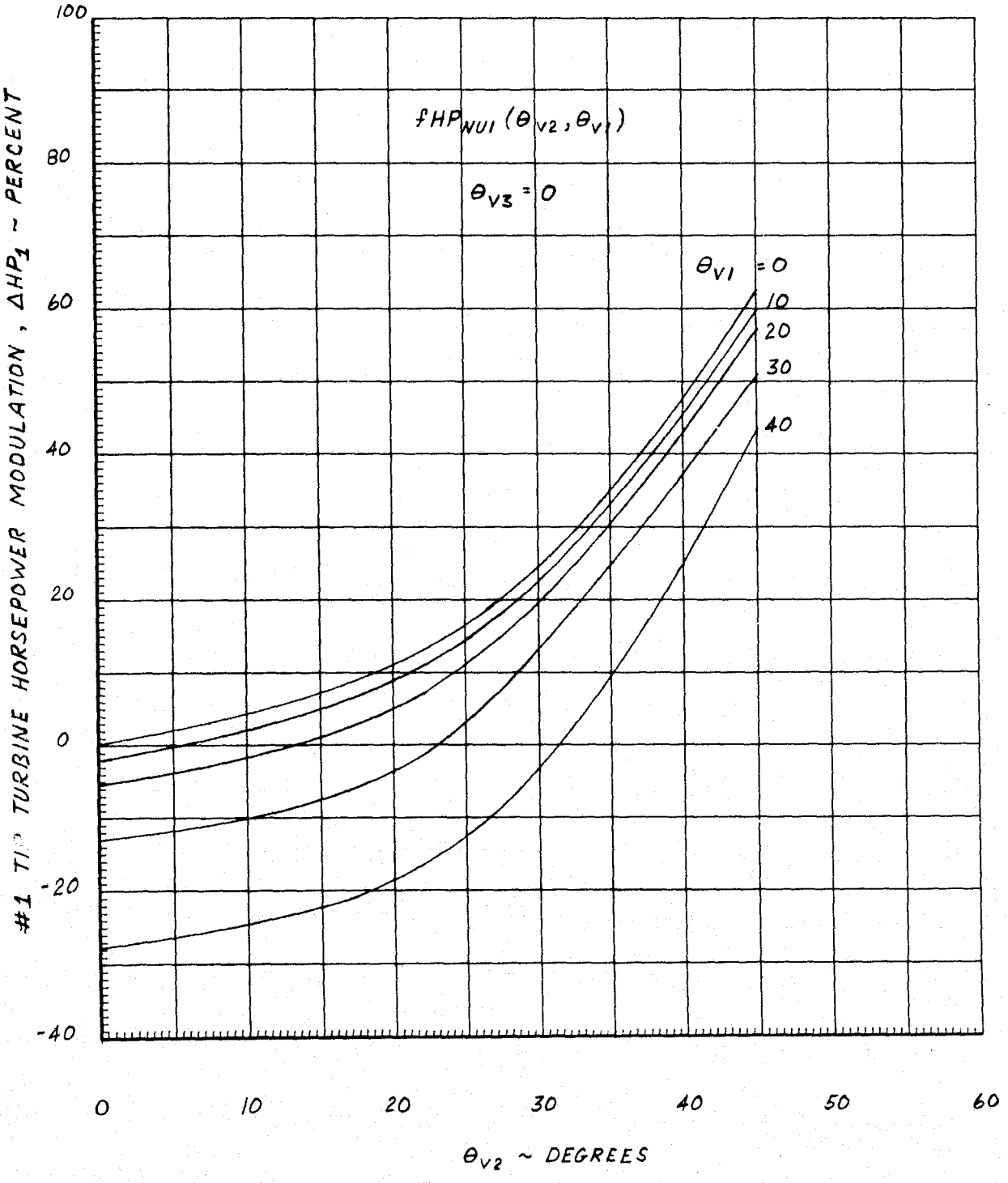

FIGURE 9-10

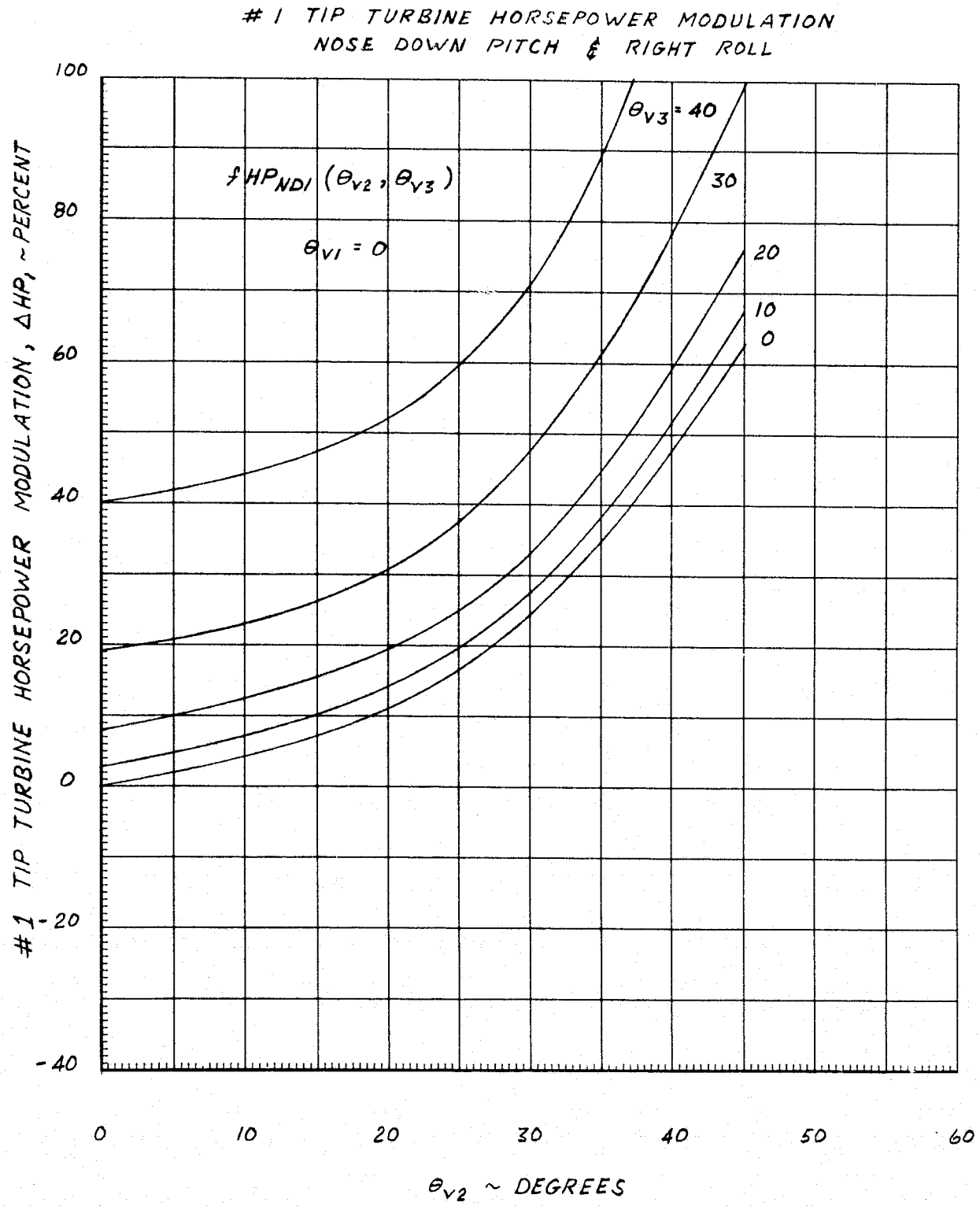
#1 TIP TURBINE HORSEPOWER MODULATION
NOSE DOWN PITCH & RIGHT ROLL
#1 TIP TURBINE HORSEPOWER MODULATION, ΔHP, ~ PERCENT
100
80
60
40
20
0
-20
-40
f HP_NDI (θV2, θV3)
θV1 = 0
θV3 = 40
30
20
10
0
0
10
20
30
40
50
60
θV2 ~ DEGREES

FIGURE 9-11

#1 TIP TURBINE HORSEPOWER MODULATION DATA POINTS

(PERCENT MODULATION)

NOSE UP PITCH & RIGHT ROLL ($\theta_{V3} = 0$)

θ_{V1} \ θ_{V2}	0	10	20	30	40
0	0.0	4.2	11.2	24.4	47.7
10	-1.6	2.2	9.0	22.7	46.0
20	-5.3	-1.8	4.7	19.3	43.3
30	-13.0	-10.0	-3.8	13.2	37.2
40	-27.6	-24.5	-19.2	-3.2	25.2

$f HP_{NU1} (\theta_{V2}, \theta_{V1})$

NOSE DOWN PITCH & RIGHT ROLL ($\theta_{V1} = 0$)

θ_{V3} \ θ_{V2}	0	10	20	30	40
0	0.0	4.2	11.2	24.4	47.7
10	3.1	7.1	14.1	27.4	51.7
20	8.4	12.4	19.4	33.0	59.3
30	19.5	22.9	30.8	47.6	78.4
40	40.0	44.1	52.1	71.0	118.0

$f HP_{ND1} (\theta_{V2}, \theta_{V3})$

FIGURE 9-12

#2 TIP TURBINE HORSEPOWER MODULATION
NOSE UP PITCH & RIGHT ROLL

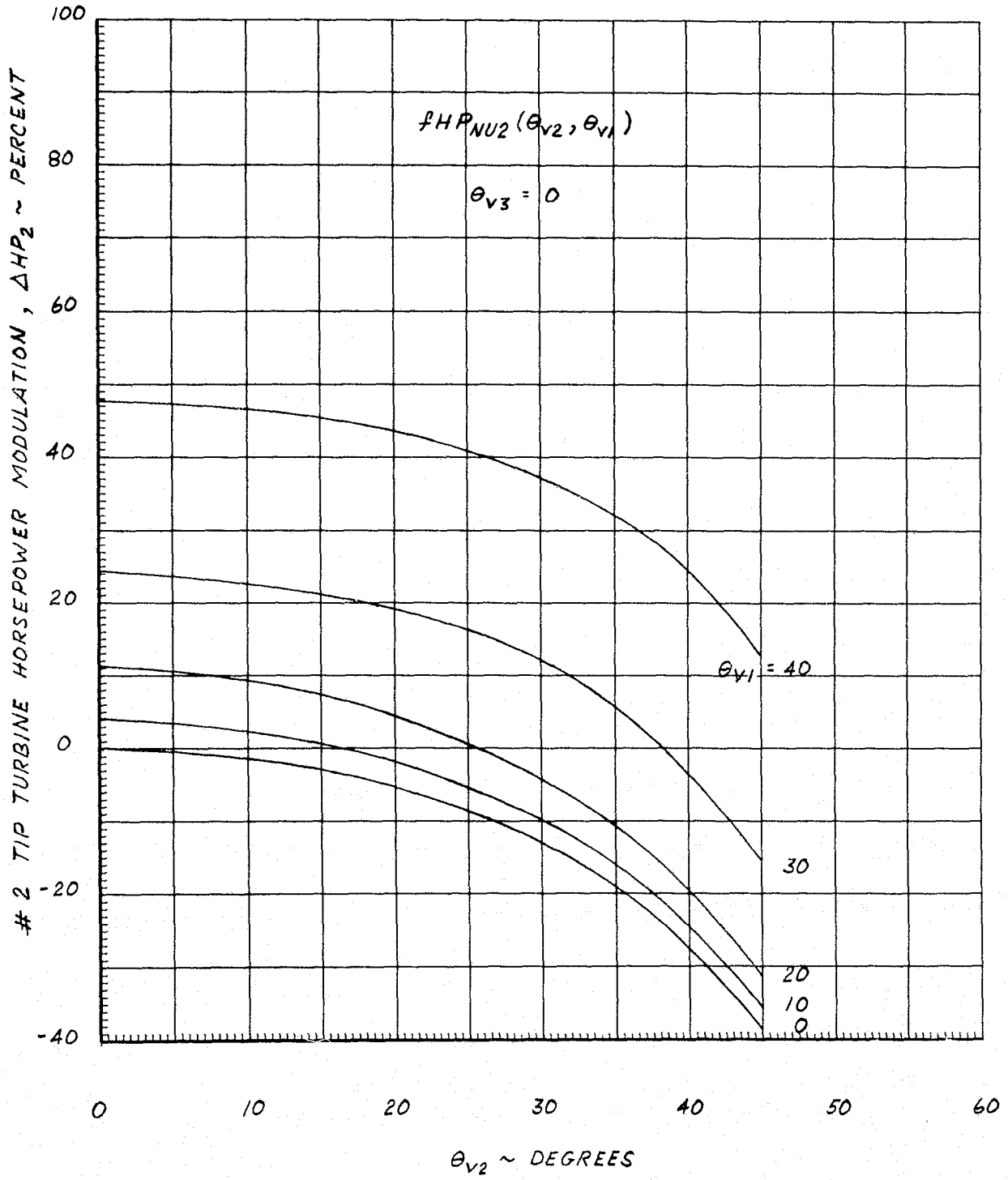

FIGURE 9-13

2 TIP TURBINE HORSEPOWER MODULATION
NOSE DOWN PITCH & RIGHT ROLL

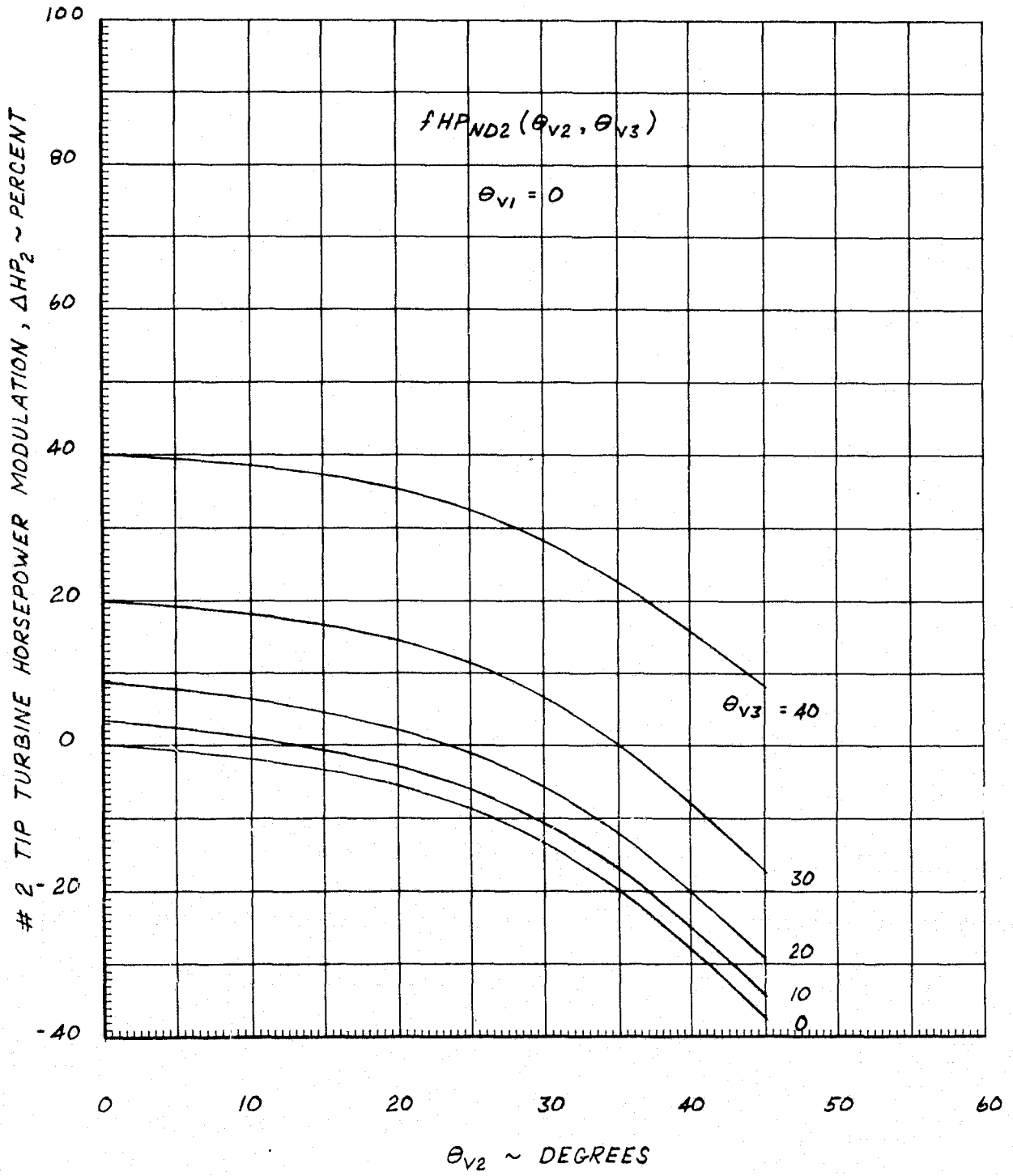

FIGURE 9-14

#2 TIP TURBINE HORSEPOWER MODULATION DATA POINTS

(PERCENT MODULATION)

NOSE UP PITCH & RIGHT ROLL ($\theta_{V3} = 0$)

θ_{V1} \ θ_{V2}	0	10	20	30	40
0	0.0	-1.6	-5.3	-13.0	-27.6
10	4.2	2.2	-1.8	-10.0	-24.5
20	11.2	9.0	4.7	-3.8	-19.2
30	24.4	22.7	19.3	13.2	-3.2
40	47.7	46.0	43.3	37.2	25.2

$f HP_{NU2} (\theta_{V2}, \theta_{V1})$

NOSE DOWN PITCH & RIGHT ROLL ($\theta_{V1} = 0$)

θ_{V3} \ θ_{V2}	0	10	20	30	40
0	0.0	-1.6	-5.3	-13.0	-27.6
10	3.1	1.1	-2.8	-10.6	-24.8
20	8.4	6.4	2.1	-5.7	-20.0
30	19.5	18.1	14.6	6.8	-7.8
40	40.0	38.7	35.4	28.2	15.9

$f HP_{ND2} (\theta_{V2}, \theta_{V3})$

FIGURE 9-15

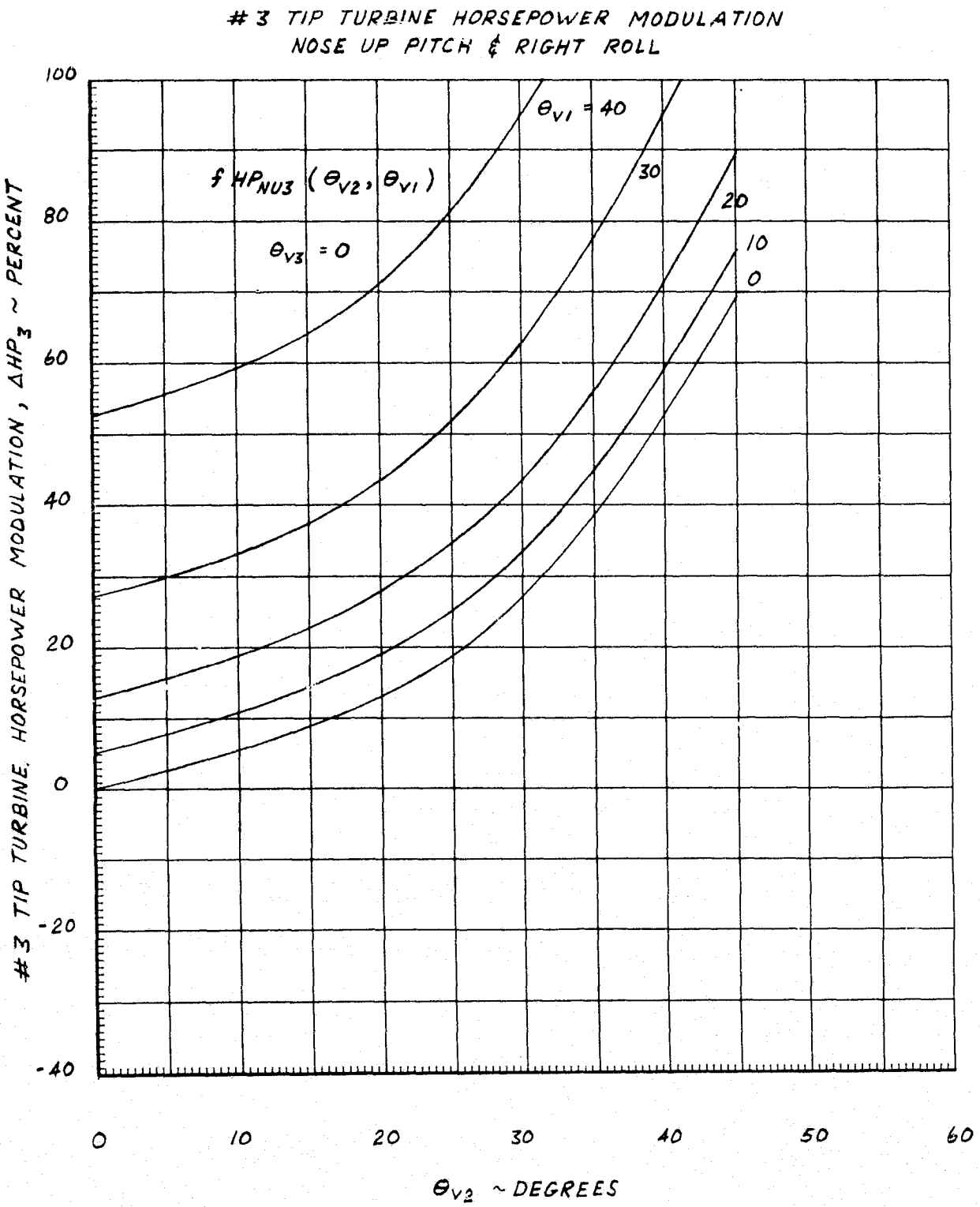
#3 TIP TURBINE HORSEPOWER MODULATION
NOSE UP PITCH & RIGHT ROLL
$f\,HP_{NU3}\,(\theta_{V2}, \theta_{V1})$
$\theta_{V3} = 0$
$\theta_{V1} = 40$
30
20
10
0
100
80
60
40
20
0
-20
-40
#3 TIP TURBINE HORSEPOWER MODULATION, ΔHP_3 ~ PERCENT
0
10
20
30
40
50
60
θ_{V2} ~ DEGREES

FIGURE 9-16

#3 TIP TURBINE HORSEPOWER MODULATION
NOSE DOWN PITCH & RIGHT ROLL

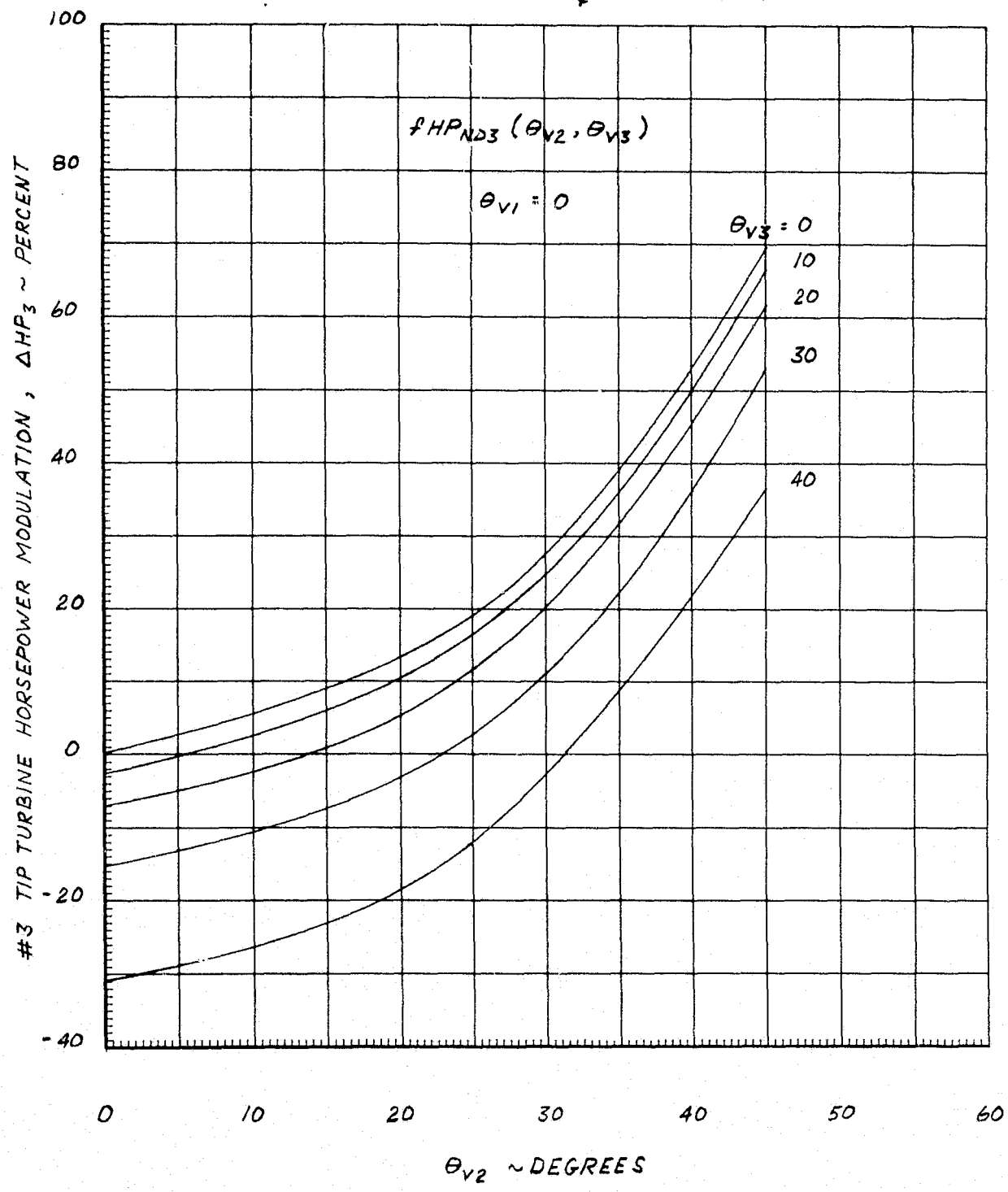

FIGURE 9-17

#3 TIP TURBINE HORSEPOWER MODULATION DATA POINTS

(PERCENT MODULATION)

NOSE UP PITCH & RIGHT ROLL ($\theta_{V3} = 0$)

θ_{V1} \ θ_{V2}	0	10	20	30	40	
0	0.0	5.6	13.0	27.2	52.8	
10	5.6	10.9	19.0	33.3	59.3	
20	13.0	19.0	27.9	43.4	71.2	$f HP_{NU3}(\theta_{V2}, \theta_{V1})$
30	27.2	33.3	43.4	62.8	94.9	
40	52.8	59.3	71.2	94.9	130.0	

NOSE DOWN PITCH & RIGHT ROLL ($\theta_{V1} = 0$)

θ_{V3} \ θ_{V2}	0	10	20	30	40	
0	0	5.6	13.0	27.2	52.8	
10	-2.6	2.6	10.3	24.8	50.0	
20	-6.9	-2.3	5.2	20.3	45.4	$f HP_{ND3}(\theta_{V2}, \theta_{V3})$
30	-15.3	-10.6	-3.1	11.2	36.1	
40	-30.9	-26.2	-18.5	-2.4	21.9	

FIGURE 9-18

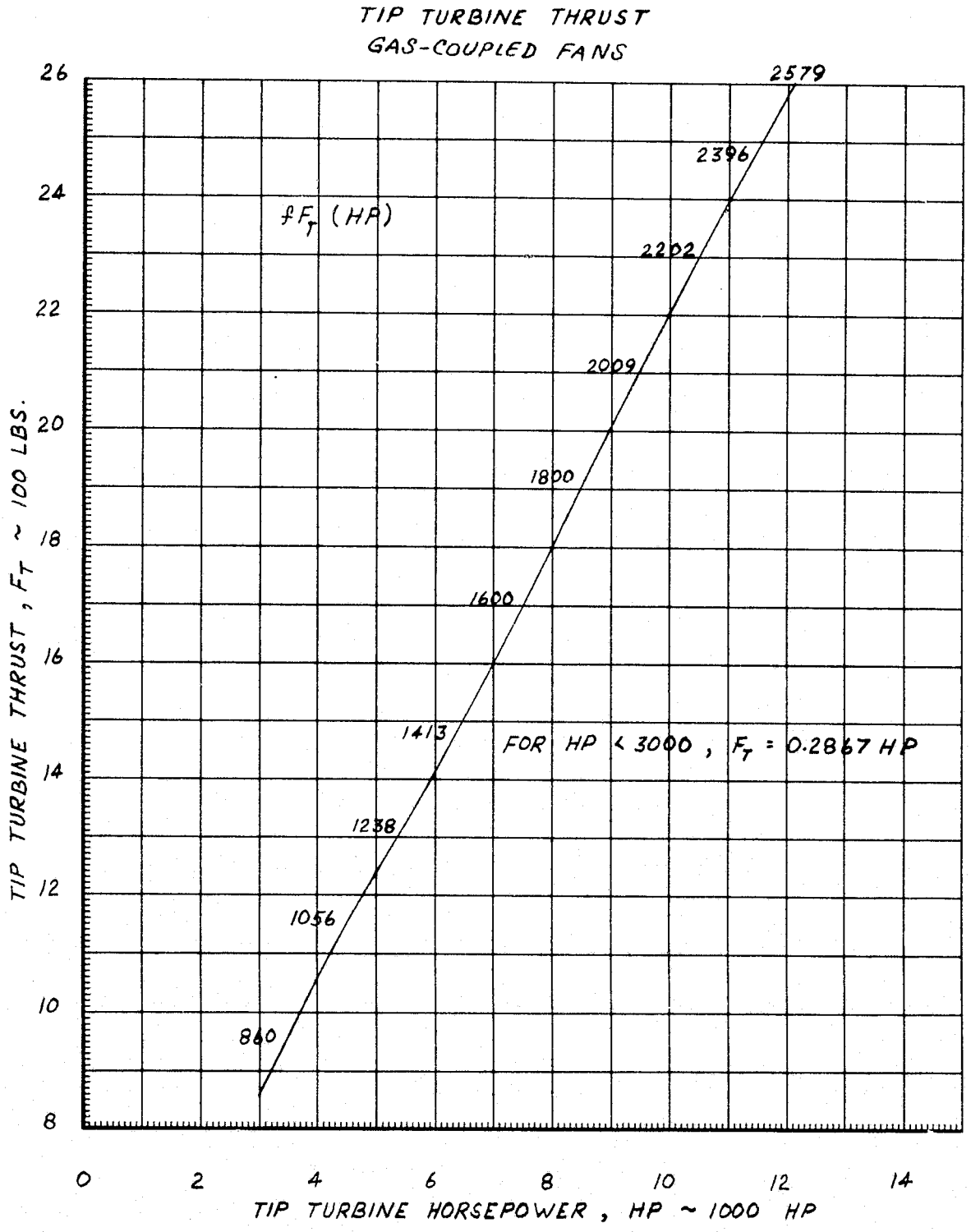

FIGURE 9-19

ENGINE FAILURE TABLES - GAS COUPLED FANS

POWERED-LIFT FLIGHT (INTERCONNECT VALVES OPEN AND DUMP VALVE CLOSED)

$I\theta_{IV} = 0$ .AND. $I\theta_{DUMP} = 1$	K_{HP1}	K_{TT1}	K_{HP2}	K_{TT2}	K_{HP3}	K_{TT3}
NORMAL OPERATION	1.0	1.0	1.0	1.0	1.0	1.0
$N_1 = 0$ .AND. $N_2 = 0$ .AND. $N_3 = 0$	0.0	0.0	0.0	0.0	0.0	0.0
$N_1 = 0$ .AND. $N_2 = 0$	0.333	0.333	0.333	0.333	0.333	0.333
$N_1 = 0$ .AND. $N_3 = 0$	0.30	0.30	0.333	0.333	0.30	0.30
$N_2 = 0$ .AND. $N_3 = 0$	0.333	0.333	0.30	0.30	0.30	0.30
$N_1 = 0$	.582	.555	.607	.572	.571	.534
$N_2 = 0$	.607	.572	.582	.555	.571	.534
$N_3 = 0$	.607	.572	.607	.572	.571	.534

AERODYNAMIC FLIGHT (INTERCONNECT VALVES CLOSED OR DUMP VALVE OPEN)

$I\theta_{IV} = 1$ .OR. $I\theta_{DUMP} = 0$	K_{HP1}	K_{TT1}	K_{HP2}	K_{TT2}	K_{HP3}	K_{TT3}
NORMAL OPERATION	1.0	1.0	1.0	1.0	1.0	1.0
$N_1 = 0$ .AND. $N_2 = 0$ .AND. $N_3 = 0$	0.0	0.0	0.0	0.0	1.0	1.0
$N_1 = 0$ .AND. $N_2 = 0$ .AND. $I\theta_{IV} = 0$	0.5	0.5	0.5	0.5	1.0	1.0
$N_1 = 0$ .AND. $N_3 = 0$ .AND. $I\theta_{IV} = 0$	0.47	0.47	0.5	0.5	1.0	1.0
$N_2 = 0$ .AND. $N_3 = 0$ .AND. $I\theta_{IV} = 0$	0.5	0.5	0.47	0.47	1.0	1.0
$N_1 = 0$ .AND. $I\theta_{IV} = 0$	0.96	0.96	1.0	1.0	1.0	1.0
$N_2 = 0$ .AND. $I\theta_{IV} = 0$	1.0	1.0	0.96	0.96	1.0	1.0

The corresponding math model for the three engines used in the shaft-coupled configuration is presented in Figure 9-20. The inputs here are: engine fuel signal (δV_f, described in Section 8), the three individual throttle lever positions set by the pilot (δ_1, δ_2, and δ_3), and fan speed and thrust vector angle command (N% and θ_J, respectively). The outputs are: total horsepower generated by the three engines (HP_E), the three individual engine rotor speeds expressed in percent units (N_1, N_2, N_3) and in radians per second (ω_1, ω_2, ω_3).

The tabular and plotted data needed in above block diagram are presented in Figures 9-21 through 9-23.

FIGURE 9-20

THREE ENGINES - DYNAMIC MODEL

(SHAFT FAN SYSTEM)

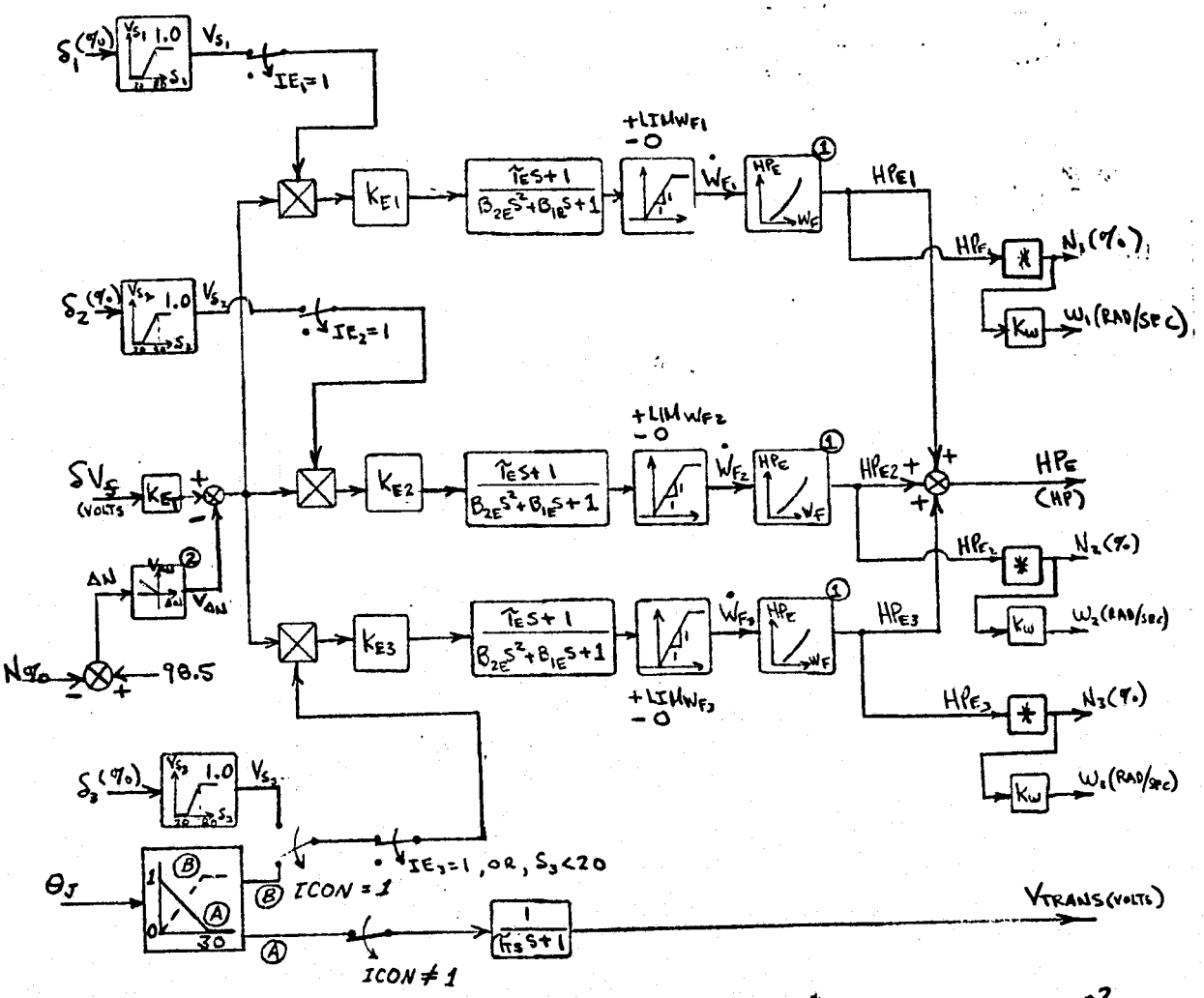

FIGURE 9-21

ENGINE MODEL PARAMETERS

(SHAFT-COUPLED FANS)

B_{1E}	Engine Transfer Function Denominator Coefficient	.0833	sec
B_{2E}	Engine Transfer Function Denominator Coefficient	.00694	sec^2
K_{ET}	Fuel Flow Forward Path Gain	4000	lb/hr/volt
K_{E1}	Fuel Flow Gain - Engine No. 1	1.032	(dimensionless)
K_{E2}	Fuel Flow Gain - Engine No. 2	1.032	(dimensionless)
K_{E3}	Fuel Flow Gain - Engine No. 3	.936	(dimensionless)
K_w	Fuel Flow Conversion Constant	15.81	rad/sec/percent
LIM_{WF1}	Fuel Flow Limit - Engine No. 1	4280	lb/hr
LIM_{WF2}	Fuel Flow Limit - Engine No. 2	4280	lb/hr
LIM_{WF3}	Fuel Flow Limit - Engine No. 3	3600	lb/hr
τ_E	Time Constant - Engine Transfer Function	0.0	sec
τ_{TS}	Time Constant - Nozzle Angle to Fan Blade 3	0.6	sec

FIGURE 9-22

ENGINE HORSEPOWER VS FUEL FLOW

(SHAFT-COUPLED SYSTEM)

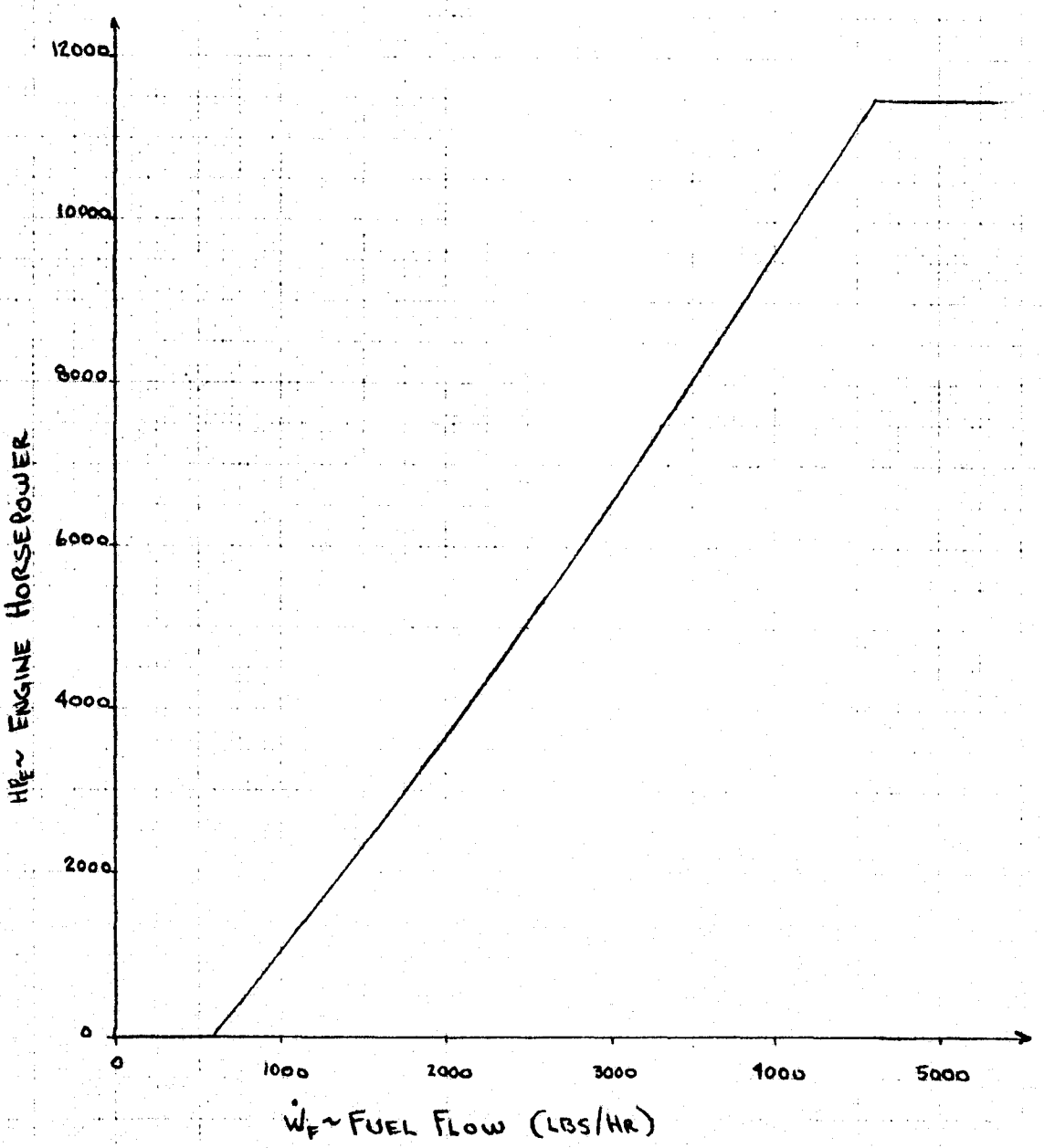

Figure 9-13

SPEED LIMITER SCHEDULE

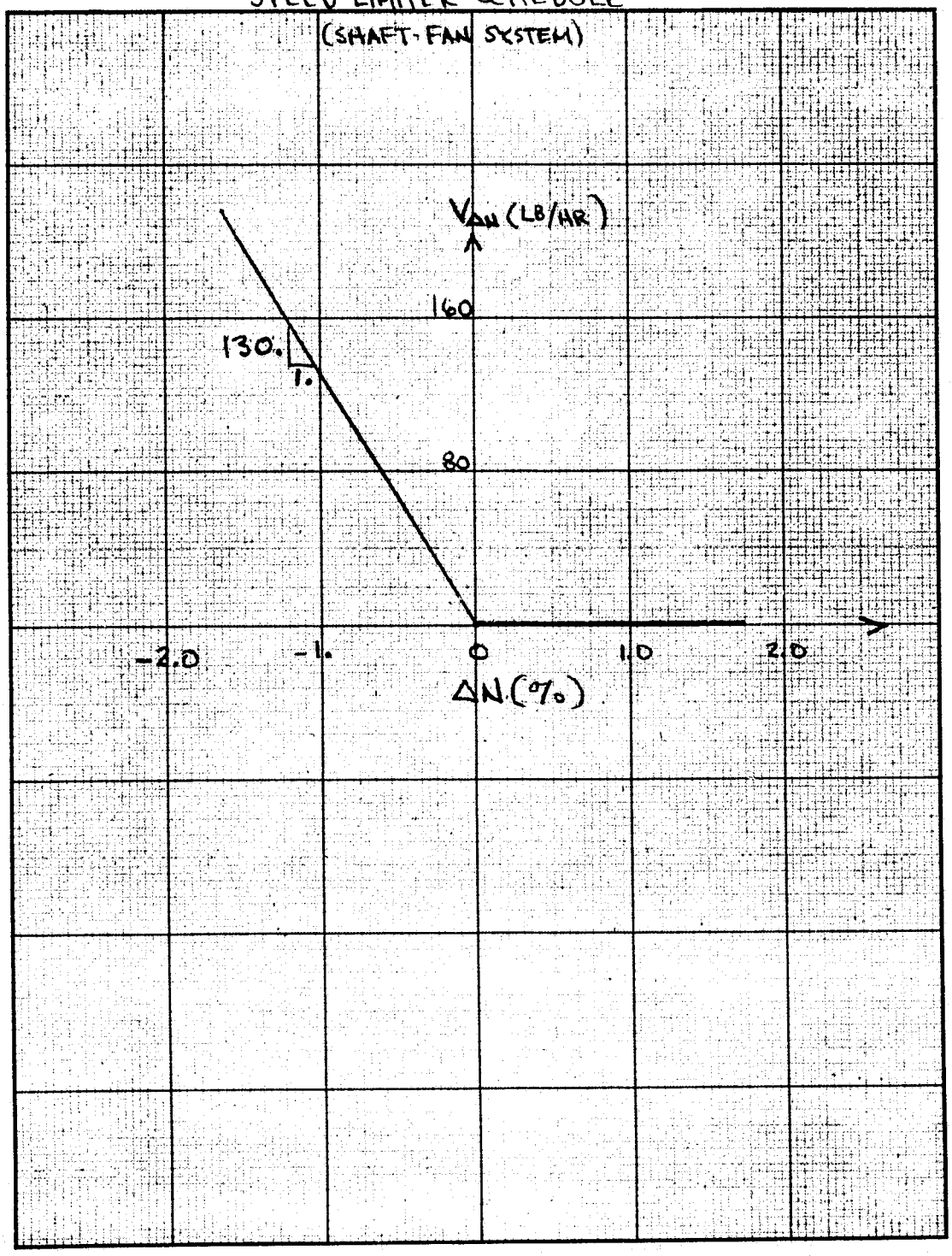

10. FAN DYNAMICS

The fan dynamics model of Figure 10-1 is typical of the three fans used in the gas-coupled configuration of the aircraft; however, as indicated by the subscript "i", the diagram applies to a specific fan. When i = 1, the diagram applies to the left lift/cruise fan, i = 2, the right lift/cruise fan, and i = 3 designates the lift fan.

The inputs to each of the three fans are: tip turbine gas horsepower (HP_i), tip turbine residual thrust (F_{Ti}), and the X-component (u_B) of airspeed. The derivation of horsepower and residual thrust inputs is described in Section 9.

The outputs from each fan model are gross uninstalled thrust (F_{GUi}) and fan airflow ($\dot{m}_{Fi}$). Most of the functions included in fan model computations are represented by exponential equations listed in Figure 10-2. Only the fan gross thrust ratio (F_G/F_{GO}) has to be depicted in graphical form, as shown in Figure 10-3.

The three fans used in the shaft-coupled aircraft configuration are represented by the block diagram of Figure 10-4. The main inputs here are the total horsepower, HP_E, supplied by the three engines, and the three individual blade pitch angle signals, β_1, β_2, and β_3. The computation of the total engine horsepower is described in Section 9 and the actuators for the fan blade pitch angles are described in Section 7. The remaining input, V_{CLUTCH}, is the forward fan clutch signal which is generated as described in Section 8.

The fan model outputs are essentially the same as those provided in the gas-coupled configuration. They are the three gross uninstalled thrust forces (F_{GU1}, F_{GU2}, F_{GU3}) and the individual airflows for each of the three fans ($\dot{m}_{F1}$, $\dot{m}_{F2}$, $\dot{m}_{F3}$). The constants used in the shaft-coupled fan diagram are listed in Figure 10-5. The lift fan and lift/cruise fan thrust plots are presented in

FIGURE 10-1
FAN DYNAMIC MODEL
GAS-COUPLED FANS

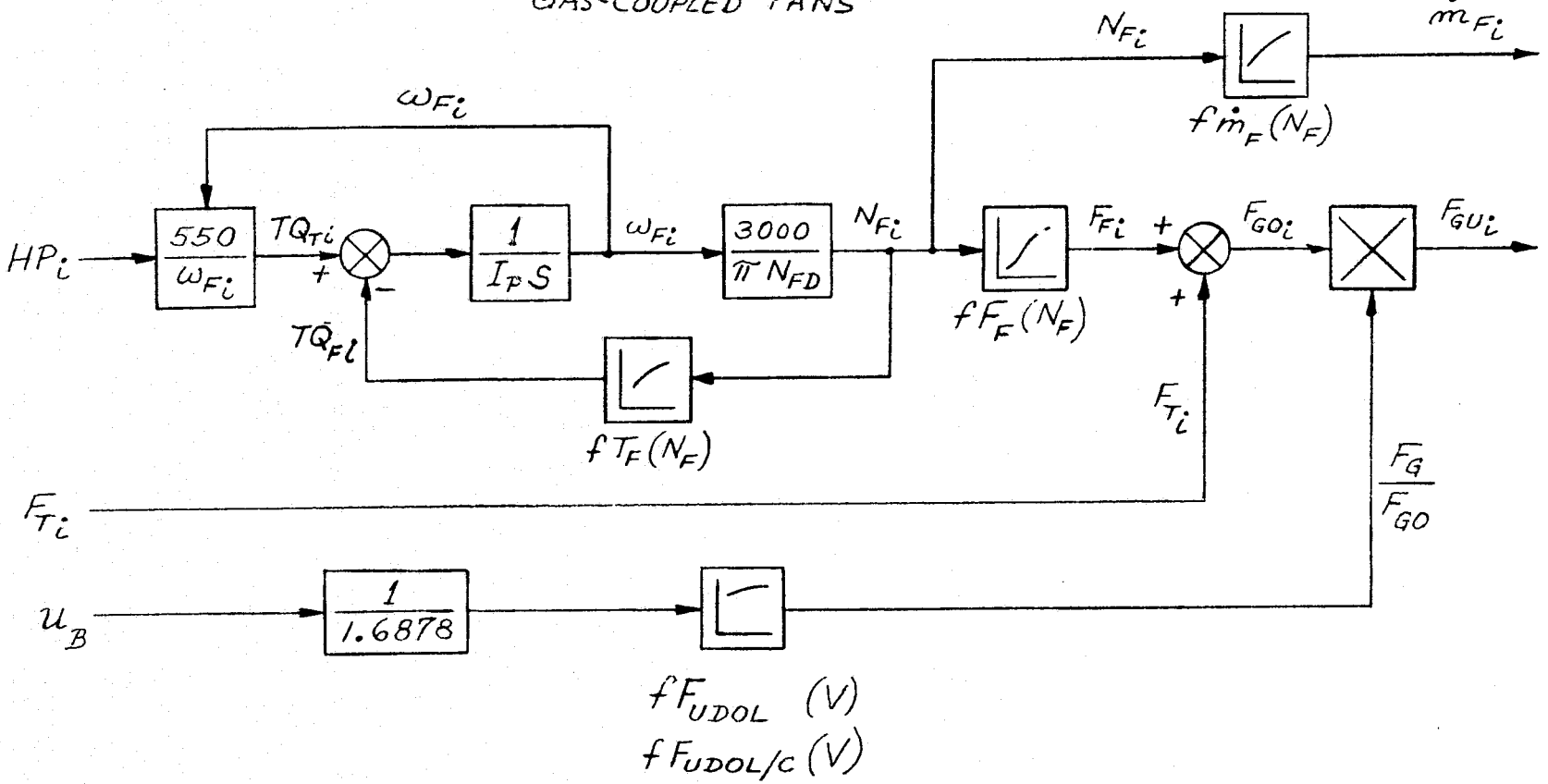

$i = 1, 2, 3$
#1 - LEFT LIFT/CRUISE FAN
#2 - RIGHT LIFT/CRUISE FAN
#3 - LIFT FAN

FIGURE 10-2

FAN DYNAMIC MODEL DATA
GAS FAN

Fan Stream Thrust vs. Fan Speed, $fF_F(N_F)$:

$$F_{F_i} = 0.6513\ (N_{F_i})^{2.152} \qquad \text{lbs}$$

Fan Airflow vs. Fan Speed, $f\dot{m}_F(N_F)$:

$$\dot{m}_{F_i} = 0.1371\ (N_{F_i})^{1.071} \qquad \text{slugs/sec}$$

Fan Torque vs. Fan Speed, $fT_F(N_F)$:

$$TQ_{F_i} = 1.203\ (N_{F_i})^{2.005} \qquad \text{ft-lbs}$$

FAN DYNAMIC MODEL PARAMETERS.

I_P	Fan Rotor Polar Moment of Inertia	21.5 slug ft^2
N_{FD}	Fan Design Speed	4370.0 RPM

FIGURE 10-3

FAN GROSS THRUST RATIO

GAS-COUPLED FANS

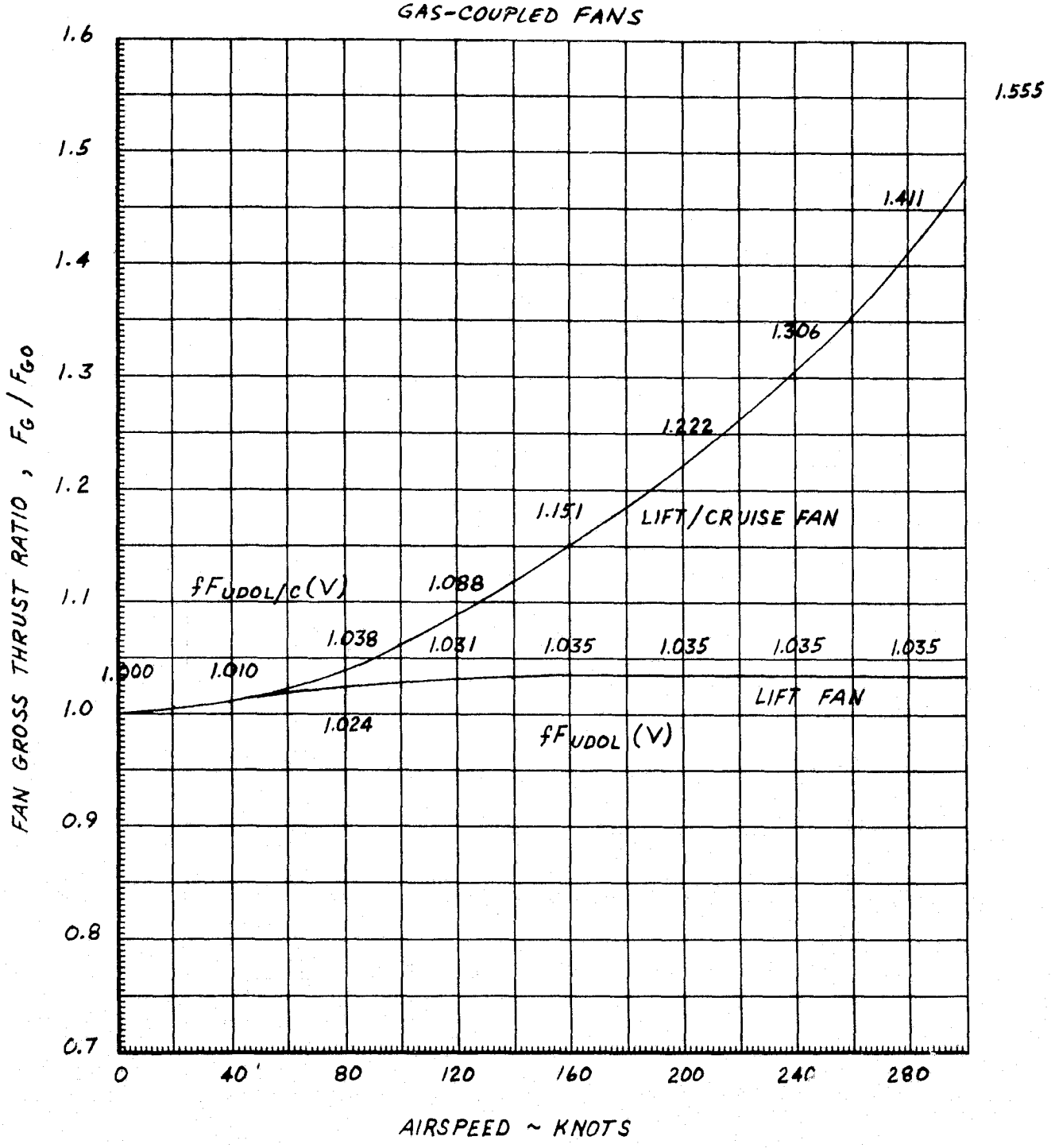

FIGURE 10-4

THREE FANS - DYNAMIC MODEL

(SHAFT-COUPLED SYSTEM)

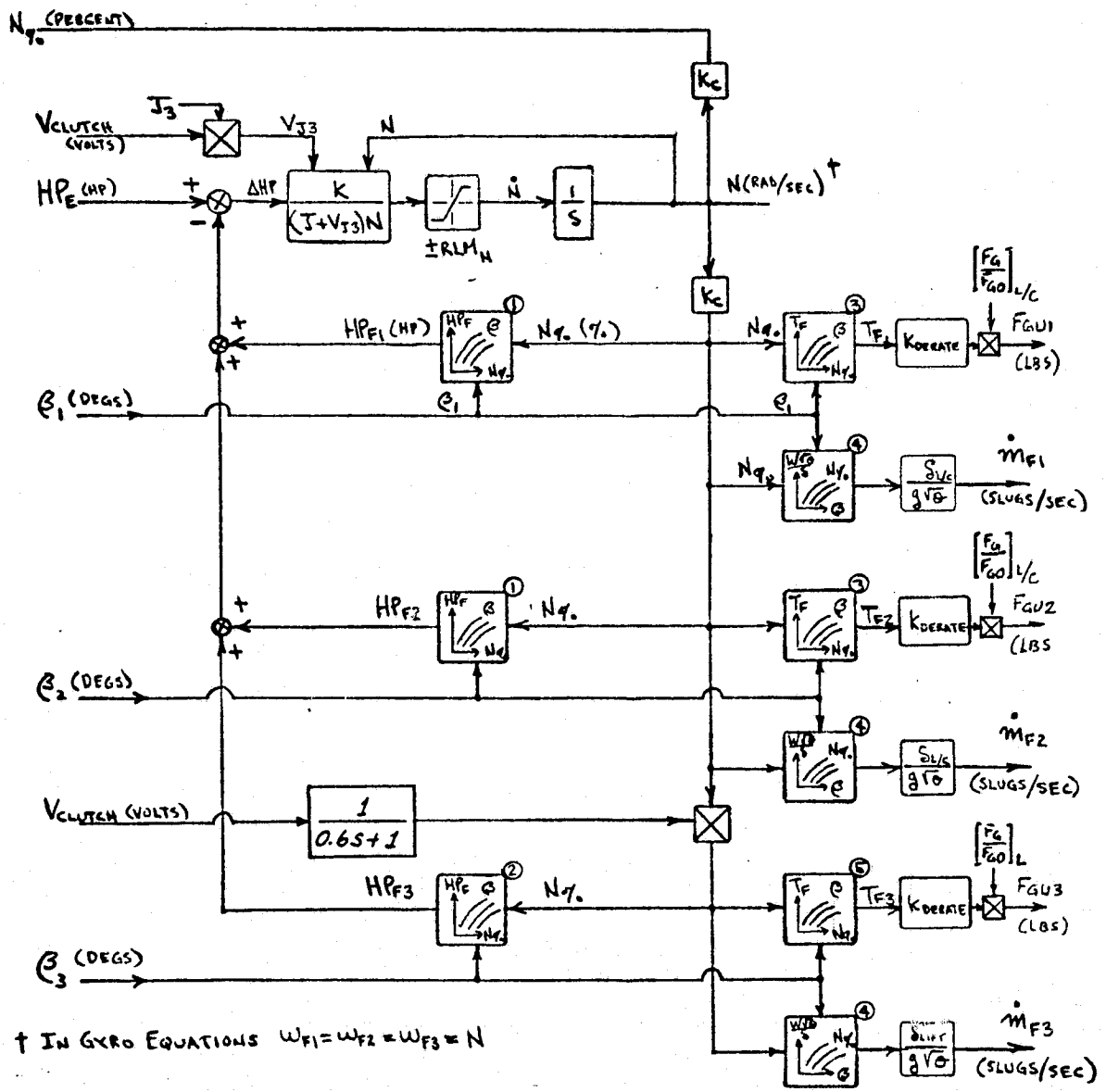

† IN GYRO EQUATIONS $W_{F1} = W_{F2} = W_{F3} \equiv N$

① FAN HP VS. FAN SPEED (LIFT/CRUISE),
② FAN HP VS. FAN SPEED (LIFT)
③ FAN THRUST VS FAN SPEED (LIFT/CRUISE)
④ FAN INLET CORRECTED FLOW VS. BLADE ANGLE
⑤ FAN THRUST VS. FAN SPEED (LIFT)

FIGURE 10-5

FAN DYNAMICS - SYSTEM PARAMETERS

(SHAFT-COUPLED FANS)

g	Gravitational Constant	32.2 ft/sec^2
J	Inertia of the Two L/C Fans	28.5 slug ft^2
J_3	Inertia of the Lift Fan	14.3 slug ft^2
K	Conversion of Units Constant	550. (dimensionless)
K_c	Conversion of Units Constant	.270 percent sec/rad
K_{DERATE}	Fan Thrust Multiplication Factor	1.0333 (dimensionless)
RLM_N	Fan Acceleration Limit	1000 rad/sec^2
δ_{LIFT}	Fan Airflow Correction Factor	.985 (dimensionless)
$\delta_{L/C}$	Fan Airflow Correction Factor	.990 (dimensionless)
$\sqrt{\theta}$	Fan Airflow Temperature Correction Factor	1.03 (dimensionless)

Figures 10-6 and 10-7, respectively. The fan horsepower, required to maintain constant fan speed with each type of fan, is plotted in Figures 10-8 and 10-9. The fan inlet corrected airflow, applicable to all shaft-coupled fans, is presented in Figure 10-10.

FIGURE 10-6

FAN THRUST vs % FAN SPEED

(SHAFT-COUPLED LIFT FAN)

FOR $N_{\%} < 60$ EXTEND LINEARILY TO ZERO AT $N_{\%} = 0$

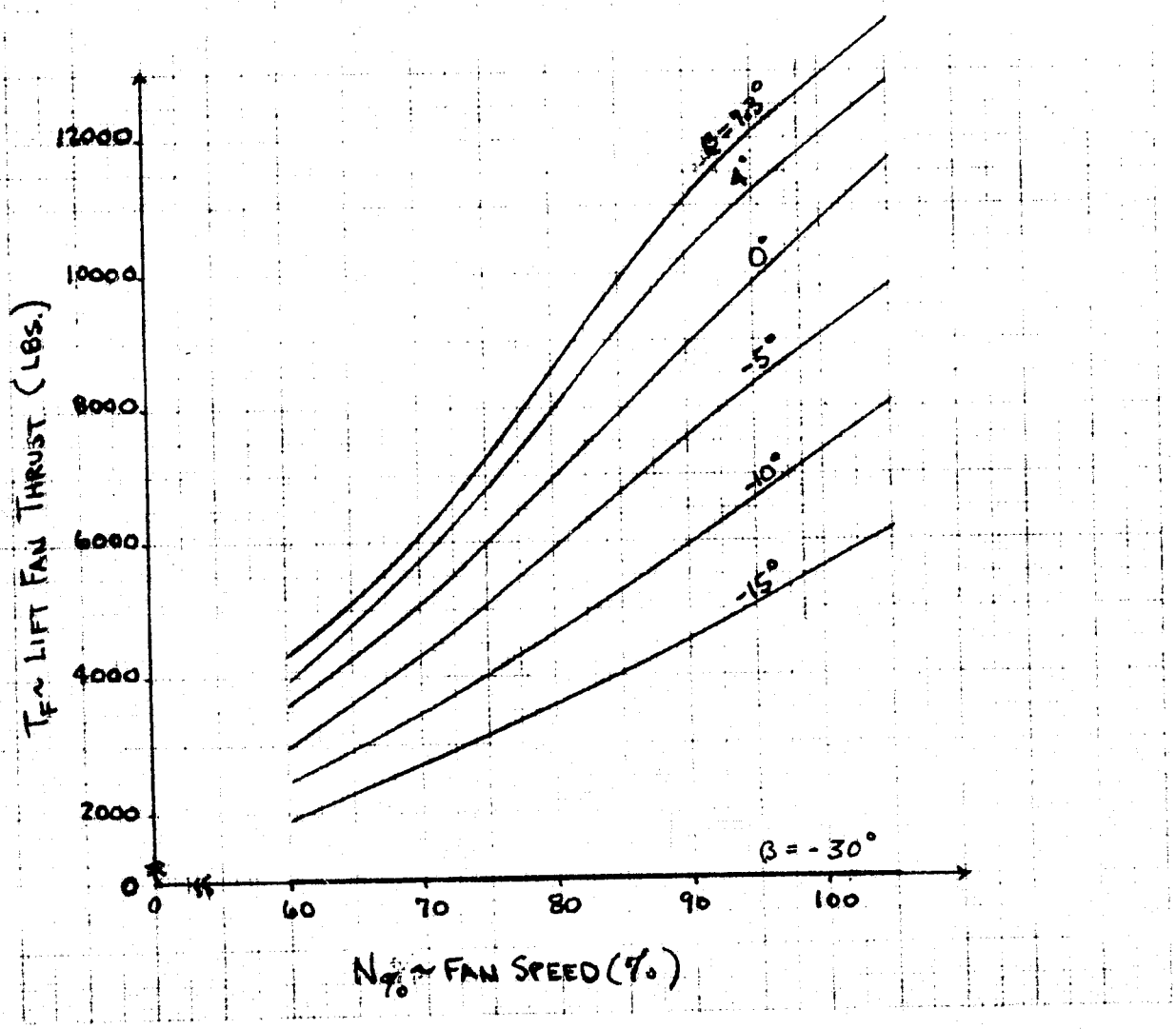

FIGURE 10-7

FAN THRUST VS % FAN SPEED

(SHAFT-COUPLED LIFT/CRUISE FAN)

FOR $N_{\%} < 60$ EXTEND LINEARILY TO ZERO AT $N_{\%} = 0$

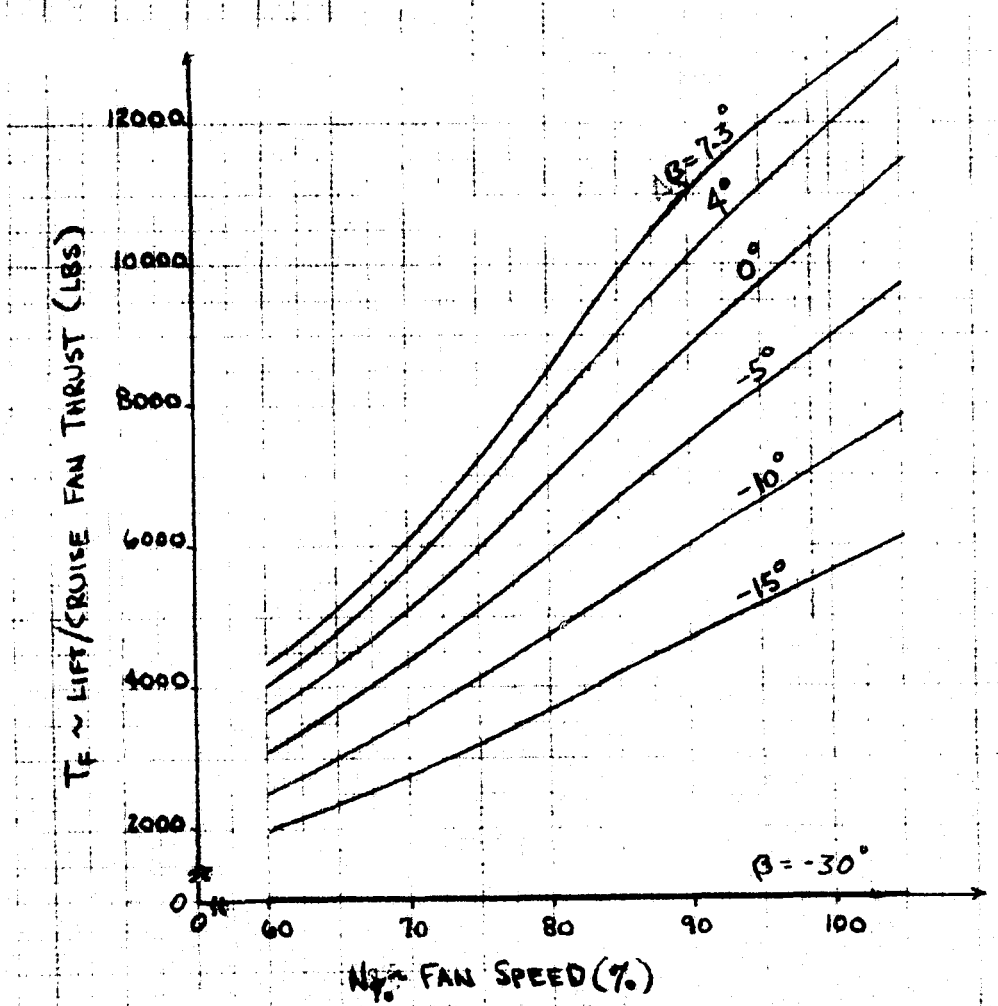

FIGURE 10-8

FAN HORSEPOWER VS % FAN SPEED

(SHAFT-COUPLED LIFT FAN)

FOR $N_{\%} < 60$ EXTEND LINEARILY TO ZERO AT $N_{\%} = 0$

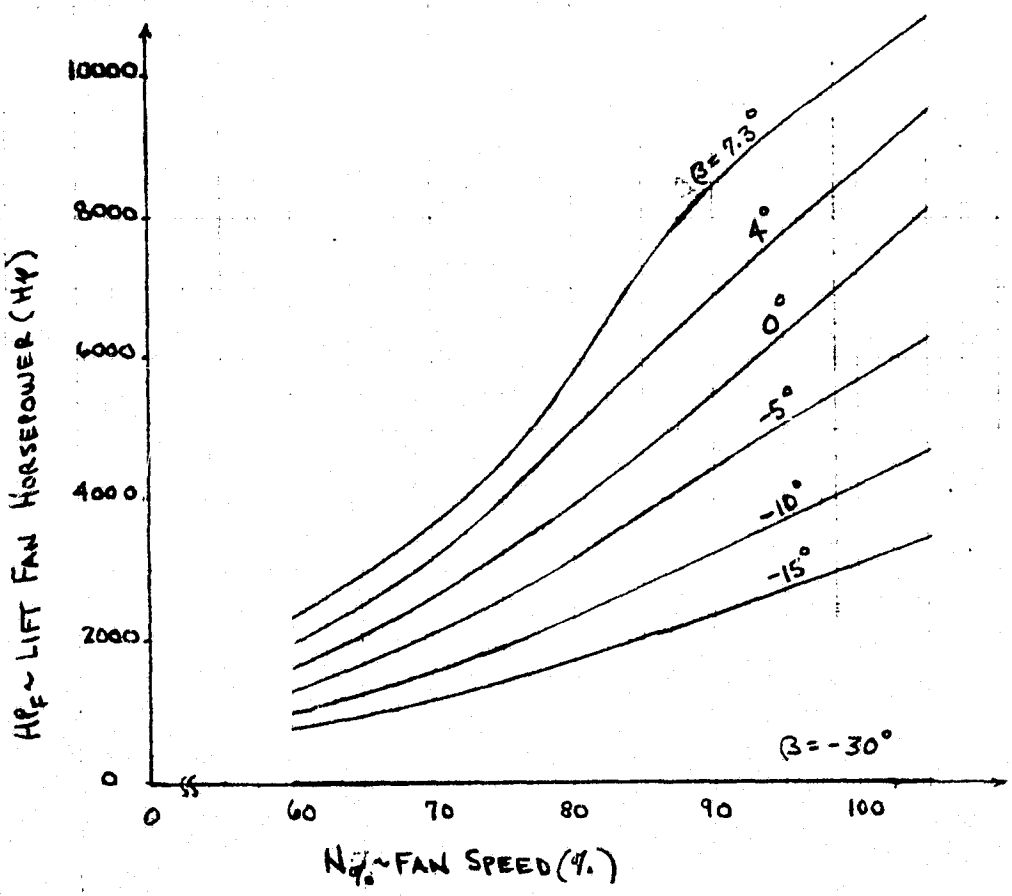

FIGURE 10-9

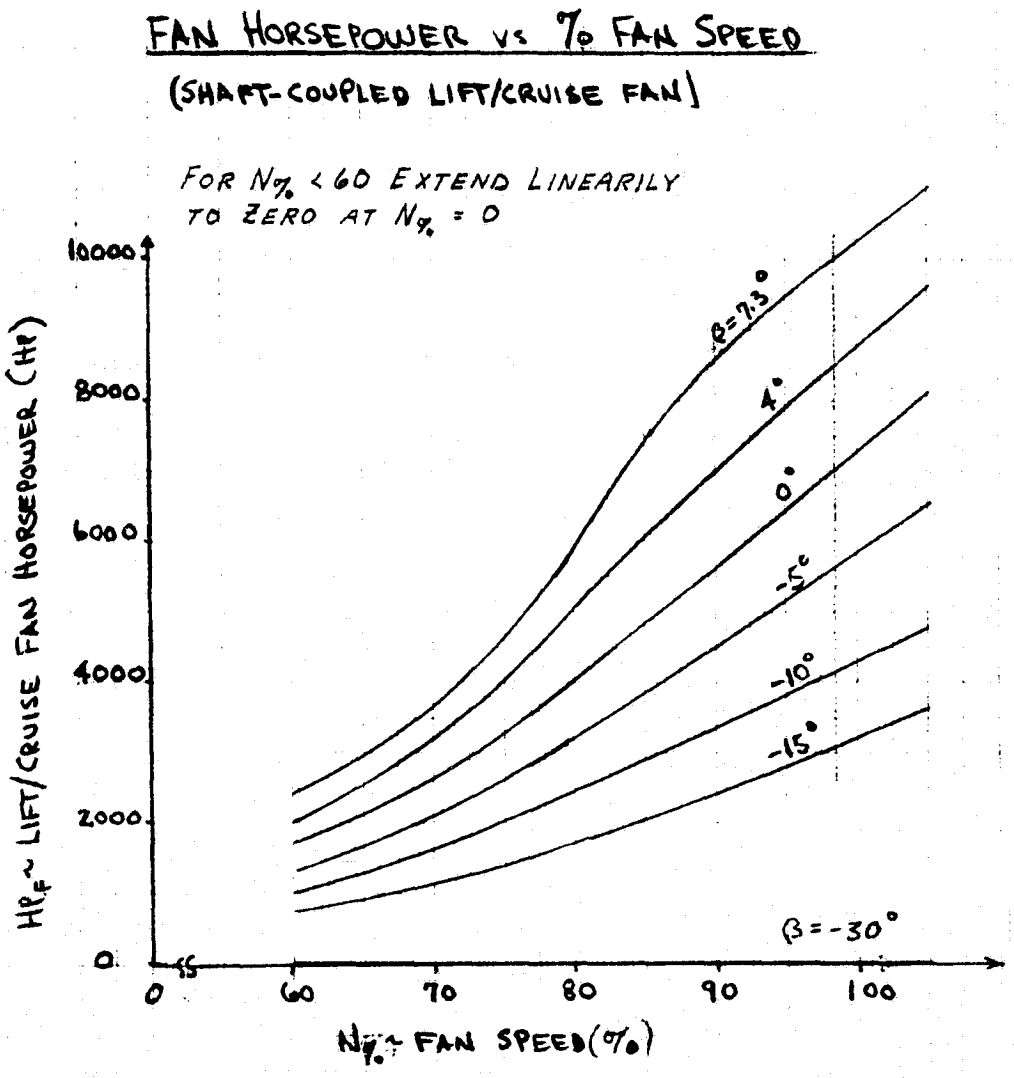
FAN HORSEPOWER vs % FAN SPEED
(SHAFT-COUPLED LIFT/CRUISE FAN)
FOR $N_{\%}$ < 60 EXTEND LINEARILY TO ZERO AT $N_{\%}$ = 0
HP_F ~ LIFT/CRUISE FAN HORSEPOWER (HP)
10000
8000
6000
4000
2000
0
55
0
60
70
80
90
100
$N_{\%}$ ~ FAN SPEED (%)
β = 7.3°
4°
0°
-5°
-10°
-15°
β = -30°

FIGURE 10-10

FAN INLET CORRECTED FLOW VS BLADE ANGLE

(SHAFT-COUPLED FANS)

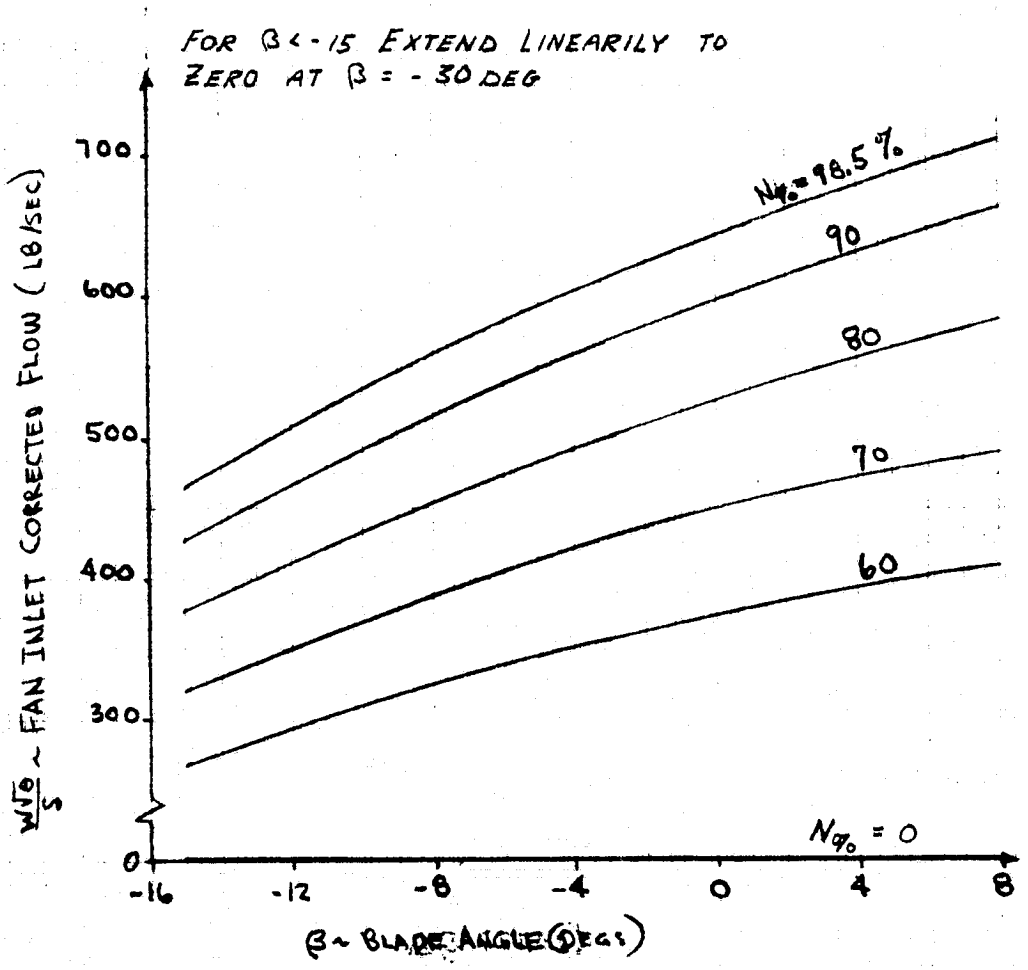

11. THRUST VECTORING SYSTEM

The main fan thrust vectoring is forward and aft thrust deflection commanded by the pilot through the thrust transition lever, ζ_{TL}. Block diagram of Figure 11-1 shows the system which transforms pilot commands into left and right lift/cruise nozzle deflections, θ_1 and θ_2 respectively, and into appropriate forward fan louver angle, θ_3. The constants used in this system are listed in Figure 11-2. Two fan thrust vector schedules are used in the thrust vectoring diagram and are plotted in Figures 11-3 and 11-4.

The thrust of all three fans also can be deflected sideward for aircraft yaw control. Sideward thrust deflection is depicted in Figure 11-5 by parameters α_1, α_2, and α_3. Changes in thrust application points are represented by incremental displacement parameters Δx_1, Δx_2, Δx_3, Δz_1, and Δz_2. The diagram of Figure 11-5 also shows the actual gross thrust (F_{G1}, F_{G2}, and F_{G3}) adjusted from gross uninstalled thrust of each fan (F_{GU1}, F_{GU2}, and F_{GU3}) as a function of TRM parameters σ_1, σ_2, and σ_3 and thrust vector angle (θ_1, θ_2, and θ_3).

All fan thrust functions depicted in Figure 11-5 are supplemented by several pages of detailed data. Figure 11-6 presents the equations defining displacements in thrust application points. Figures 11-7 and 11-8 present thrust reduction ratios (F_{G1}/F_{GU1}, F_{G2}/F_{GU2}, F_{G3}/F_{GU3}) plotted as function of thrust vector angles and TRM parameters. Figures 11-9 and 11-10 present sideward thrust deflection angles (α_1, α_2, α_3) plotted as a function of yaw vane angles and thrust vector angles.

FIGURE 11-1
THRUST VECTORING SYSTEM

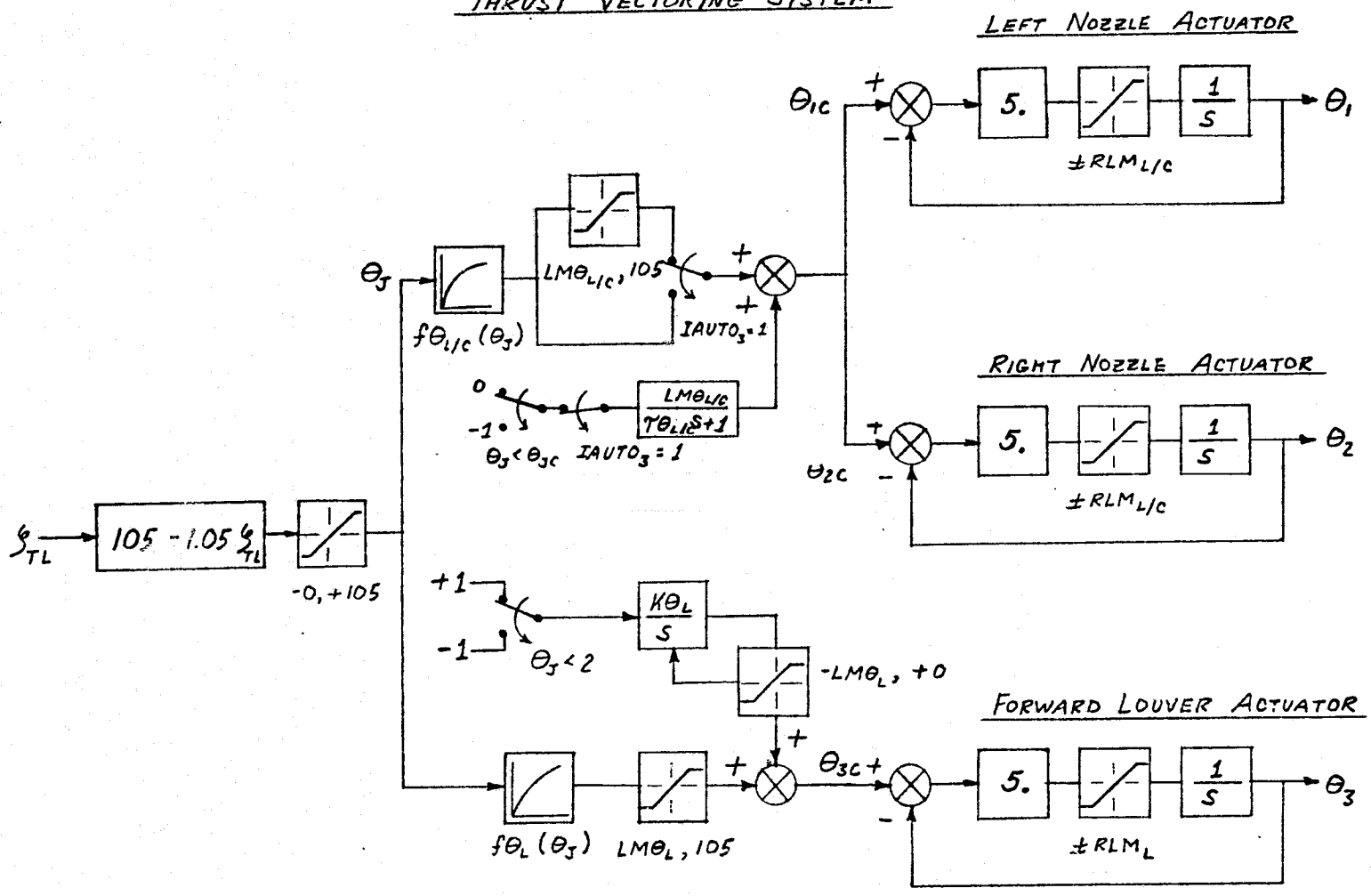

FIGURE 11-2

THRUST VECTORING SYSTEM PARAMETERS

$LM\theta_{L/C}$	Lift/Cruise Thrust Vector Limit	30.0 deg
$LM\theta_{L}$	Lift Fan Thrust Vector Limit	30.0 deg
$\tau\theta_{L/C}$	Lift/Cruise Conversion Time Constant	0.6 sec
$K\theta_{L}$	Lift Fan Conversion Vector Rate	30.0 deg/sec
$RLM_{L/C}$	Lift/Cruise Vector Rate Limit	50.0 deg/sec
RLM_{L}	Lift Fan Vector Rate Limit	50.0 deg/sec
θ_{JC}	Conversion Vector Angle	30.0 deg

FIGURE 11-3

LIFT FAN THRUST VECTOR SCHEDULE

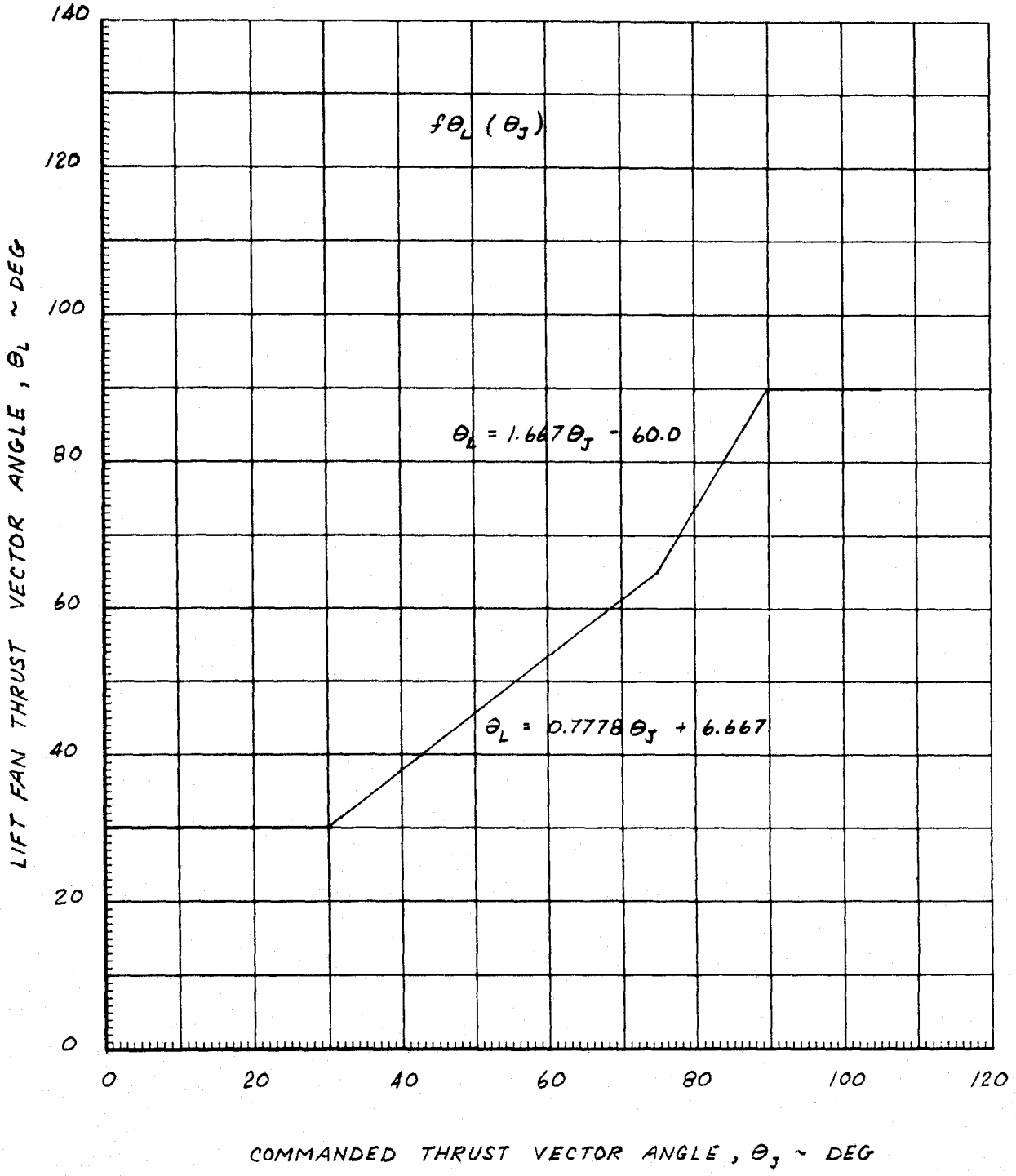

FIGURE 11-4

LIFT / CRUISE FAN THRUST VECTOR SCHEDULE

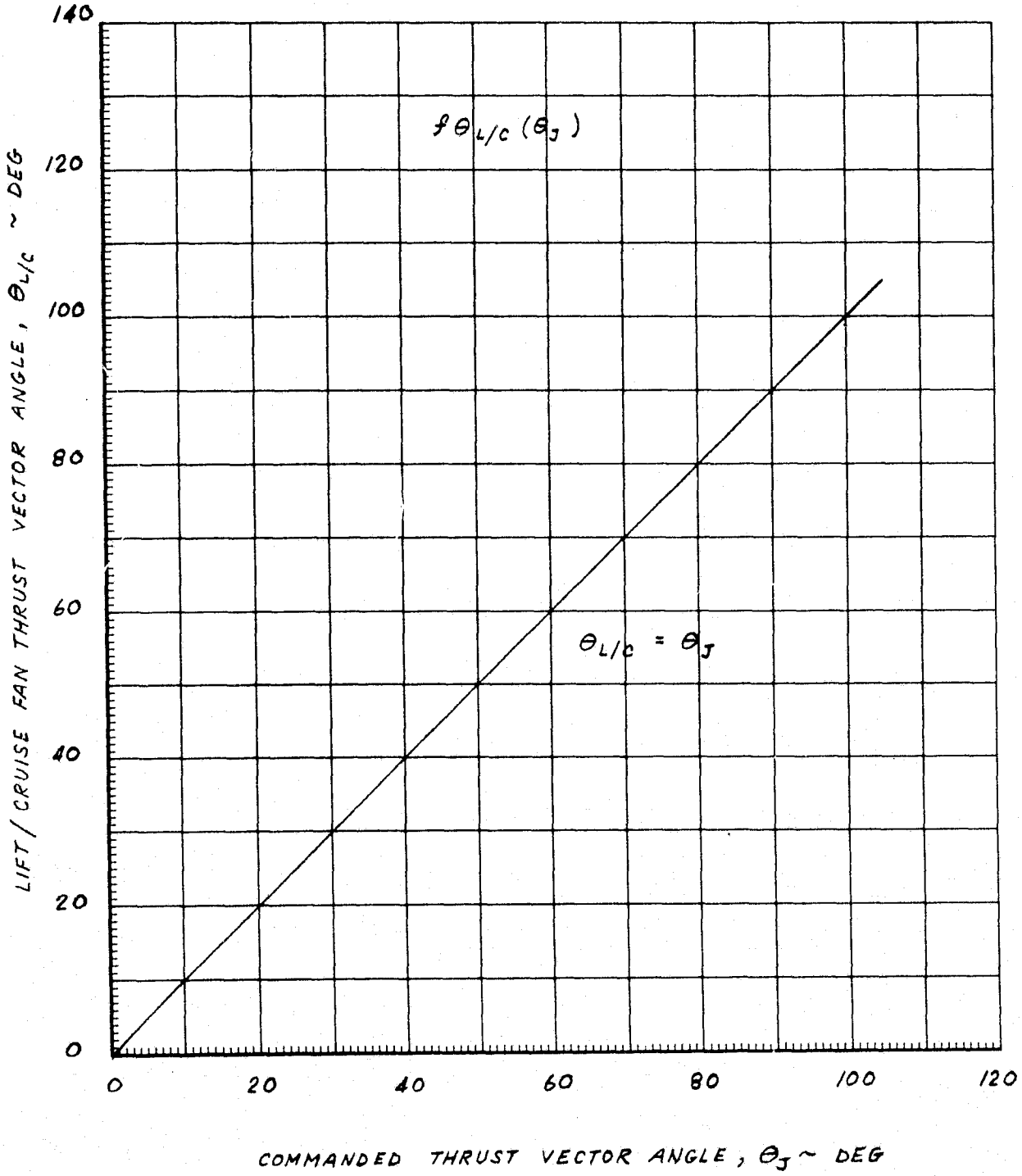

FIGURE 11-5

THRUST VECTORING NOZZLE & LOUVER PERFORMANCE

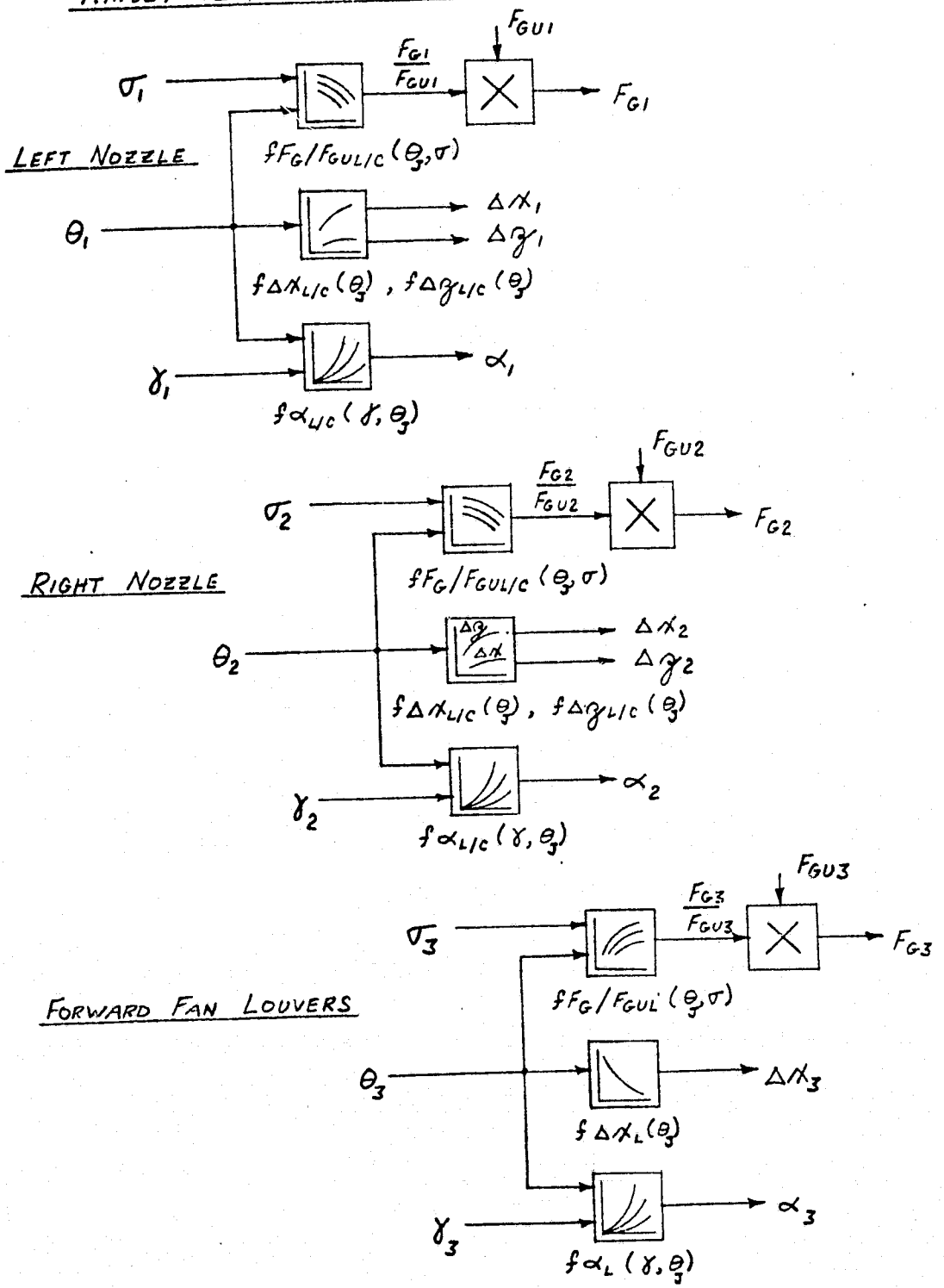

FIGURE 11-6

THRUST VECTORING SYSTEM DATA

Thrust Application Point vs. Vector Angle.

Lift/Cruise Fan: $f\Delta x_{L/C}(\theta_J)$ and $f\Delta z_{L/C}(\theta_J)$

$$\Delta x = 2.583\ (1 - \sin\theta_J)$$

$$\Delta z = -2.583\ \cos\theta_J$$

Lift Fan: $f\Delta x_L(\theta_J)$

$$\Delta x = -2.667\ \cos\theta_3$$

FIGURE 11-7

LIFT FAN GROSS THRUST VS θ_J AND TRM

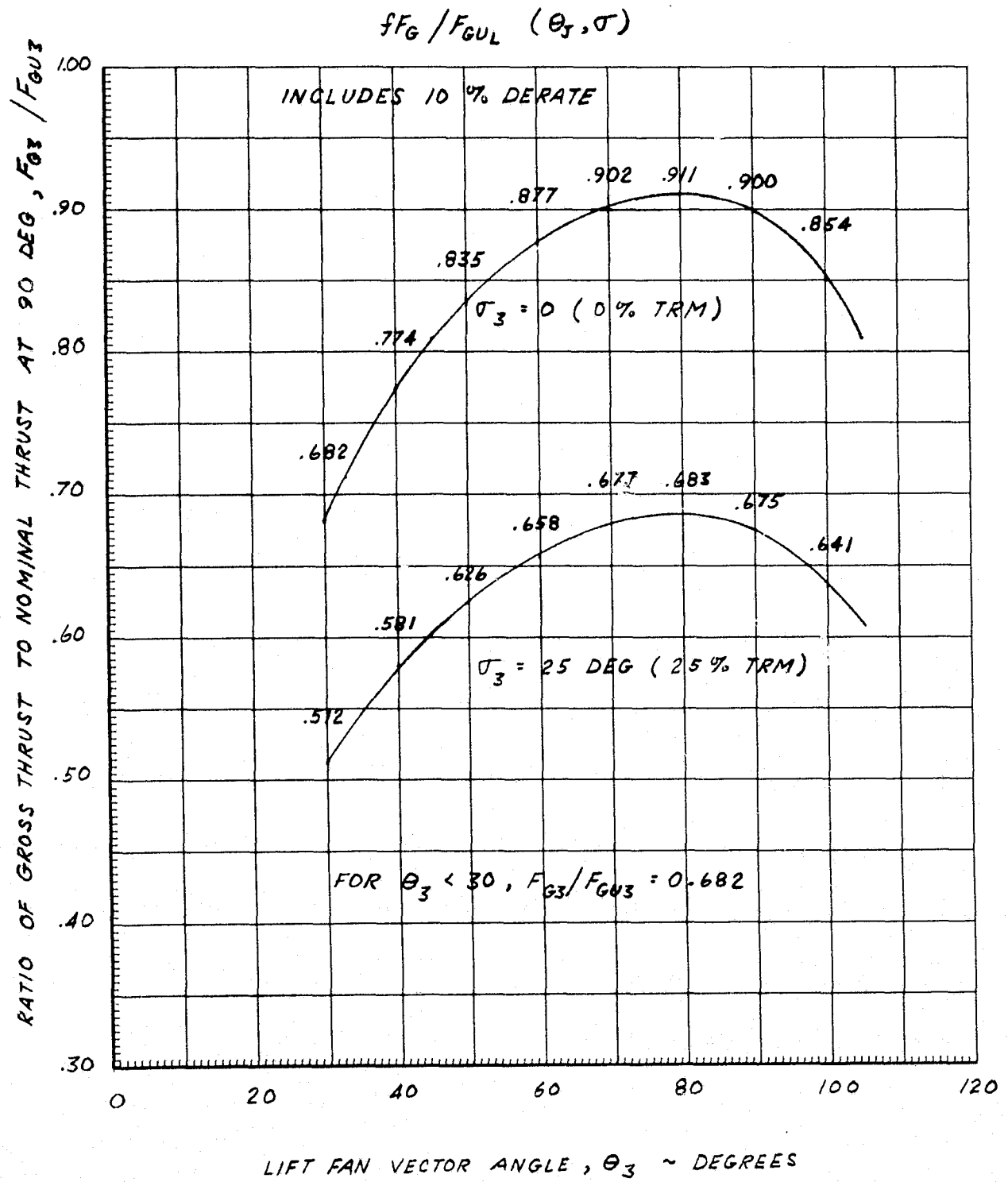

FIGURE 11-8

LIFT / CRUISE FAN GROSS THRUST VS θ_J AND TRM

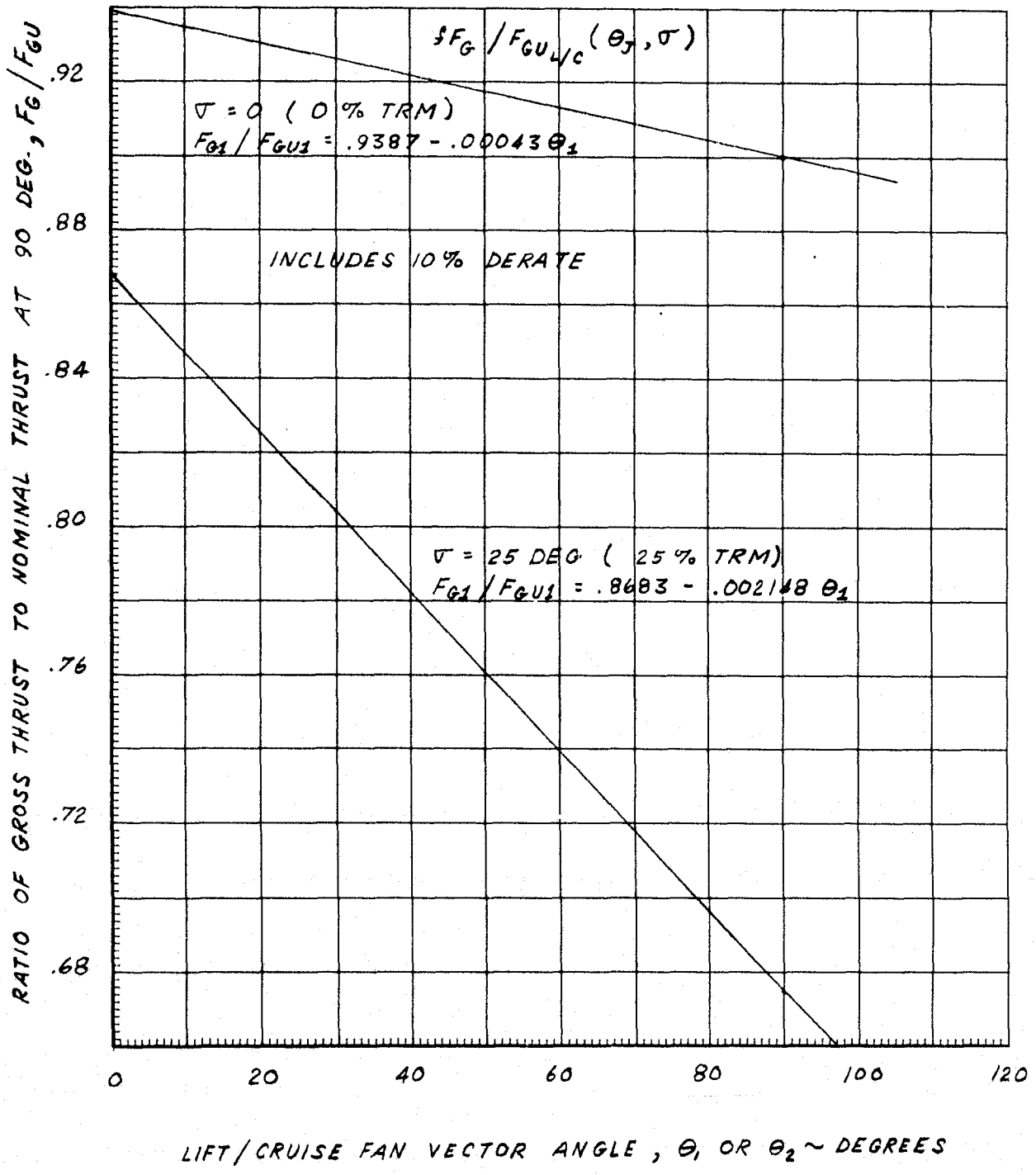

FIGURE 11-9

LIFT FAN YAW VANE EFFECTIVENESS VS. VECTOR ANGLE

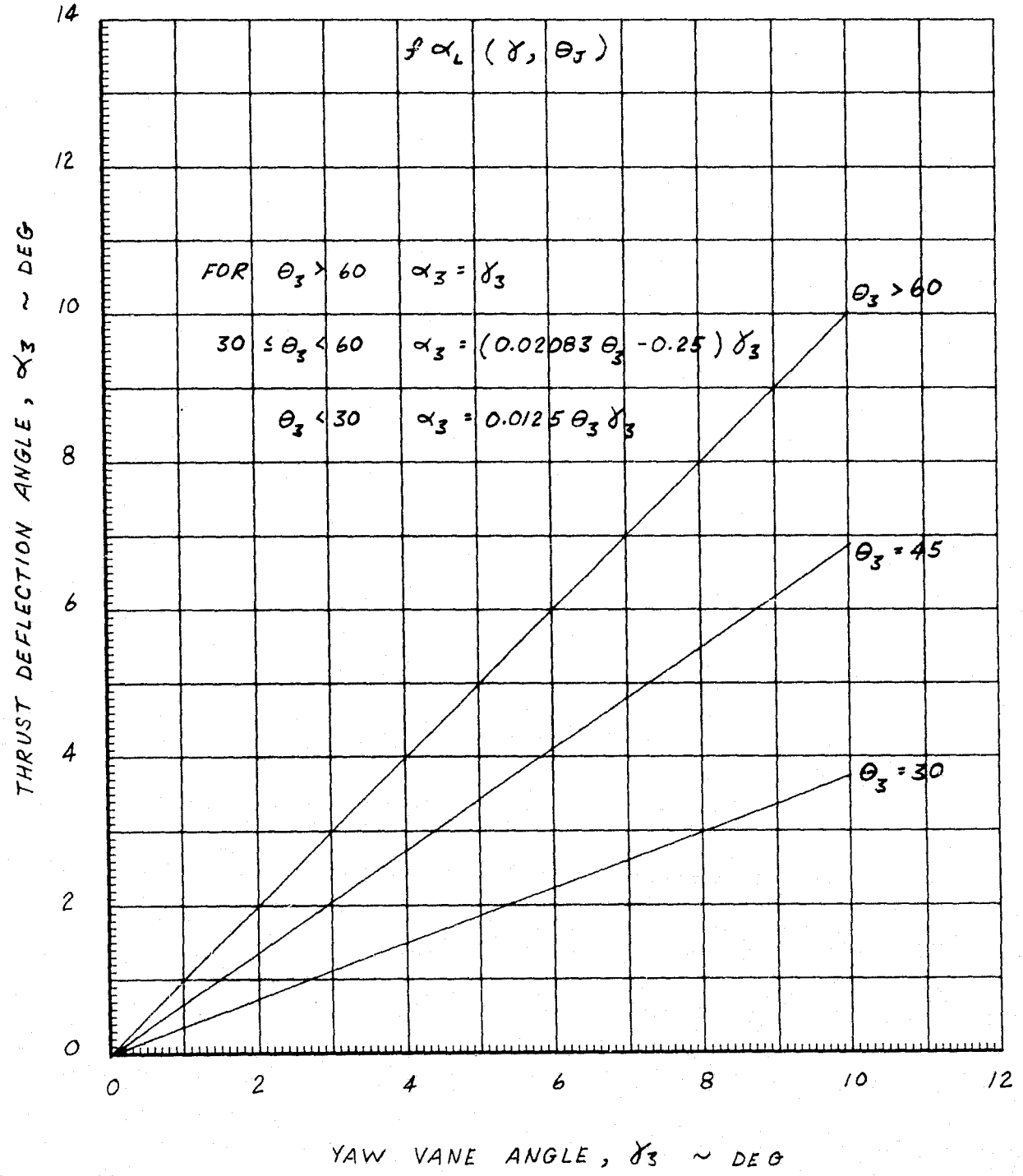

FIGURE 11-10

LIFT/CRUISE YAW VANE EFFECTIVENESS VS. VECTOR ANGLE

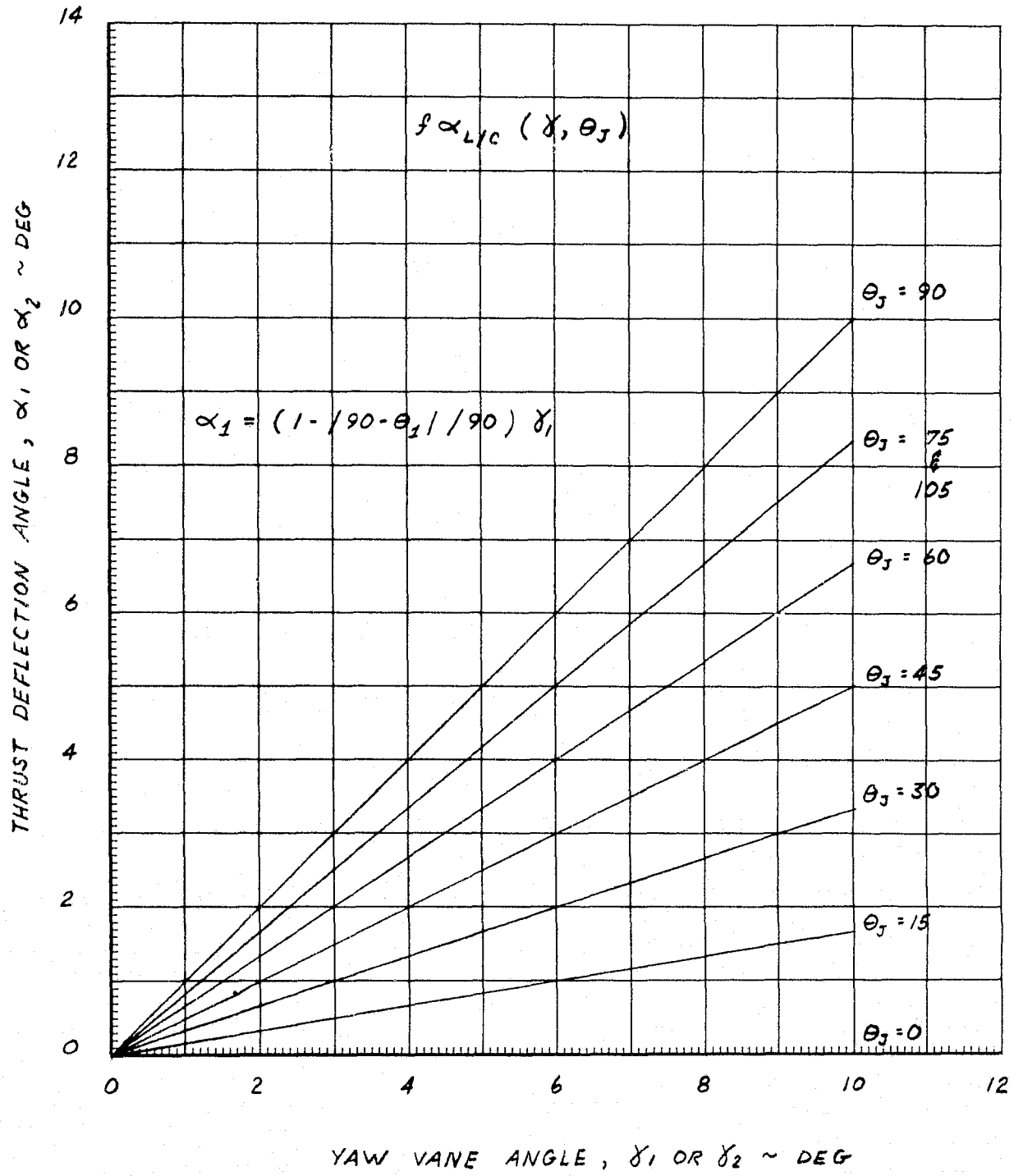

12. FAN FORCE AND MOMENT COMPUTATION AND RESOLUTION

In order to compute total fan thrust forces and moments, thrust of each fan is first resolved into components along the three body axes. The resolution equations are listed in Figure 12-1. Thrust components of each fan are summed separately for each body axis to give the total fan thrust force along each axis (X_F, Y_F, Z_F). Total aircraft moments produced by fan thrust (L_F, M_F, N_F) are also computed separately for each axis, as shown in Figure 12-1. The thrust moment arms are defined in Figure 12-2 and the displacements in thrust application point, used in Figure 12-2, are defined in Section 11.

FIGURE 12-1
FORCE AND MOMENT COMPUTATION AND RESOLUTION

FAN THRUST COMPONENTS

$$F_{X1} = F_{G1} \cos\theta_1 \cos\alpha_1$$
$$F_{Y1} = F_{G1} \sin\alpha_1$$
$$F_{Z1} = -F_{G1} \sin\theta_1 \cos\alpha_1$$

$$F_{X2} = F_{G2} \cos\theta_2 \cos\alpha_2$$
$$F_{Y2} = F_{G2} \sin\alpha_2$$
$$F_{Z2} = -F_{G2} \sin\theta_2 \cos\alpha_2$$

$$F_{X3} = F_{G3} \cos\theta_3 \cos\alpha_3$$
$$F_{Y3} = F_{G3} \sin\alpha_3$$
$$F_{Z3} = -F_{G3} \sin\theta_3 \cos\alpha_3$$

TOTAL FAN FORCES

$$X_F = F_{X1} + F_{X2} + F_{X3}$$
$$Y_F = F_{Y1} + F_{Y2} + F_{Y3}$$
$$Z_F = F_{Z1} + F_{Z2} + F_{Z3}$$

TOTAL FAN MOMENTS

$$L_F = \eta_{TL/C}(F_{Z2} - F_{Z1}) - \zeta_{TL/C}(F_{Y1} + F_{Y2}) - \zeta_{TL} F_{Y3}$$
$$M_F = \zeta_{TL/C}(F_{X1} + F_{X2}) - \chi_{TL/C}(F_{Z1} + F_{Z2}) + \zeta_{TL} F_{X3} - \chi_{TL} F_{Z3}$$
$$N_F = \chi_{TL/C}(F_{Y1} + F_{Y2}) + \eta_{TL/C}(F_{X1} - F_{X2}) + \chi_{TL} F_{Y3}$$

FIGURE 12-2

FAN THRUST APPLICATION POINTS

GAS-COUPLED FANS

$x_{TL/C}$	LIFT/CRUISE FAN	$-9.26 + \Delta x_1$	FT
$y_{TL/C}$		7.54	FT
$z_{TL/C}$		$2.23 + \Delta z_1$	FT
x_{TL}	LIFT FAN	$20.32 + \Delta x_3$	FT
z_{TL}		3.35	FT

SHAFT-COUPLED FANS

$x_{TL/C}$	LIFT/CRUISE FAN	$-10.17 + \Delta x_1$	FT
$y_{TL/C}$		5.48	FT
$z_{TL/C}$		$3.12 + \Delta z_1$	FT
x_{TL}	LIFT FAN	$19.63 + \Delta x_3$	FT
z_{TL}		3.74	FT

13. RAM DRAG FORCES AND MOMENTS

The ram drag forces and moments are computed from fan and engine airflows and from the total linear and angular velocities relative to ambient air. The computation of engine airflows for the gas-coupled configuration is described in Section 8 (Power Lever and Throttle Gearing), but in the shaft-coupled configuration the engine airflows are included in the fan airflows, except for engine No. 3. The effects of this engine (with inlet located near c.g.) were neglected. The fan airflows for both configurations are computed in Section 10. The fan and engine airflows in the gas-coupled system are computed separately for each fan and engine in order to simulate the effects of engine shutdowns and failures. Data available for the shaft-coupled system was insufficient to separate the engine and fan airflow effects.

The ram drag effects are initially expressed in the form of ram drag derivatives defined in Figure 13-1. The derivatives are multiplied by appropriate linear and angular velocity components to compute the total ram drag forces and moments defined in Figure 13-2. Fan and engine inlet locations for the equations of Figure 13-1 are listed in Figure 13-3.

FIGURE 13-1
RAM DRAG FORCES AND MOMENTS

RAM DRAG DERIVATIVES

$$X_u = -\dot{m}_{F1} - \dot{m}_{F2} - \dot{m}_{F3} - \dot{m}_{E1} - \dot{m}_{E2} - \dot{m}_{E3}$$

$$M_u = -z_{FL/C}(\dot{m}_{F1} + \dot{m}_{F2}) - z_{FL}\dot{m}_{F3} - z_{EL/C}(\dot{m}_{E1} + \dot{m}_{E2}) - z_{EL}\dot{m}_{E3}$$

$$M_w = x_{FL/C}(\dot{m}_{F1} + \dot{m}_{F2}) + x_{FL}\dot{m}_{F3} + x_{EL/C}(\dot{m}_{E1} + \dot{m}_{E2}) + x_{EL}\dot{m}_{E3}$$

$$M_q = -[x_{FL/C}^2 + z_{FL/C}^2](\dot{m}_{F1} + \dot{m}_{F2}) - [x_{FL}^2 + z_{FL}^2]\dot{m}_{F3}$$
$$- [x_{EL/C}^2 + z_{EL/C}^2](\dot{m}_{E1} + \dot{m}_{E2}) - [x_{EL}^2 + z_{EL}^2]\dot{m}_{E3}$$

$$Z_w = X_u$$

$$X_q = M_u$$

$$Z_q = M_w$$

$$L_p = -[y_{FL/C}^2 + z_{FL/C}^2](\dot{m}_{F1} + \dot{m}_{F2}) - z_{FL}^2\dot{m}_{F3}$$
$$- [y_{EL/C}^2 + z_{EL/C}^2](\dot{m}_{E1} + \dot{m}_{E2}) - z_{EL}^2\dot{m}_{E3}$$

$$N_r = -[x_{FL/C}^2 + y_{FL/C}^2](\dot{m}_{F1} + \dot{m}_{F2}) - x_{FL}^2\dot{m}_{F3}$$
$$- [x_{EL/C}^2 + y_{EL/C}^2](\dot{m}_{E1} + \dot{m}_{E2}) - x_{EL}^2\dot{m}_{E3}$$

$$L_r = x_{FL/C}z_{FL/C}(\dot{m}_{F1} + \dot{m}_{F2}) + x_{FL}z_{FL}\dot{m}_{F3}$$
$$+ x_{EL/C}z_{EL/C}(\dot{m}_{E1} + \dot{m}_{E2}) + x_{EL}z_{EL}\dot{m}_{E3}$$

$$N_p = L_r$$

$$Y_r = Z_w$$

$$Y_p = L_r = -X_q$$

$$Y_r = N_r = -Z_q$$

FIGURE 13-2

TOTAL RAM DRAG FORCES

$$X_{RAM} = X_u u_B + X_q q_T$$
$$Y_{RAM} = Y_v v_B + Y_p p_T + Y_r r_T$$
$$Z_{RAM} = Z_w w_B + Z_q q_T$$

TOTAL RAM DRAG MOMENTS

$$L_{RAM} = L_v v_B + L_p p_T + L_r r_T$$
$$M_{RAM} = M_u u_B + M_w w_B + M_q q_T$$
$$N_{RAM} = N_v v_B + N_p p_T + N_r r_T$$

FIGURE 13-3

FAN AND ENGINE INLET LOCATIONS

$x_{FL/C}$	LIFT/CRUISE FAN	−1.06 FT
$y_{FL/C}$		7.54 FT
$z_{FL/C}$		−0.50 FT
x_{FL}	LIFT FAN	20.25 FT
z_{FL}		−1.38 FT
$x_{EL/C}$	LIFT/CRUISE ENGINE	9.92 FT
$y_{EL/C}$		4.33 FT
$z_{EL/C}$		0.54 FT
x_{EL}	LIFT ENGINE	0.42 FT
z_{EL}		−4.38 FT

14. AERODYNAMIC FORCES AND MOMENTS

The primary purpose of equations and definitions presented in this section is to transform or redefine the aerodynamic quantities such that they can be first computed in one part of simulation math model and then used correctly in other parts of the model. As in most simulations, the main transformations are those between stability and body axes; i.e. aircraft angular rates are transformed from body to stability axes, while aerodynamic forces and moments are transformed from stability to body axes.

The first set of equations in Figure 14-1 defines three of the main simulation parameters: aircraft velocity (V), angle of attack (α), and angle of sideslip (β). These parameters are computed from body axes velocity components u_B, v_B, and w_B.

Figure 14-2 includes equations defining the dynamic pressure ($\bar{q}$), jet velocity ratios (V/V_J) for all three fans, thrust vector angles (θ_{LCLEFT}, $\theta_{LCRIGHT}$, θ_{NL}), and total gross thrust (T). Transformations of aerodynamic forces and moments to body axes are defined in Figure 14-3. The constant aerodynamic force and moment parameters are listed in Figure 14-4.

FIGURE 14-1
AERODYNAMIC FORCE AND MOMENT EQUATIONS

AIRSPEED, ANGLE OF ATTACK, AND SIDESLIP ANGLE

$$V = \sqrt{u_B^2 + v_B^2 + w_B^2}$$

$$\alpha = \tan^{-1} \frac{w_B}{u_B}$$

$$\beta = \tan^{-1} \frac{v_B}{\sqrt{u_B^2 + w_B^2}}$$

ANGLE OF ATTACK - TABLE LOOKUP

$$\alpha_F = F_\alpha \alpha + F_\theta \theta$$

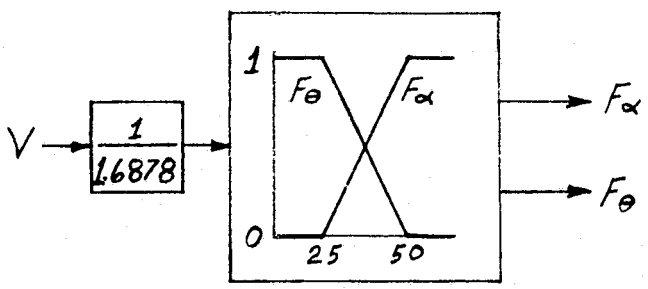

ANGULAR VELOCITY IN STABILITY AXES

$$p_{ST} = p_T \cos\alpha_F + r_T \sin\alpha_F$$

$$q_{ST} = q_T$$

$$r_{ST} = -p_T \sin\alpha_F + r_T \cos\alpha_F$$

FIGURE 14-2

NONDIMENSIONAL ANGULAR VELOCITIES

$$\hat{\theta} = \frac{q_{ST}\bar{C}}{2V} \qquad \hat{p} = \frac{p_{ST}b}{2V}$$

$$\hat{\alpha} = \frac{\dot{\alpha}_F\bar{C}}{2V} \qquad \hat{r} = \frac{r_{ST}b}{2V}$$

JET VELOCITY RATIOS

$$\bar{q} = \frac{1}{2}\rho V^2$$

$$\left(\frac{V}{V_J}\right)_{LCLEFT} = \frac{V}{F_{G1}}\left(\dot{m}_{E1} + \dot{m}_{F1}\right)$$

$$\left(\frac{V}{V_J}\right)_{LCRIGHT} = \frac{V}{F_{G2}}\left(\dot{m}_{E2} + \dot{m}_{F2}\right)$$

$$\left(\frac{V}{V_J}\right)_{NL} = \frac{V}{F_{G3}}\left(\dot{m}_{E3} + \dot{m}_{F3}\right)$$

THRUST VECTOR ANGLES AND GROSS THRUST

$$\theta_{LCLEFT} = \theta_1$$

$$\theta_{LCRIGHT} = \theta_2$$

$$\theta_{NL} = \theta_3$$

$$T_{LC_{LEFT}} = F_{G1}$$

$$T_{LC_{RIGHT}} = F_{G2}$$

$$T_{NL} = F_{G3}$$

FIGURE 14-3

AERODYNAMIC FORCES IN BODY AXES

$$X_A = -D\cos\alpha_F + L\sin\alpha_F$$

$$Y_A = SF$$

$$Z_A = -D\sin\alpha_F - L\cos\alpha_F$$

AERODYNAMIC MOMENTS IN BODY AXES

$$L_A = RM\cos\alpha_F - YM\sin\alpha_F$$

$$M_A = PM$$

$$N_A = RM\sin\alpha_F + YM\cos\alpha_F$$

FIGURE 14-4

AERODYNAMIC FORCE AND MOMENT PARAMETERS

S_w	Wing Area	342.05 ft^2
$\bar{c}$	Mean Aerodynamic Chord	8.38 ft
b	Wing Span	44.43 ft
ρ	Atmospheric Density	0.002246 $slug/ft^3$

15. AERODYNAMIC DATA

The aerodynamic data and equations needed to define the pertinent aerodynamic parameters in stability axes are provided in this section. Definition of longitudinal parameters lift (L), drag (D), and pitching moment (PM) are included and the expressions for these three parameters are presented in Figure 15-1. The main lateral-directional parameters, aerodynamic sideforce (SF), yawing moment (YM), and rolling moment (RM), are defined in Figure 15-2. The associated detailed expressions for longitudinal parameters are presented in Figure 15-3, and equivalent lateral-directional parameter expressions are listed in Figure 15-4.

The basic constants which enter the calculations of aerodynamic parameters are tabulated in Figure 15-5. All other aerodynamic data are presented either as plots or as tabulated data in Figures 15-6 through 15-64. These data are based on wind tunnel results obtained from two sources:

- o MCAIR sponsored small scale wind tunnel tests
- o Large scale testing of a powered model at NASA Ames as reported in Reference listed below (*).

The data applies in the stability axes coordinate system and can be entered in the same form into equations listed in Section 14.

Most of the aerodynamic data graphs are plotted versus fuselage angle of attack, α_F, which is defined in Section 14. The plotted aerodynamic data is typically presented for a fuselage angle of attack range from zero to 32 degrees. The angle α_F is defined equal to airplane pitch angle (θ) at velocities below 25 knots and equal to conventional airplane angle of attack at velocities above 50 knots. Between 25 and 50 knots there is a gradual transition from one definition of α_F to the other.

Reference (*): Orr, J. K., Phillips, E. J., "Wind Tunnel and Ground Static Investigation of a Large Scale Powered Model of a Lift/Cruise Fan V/STOL Aircraft," Report MDC A4318, 2 August 1976.

FIGURE 15-1

SIMULATION MATHEMATICAL MODEL
TOTAL AERODYNAMIC CONTRIBUTIONS
LONGITUDINAL

$$L = \tfrac{1}{2}\rho V^2 S_W \left[C_{L_{WB}} + \Delta C_{L_{GEAR}} \delta_{GEAR} + \Delta C_{L_{DOORS}} + \Delta C_{L_{FLAP}} + \Delta C_{L_{AILERON}} + \left(\frac{S_t}{S_W}\right)(\eta_t)(C_{L_t}\cos\epsilon - C_{D_t}\sin\epsilon) + C_{L_{\dot\theta}}\hat{\dot\theta} + C_{L_{\dot\alpha}}\hat{\dot\alpha} + \Delta C_{L_{GE}} \right] + (\Delta L)_{POWER}$$

$$D = \tfrac{1}{2}\rho V^2 S_W \left[C_{D_{WB}} + \Delta C_{D_{GEAR}} \delta_{GEAR} + \Delta C_{D_{DOORS}} + \Delta C_{D_{FLAP}} + \Delta C_{D_{AILERON}} + \left(\frac{S_t}{S_W}\right)(\eta_t)(C_{D_t}\cos\epsilon + C_{L_t}\sin\epsilon) + \Delta C_{D_{GE}} \right] + (\Delta D)_{POWER}$$

$$PM = \tfrac{1}{2}\rho V^2 S_W \bar{c} \left[C_{m_{WB}} + \Delta C_{m_{GEAR}} \delta_{GEAR} + \Delta C_{m_{DOORS}} + \Delta C_{m_{FLAP}} + \Delta C_{m_{AILERON}} + \left(\frac{S_t}{S_W}\right)(\eta_t)\left(-C_{L_t}\left\{\frac{\ell_t}{\bar{c}}\cos(\alpha_F - \epsilon) + \frac{Z_t}{\bar{c}}\sin(\alpha_F - \epsilon)\right\} + C_{D_t}\left\{\frac{Z_t}{\bar{c}}\cos(\alpha_F - \epsilon) - \frac{\ell_t}{\bar{c}}\sin(\alpha_F - \epsilon)\right\}\right) + C_{m_{\dot\theta}}\hat{\dot\theta} + C_{m_{\dot\alpha}}\hat{\dot\alpha} + \Delta C_{m_{GE}} \right] + \left(\frac{\Delta PM}{\bar{c}}\right)_{POWER} \bar{c}$$

FIGURE 15-2

SIMULATION MATHEMATICAL MODEL
TOTAL AERODYNAMIC CONTRIBUTIONS
LATERAL-DIRECTIONAL

$$SF = \frac{1}{2}\rho V^2 S_w \left[\left(C_{Y_\beta} + \Delta C_{Y_{\beta_{DOORS}}} + \Delta C_{Y_{\beta_{FLAP}}} + \Delta C_{Y_{\beta_{AILERON}}} + \Delta C_{Y_{\beta_{GE}}} \right) \beta + \Delta C_{Y_{AILERON}} + \Delta C_{Y_{RUDDER}} + C_{Y_p} \hat{p} + C_{Y_r} \hat{r} \right] + (\Delta SF)_{POWER}$$

$$YM = \frac{1}{2}\rho V^2 S_w b \left[\left(C_{n_\beta} + \Delta C_{n_{\beta_{DOORS}}} + \Delta C_{n_{\beta_{FLAP}}} + \Delta C_{n_{\beta_{AILERON}}} + \Delta C_{n_{\beta_{GE}}} \right) \beta + \Delta C_{n_{AILERON}} + \Delta C_{n_{RUDDER}} + C_{n_p} \hat{p} + C_{n_r} \hat{r} \right] + \left(\frac{\Delta YM}{b} \right)_{POWER} b$$

$$RM = \frac{1}{2}\rho V^2 S_w b \left[\left(C_{\ell_\beta} + \Delta C_{\ell_{\beta_{DOORS}}} + \Delta C_{\ell_{\beta_{FLAP}}} + \Delta C_{\ell_{\beta_{AILERON}}} + \Delta C_{\ell_{\beta_{GE}}} \right) \beta + \Delta C_{\ell_{AILERON}} + \Delta C_{\ell_{RUDDER}} + C_{\ell_p} \hat{p} + C_{\ell_r} \hat{r} \right] + \left(\frac{\Delta RM}{b} \right)_{POWER} b$$

FIGURE 15-3

SIMULATION MATHEMATICAL MODEL

AERODYNAMIC COMPONENT SUMMATION EQUATIONS

LONGITUDINAL

DEPENDENT VARIABLE(S)	COMPONENT SUMMATION EQUATION
Effect of Fan Closure Doors	$\Delta C_{L_{DOORS}} = \Delta C_{L_{NL}} \delta_{NL_{DOOR}} + 2\,\Delta C_{L_{LC}} \delta_{LC_{DOOR}}$ $\Delta C_{D_{DOORS}} = \Delta C_{D_{NL}} \delta_{NL_{DOOR}} + 2\,\Delta C_{D_{LC}} \delta_{LC_{DOOR}}$ $\Delta C_{m_{DOORS}} = \Delta C_{m_{NL}} \delta_{NL_{DOOR}} + 2\,\Delta C_{m_{LC}} \delta_{LC_{DOOR}}$
Effect of Aileron Deflection (Basic Aerodynamic Parameters)	$\Delta C_{L_{AILERON}} = \Delta C_{L_{LEFT\ AILERON}} + \Delta C_{L_{RIGHT\ AILERON}}$ $\Delta C_{D_{AILERON}} = \Delta C_{D_{LEFT\ AILERON}} + \Delta C_{D_{RIGHT\ AILERON}}$ $\Delta C_{m_{AILERON}} = \Delta C_{m_{LEFT\ AILERON}} + \Delta C_{m_{RIGHT\ AILERON}}$
Downwash at the Horizontal Tail Effect of Drooped Aileron Deflection Power Induced Effects	$\epsilon = \epsilon_{WB} + \Delta\epsilon_{FLAP} + \Delta\epsilon_{AILERON} + \Delta\epsilon_{POWER} + \Delta\epsilon_{GE}$ $\Delta\epsilon_{AILERON} = \frac{1}{2}\left[(\Delta\epsilon)_{LEFT\ AILERON} + (\Delta\epsilon)_{RIGHT\ AILERON}\right]$ $\Delta\epsilon_{POWER} = \left[(\Delta\epsilon)_{NL_{POWER}}\right]_{\Theta_{NL}} + \frac{1}{2}\left\{\left[(\Delta\epsilon)_{LC_{POWER}}\right]_{\Theta_{LC_{LEFT}}} + \left[(\Delta\epsilon)_{LC_{POWER}}\right]_{\Theta_{LC_{RIGHT}}}\right\}$
Tail Efficiency Factor Effect of Drooped Aileron Deflection Power Induced Effects	$\eta_t = \eta_{t_{WB}} + \Delta\eta_{t_{FLAP}} + \Delta\eta_{t_{AILERON}} + \Delta\eta_{t_{POWER}} + \Delta\eta_{t_{GE}}$ $\Delta\eta_{t_{AILERON}} = \frac{1}{2}\left[(\Delta\eta_t)_{LEFT\ AILERON} + (\Delta\eta_t)_{RIGHT\ AILERON}\right]$ $\Delta\eta_{t_{POWER}} = \left[(\Delta\eta_t)_{NL_{POWER}}\right]_{\Theta_{NL}} + \frac{1}{2}\left\{\left[(\Delta\eta_t)_{LC_{POWER}}\right]_{\Theta_{LC_{LEFT}}} + \left[(\Delta\eta_t)_{LC_{POWER}}\right]_{\Theta_{LC_{RIGHT}}}\right\}$
Horizontal Tail Characteristics	$\alpha_t = \alpha_F - \epsilon + \delta_H$
Power Induced Effects Basic Aerodynamic Parameters Effect of Ground Proximity Effect of Roll Angle	$(\ )_{POWER} = (\ )_{NL_{POWER}} + \Sigma(\ )_{LC_{POWER}} + \left[\Delta(\ )_{NL_{POWER}}\right]_{GE} + \Sigma\left[\Delta(\ )_{LC_{POWER}}\right]_{GE} + \Sigma\left[\Delta(\ )_{POWER}\right]_{\phi}$ $(\ )_{NL_{POWER}} + \Sigma(\ )_{LC_{POWER}} = \left[\left(\frac{\Delta X}{T}\right)^*_{NL_{POWER}}\right]_{\Theta_{NL}} T_{NL} + \frac{1}{2}\left\{\left[\left(\frac{\Delta X}{T}\right)^*_{LC_{POWER}}\right]_{\Theta_{LC_{LEFT}}} T_{LC_{LEFT}} + \left[\left(\frac{\Delta X}{T}\right)^*_{LC_{POWER}}\right]_{\Theta_{LC_{RIGHT}}} T_{LC_{RIGHT}}\right\}$ $\left[\Delta(\ )_{NL_{POWER}}\right]_{GE} + \Sigma\left[\Delta(\ )_{LC_{POWER}}\right]_{GE}$ = SAME FORM AS THAT ASSOCIATED WITH FIGURE 10 $\Sigma\left[\Delta(\ )_{POWER}\right]_{\phi}$ = SAME FORM AS THAT ASSOCIATED WITH FIGURE 10

* $\frac{\Delta X}{T}$ represents L, D or $\frac{PM}{c}$

FIGURE 15-4

SIMULATION MATHEMATICAL MODEL
AERODYNAMIC COMPONENT SUMMATION EQUATIONS
LATERAL-DIRECTIONAL

DEPENDENT VARIABLE(S)	COMPONENT SUMMATION EQUATIONS
Effect of Fan Closure Doors	$\Delta C_{Y_{\beta\ DOORS}} = \Delta C_{Y_{\beta\ NL}} \delta_{NL\ DOOR} + \Sigma\, \Delta C_{Y_{\beta\ LC}} \delta_{LC\ DOOR}$ $\Delta C_{n_{\beta\ DOORS}} = \Delta C_{n_{\beta\ NL}} \delta_{NL\ DOOR} + \Sigma\, \Delta C_{n_{\beta\ LC}} \delta_{LC\ DOOR}$ $\Delta C_{\ell_{\beta\ DOORS}} = \Delta C_{\ell_{\beta\ NL}} \delta_{NL\ DOOR} + \Sigma\, \Delta C_{\ell_{\beta\ LC}} \delta_{LC\ DOOR}$
Effect of Drooped Aileron Deflection	$\Delta C_{Y_{\beta\ AILERON}} = \Delta C_{Y_{\beta\ LEFT\ AILERON}} + \Delta C_{Y_{\beta\ RIGHT\ AILERON}}$ $\Delta C_{n_{\beta\ AILERON}} = \Delta C_{n_{\beta\ LEFT\ AILERON}} + \Delta C_{n_{\beta\ RIGHT\ AILERON}}$ $\Delta C_{\ell_{\beta\ AILERON}} = \Delta C_{\ell_{\beta\ LEFT\ AILERON}} + \Delta C_{\ell_{\beta\ RIGHT\ AILERON}}$
Aileron Effectiveness	$\Delta C_{Y_{AILERON}} = \Delta C_{Y_{LEFT\ AILERON}} + \Delta C_{Y_{RIGHT\ AILERON}}$ $\Delta C_{n_{AILERON}} = \Delta C_{n_{LEFT\ AILERON}} + \Delta C_{n_{RIGHT\ AILERON}}$ $\Delta C_{\ell_{AILERON}} = \Delta C_{\ell_{LEFT\ AILERON}} + \Delta C_{\ell_{RIGHT\ AILERON}}$
Power Induced Effects Basic Aerodynamic Parameters Effect of Ground Proximity Effect of Roll Angle	$()_{POWER} = ()_{NL\ POWER} + \Sigma()_{LC_{POWER}} + \left[\Delta()_{NL_{POWER}}\right]_{GE} + \Sigma\left[\Delta()_{LC\ POWER}\right]_{GE} + \Sigma\left[\Delta()_{POWER}\right]_{\phi}$ $()_{NL_{POWER}} + \Sigma()_{LC_{POWER}} = \left[\left(\frac{\Delta X}{T}\right)^{*}_{NL_{POWER}}\right]_{\delta_{NL}} T_{NL} + \frac{1}{2}\left\{\left[\left(\frac{\Delta X}{T}\right)^{*}_{LC_{POWER}}\right]_{\delta_{LC_{LEFT}}} T_{LC_{LEFT}} + \left[\left(\frac{\Delta X}{T}\right)^{*}_{LC_{POWER}}\right]_{\delta_{LC_{RIGHT}}} T_{LC_{RIGHT}}\right\}$ $\left[\Delta()_{NL_{POWER}}\right]_{GE} + \Sigma\left[\Delta()_{LC_{POWER}}\right]_{GE}$ = SAME FORM AS THAT ASSOCIATED WITH FIGURE 25 $\Sigma\left[\Delta()_{POWER}\right]_{\phi}$ = SAME FORM AS THAT ASSOCIATED WITH FIGURE 25

* X represents SF, $\frac{YM}{b}$ or $\frac{RM}{b}$

FIGURE 15-5

PHYSICAL CHARACTERISTICS DATA

S_w	Wing Area	342.05 ft^2
b	Wing Span	44.43 ft
$\bar{c}$	Mean Aerodynamic Chord	8.38 ft
S_t	Horizontal Tail Area	75.10 ft^2
ℓ_t	Tail Moment Arm	21.20 ft
Z_t	Tail Moment Arm	8.17 ft

AIR DENSITY - 90°F DAY

ρ	Atmospheric Density	0.002246 $slug/ft^3$

FIGURE 15-6

WING-BODY LIFT CHARACTERISTICS
AERODYNAMIC FLIGHT CONFIGURATION

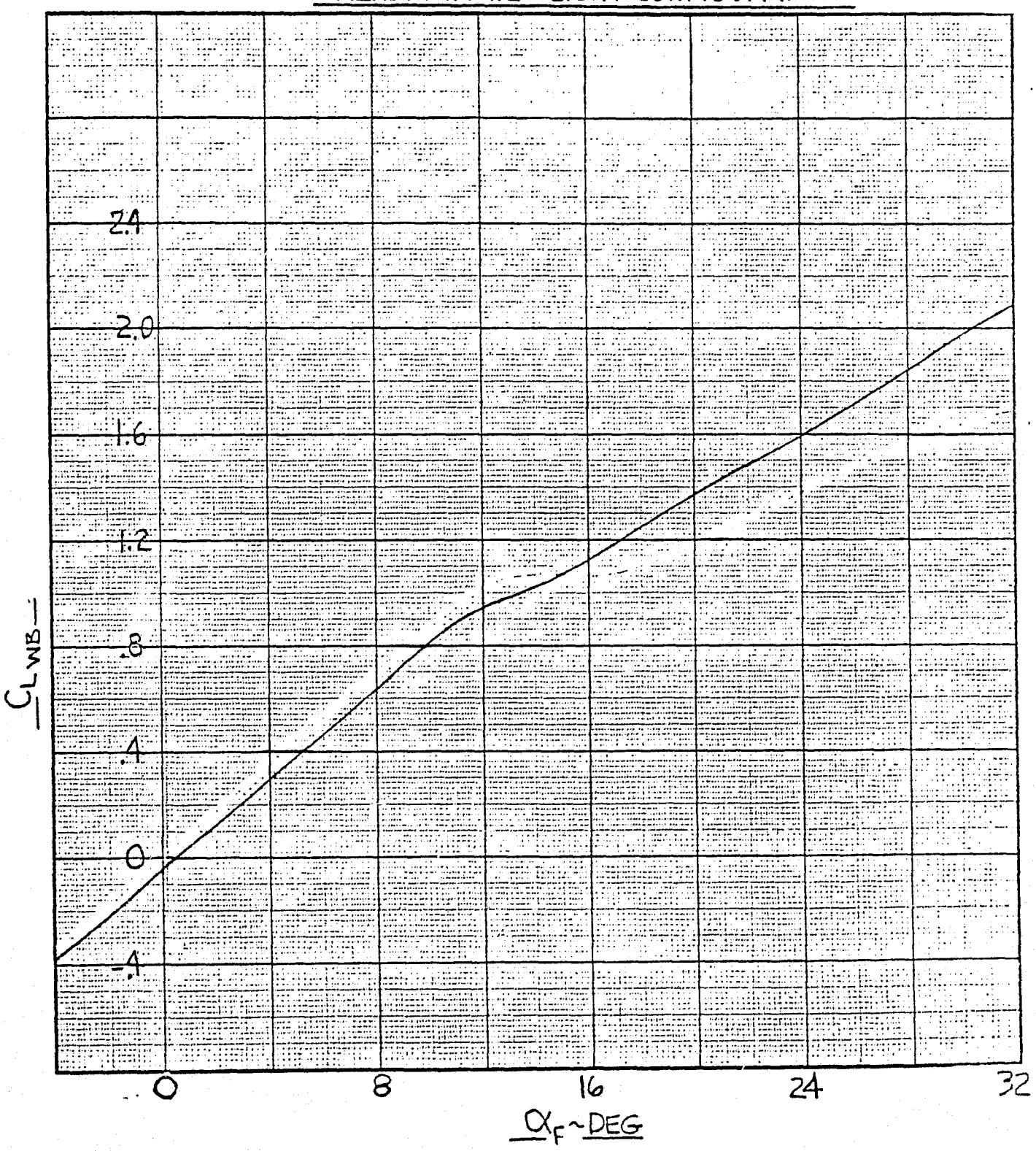

FIGURE 15-7
WING-BODY DRAG CHARACTERISTICS
AERODYNAMIC FLIGHT CONFIGURATION

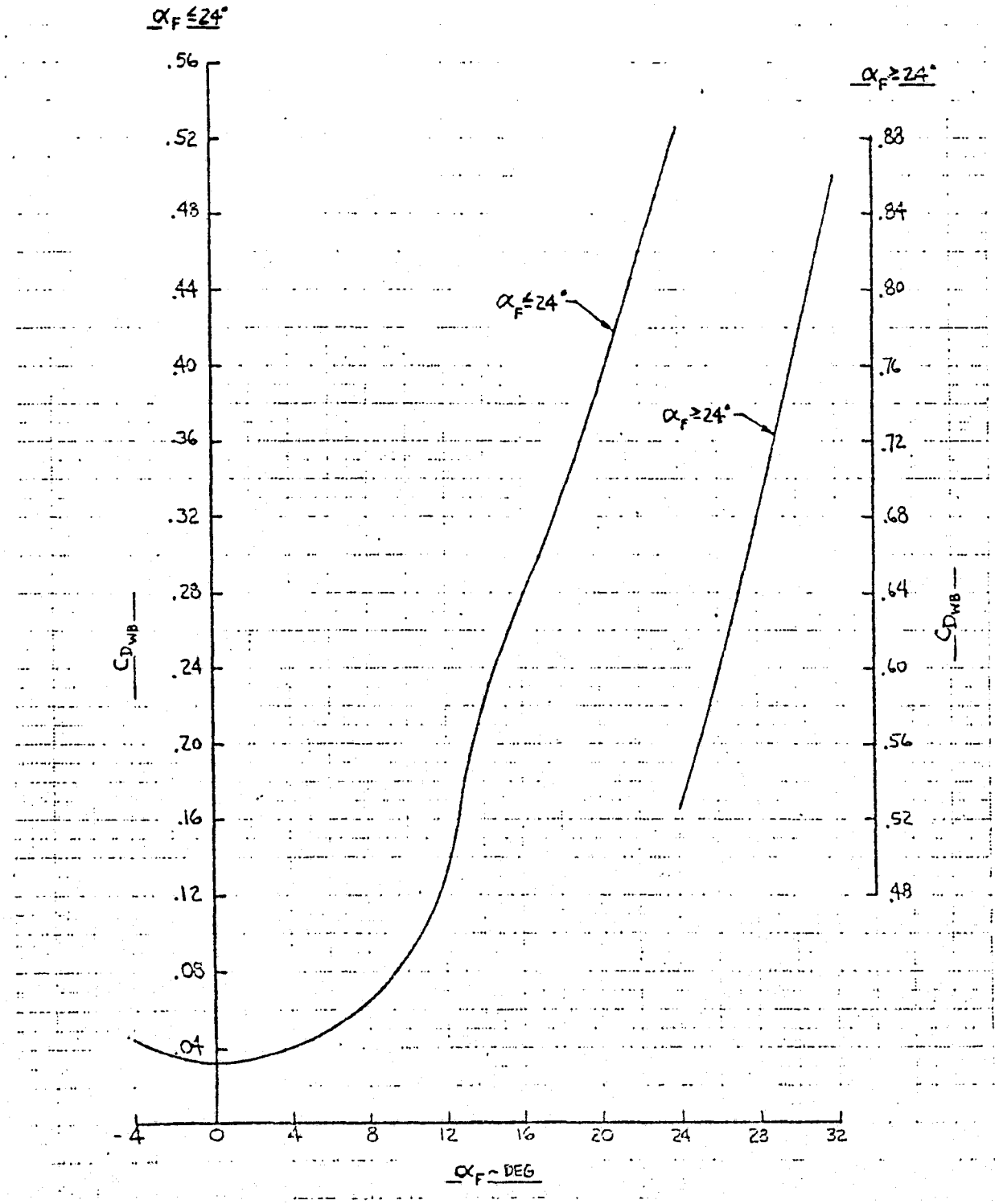

FIGURE 15-8

WING-BODY PITCHING MOMENT CHARACTERISTICS

AERODYNAMIC FLIGHT CONFIGURATION

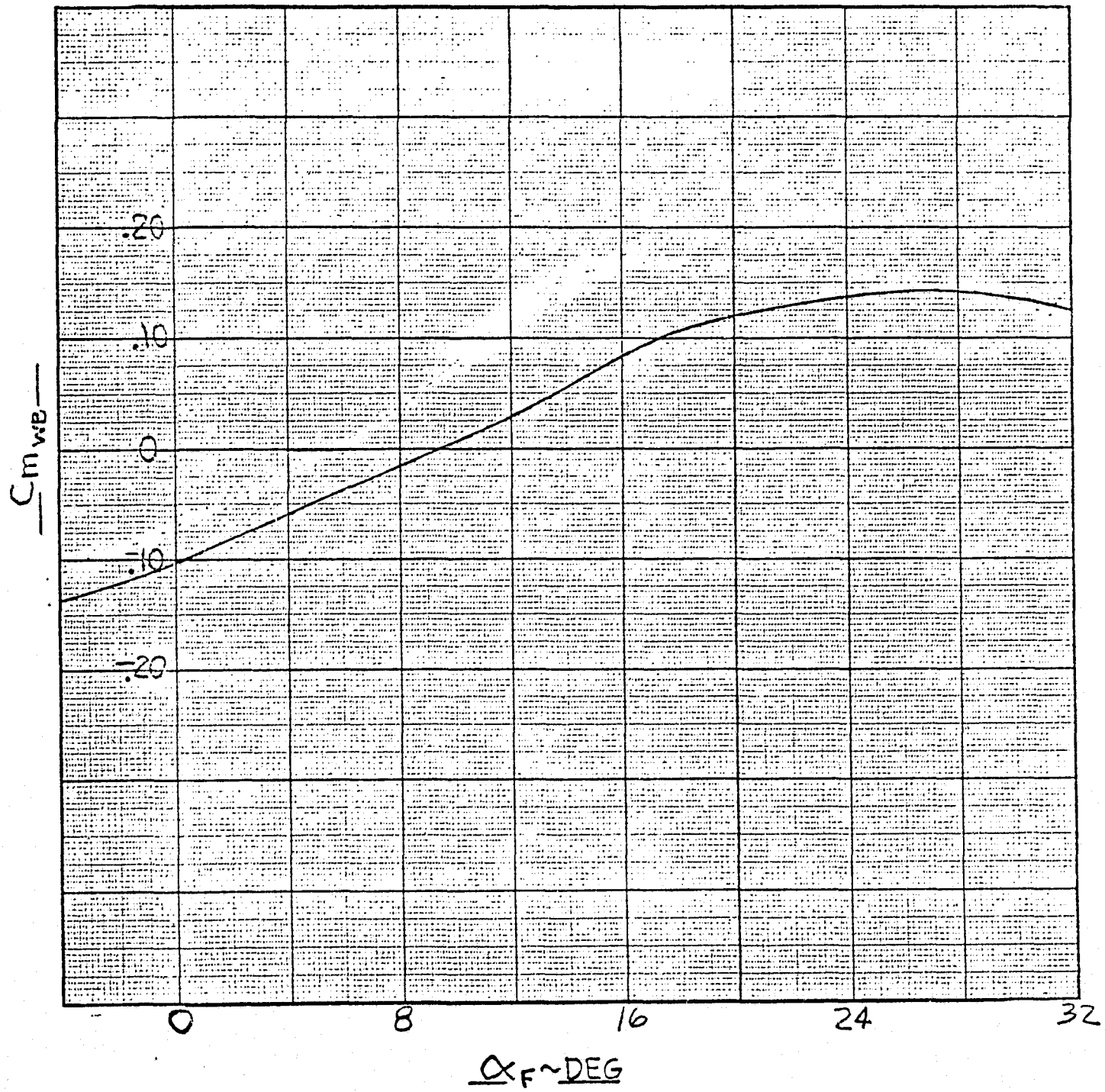

FIGURE 15-9

DOWNWASH AT THE HORIZONTAL TAIL
AERODYNAMIC FLIGHT CONFIGURATION

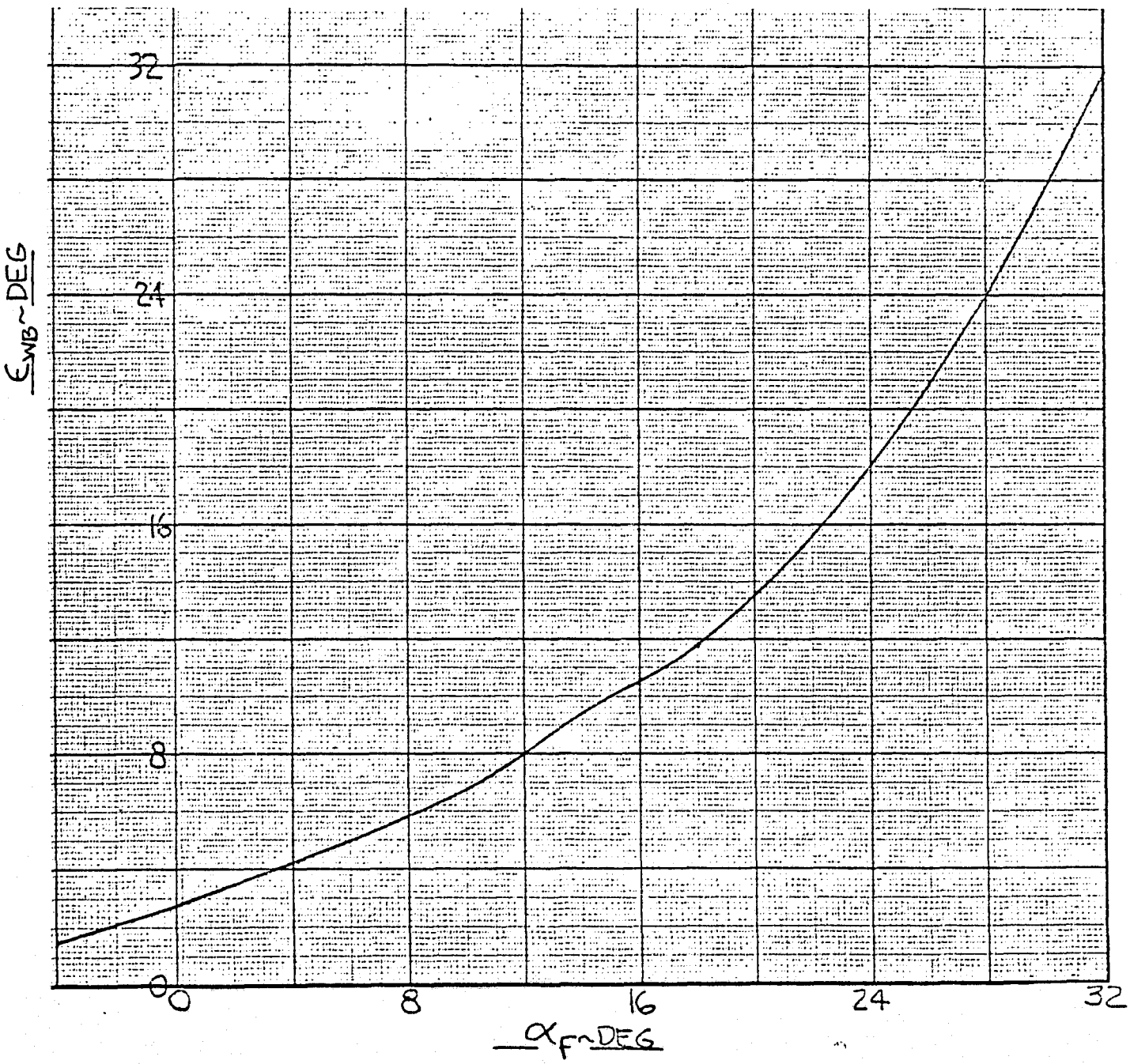

FIGURE 15-10

TAIL EFFICIENCY FACTOR
AERODYNAMIC FLIGHT CONFIGURATION

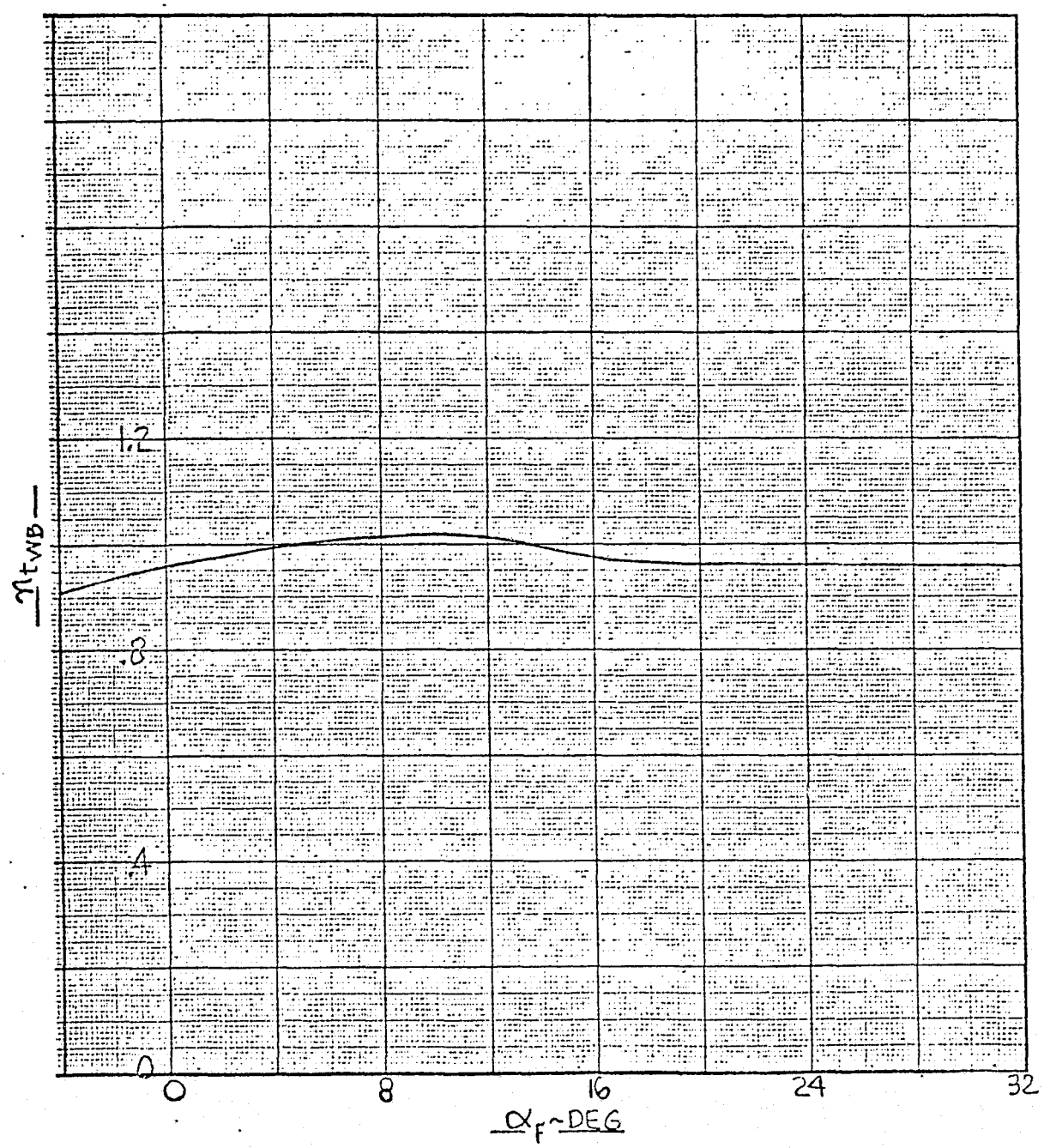

FIGURE 15-11

EFFECT OF FAN CLOSURE DOORS

$$\Delta C_{L_{NL}} = 0$$

$$\Delta C_{L_{LC}} = 0$$

$$\Delta C_{D_{NL}} = 0$$

$$\Delta C_{D_{LC}} = 0$$

$$\Delta C_{m_{NL}} = 0$$

$$\Delta C_{m_{LC}} = 0$$

EFFECT OF LANDING GEAR

$$\Delta C_{L_{GEAR}} = 0$$

$$\Delta C_{D_{GEAR}} = 0.0234$$

$$\Delta C_{m_{GEAR}} = -0.0209$$

FIGURE 15-12

EFFECT OF FLAP DEFLECTION ON LIFT

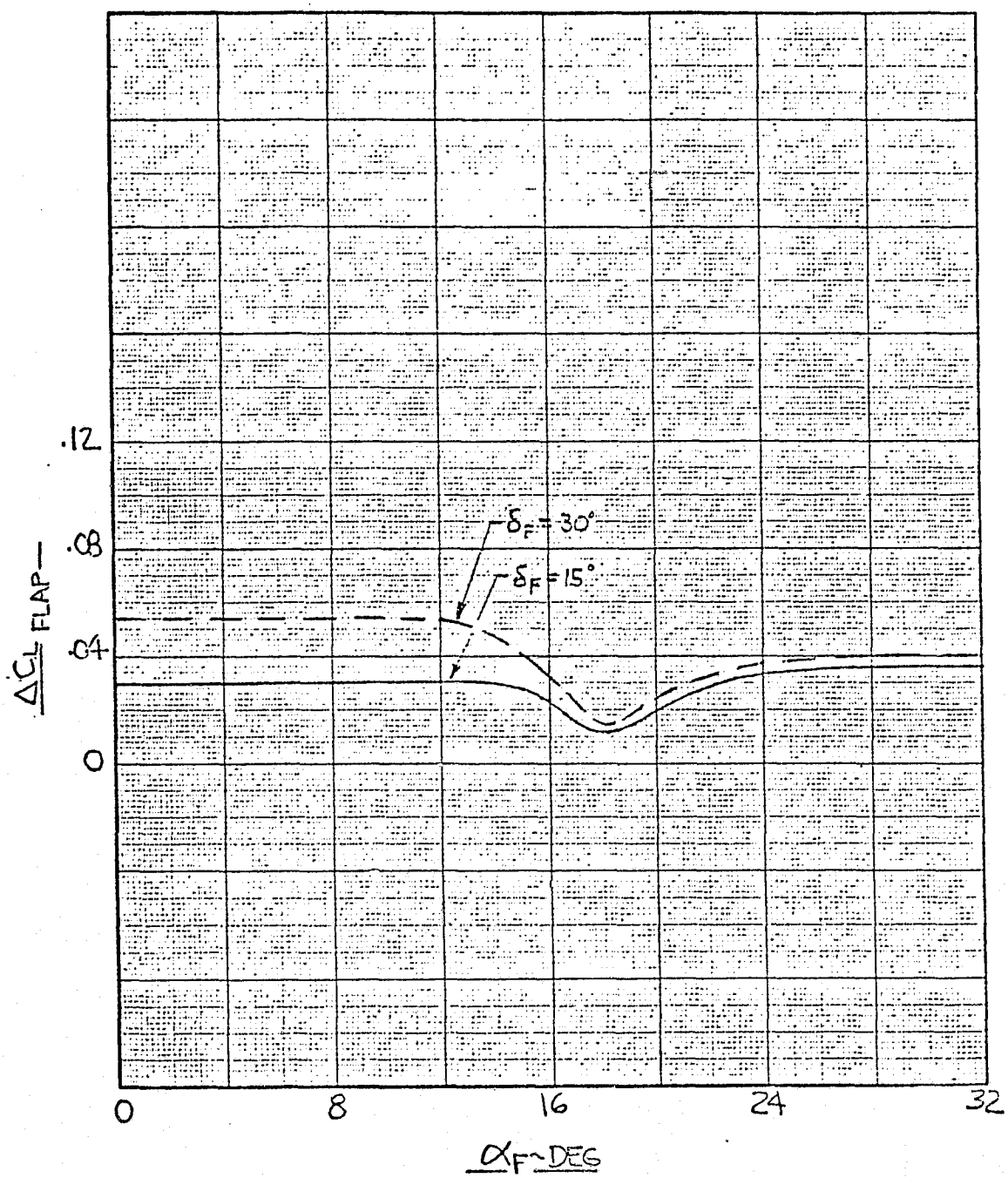

FIGURE 15-13

EFFECT OF FLAP DEFLECTION ON DRAG

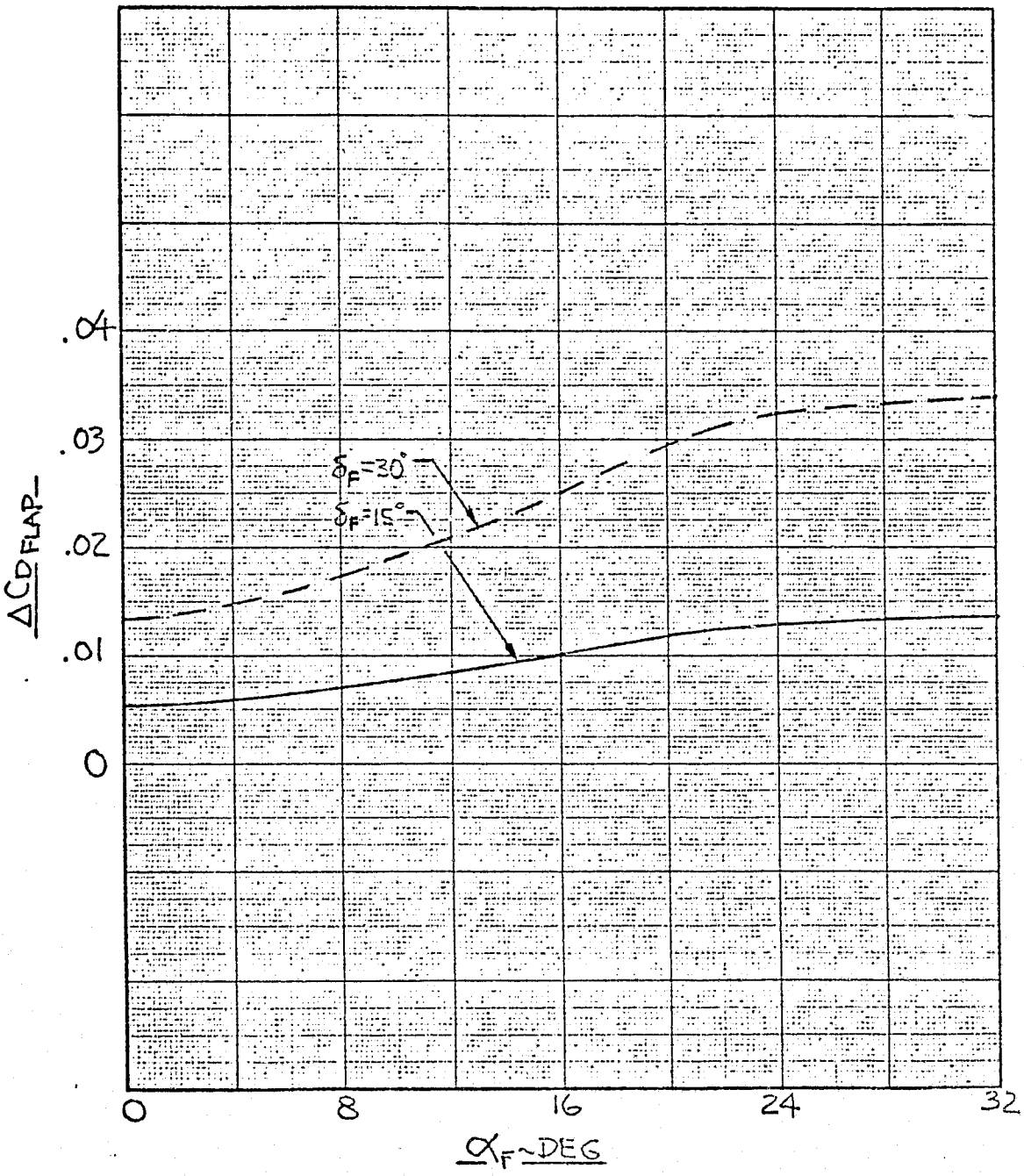

FIGURE 15-14

EFFECT OF FLAP DEFLECTION ON PITCHING MOMENT

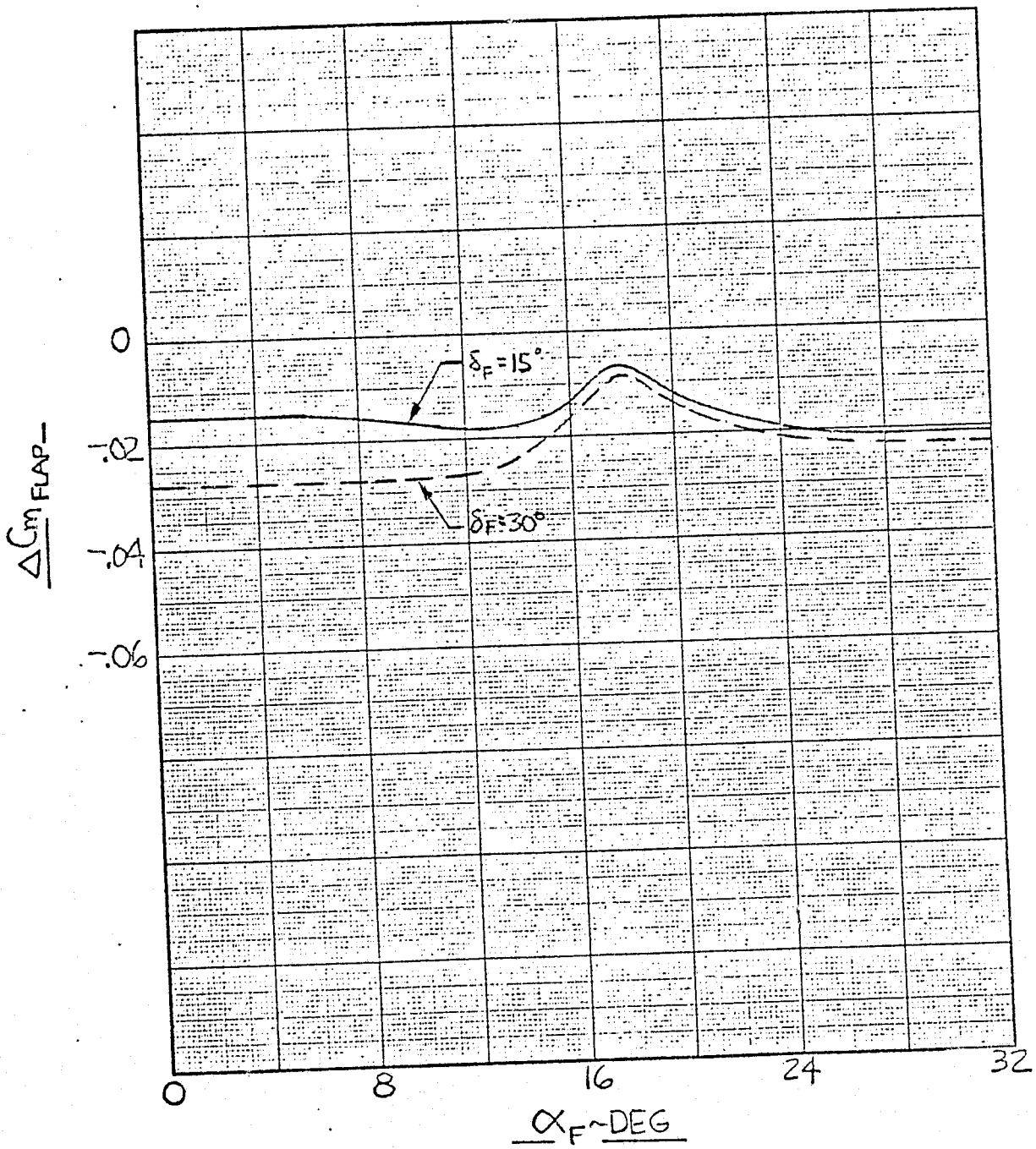

FIGURE 15-15

EFFECT OF AILERON DEFLECTION ON LIFT
ALL (V/V_J)

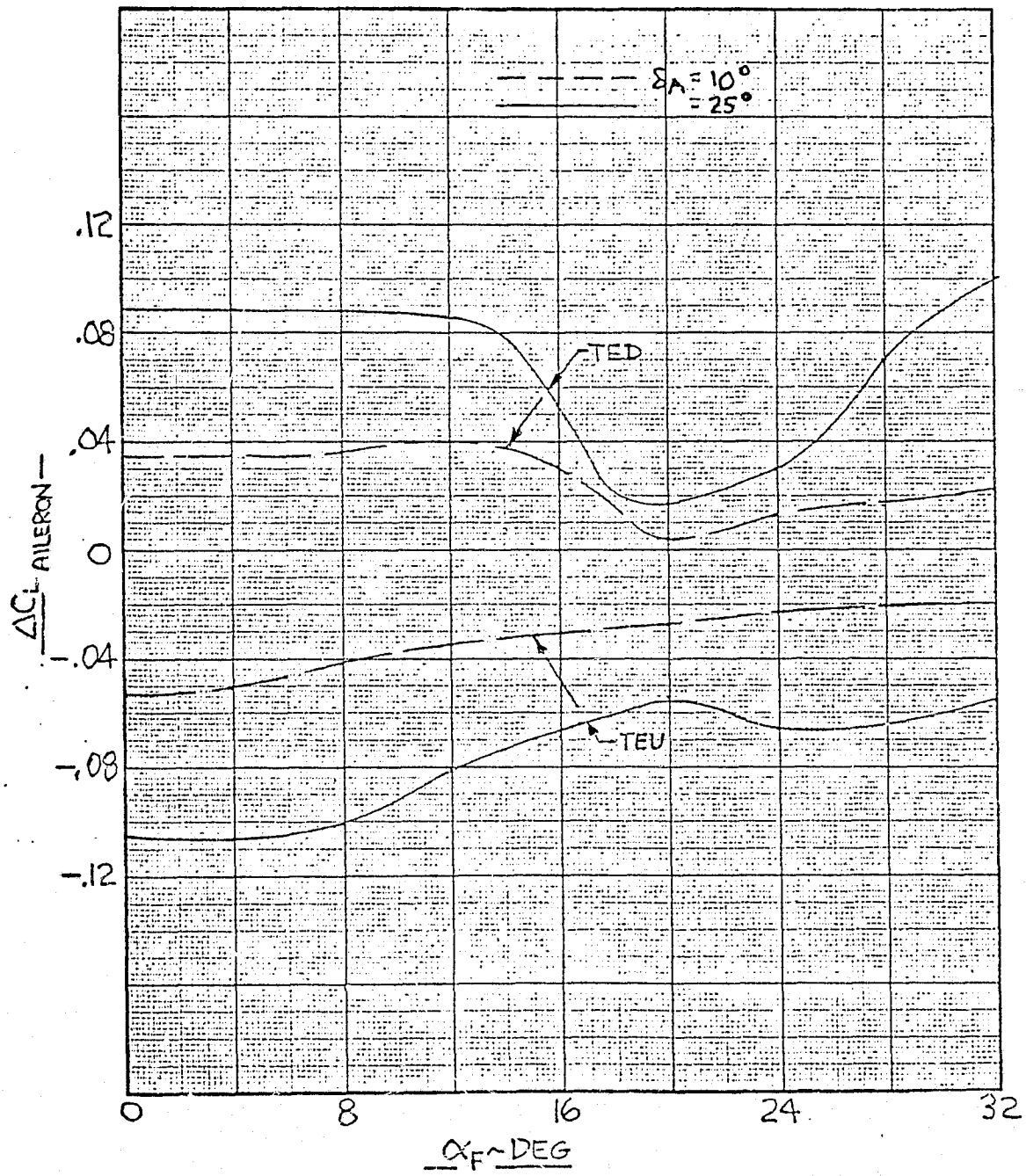

FIGURE 15-16

EFFECT OF AILERON DEFLECTION ON DRAG
ALL (V/V_J)

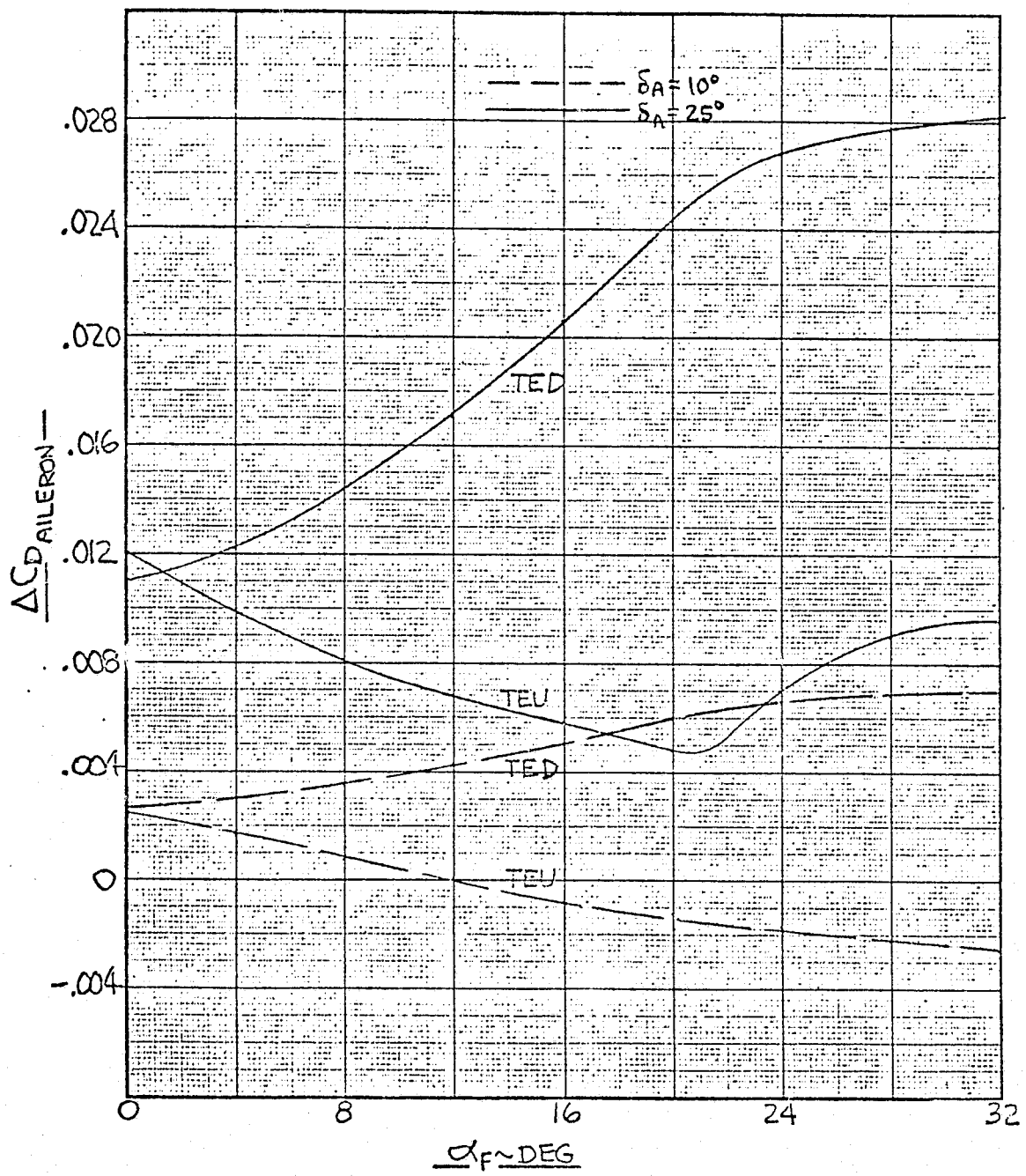

FIGURE 15-17

EFFECT OF AILERON DEFLECTION ON PITCHING MOMENT

ALL (V/V_J)

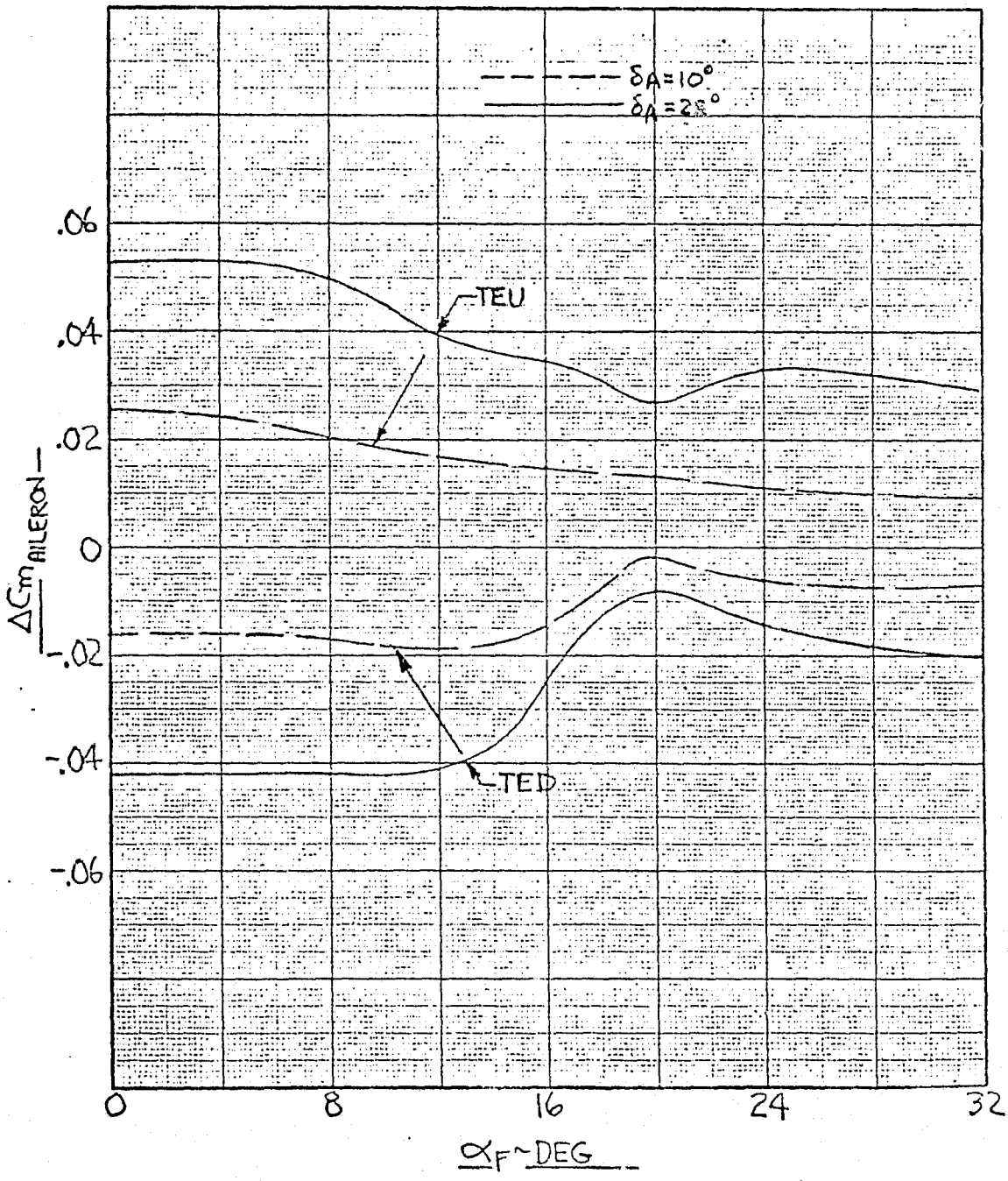

FIGURE 15-18

EFFECT OF FLAP AND AILERON
ON DOWNWASH AT THE HORIZONTAL TAIL

$$\Delta\varepsilon_{FLAP} = 0$$

$$\Delta\varepsilon_{AILERON} = 0$$

EFFECT OF FLAP AND AILERON
ON TAIL EFFICIENCY FACTOR

$$\Delta\eta_{t_{FLAP}} = 0$$

$$\Delta\eta_{t_{AILERON}} = 0$$

FIGURE 15-19

HORIZONTAL TAIL LIFT CHARACTERISTICS

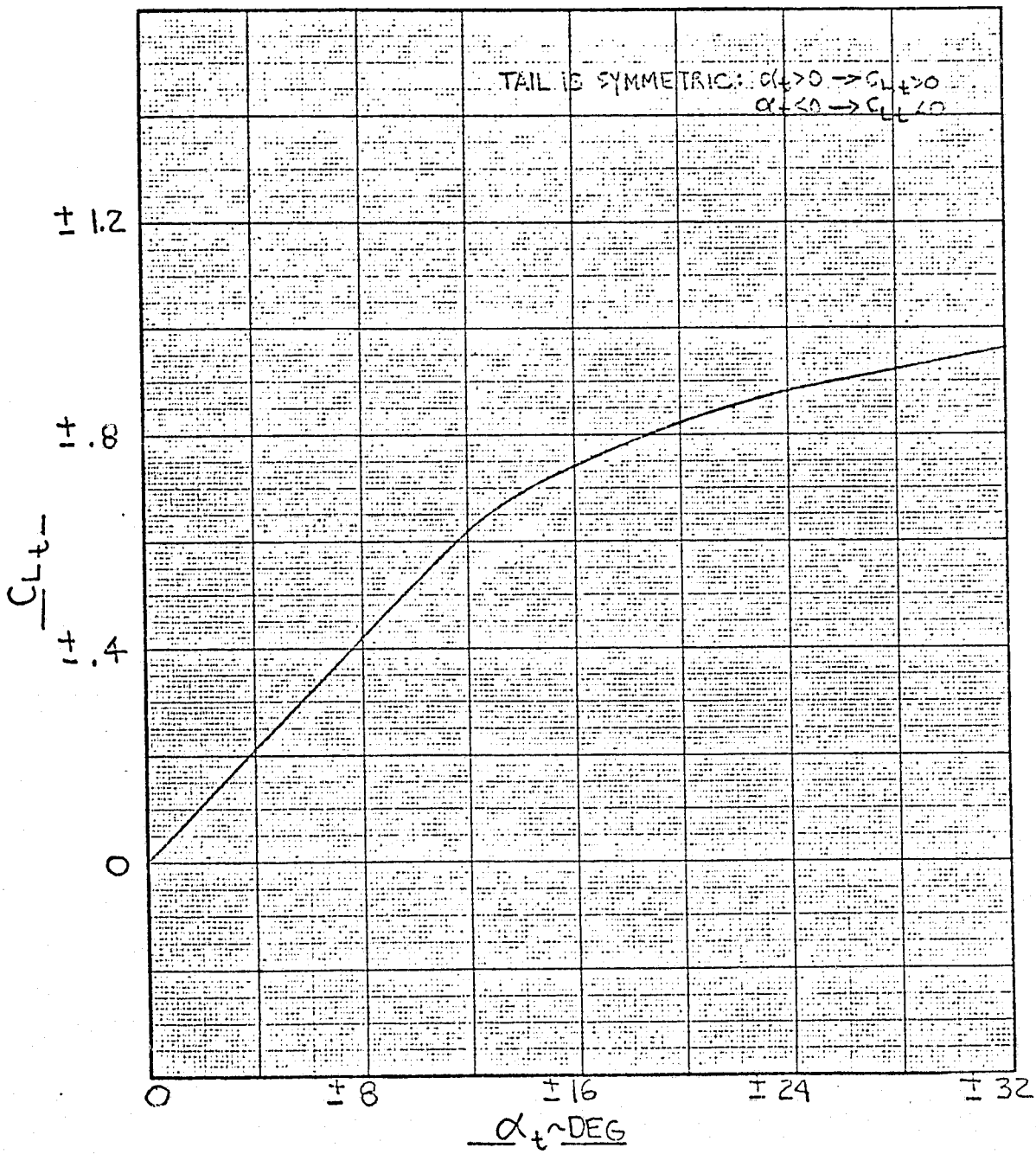

FIGURE 15-20

HORIZONTAL TAIL DRAG CHARACTERISTICS

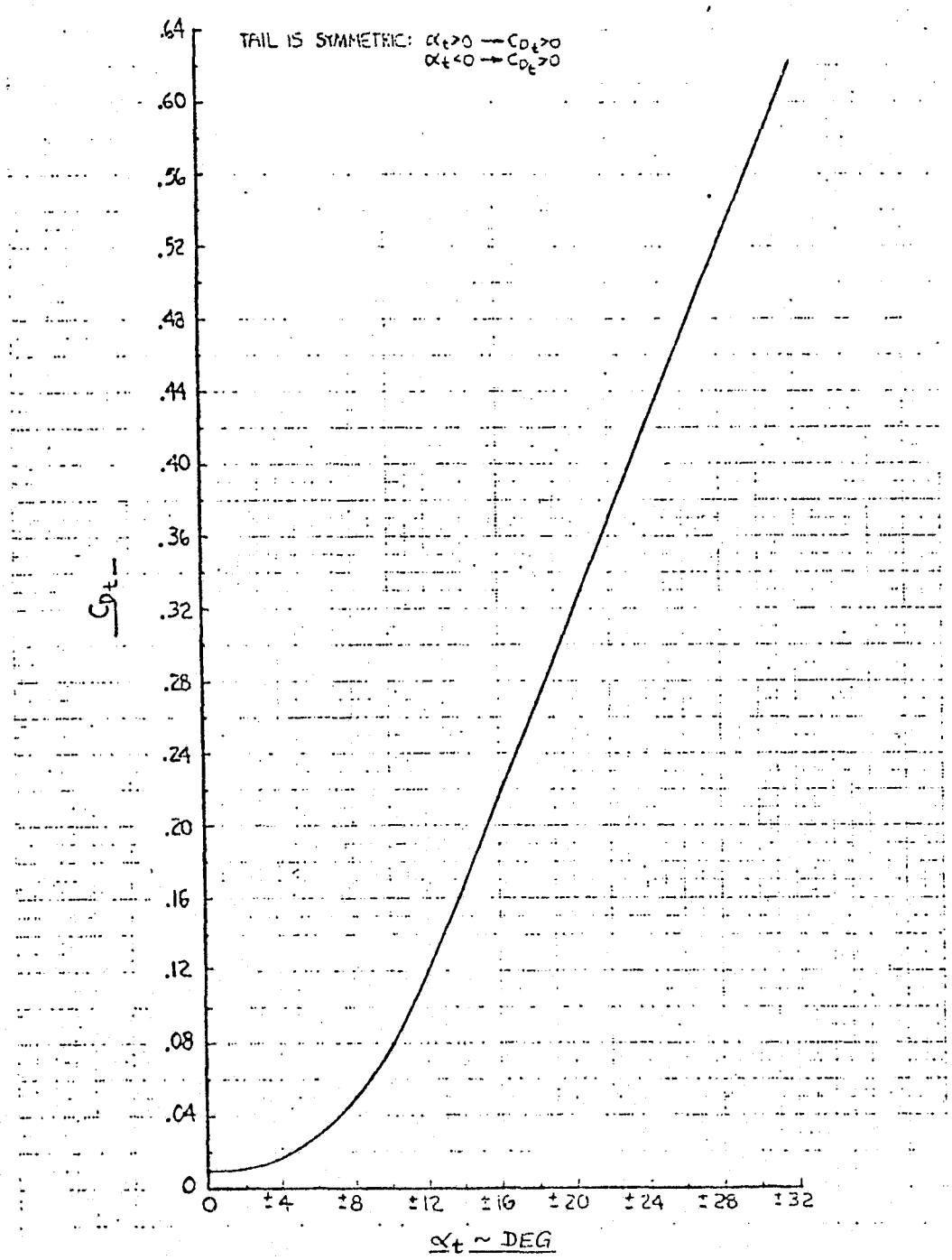

FIGURE 15-21

POWER INDUCED LIFT USING
NOSE LIFT UNIT AND LIFT CRUISE UNITS
ALL α_F REVISION A: 25 JUNE 1976

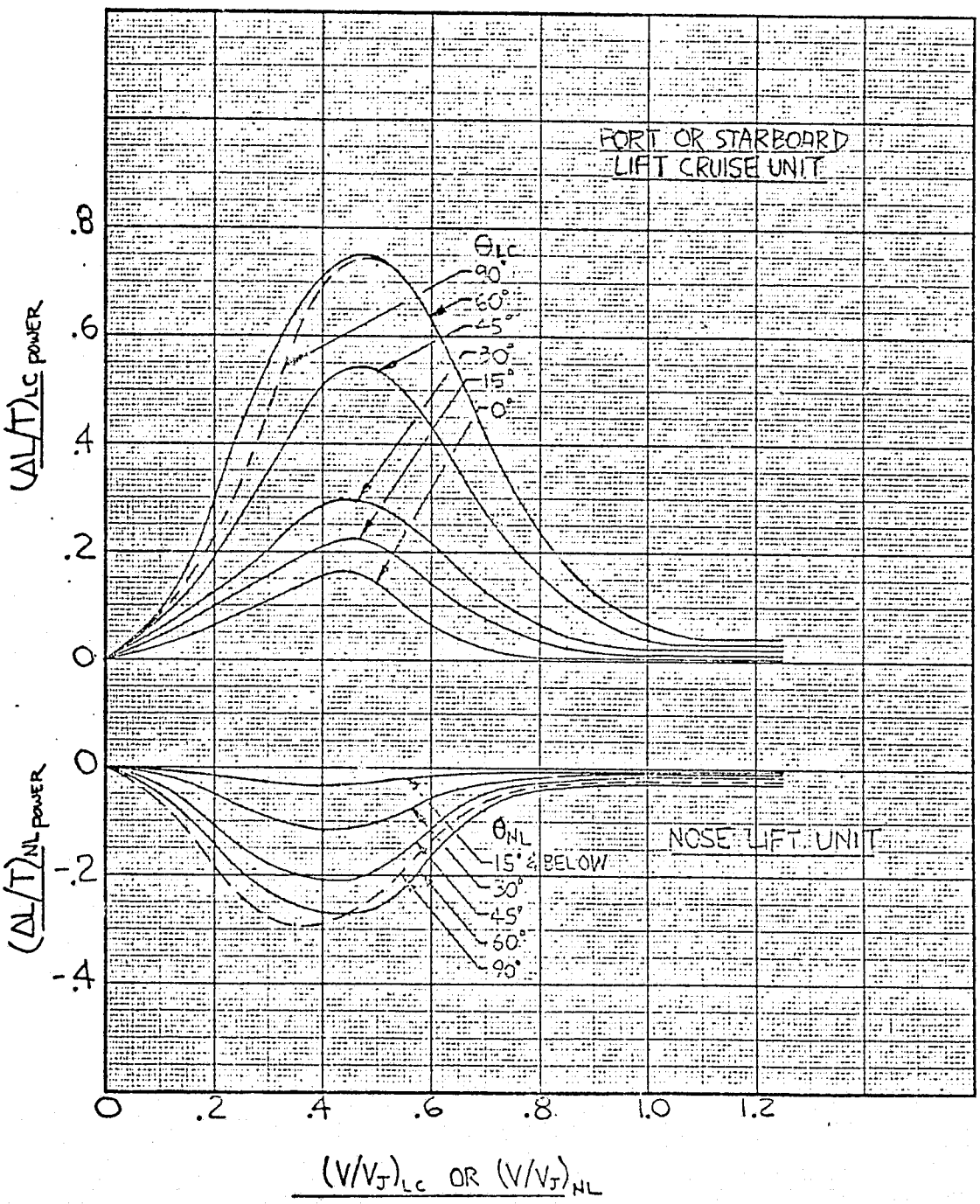

FIGURE 15-22

POWER INDUCED DRAG AND PITCHING MOMENT USING NOSE UNIT AND LIFT CRUISE UNITS

$$\left(\frac{\Delta D}{T}\right)_{NL_{POWER}} = 0$$

$$\left(\frac{\Delta D}{T}\right)_{LC_{POWER}} = 0$$

$$\left(\frac{\Delta PM}{T\bar{c}}\right)_{NL_{POWER}} = 0$$

$$\left(\frac{\Delta PM}{T\bar{c}}\right)_{LC_{POWER}} = 0$$

FIGURE 15-23

EFFECT OF POWER ON DOWNWASH AT THE HORIZONTAL TAIL USING LIFT CRUISE UNIT

θ_{LC}=0° & 12°

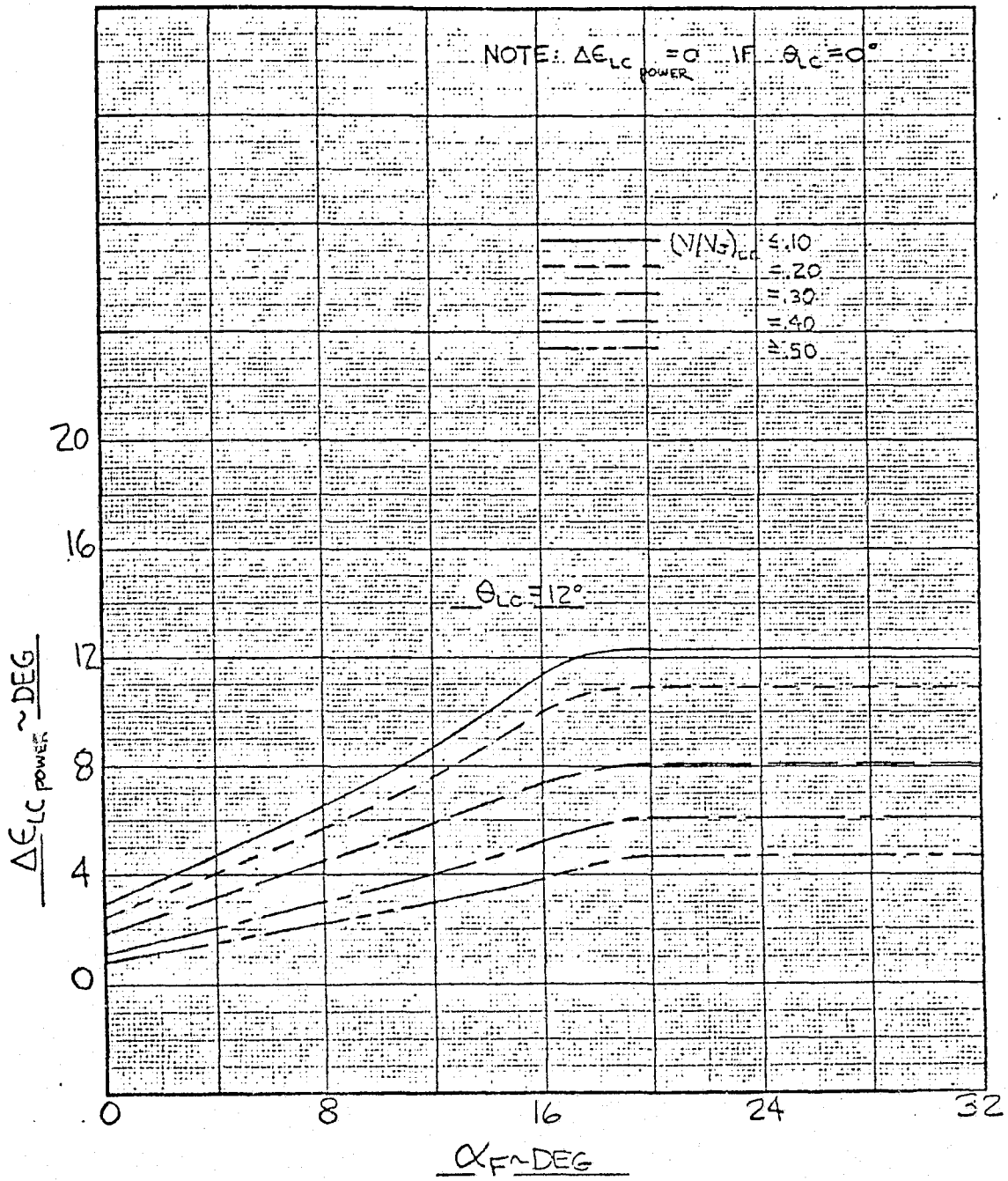

FIGURE 15-24

EFFECT OF POWER ON DOWNWASH AT THE HORIZONTAL TAIL USING LIFT CRUISE UNIT

$\theta_{LC} = 47°$

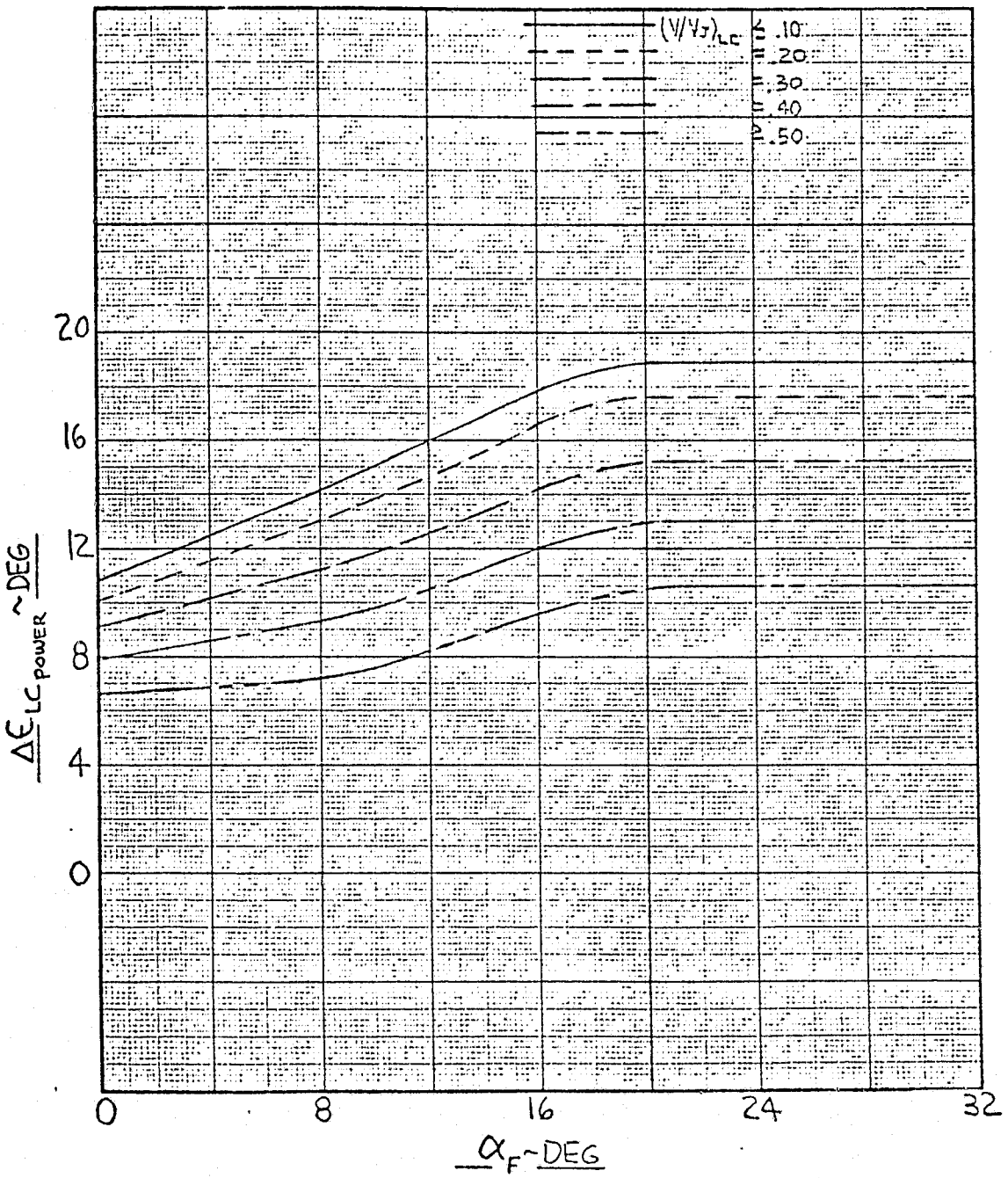

FIGURE 15-25

EFFECT OF POWER ON DOWNWASH AT THE HORIZONTAL TAIL USING LIFT CRUISE UNIT

$\theta_{LC} \geq 84°$

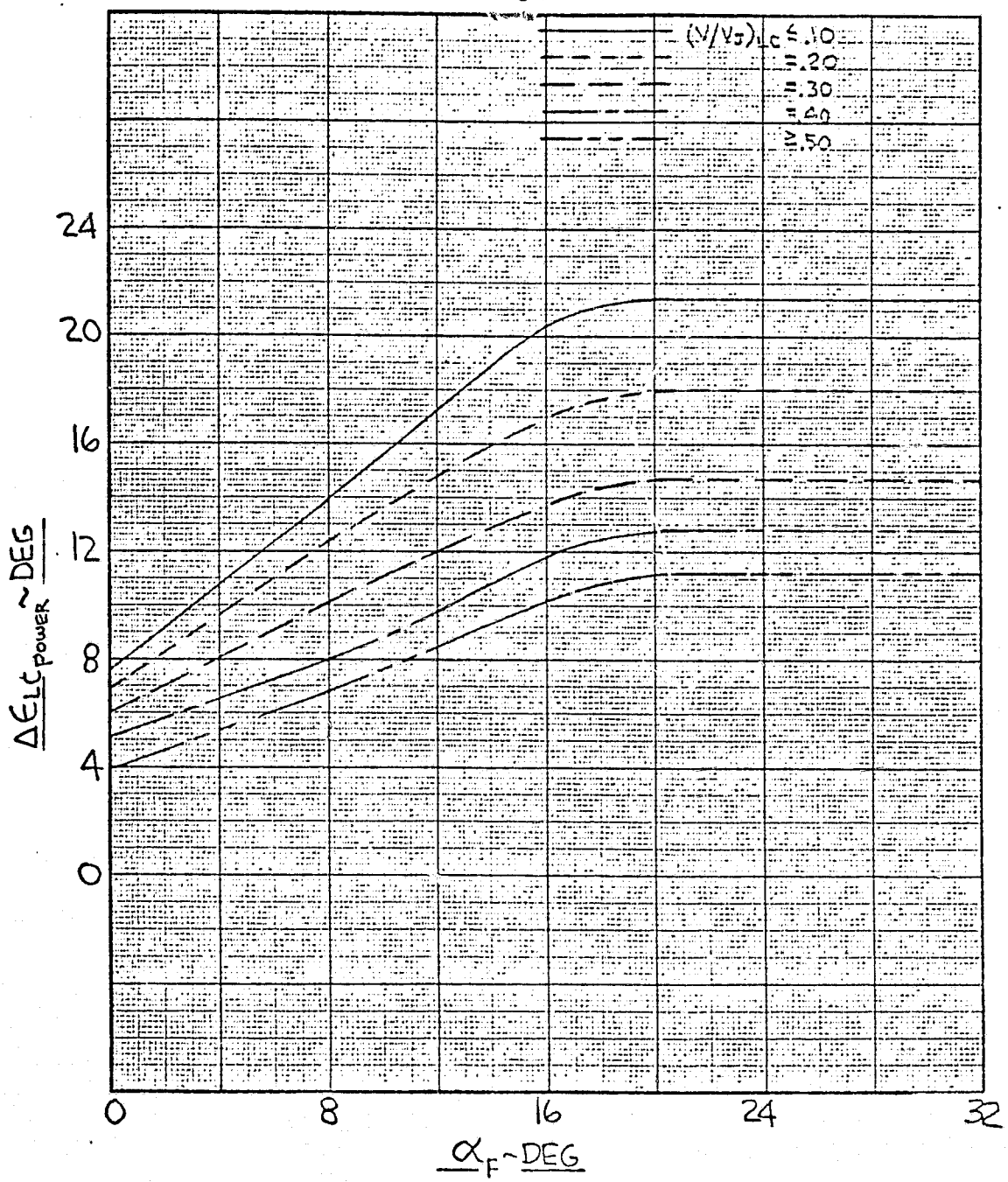

FIGURE 15-26

TABULATED PARAMETERS PERTAINING TO
POWER AND GROUND PROXIMITY EFFECTS

1) Effect of power on downwash at the horizontal tail - contribution due to nose lift unit

$$\Delta\varepsilon_{NL_{POWER}} = 0$$

2) Effect of power on tail efficiency factor

$$\Delta\eta_{t_{NL_{POWER}}} = 0$$

$$\Delta\eta_{t_{LC_{POWER}}} = 0$$

3) Effect of ground proximity on wing-body characteristics

$$\Delta C_{L_{GE}} = 0$$

$$\Delta C_{D_{GE}} = 0$$

$$\Delta C_{m_{GE}} = 0$$

4) Effect of ground proximity on downwash at the horizontal tail

$$\Delta\varepsilon_{GE} = 0$$

5) Effect of ground proximity on tail efficiency factor

$$\Delta\eta_{t_{GE}} = 0$$

FIGURE 15-27

EFFECT OF GROUND PROXIMITY
ON POWER INDUCED LONGITUDINAL CHARACTERISTICS

$$\left[\Delta\left(\frac{\Delta L}{T}\right)_{NL_{POWER}}\right]_{GE} = 0$$

$$\left[\Delta\left(\frac{\Delta L}{T}\right)_{LC_{POWER}}\right]_{GE} = 0$$

$$\left[\Delta\left(\frac{\Delta D}{T}\right)_{NL_{POWER}}\right]_{GE} = 0$$

$$\left[\Delta\left(\frac{\Delta D}{T}\right)_{LC_{POWER}}\right]_{GE} = 0$$

$$\left[\Delta\left(\frac{\Delta PM}{T\bar{c}}\right)_{NL_{POWER}}\right]_{GE} = 0$$

$$\left[\Delta\left(\frac{\Delta PM}{T\bar{c}}\right)_{LC_{POWER}}\right]_{GE} = 0$$

FIGURE 15-28

EFFECT OF ROLL ANGLE
ON POWER INDUCED LONGITUDINAL CHARACTERISTICS

$$\left[\Delta\left(\frac{\Delta L}{T}\right)_{NL_{POWER}}\right]_{\phi} = 0$$

$$\left[\Delta\left(\frac{\Delta L}{T}\right)_{LC_{POWER}}\right]_{\phi} = 0$$

$$\left[\Delta\left(\frac{\Delta D}{T}\right)_{NL_{POWER}}\right]_{\phi} = 0$$

$$\left[\Delta\left(\frac{\Delta D}{T}\right)_{LC_{POWER}}\right]_{\phi} = 0$$

$$\left[\Delta\left(\frac{\Delta PM}{T\bar{c}}\right)_{NL_{POWER}}\right]_{\phi} = 0$$

$$\left[\Delta\left(\frac{\Delta PM}{T\bar{c}}\right)_{LC_{POWER}}\right]_{\phi} = 0$$

FIGURE 15-29

LIFT AND PITCHING MOMENT DUE TO PITCH RATE

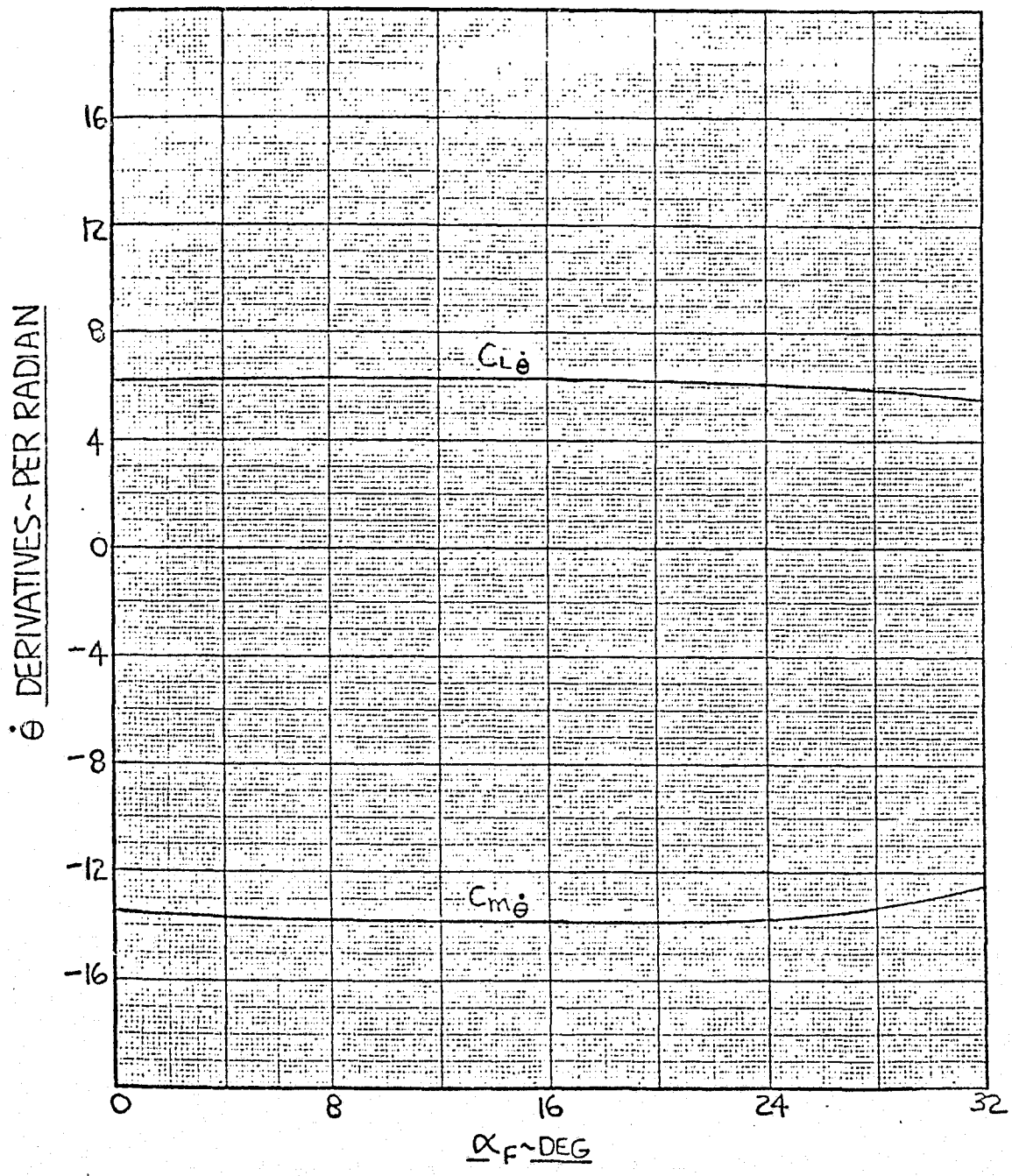

FIGURE 15-30

LIFT AND PITCHING MOMENT DUE TO RATE OF CHANGE OF ANGLE OF ATTACK

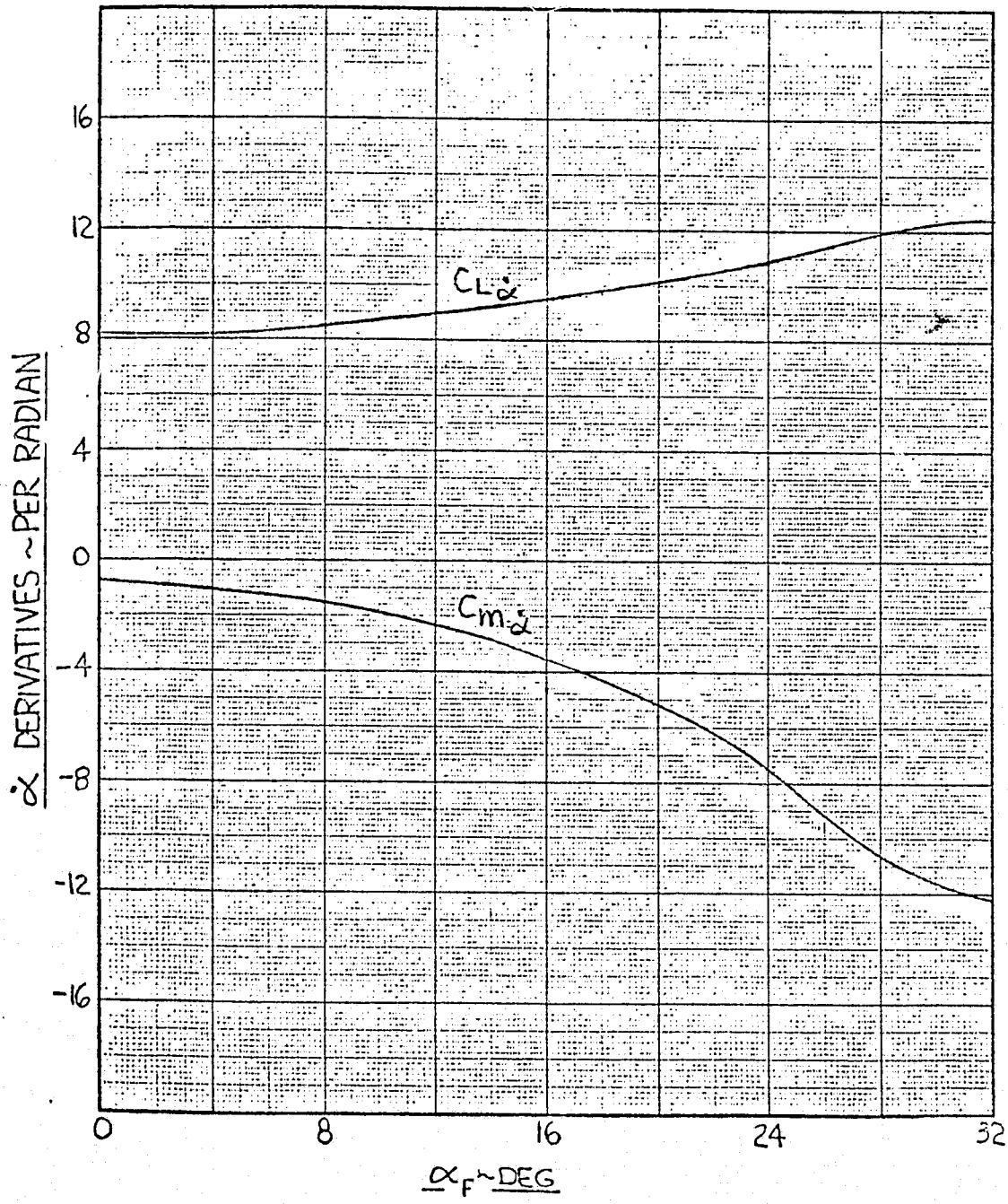

FIGURE 15-31

STATIC LATERAL-DIRECTIONAL STABILITY
AERODYNAMIC FLIGHT CONFIGURATION
STABILITY AXES

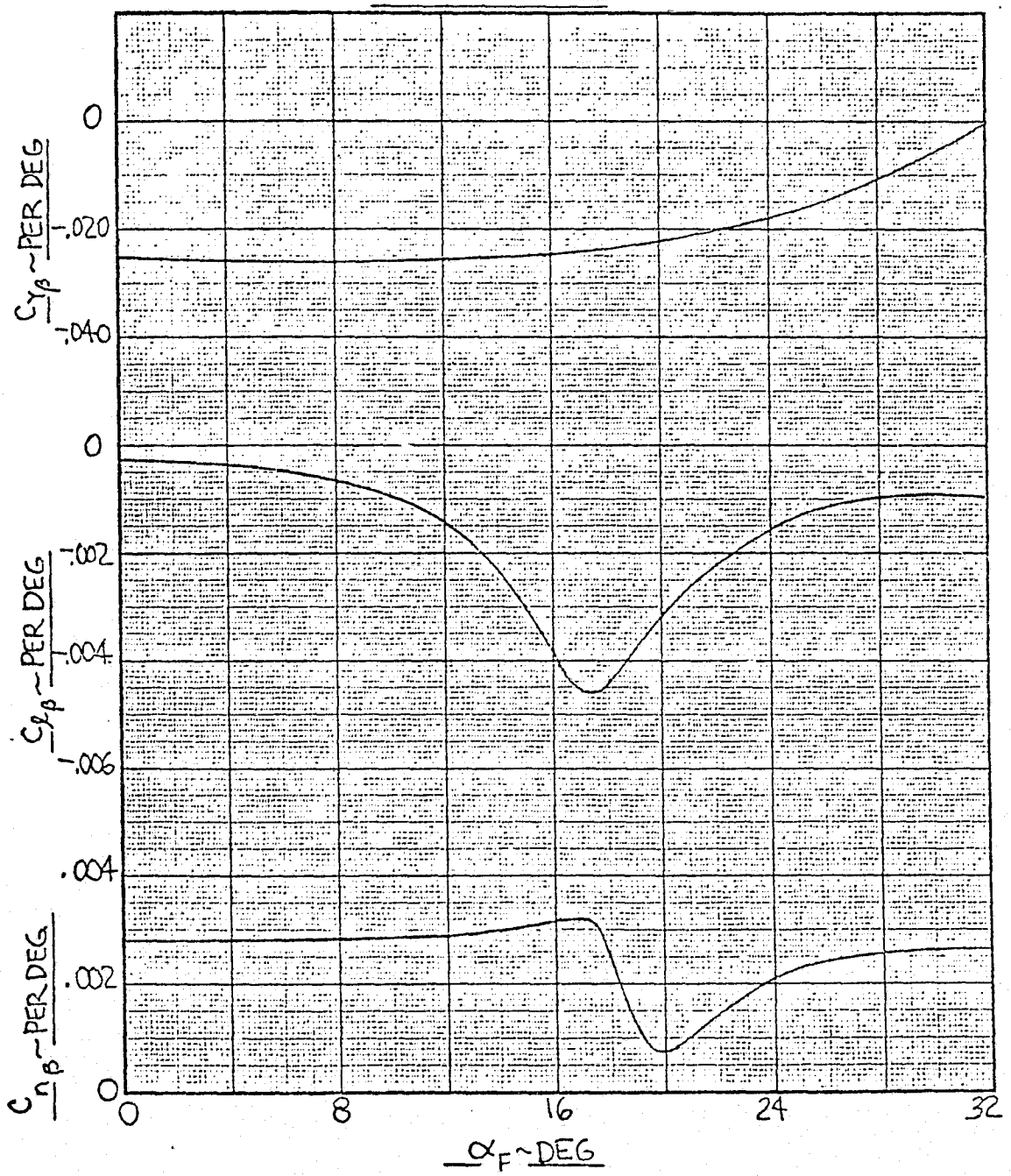

FIGURE 15-32

EFFECT OF FAN CLOSURE DOORS ON LATERAL-DIRECTIONAL STABILITY

STABILITY AXES

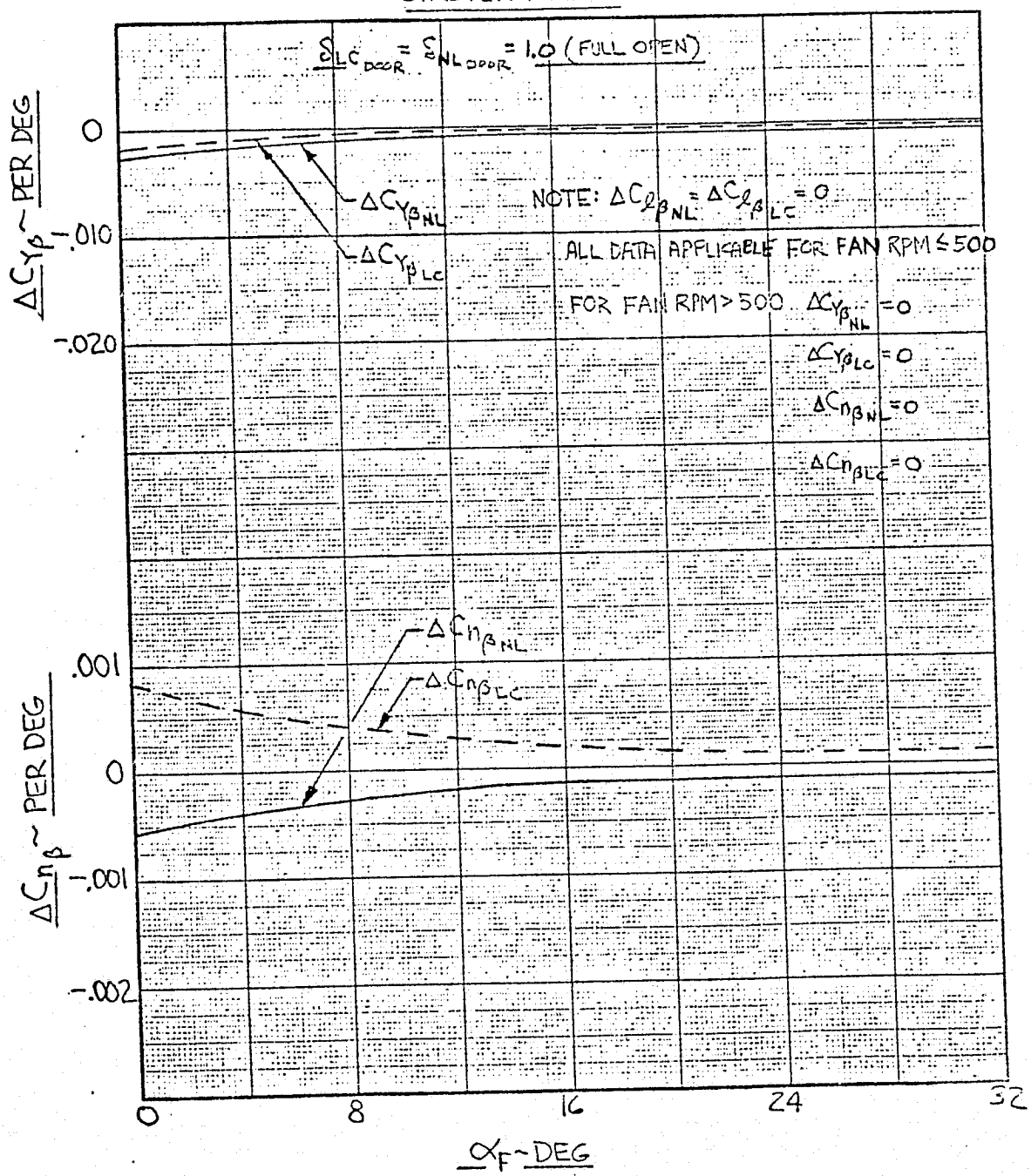

FIGURE 15-33

EFFECT OF DROOPED AILERONS
ON LATERAL-DIRECTIONAL CHARACTERISTICS

$$\Delta C_{Y_{\beta_{AILERON}}} = 0$$

$$\Delta C_{n_{\beta_{AILERON}}} = 0$$

$$\Delta C_{\ell_{\beta_{AILERON}}} = 0$$

EFFECT OF FLAP
ON LATERAL-DIRECTIONAL CHARACTERISTICS

$$\Delta C_{Y_{\beta_{FLAP}}} = 0$$

$$\Delta C_{n_{\beta_{FLAP}}} = 0$$

$$\Delta C_{n_{\beta_{FLAP}}} = 0$$

FIGURE 15-34

EFFECT OF AILERON DEFLECTION ON SIDEFORCE

STABILITY AXES

$\delta_A = 10°$

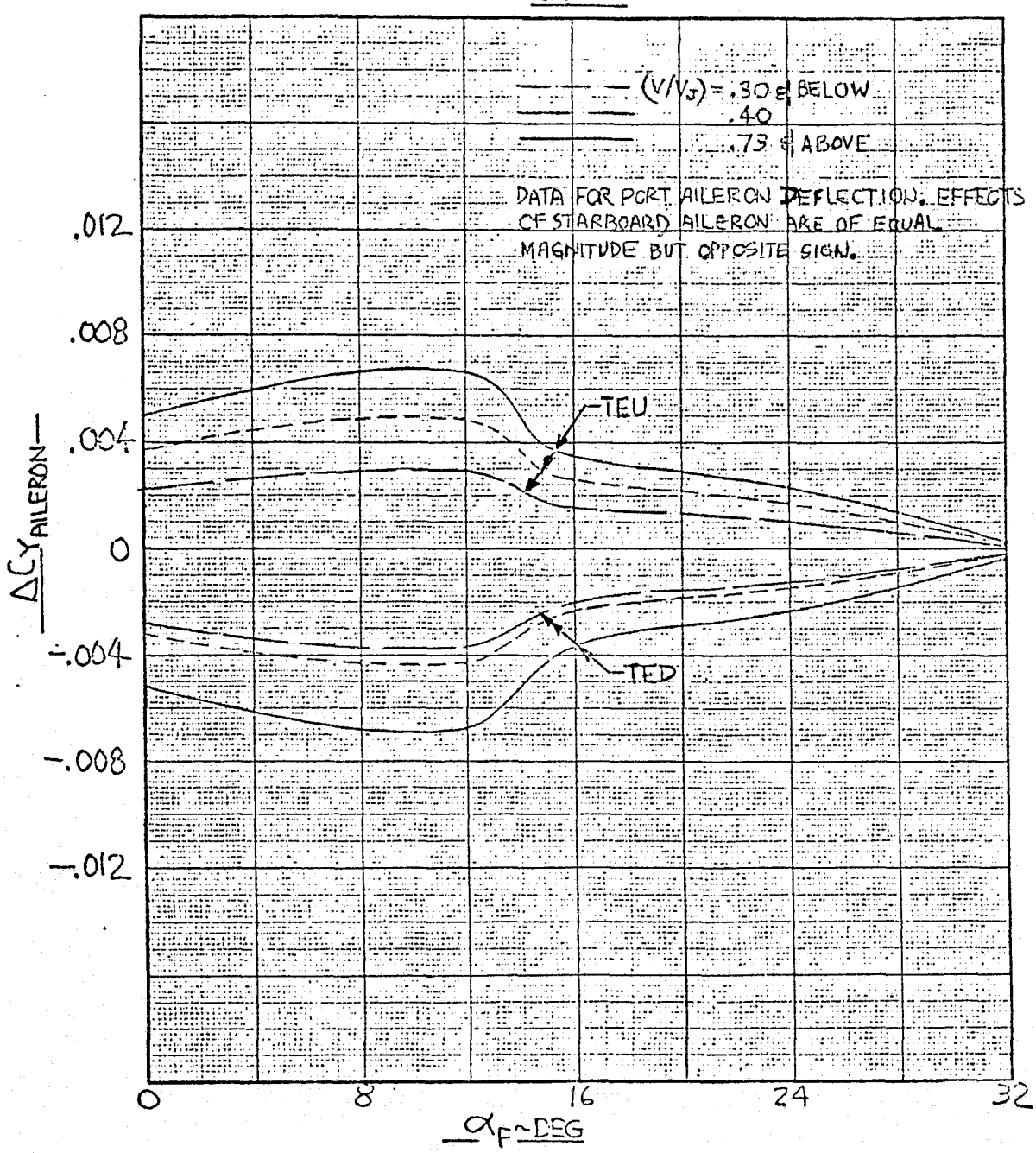

FIGURE 15-35

EFFECT OF AILERON DEFLECTION ON SIDEFORCE

STABILITY AXES

$\delta_A = 25°$

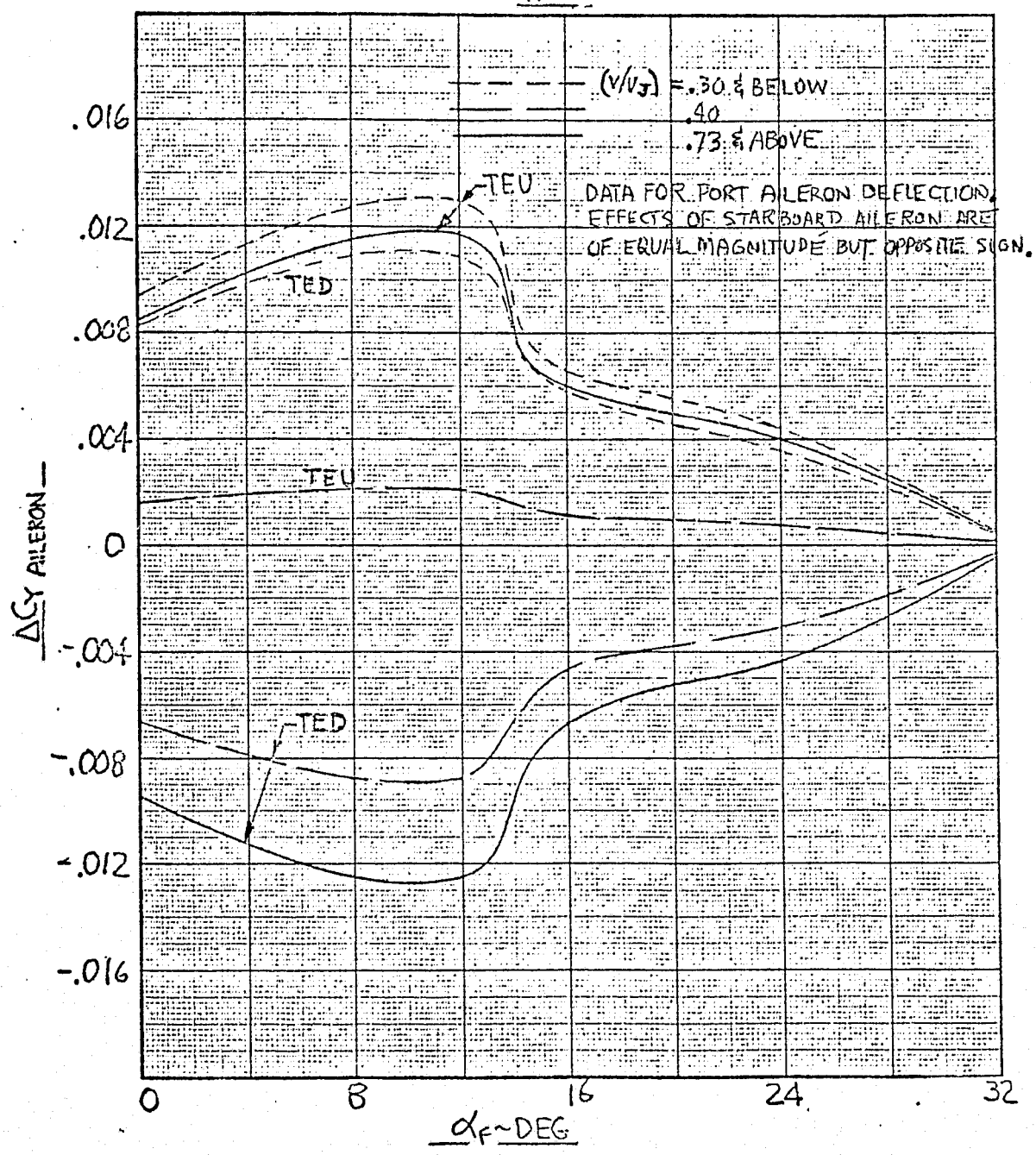

FIGURE 15-36

EFFECT OF AILERON DEFLECTION ON YAWING MOMENT
STABILITY AXES
$\delta_A = 10°$

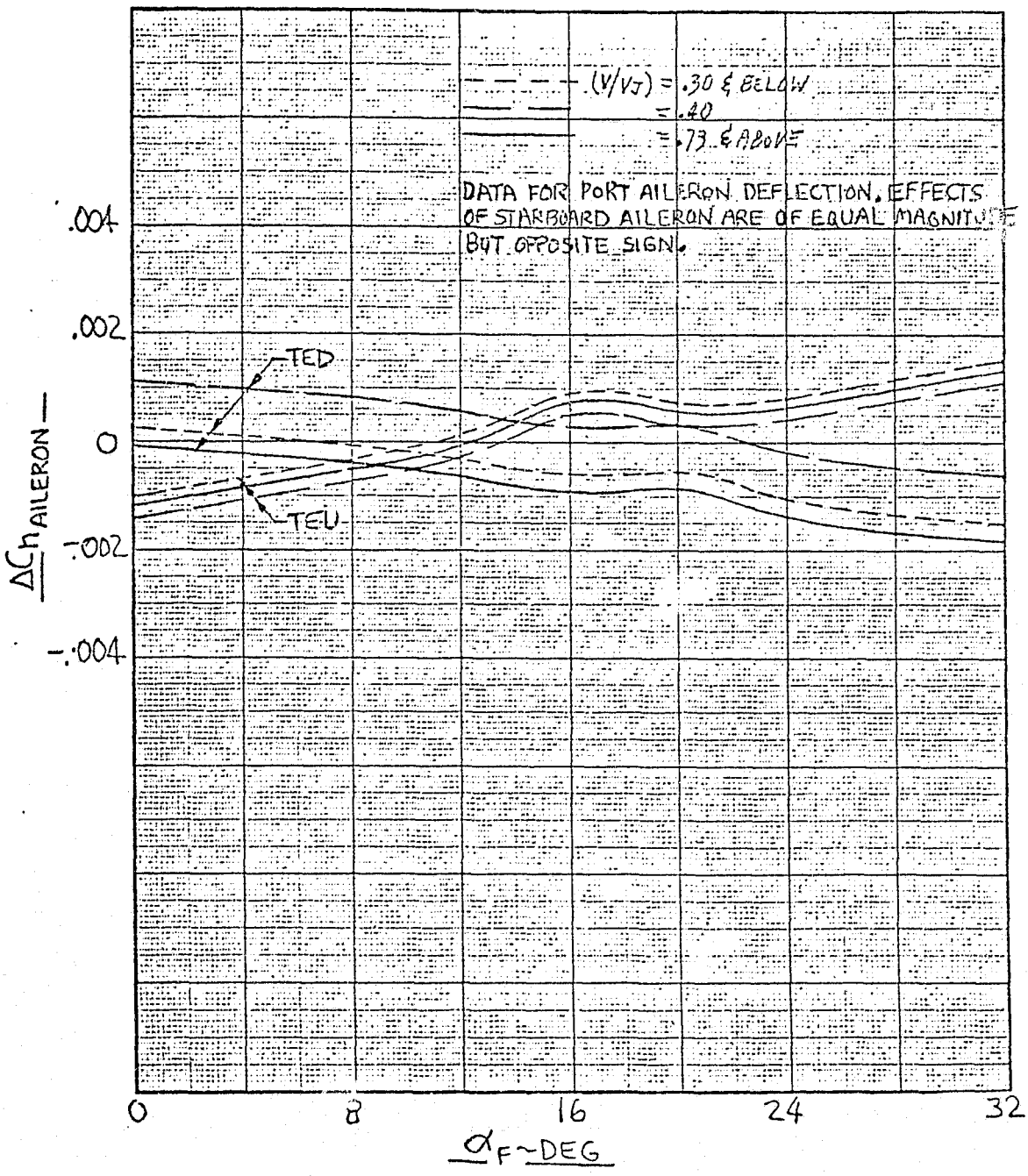

FIGURE 15-37

EFFECT OF AILERON DEFLECTION ON YAWING MOMENT

STABILITY AXES

$\delta_A = 25°$

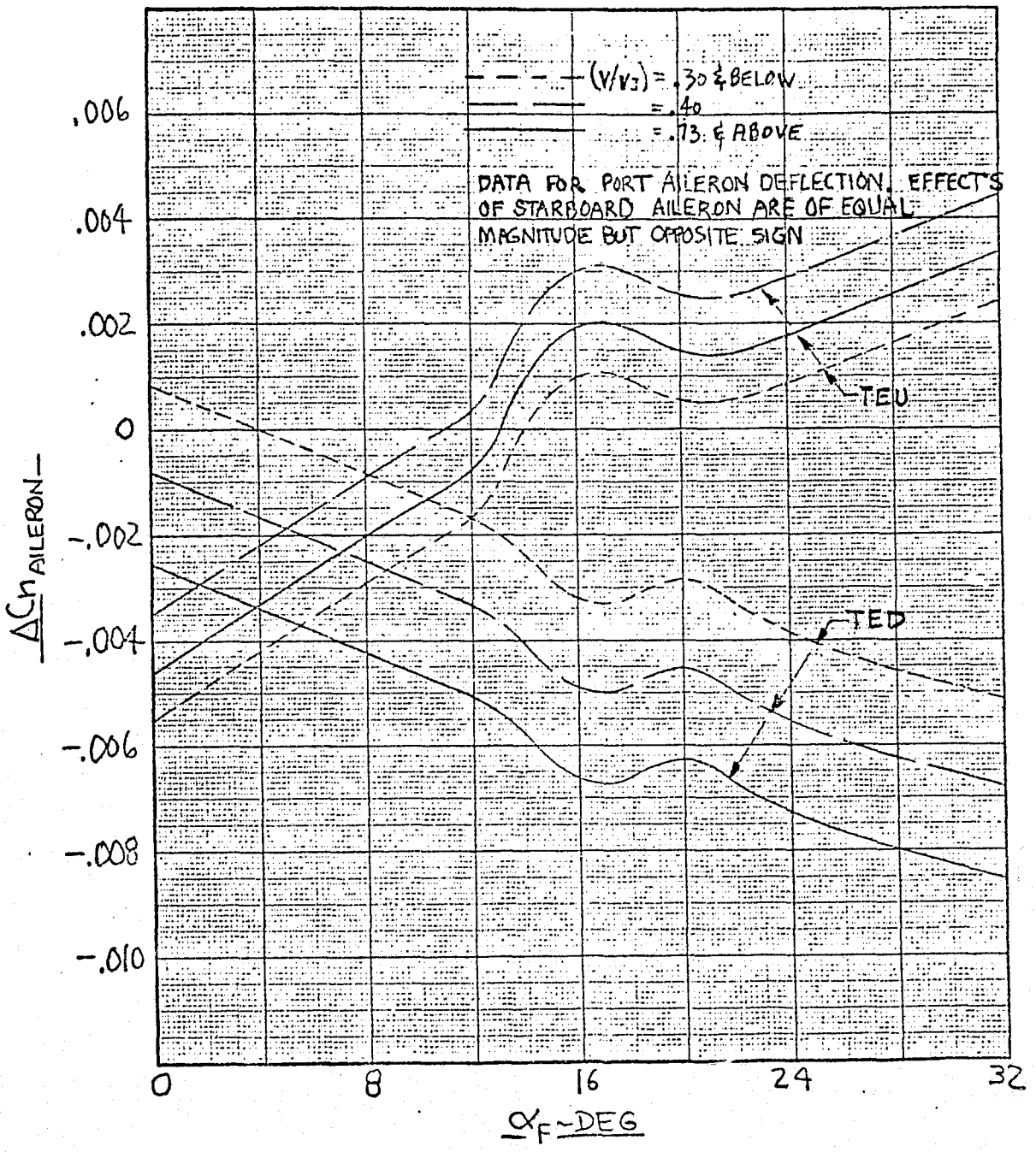

FIGURE 15-38

EFFECT OF AILERON DEFLECTION ON ROLLING MOMENT

STABILITY AXES

$\delta_A = 10°$

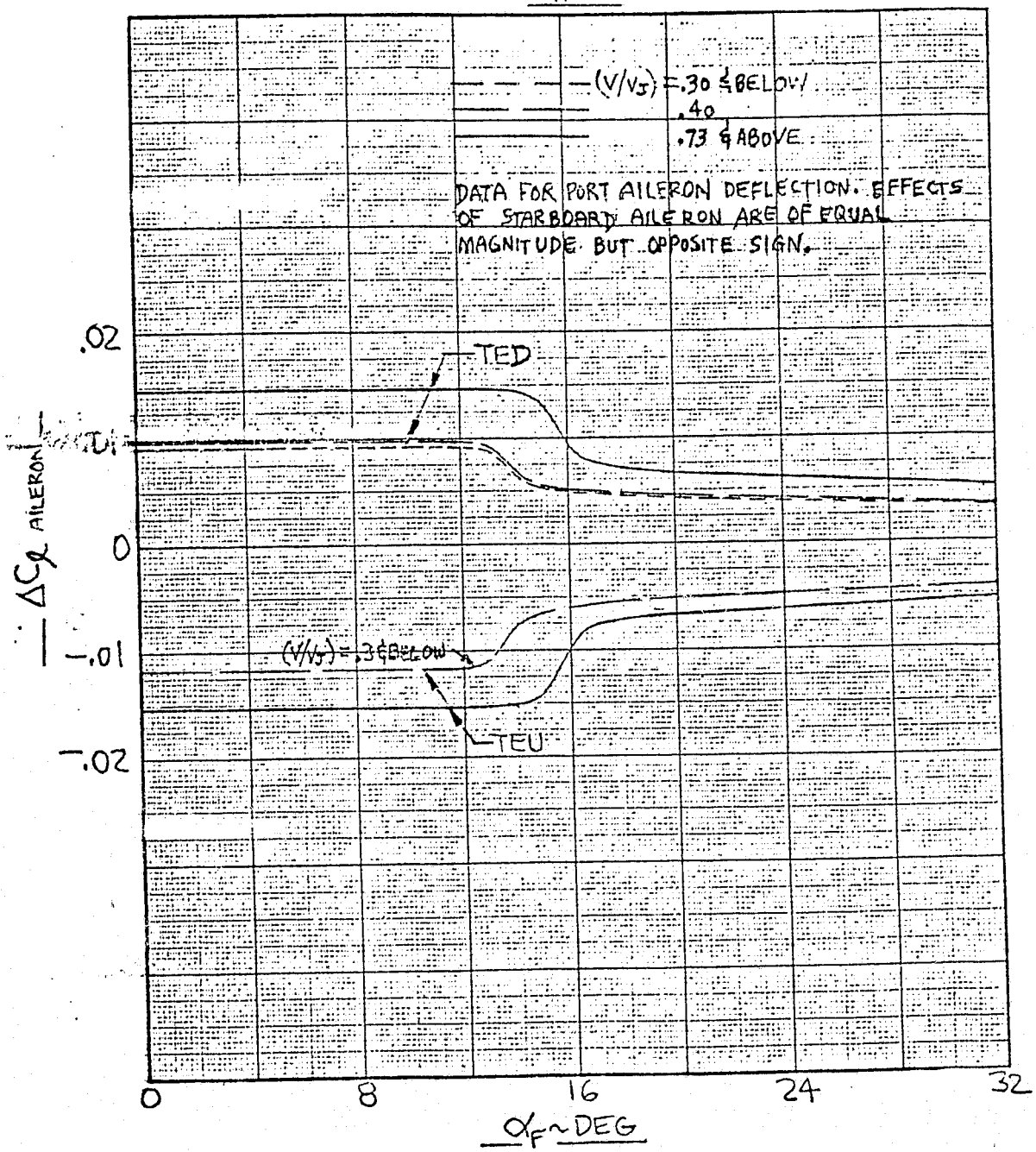

FIGURE 15-39

EFFECT OF AILERON DEFLECTION ON ROLLING MOMENT

STABILITY AXES

$\delta_A = 25°$

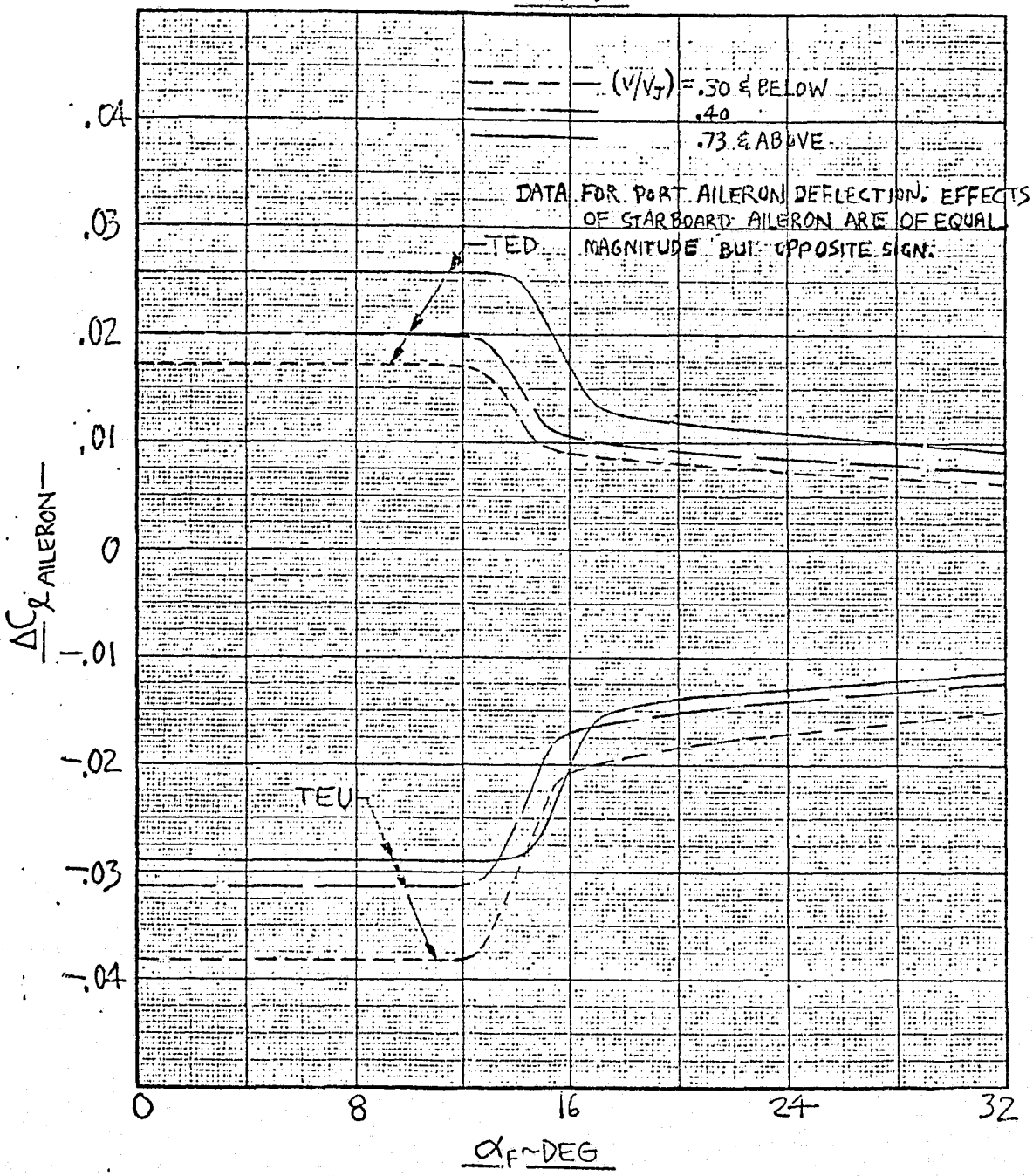

FIGURE 15-40

RUDDER EFFECTIVENESS
STABILITY AXES

$\delta_R = 23°$

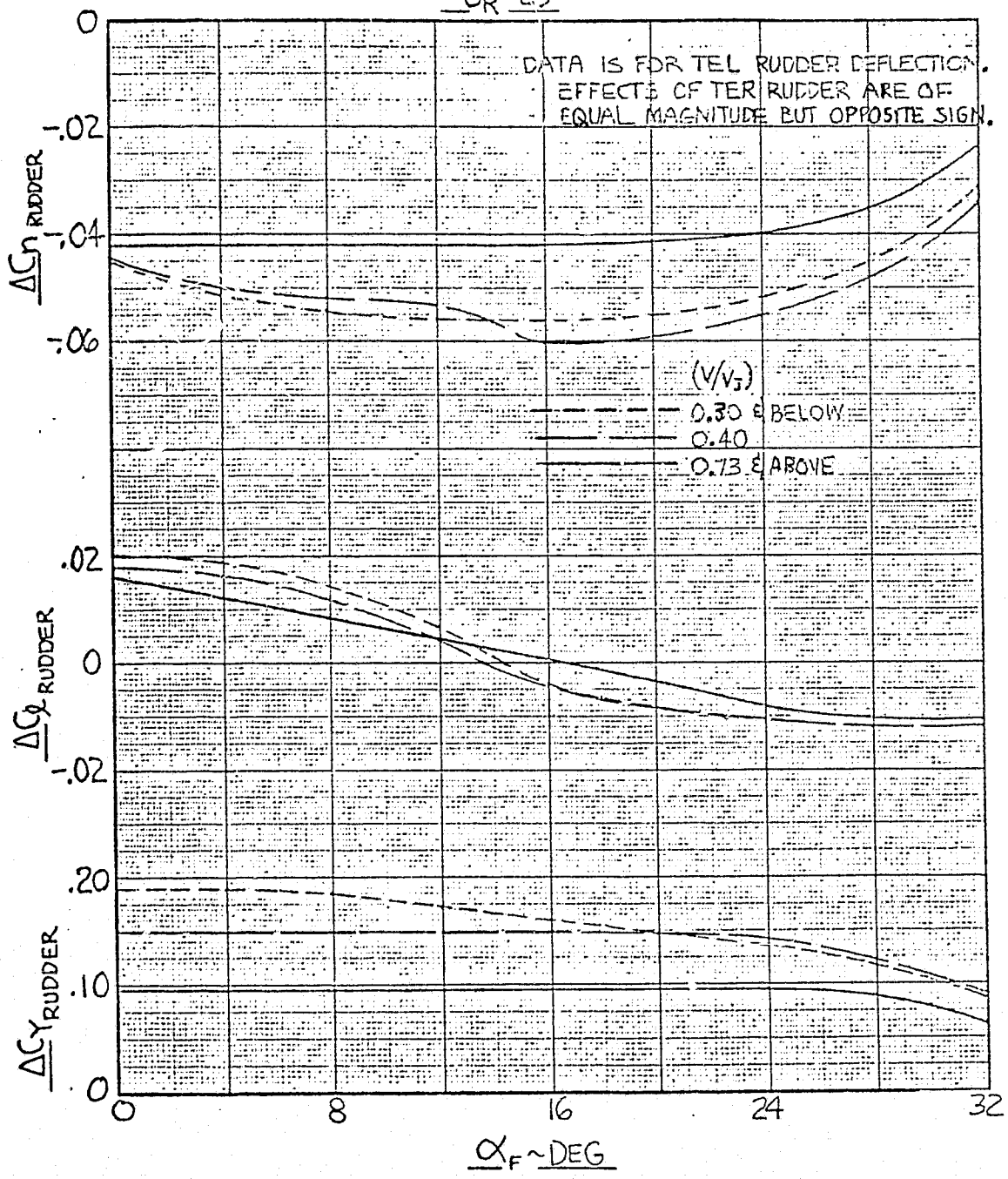

FIGURE 15-41

POWER INDUCED SIDEFORCE USING LIFT CRUISE UNIT
STABILITY AXES
$\beta = 0° \& +6°$

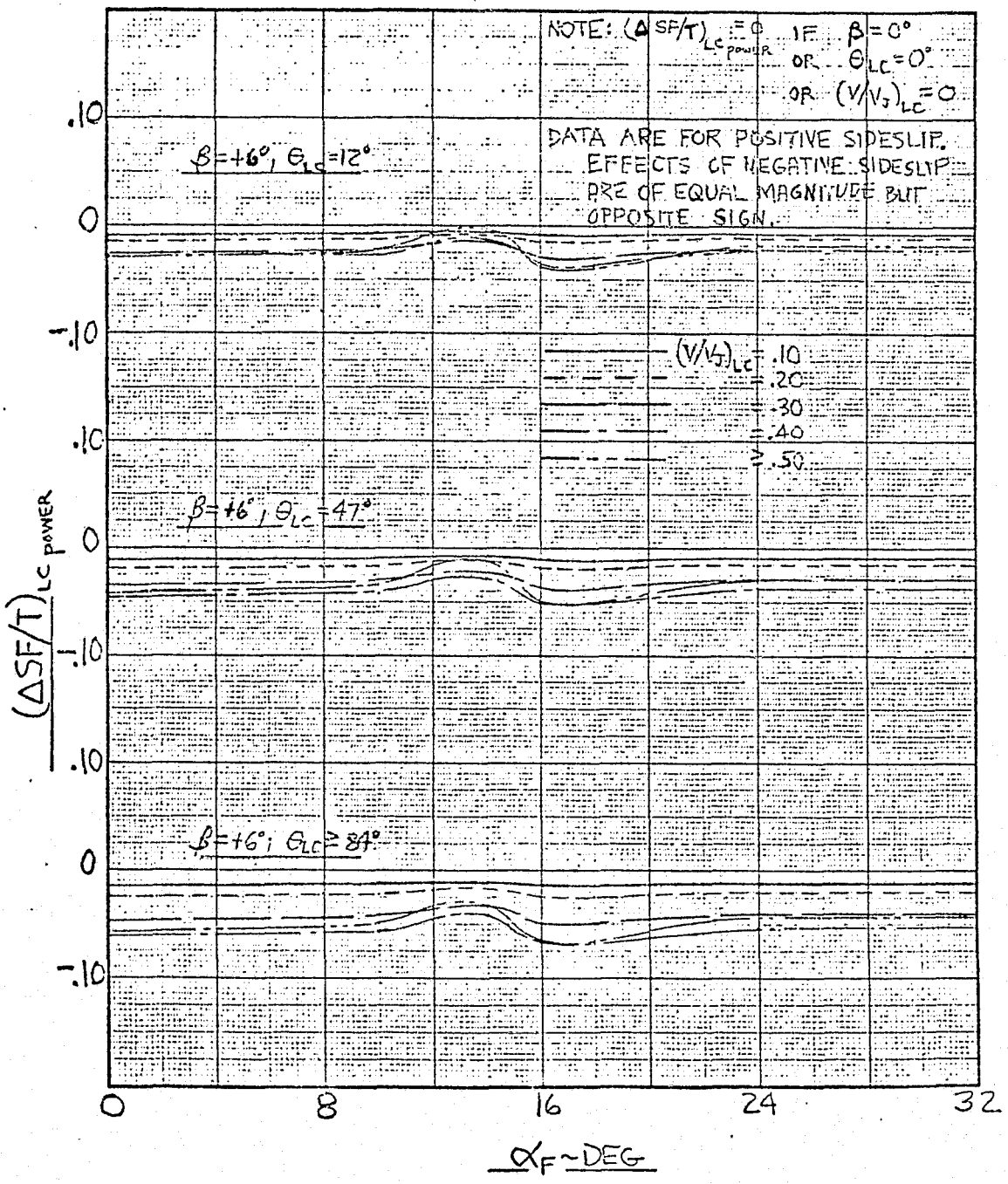

FIGURE 15-42

POWER INDUCED SIDEFORCE USING LIFT CRUISE UNIT

STABILITY AXES

$\beta = +12°$

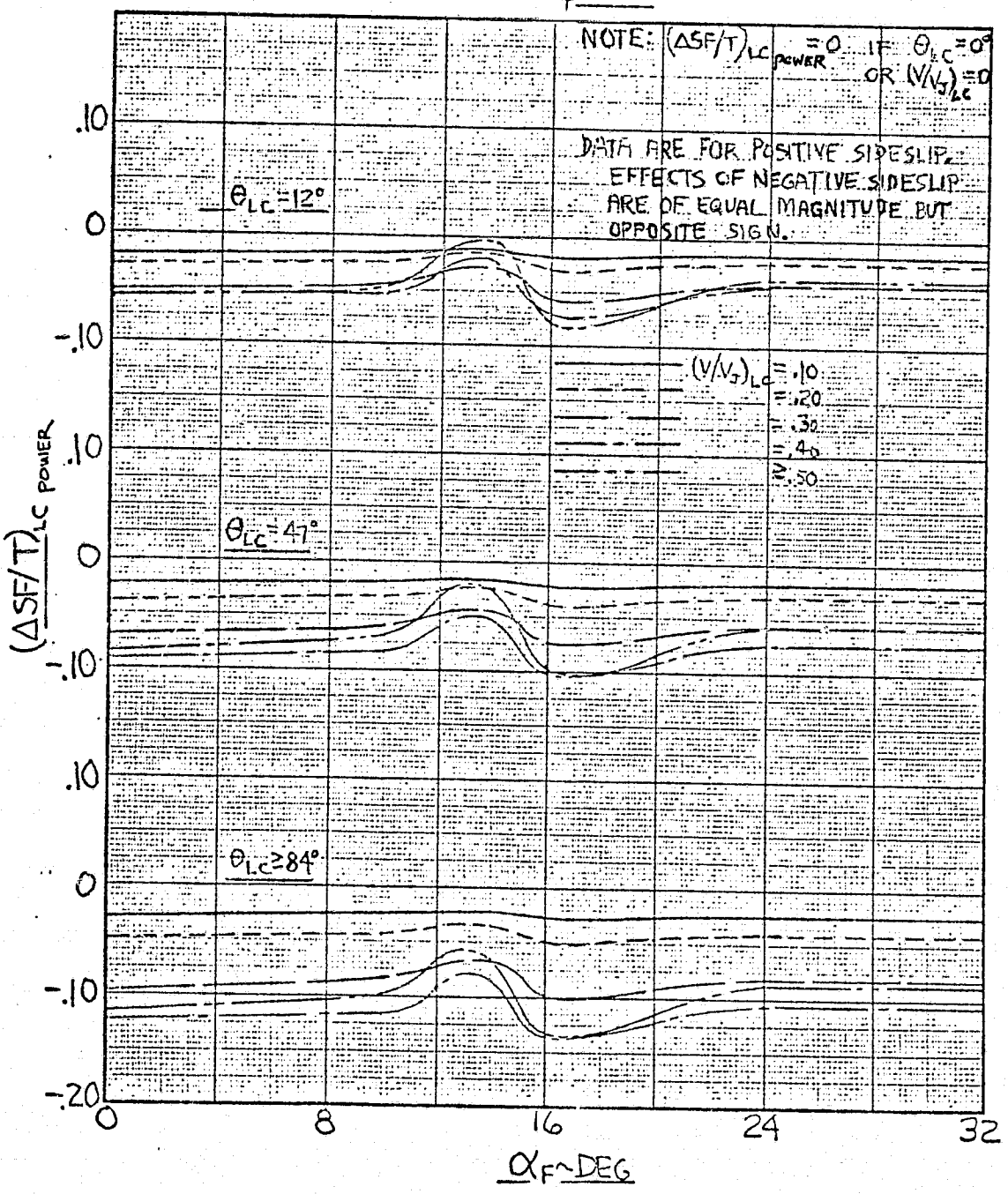

FIGURE 15-43

POWER INDUCED SIDEFORCE USING LIFT CRUISE UNIT

STABILITY AXES

$\beta = +18°$

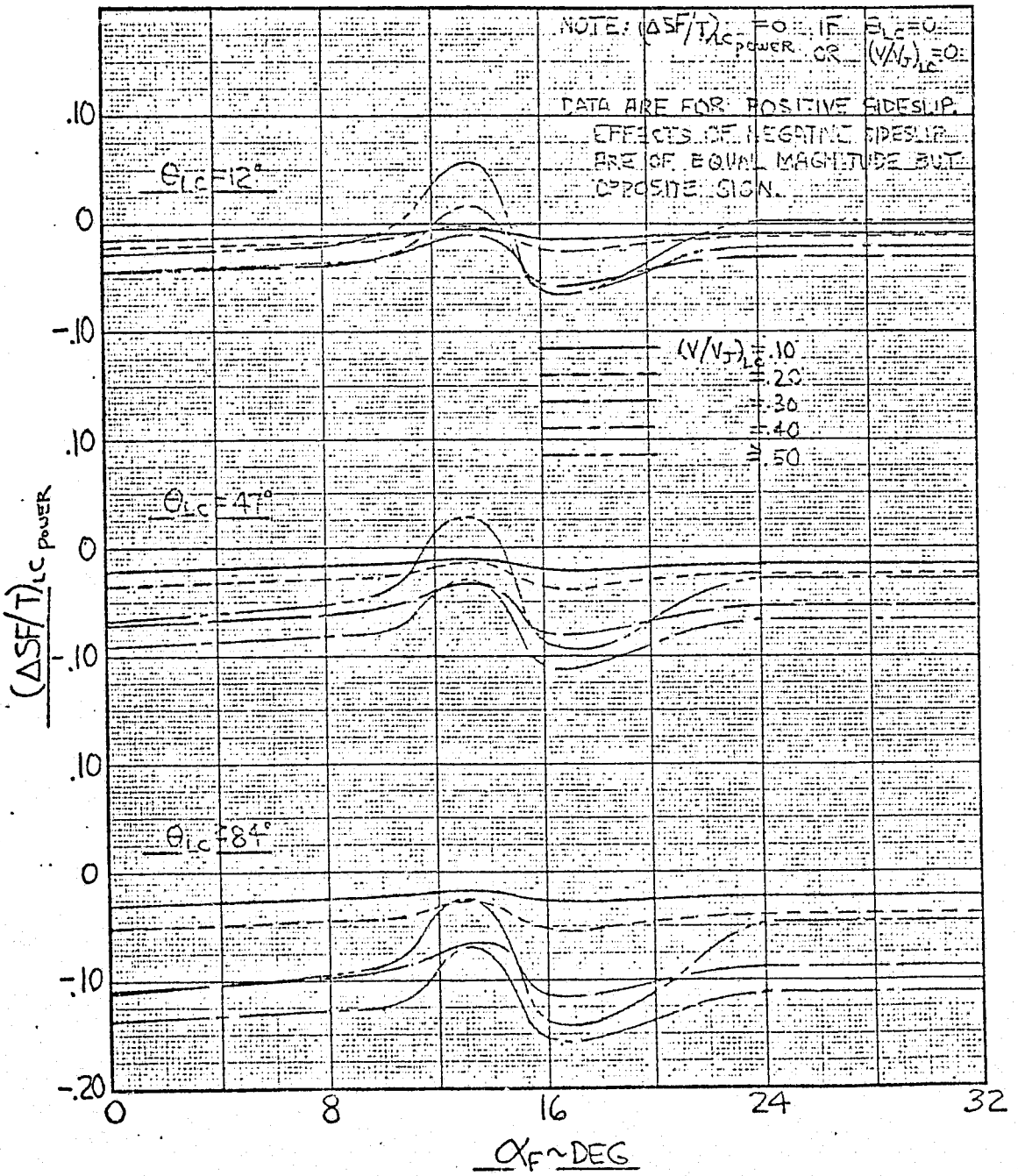

FIGURE 15-44

POWER INDUCED YAWING MOMENT USING LIFT CRUISE UNIT

STABILITY AXES

$\beta = 0° \& +6°$; $\theta_{LC} = 0° \& 12°$

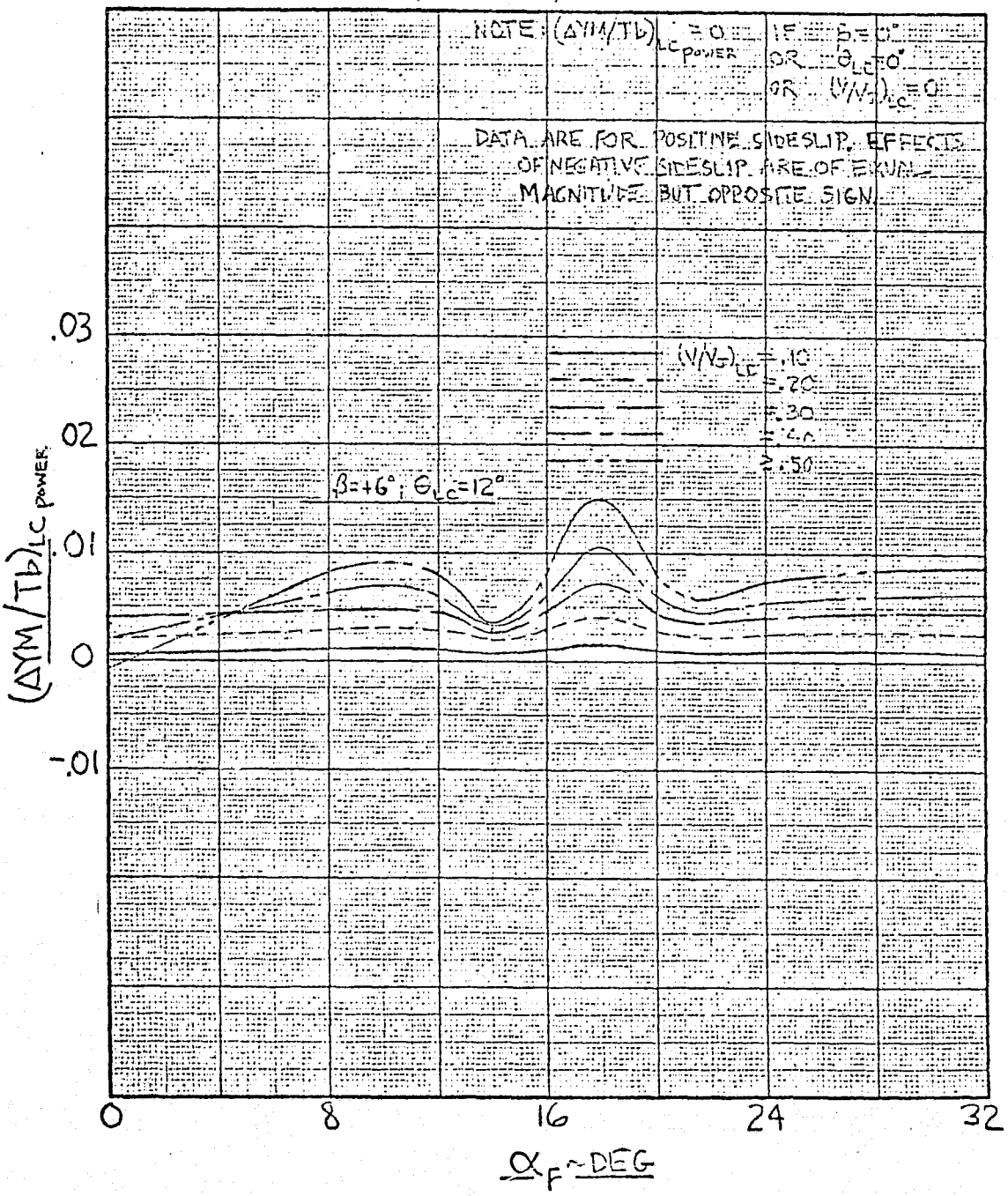

FIGURE 15-45

POWER INDUCED YAWING MOMENT USING LIFT CRUISE UNIT

STABILITY AXES

$\beta = +12°$ $\theta_{LC} = 0° \& 12°$

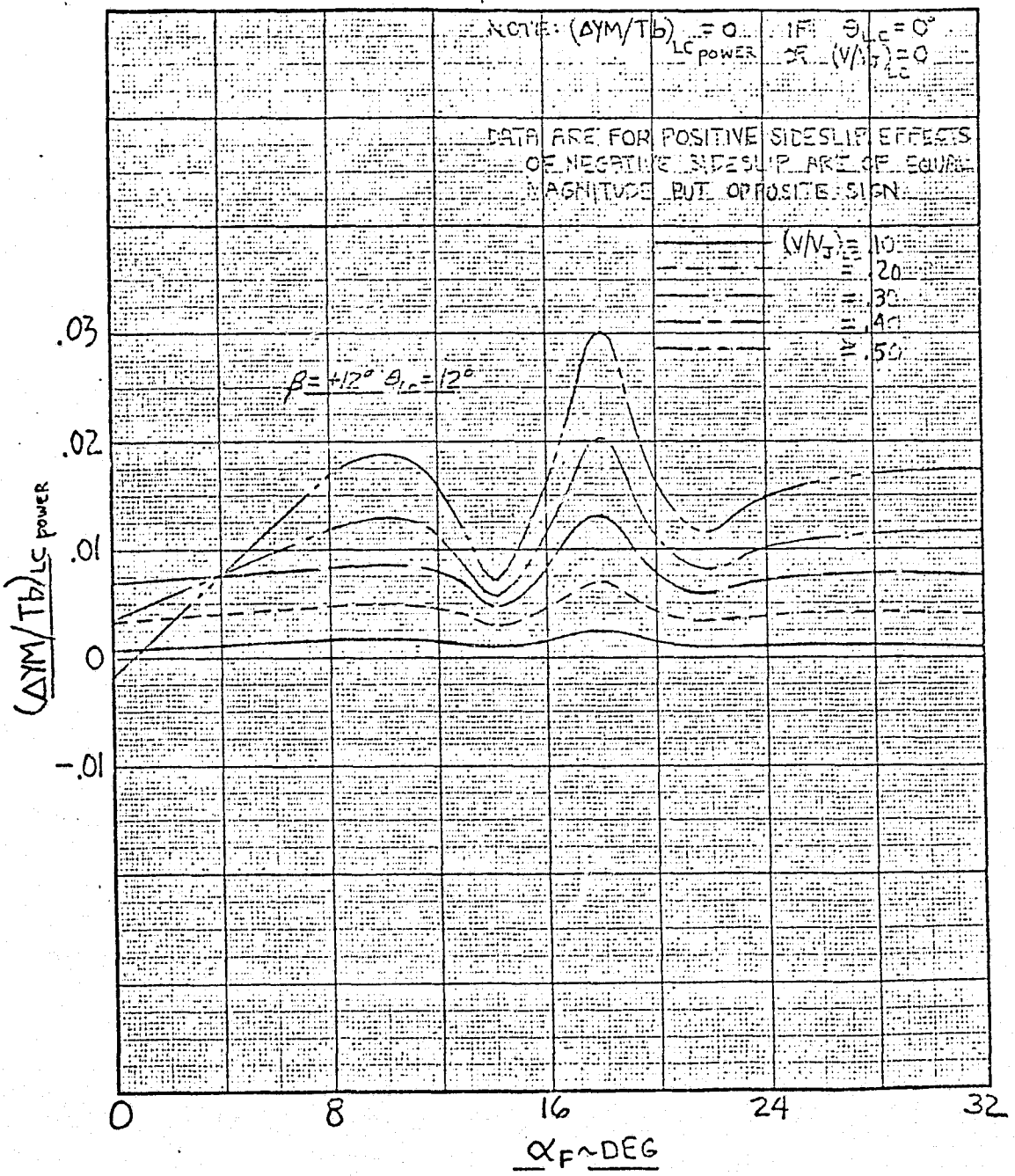

FIGURE 15-46

POWER INDUCED YAWING MOMENT USING LIFT CRUISE UNIT

STABILITY AXES

$\beta \geq +18°$; $\theta_{LC} = 0° \& 12°$

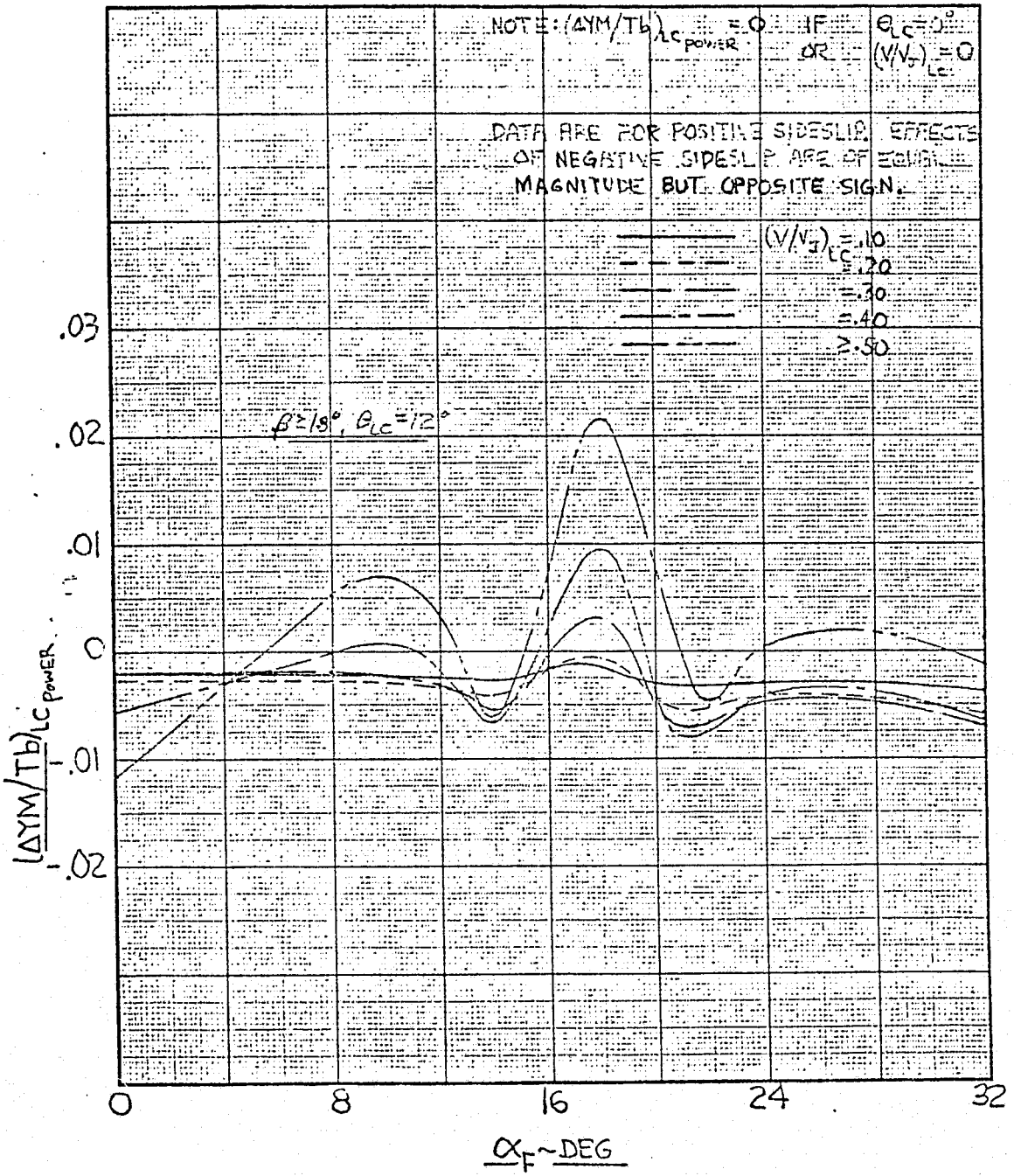

FIGURE 15-47

POWER INDUCED YAWING MOMENT USING LIFT CRUISE UNIT

STABILITY AXES

$\beta = 0°, +6°, +12°$; $\theta_{LC} = 47°$

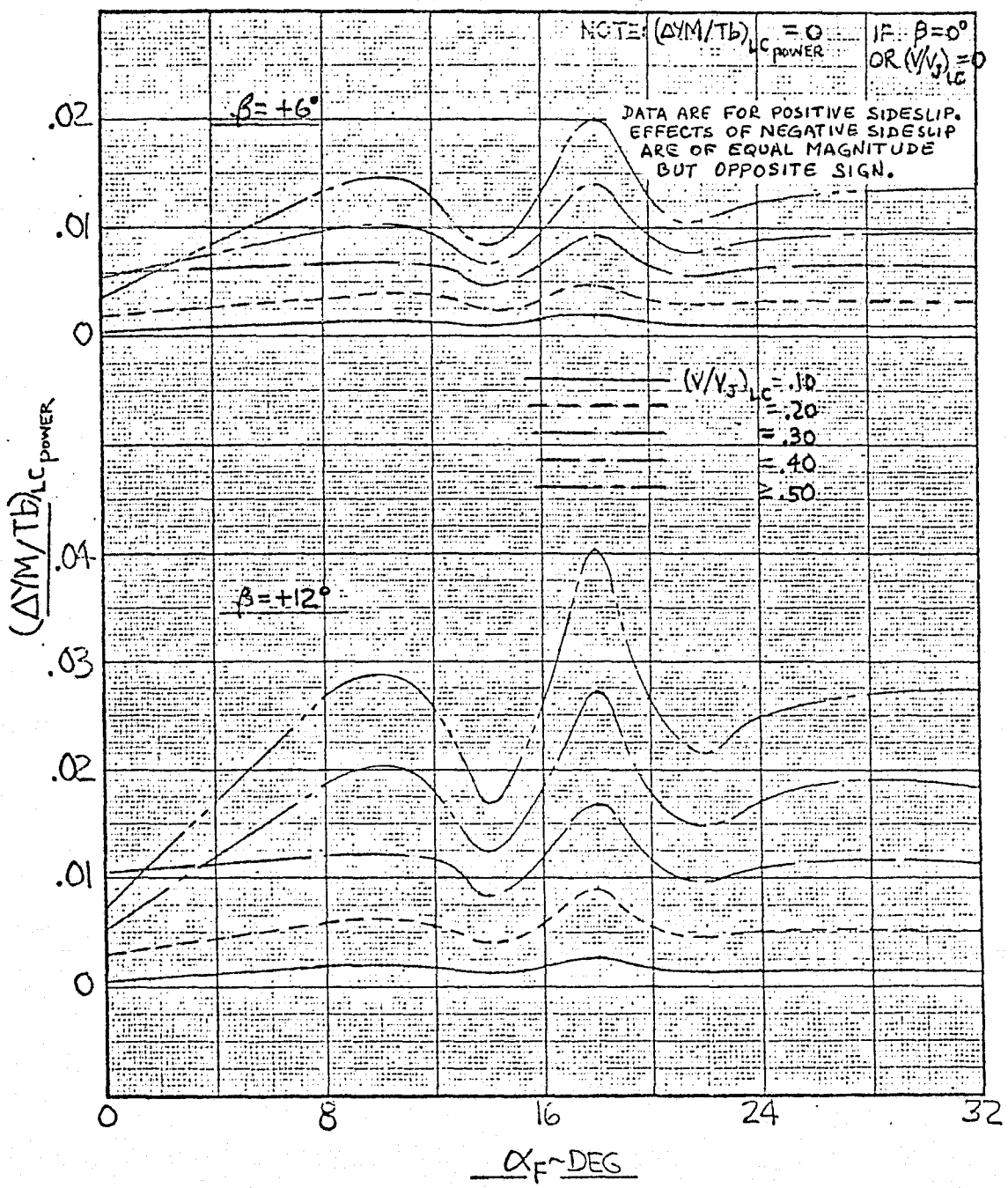

FIGURE 15-48

POWER INDUCED YAWING MOMENT USING LIFT CRUISE UNIT

STABILITY AXES

$\beta \geq +18°$; $\theta_{LC} = 47°$

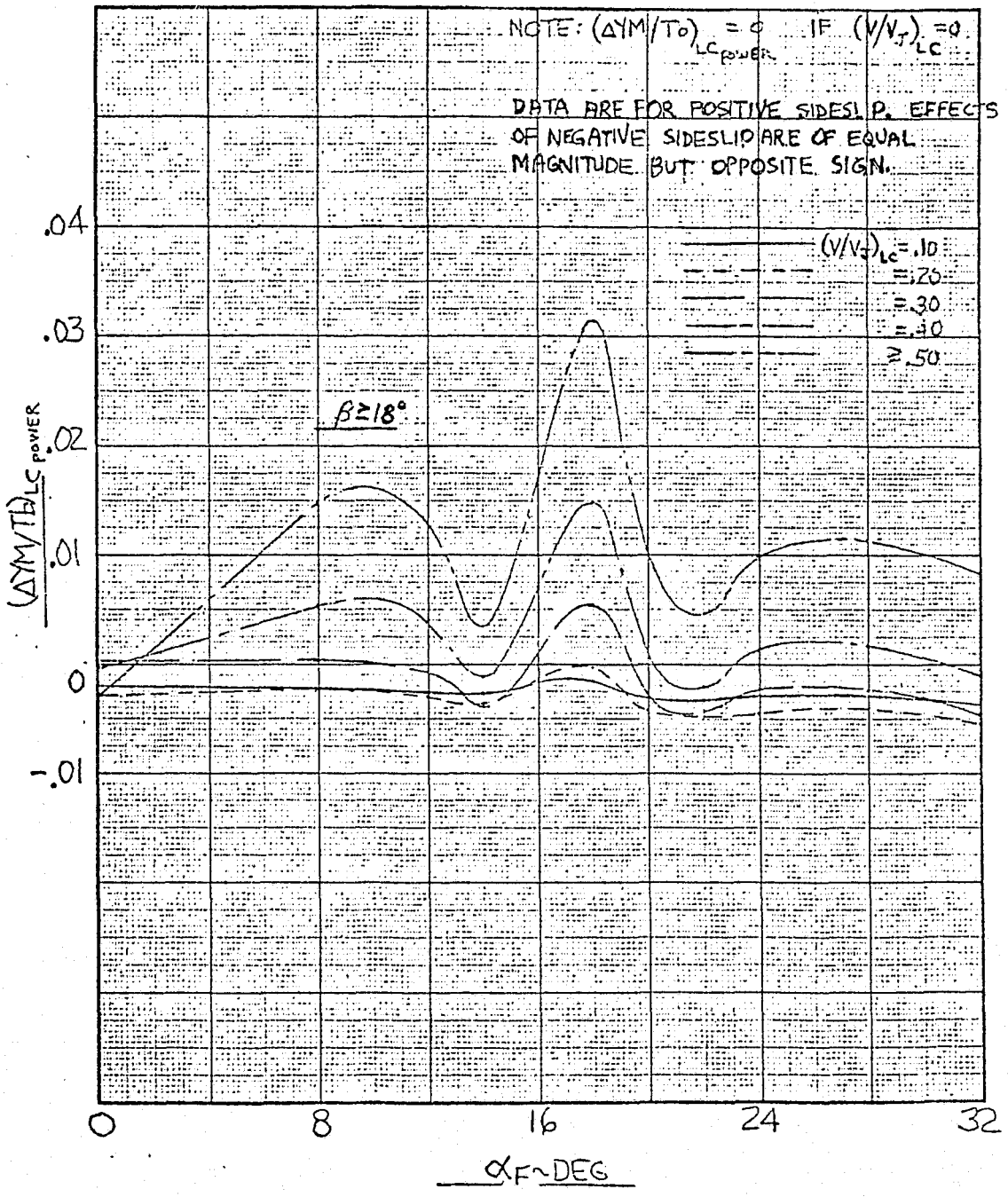

FIGURE 15-49

POWER INDUCED YAWING MOMENT USING LIFT CRUISE UNIT

STABILITY AXES

$\beta = 0°, +6°, +12°$; $\theta_{LC} \geq 84°$

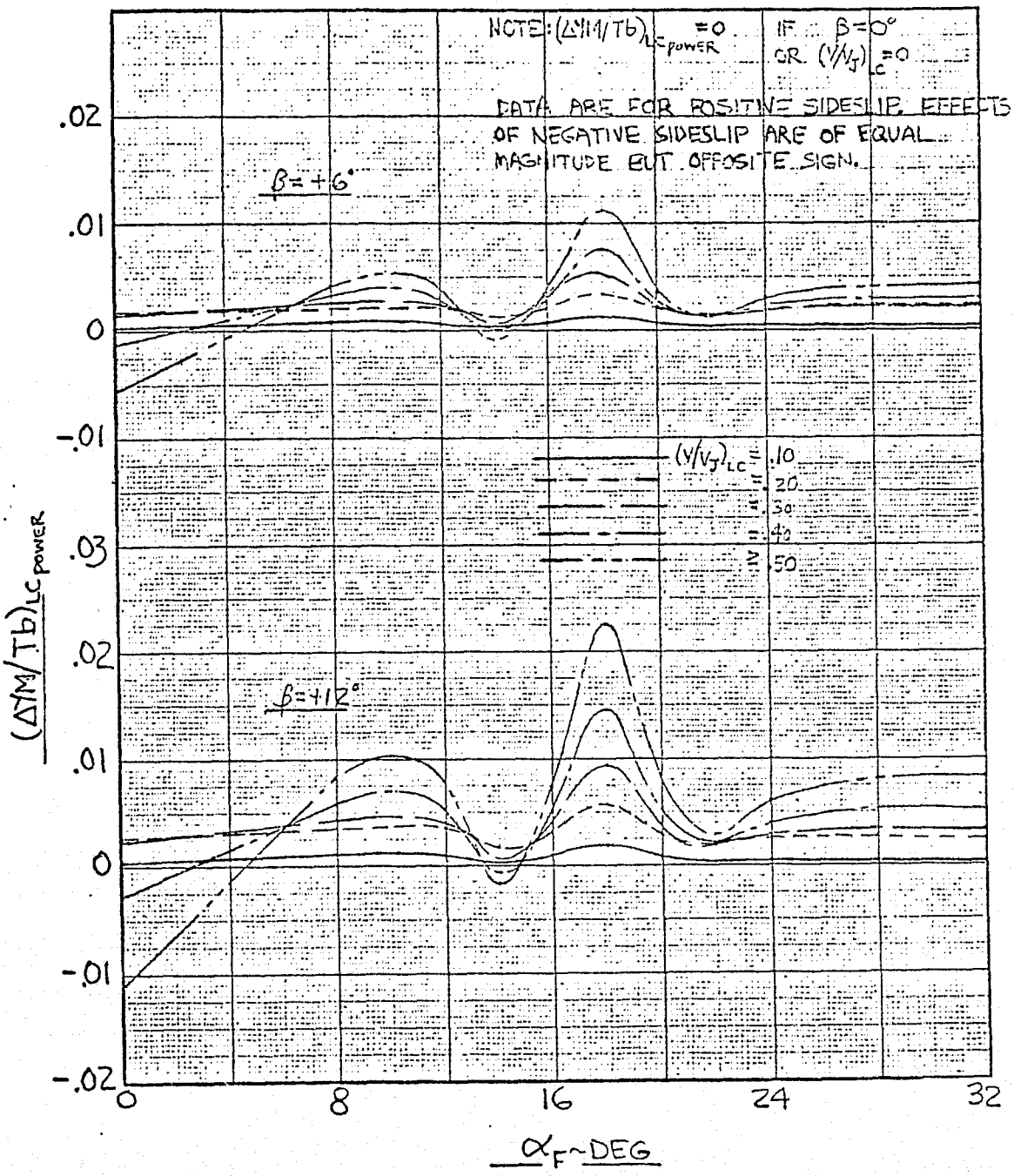

FIGURE 15-50

POWER INDUCED YAWING MOMENT USING LIFT CRUISE UNIT
STABILITY AXES

$\beta \geq 18°$ $\theta_{LC} \geq 84°$

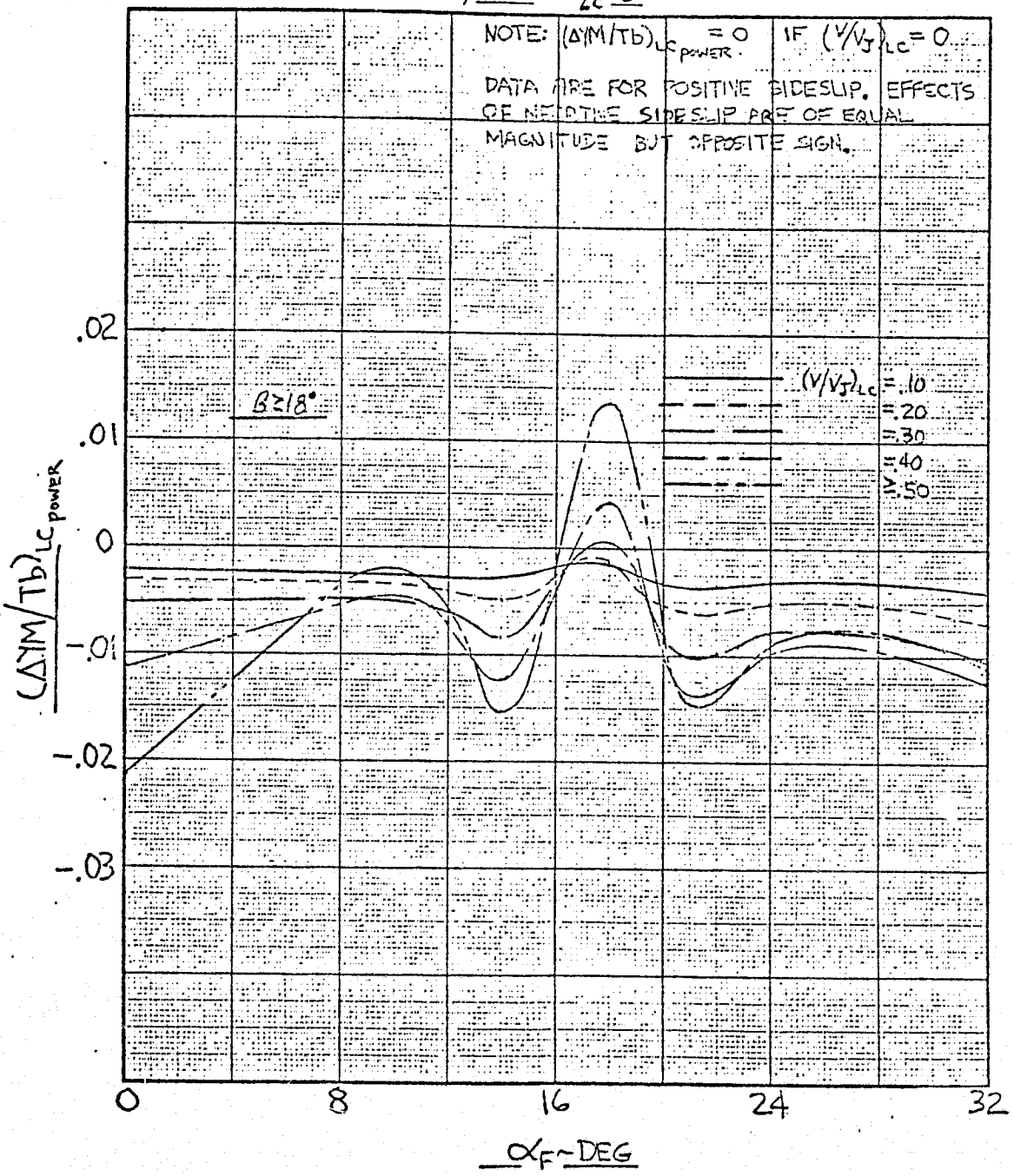

FIGURE 15-51

POWER INDUCED ROLLING MOMENT USING LIFT CRUISE UNIT

STABILITY AXES

$\beta = 0°, +6°$; $\theta_{LC} = 0°, 12°$

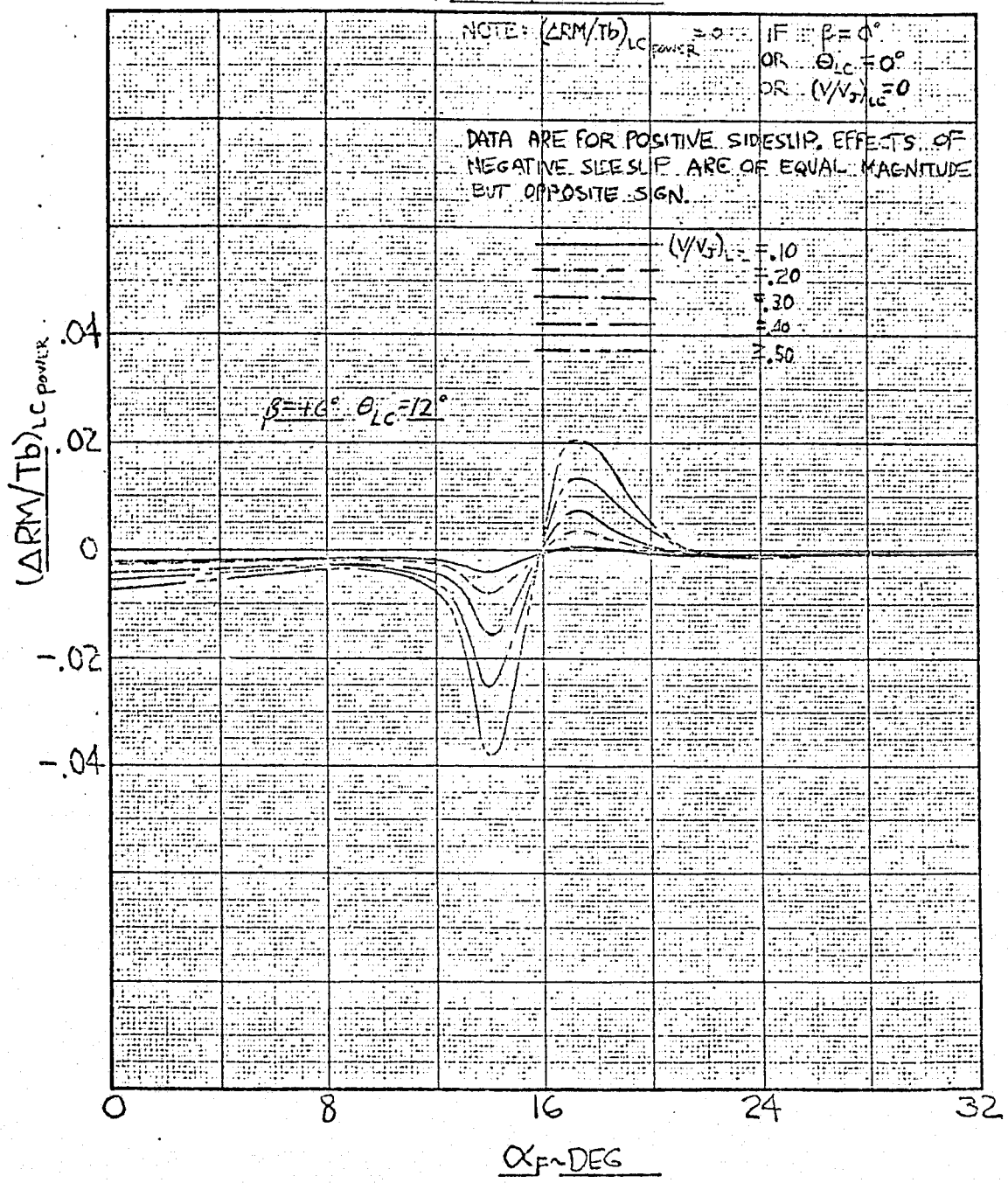

FIGURE 15-52

POWER INDUCED ROLLING MOMENT USING LIFT CRUISE UNIT

STABILITY AXES

$\beta = +12°$; $\theta_{LC} = 0°, 12°$

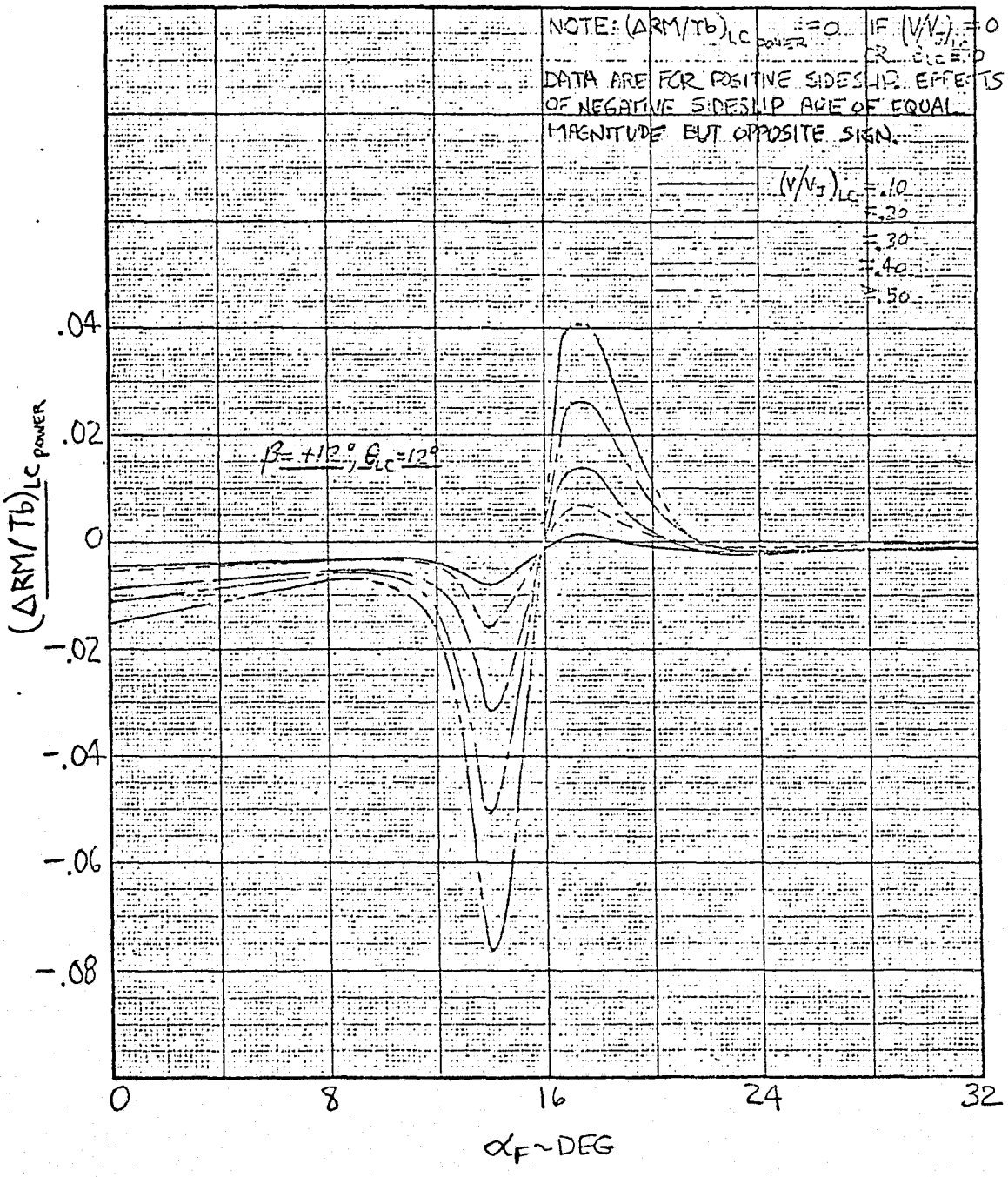

FIGURE 15-53

POWER INDUCED ROLLING MOMENT USING LIFT CRUISE UNIT

STABILITY AXES

$\beta = +18°$ $\theta_{LC} = 0°, 12°$

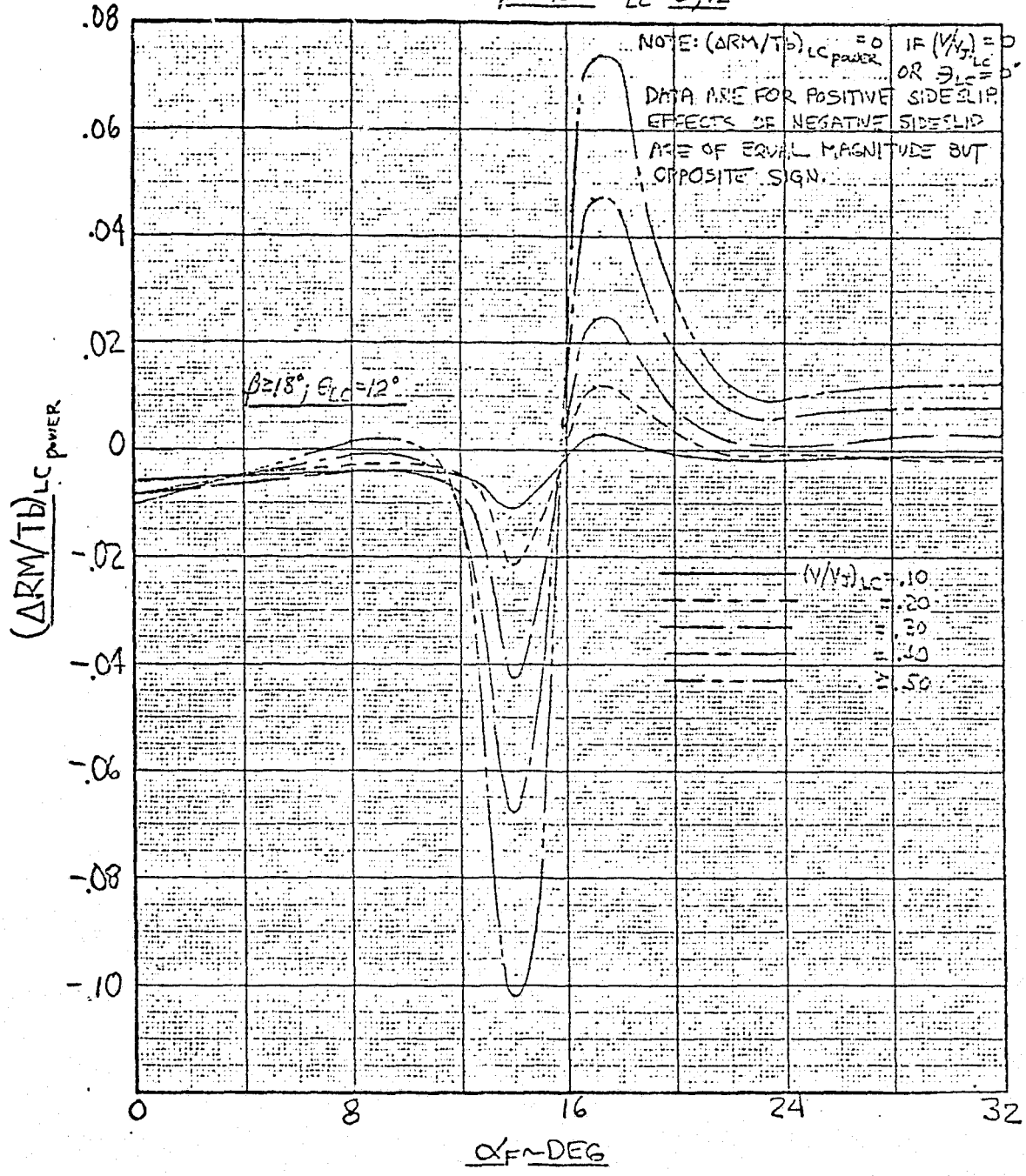

FIGURE 15-54

POWER INDUCED ROLLING MOMENT USING LIFT CRUISE UNIT

STABILITY AXES

$\beta = 0°, +6°$; $\theta_{LC} = 47°$

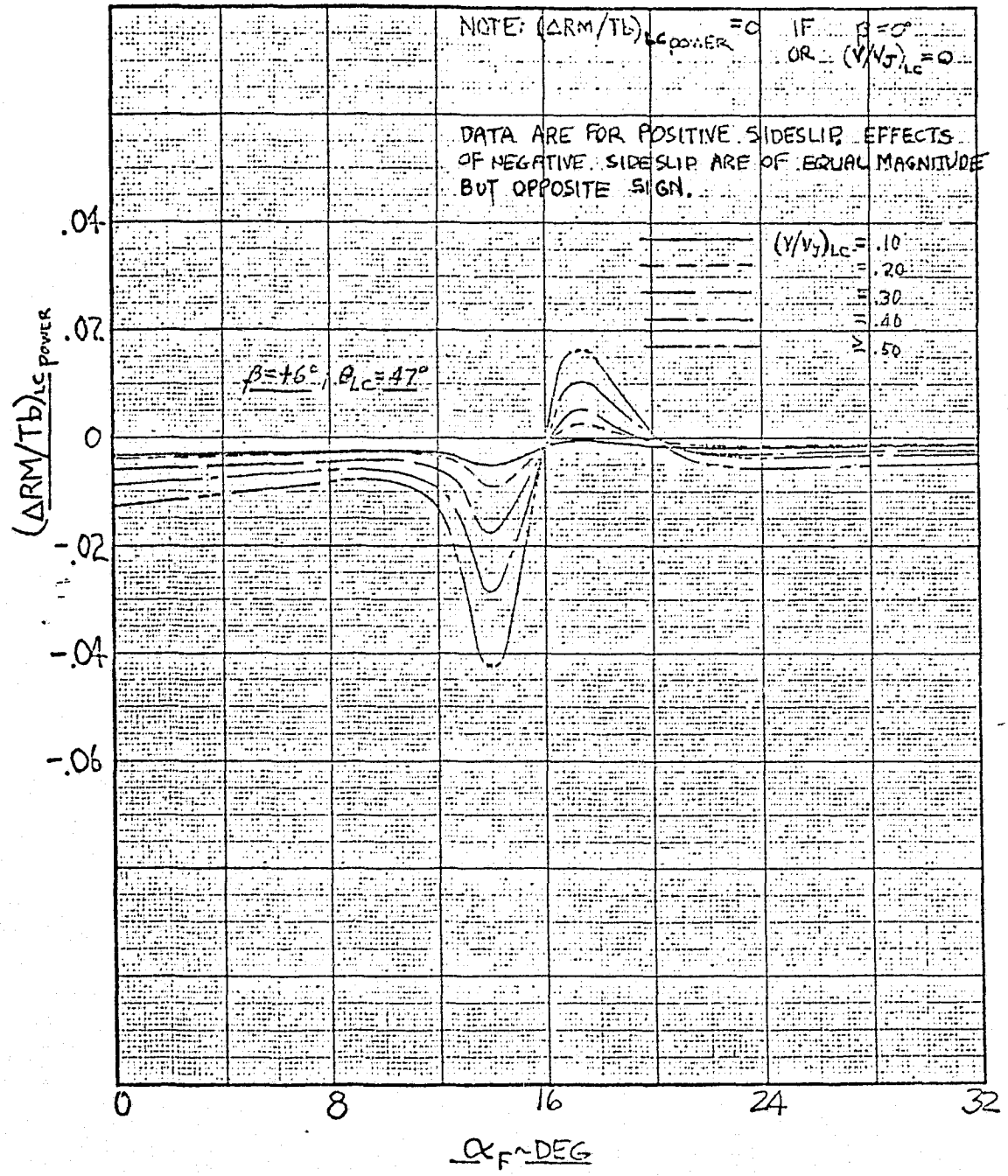

FIGURE 15-55

POWER INDUCED ROLLING MOMENT USING LIFT CRUISE UNIT

STABILITY AXES

$\beta = +12°$; $\theta_{LC} = 47°$

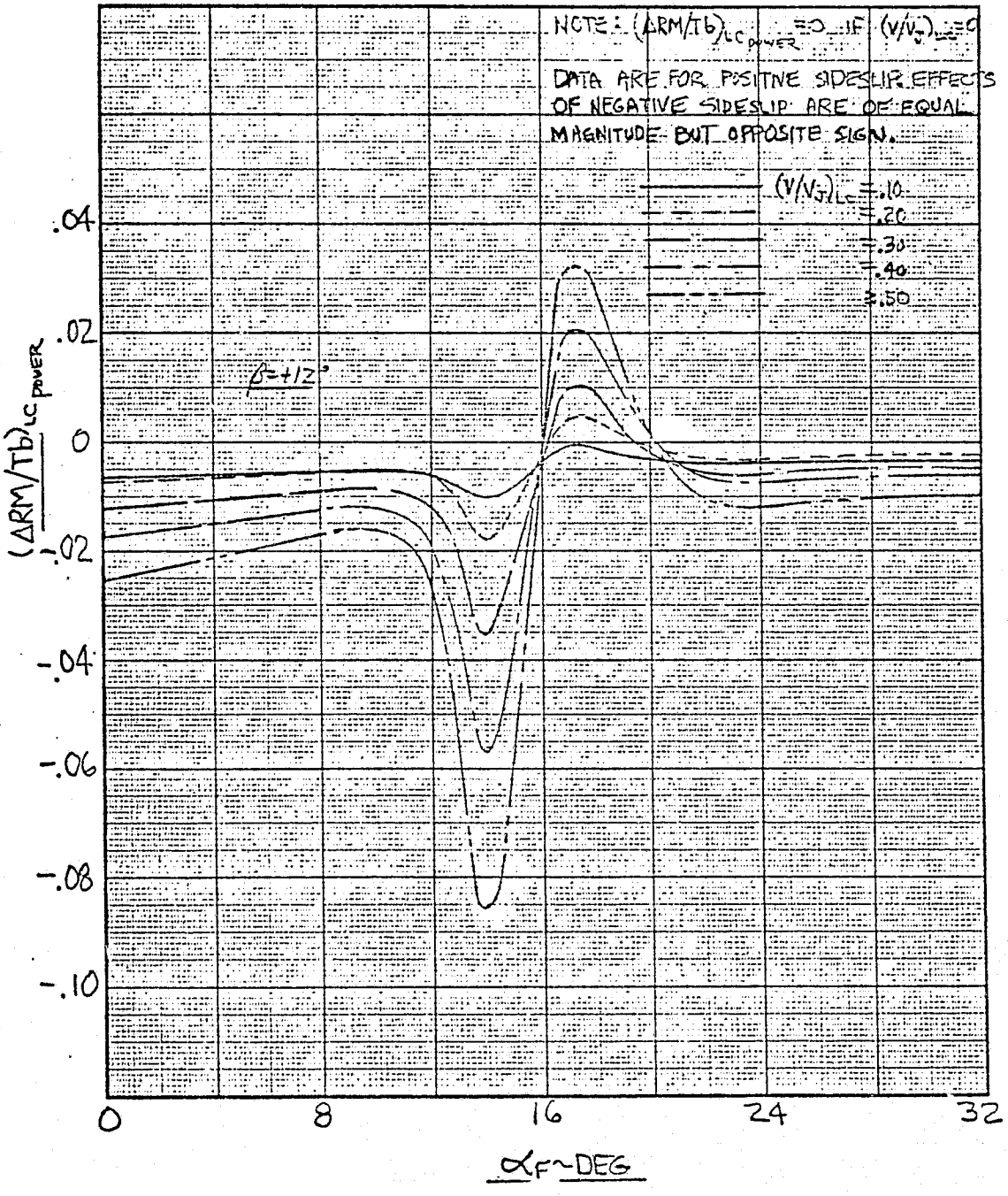

FIGURE 15-56

POWER INDUCED ROLLING MOMENT USING LIFT CRUISE UNIT

STABILITY AXES

$\beta = +18°$; $\theta_{l.c.} = 47°$

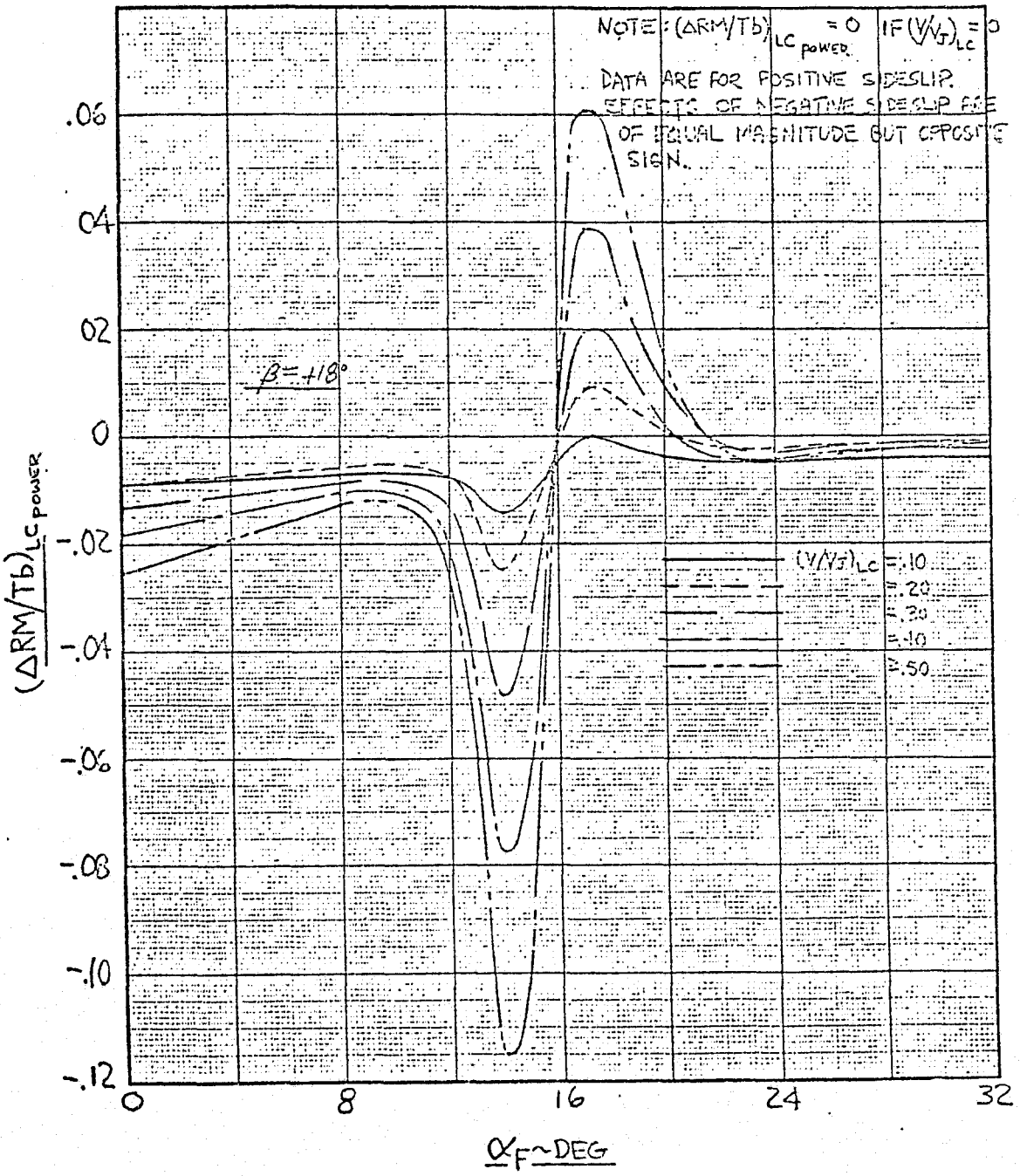

FIGURE 15-57

POWER INDUCED ROLLING MOMENT USING LIFT CRUISE UNIT

STABILITY AXES

$\beta = 0°, +6°$; $\theta_{LC} \geq 84°$

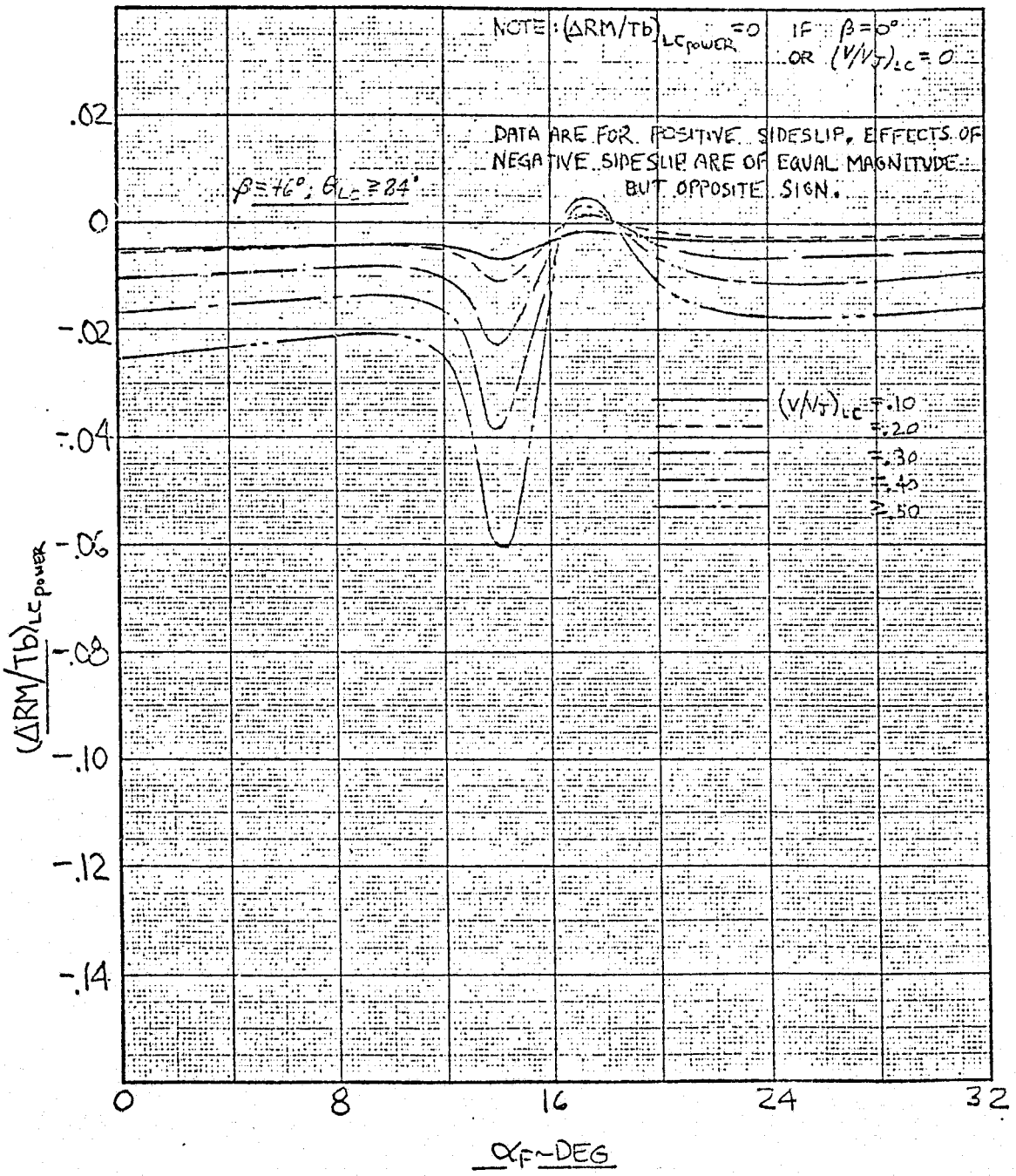

FIGURE 15-58

POWER INDUCED ROLLING MOMENT USING LIFT CRUISE UNIT

STABILITY AXES

$\beta = +12°$; $\theta_{LC} \geq 84°$

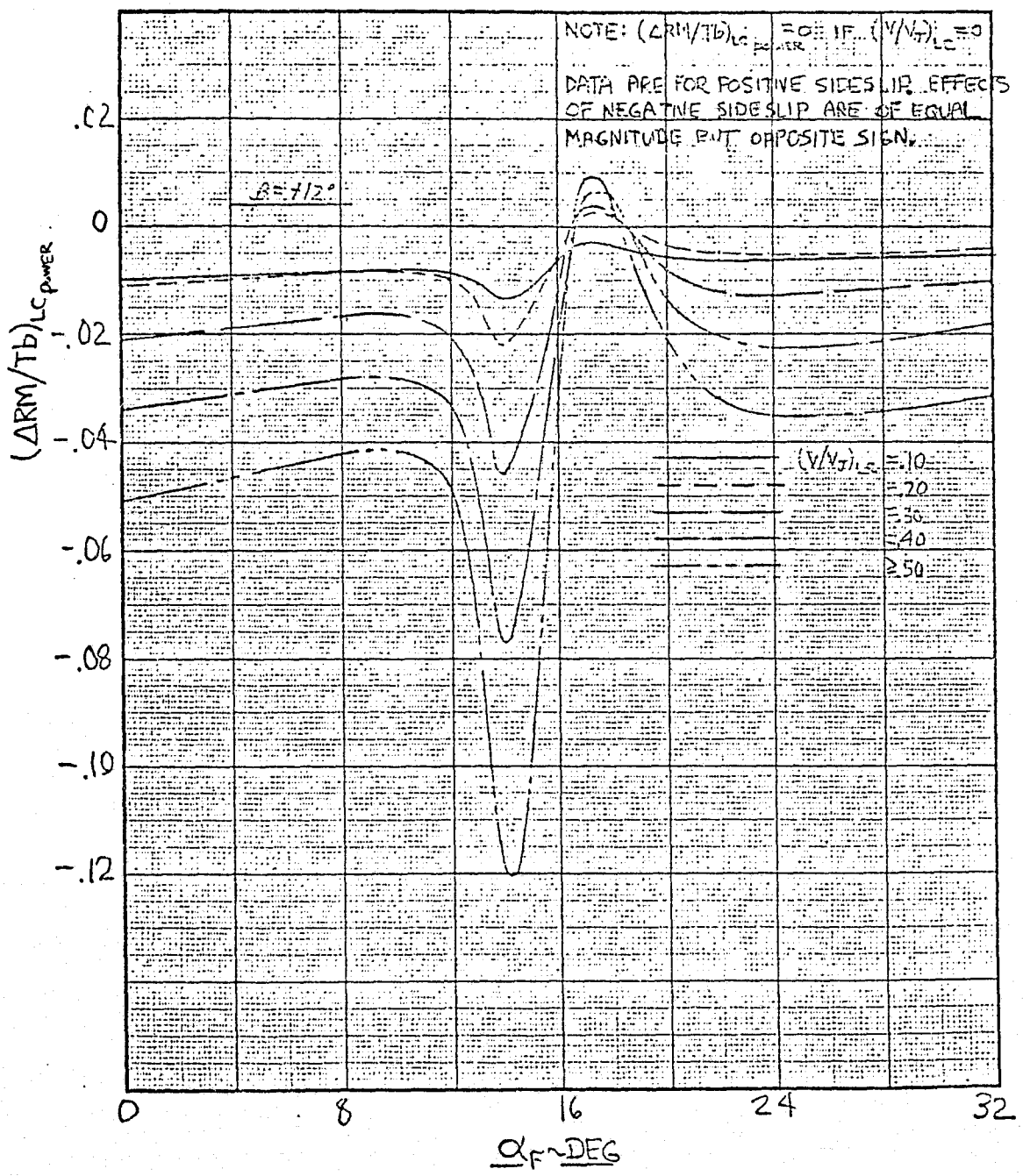

FIGURE 15-59

POWER INDUCED ROLLING MOMENT USING LIFT CRUISE UNIT

STABILITY AXES

$\beta = +18°$ $\theta_{LC} = 84°$

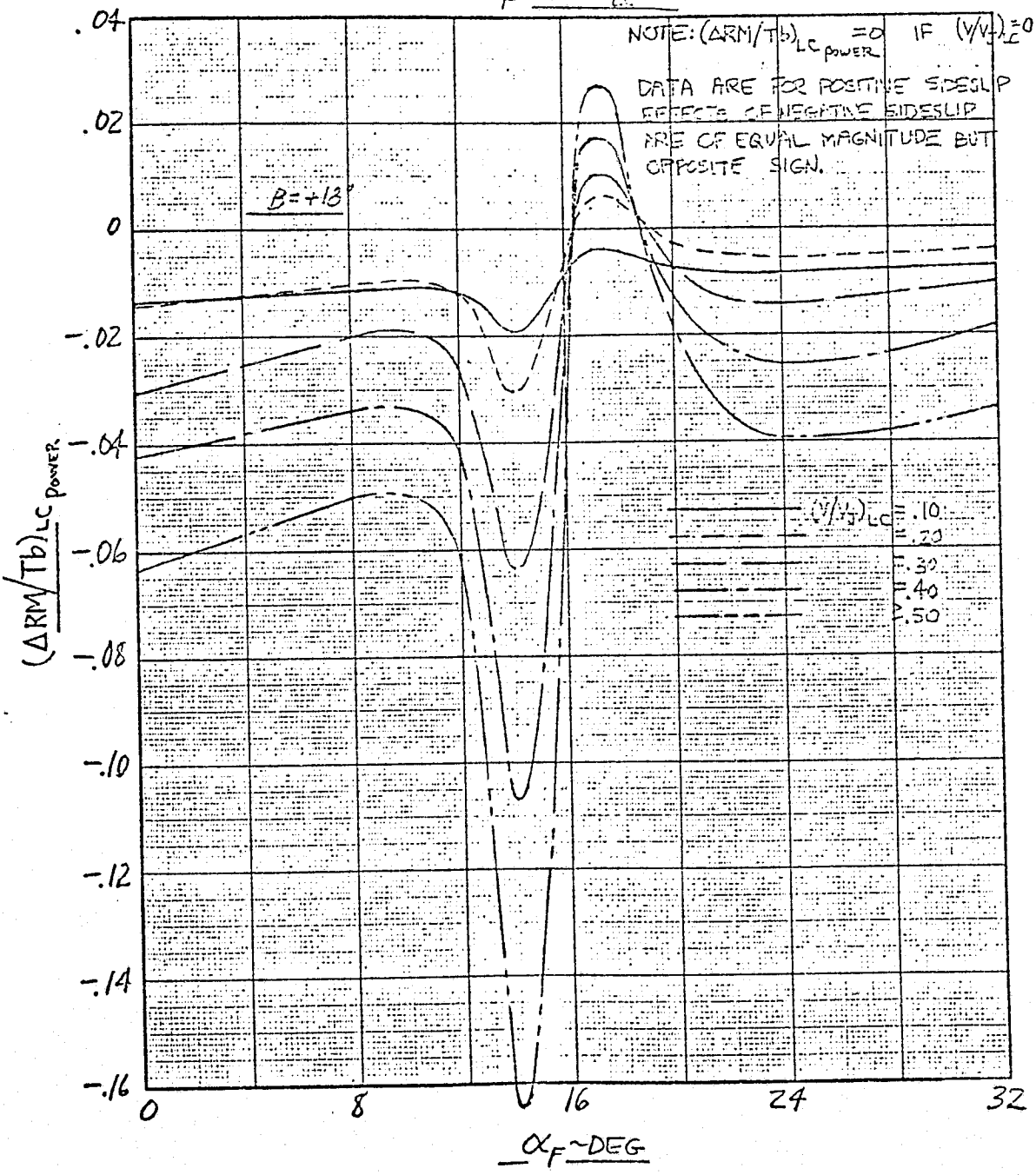

FIGURE 15-60

POWER INDUCED LATERAL-DIRECTIONAL CHARACTERISTICS USING NOSE LIFT UNIT

$$\left(\frac{\Delta SF}{T}\right)_{NL_{POWER}} = 0$$

$$\left(\frac{\Delta YM}{Tb}\right)_{NL_{POWER}} = 0$$

$$\left(\frac{\Delta RM}{Tb}\right)_{NL_{POWER}} = 0$$

EFFECTS OF GROUND PROXIMITY ON LATERAL-DIRECTIONAL CHARACTERISTICS

$$\Delta C_{Y_{\beta_{GE}}} = 0$$

$$\Delta C_{n_{\beta_{GE}}} = 0$$

$$\Delta C_{\ell_{\beta_{GE}}} = 0$$

FIGURE 15-61

EFFECTS OF GROUND PROXIMITY ON POWER INDUCED LATERAL-DIRECTIONAL CHARACTERISTICS

$$\left[\Delta\left(\frac{\Delta SF}{T}\right)_{NL_{POWER}}\right]_{GE} = 0$$

$$\left[\Delta\left(\frac{\Delta SF}{T}\right)_{LC_{POWER}}\right]_{GE} = 0$$

$$\left[\Delta\left(\frac{\Delta YM}{Tb}\right)_{NL_{POWER}}\right]_{GE} = 0$$

$$\left[\Delta\left(\frac{\Delta YM}{Tb}\right)_{LC_{POWER}}\right]_{GE} = 0$$

$$\left[\Delta\left(\frac{\Delta RM}{Tb}\right)_{NL_{POWER}}\right]_{GE} = 0$$

$$\left[\Delta\left(\frac{\Delta RM}{Tb}\right)_{LC_{POWER}}\right]_{GE} = 0$$

FIGURE 15-62

EFFECT OF ROLL ANGLE ON POWER INDUCED LATERAL-DIRECTIONAL CHARACTERISTICS

$$\left[\Delta\left(\frac{\Delta SF}{T}\right)_{NL_{POWER}}\right]_{\phi} = 0$$

$$\left[\Delta\left(\frac{\Delta SF}{T}\right)_{LC_{POWER}}\right]_{\phi} = 0$$

$$\left[\Delta\left(\frac{\Delta YM}{Tb}\right)_{NL_{POWER}}\right]_{\phi} = 0$$

$$\left[\Delta\left(\frac{\Delta YM}{Tb}\right)_{LC_{POWER}}\right]_{\phi} = 0$$

$$\left[\Delta\left(\frac{\Delta RM}{Tb}\right)_{NL_{POWER}}\right]_{\phi} = 0$$

$$\left[\Delta\left(\frac{\Delta RM}{Tb}\right)_{LC_{POWER}}\right]_{\phi} = 0$$

FIGURE 15-63

EFFECT OF ROLL RATE ON LATERAL-DIRECTIONAL CHARACTERISTICS STABILITY AXES

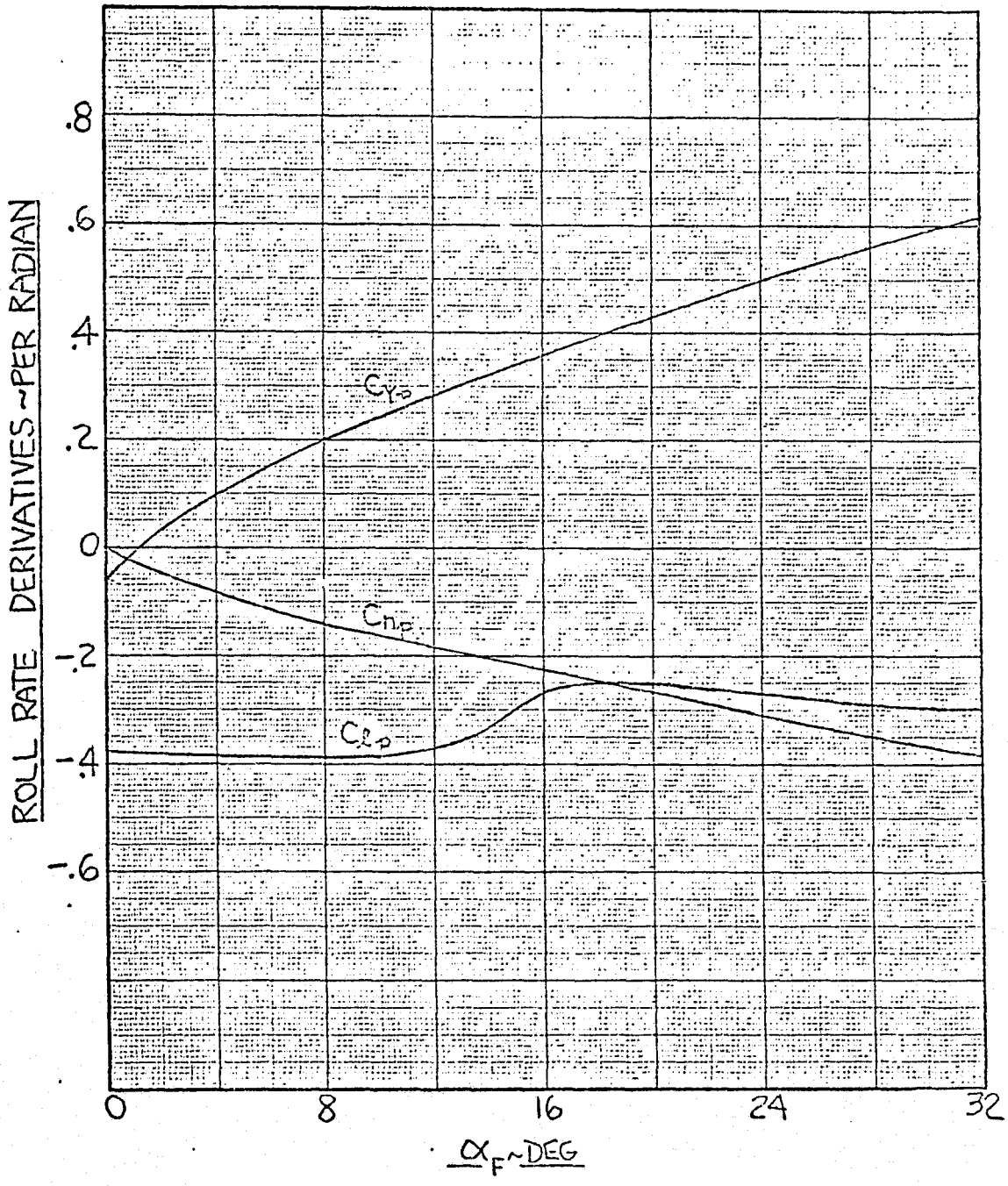

FIGURE 15-64

EFFECT OF YAW RATE ON
LATERAL-DIRECTIONAL CHARACTERISTICS
STABILITY AXES

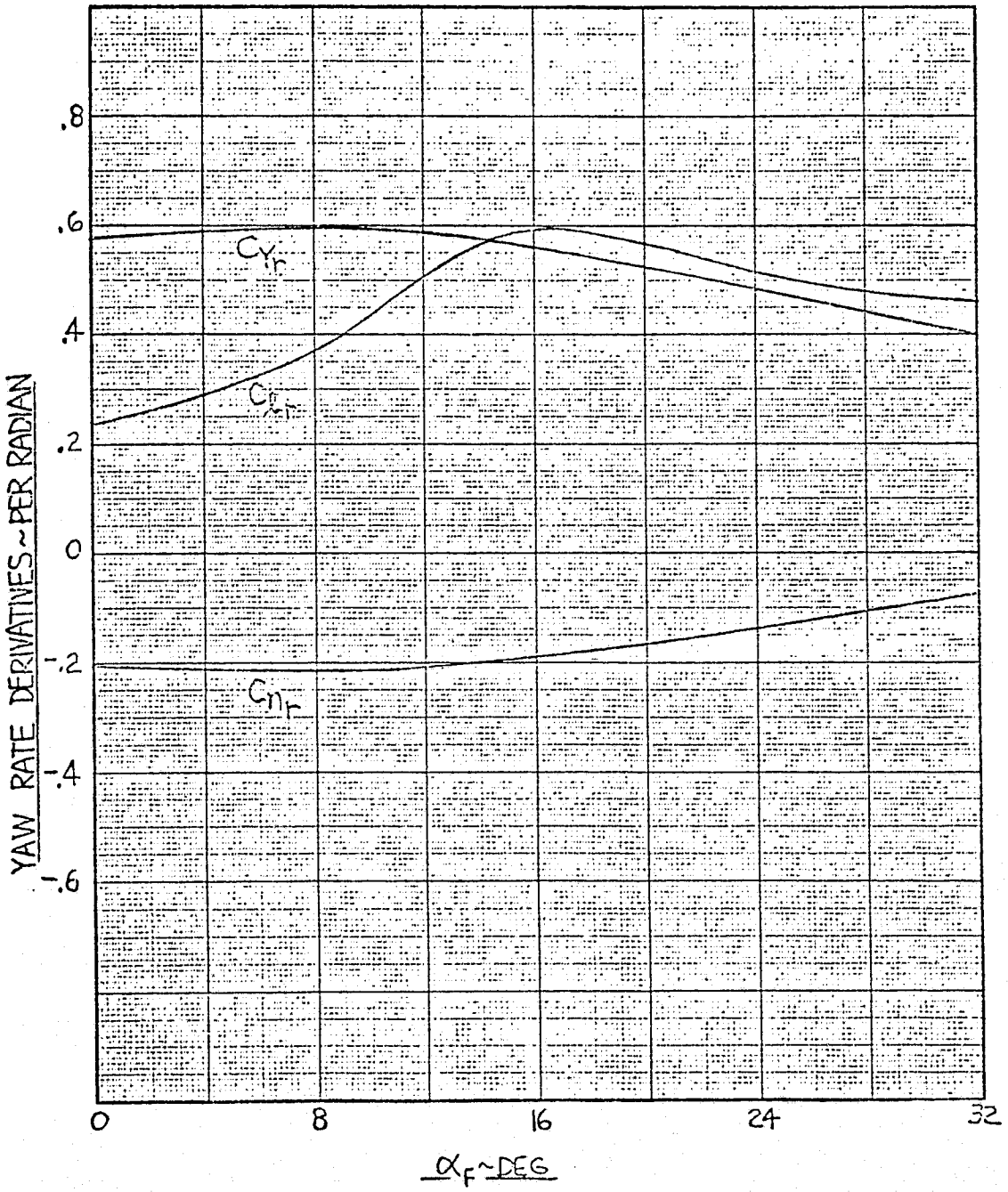

16. LANDING GEAR FORCES AND MOMENTS

Figures 16-1 through 16-3 list the equations used to simulate the landing gear. These equations are considerably simplified and were derived for the purpose of permitting simulated takeoffs and landings; they are not intended to be used to accurately simulate landing gear dynamics. The landing gear forces simulated here consist of friction forces plus linearized spring rate and damping forces.

The numerical values of constants used in landing gear equations are listed in Figure 16-4.

FIGURE 16-1

LANDING GEAR MODEL

STRUT COMPRESSION *

$$a_{NG} = (h - x_{NG} l_3 - y_{NG} m_3 - z_{NG} n_3) / n_3$$
$$a_{LMG} = (h - x_{MG} l_3 + y_{MG} m_3 - z_{MG} n_3) / n_3$$
$$a_{RMG} = (h - x_{MG} l_3 - y_{MG} m_3 - z_{MG} n_3) / n_3$$

DIRECTION COSINE DERIVATIVES

$$\dot{l}_3 = - \cos\theta\,\dot{\theta}$$
$$\dot{m}_3 = - \sin\phi \sin\theta\,\dot{\theta} + \cos\phi \cos\theta\,\dot{\phi}$$
$$\dot{n}_3 = - \cos\theta \sin\phi\,\dot{\phi} - \sin\theta \cos\phi\,\dot{\theta}$$

STRUT COMPRESSION RATES

$$\dot{a}_{NG} = [(\dot{n}_3 l_3 - n_3 \dot{l}_3) x_{NG} + (\dot{n}_3 m_3 - n_3 \dot{m}_3) y_{NG} + (n_3 \dot{h} - \dot{n}_3 h)] / n_3^2$$
$$\dot{a}_{LMG} = [(\dot{n}_3 l_3 - n_3 \dot{l}_3) x_{MG} - (\dot{n}_3 m_3 - n_3 \dot{m}_3) y_{MG} + (n_3 \dot{h} - \dot{n}_3 h)] / n_3^2$$
$$\dot{a}_{RMG} = [(\dot{n}_3 l_3 - n_3 \dot{l}_3) x_{MG} + (\dot{n}_3 m_3 - n_3 \dot{m}_3) y_{MG} + (n_3 \dot{h} - \dot{n}_3 h)] / n_3^2$$

OLEO FORCES

$$Z_{NG} = b_{NG} \dot{a}_{NG} + k_{NG} a_{NG}$$
$$Z_{LMG} = b_{MG} \dot{a}_{LMG} + k_{MG} a_{LMG}$$
$$Z_{RMG} = b_{MG} \dot{a}_{RMG} + k_{MG} a_{RMG}$$

* IF $a_{(\,)} \geq 0$, ALL FORCES ($X_{(\,)}$, $Y_{(\,)}$, & $Z_{(\,)}$) ON THAT WHEEL ARE ZERO.

FIGURE 16-2
LANDING GEAR MODEL (CONTINUED)

GEAR REACTIONS FOR ROLLING AND SLIDING

$$X1_{NG} = [-M_A - M_F - M_{RAM} + (X_A + X_F + X_{RAM} + Wl_3)g_{MG} + Z_{NG}x_{NG} + Z_{LMG}x_{MG} + Z_{RMG}x_{MG}] / (g_{NG} - g_{MG})$$

$$X1_{MG} = \tfrac{1}{2}[M_A + M_F + M_{RAM} - (X_A + X_F + X_{RAM} + Wl_3)g_{NG} - Z_{NG}x_{NG} - Z_{LMG}x_{MG} - Z_{RMG}x_{MG}] / (g_{NG} - g_{MG})$$

$$Y1_{NG} = [-N_A - N_F - N_{RAM} + (Y_A + Y_F + Y_{RAM} + Wm_3)x_{MG}] / (x_{NG} - x_{MG})$$

$$Y1_{MG} = \tfrac{1}{2}[N_A + N_F + N_{RAM} - (Y_A + Y_F + Y_{RAM} + Wm_3)x_{NG}] / (x_{NG} - x_{MG})$$

ROLLING FRICTION FORCES

$$X_{NG} = Z_{NG}\mu_R \operatorname{sign} u_{IB} \qquad |u_{IB}| > 0$$
$$= -Z_{NG}\mu_R \operatorname{sign} X1_{NG} \qquad |u_{IB}| = 0,\ |X1_{NG}| > |Z_{NG}\mu_R|$$
$$= X1_{NG} \qquad |u_{IB}| = 0,\ |X1_{NG}| \le |Z_{NG}\mu_R|$$

$$X_{LMG} = Z_{LMG}\mu_R \operatorname{sign} u_{IB} \qquad |u_{IB}| > 0$$
$$= -Z_{LMG}\mu_R \operatorname{sign} X1_{MG} \qquad |u_{IB}| = 0,\ |X1_{MG}| > |Z_{LMG}\mu_R|$$
$$= X1_{MG} \qquad |u_{IB}| = 0,\ |X1_{MG}| \le |Z_{LMG}\mu_R|$$

$$X_{RMG} = Z_{RMG}\mu_R \operatorname{sign} u_{IB} \qquad |u_{IB}| > 0$$
$$= -Z_{RNG}\mu_R \operatorname{sign} X1_{MG} \qquad |u_{IB}| = 0,\ |X1_{MG}| > |Z_{RMG}\mu_R|$$
$$= X1_{MG} \qquad |u_{IB}| = 0,\ |X1_{MG}| \le |Z_{RMG}\mu_R|$$

FIGURE 16-3
LANDING GEAR MODEL (CONTINUED)

SLIDING FRICTION FORCES

$$Y_{NG} = Z_{NG}\mu_s \operatorname{sign} v_{IB} \qquad |v_{IB}| > 0$$
$$= -Z_{NG}\mu_s \operatorname{sign} Y1_{NG} \qquad |v_{IB}| = 0,\ |Y1_{NG}| > |Z_{NG}\mu_s|$$
$$= Y1_{NG} \qquad |v_{IB}| = 0,\ |Y1_{NG}| \le |Z_{NG}\mu_s|$$

$$Y_{LMG} = Z_{LMG}\mu_s \operatorname{sign} v_{IB} \qquad |v_{IB}| > 0$$
$$= Z_{LMG}\mu_s \operatorname{sign} Y1_{MG} \qquad |v_{IB}| = 0,\ |Y1_{MG}| > |Z_{LMG}\mu_s|$$
$$= Y1_{MG} \qquad |v_{IB}| = 0,\ |Y1_{MG}| \le |Z_{LMG}\mu_s|$$

$$Y_{RMG} = Z_{RMG}\mu_s \operatorname{sign} v_{IB} \qquad |v_{IB}| > 0$$
$$= -Z_{RMG}\mu_s \operatorname{sign} Y1_{MG} \qquad |v_{IB}| = 0,\ |Y1_{MG}| > |Z_{RMG}\mu_s|$$
$$= Y1_{MG} \qquad |v_{IB}| = 0,\ |Y1_{MG}| \le |Z_{RMG}\mu_s|$$

TOTAL GEAR FORCES

$$X_{LG} = X_{NG} + X_{LMG} + X_{RMG}$$
$$Y_{LG} = Y_{NG} + Y_{LMG} + Y_{RMG}$$
$$Z_{LG} = Z_{NG} + Z_{LMG} + Z_{RMG}$$

TOTAL GEAR MOMENTS

$$L_{LG} = -Y_{NG}\zeta_{NG} - Y_{LMG}\zeta_{MG} - Y_{RMG}\zeta_{MG} - Z_{LMG}\eta_{MG} + Z_{RMG}\eta_{MG}$$
$$M_{LG} = X_{NG}\zeta_{NG} + X_{LMG}\zeta_{MG} + X_{RMG}\zeta_{MG} - Z_{NG}\xi_{NG} - Z_{LMG}\xi_{MG} - Z_{RMG}\xi_{MG}$$
$$N_{LG} = X_{LMG}\eta_{MG} - X_{RMG}\eta_{MG} + Y_{NG}\xi_{NG} + Y_{LMG}\xi_{MG} + Y_{RMG}\xi_{MG}$$

FIGURE 16-4

LANDING GEAR MODEL DATA

x_{NG}	Nose Gear x Location	9.33 ft
y_{NG}	Nose Gear y Location	0.00 ft
z_{NG}	Nose Gear z Location	10.31 ft
x_{MG}	Main Gear x Location	-3.66 ft
y_{MG}	Main Gear y Location	8.91 ft
z_{MG}	Main Gear z Location	9.35 ft
μ_R	Coefficient of Rolling Friction	0.02
μ_S	Coefficient of Sliding Friction	0.50
k_{NG}	Nose Gear Spring Rate	6750 lb/ft
b_{NG}	Nose Gear Damping	4500 lb-sec/ft
k_{MG}	Main Gear Spring Rate	8590 lb/ft
b_{MG}	Main Gear Damping	1300 lb-sec/ft

17. WIND MODEL

The wind model used in the simulation program provides a mean wind and a superimposed continuous random wind turbulence. The wind model parameters, such as the mean wind magnitude (V_{WIND}) and direction (ψ_{WIND}), are selected during the study as necessary to simulate the ambient conditions desired for specific simulation runs. The random turbulence is generated using a modified Dryden form of the spectra for the turbulence velocities.

The wind model parameters and the equations defining the mean wind components are presented in Figure 17-1. The Dryden filters used to shape the gust spectra are listed in Figure 17-2.

FIGURE 17-1
WIND MODEL

MEAN WIND COMPONENTS

$$W_X = -V_{WIND} \cos \Psi_{WIND}$$
$$W_Y = -V_{WIND} \sin \Psi_{WIND}$$
$$W_Z = 0$$

TURBULENCE INTENSITIES

$$\sigma_u = \sigma_v = 0.2\, V_{WIND}$$

$$\sigma_w = \sqrt{\frac{h}{5.357\bar{c}}}\,(0.5 + 0.001h)\,\sigma_u \qquad h \le 5.357\bar{c}$$
$$= (0.5 + 0.001h)\,\sigma_u \qquad 5.357\bar{c} < h < 500\ FT$$
$$= \sigma_u \qquad h \ge 500\ FT$$

$$L_u = L_v = 600\ FT \qquad h \le 260\ FT$$
$$= 340 + h \qquad h > 260\ FT$$

$$L_w = 8.25\,\bar{c} \qquad h \le 5.357\bar{c}$$
$$= 1.54\,h \qquad 5.357\bar{c} \le h \le 260\ FT$$
$$= 140 + h \qquad h > 260\ FT$$

WIND MODEL CONSTANT PARAMETERS

$\bar{c}$	MEAN AERODYNAMIC CHORD	8.38 FT
b	WING SPAN	44.43 FT

FIGURE 17-2

DRYDEN FILTERS

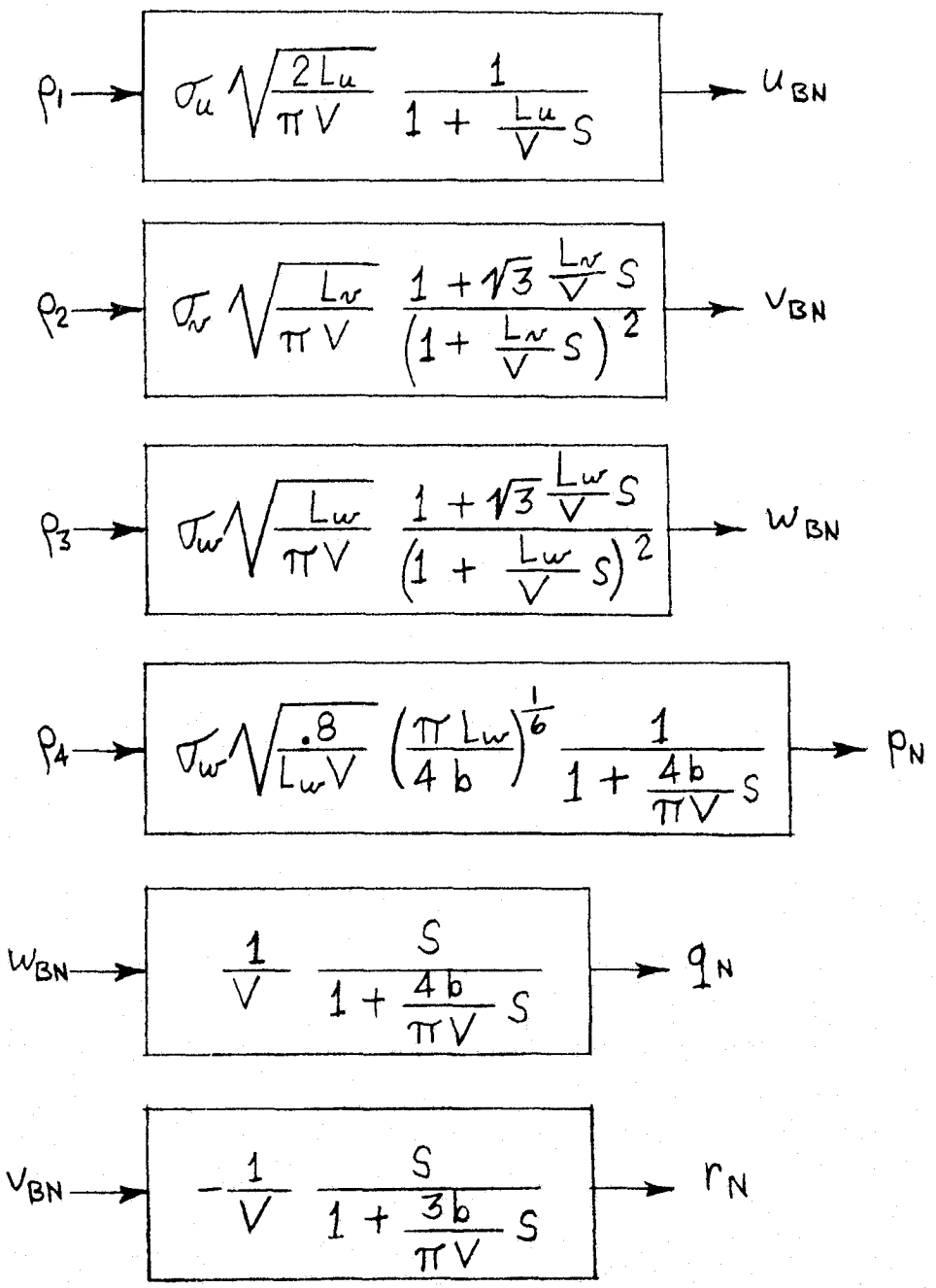

18. FUEL SYSTEM

In the math model of the fuel system the fuel consumption rates for the three engines are first summed, the total fuel consumption rate is then integrated and the result is continuously subtracted from the fuel quantity initially stored on the airplane. The result of the subtraction is the total remaining on-board fuel. The sum of the empty airplane weight and the remaining fuel weight is the current total airplane weight (W).

The described summations and integration are depicted schematically in Figure 18-1. Associated constants are tabulated in Figure 18-2.

FIGURE 18-1
FUEL SYSTEM

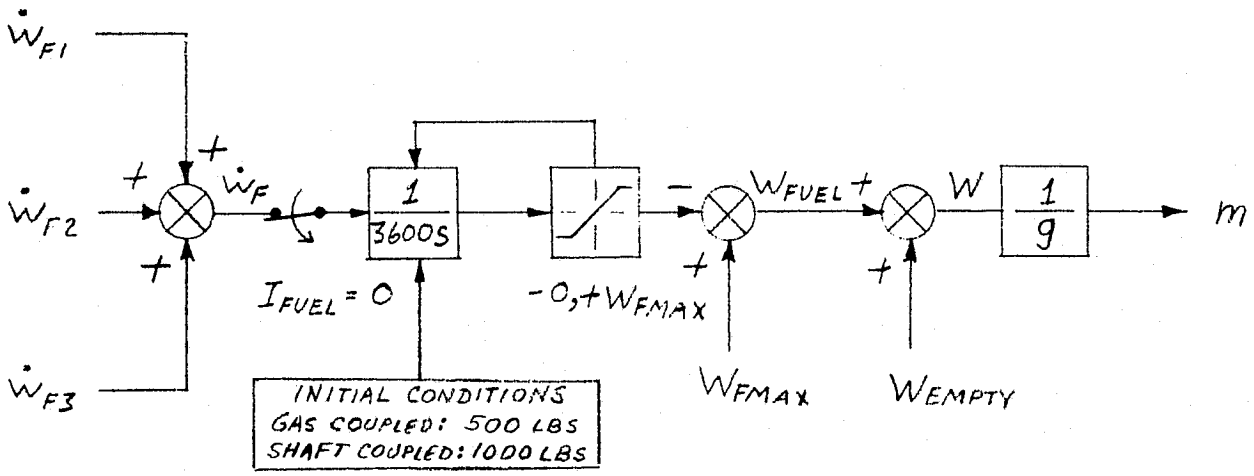

$$W_{GAUGE} = 100 \frac{W_{FUEL}}{W_{FMAX}}$$

FIGURE 18-2

FUEL SYSTEM PARAMETERS

I_{FUEL}	Fuel Usage Discrete	1
W_{FMAX}	Maximum Usable Fuel	6500. lb (gas) 4500. lb (shaft)
W_{EMPTY}	Airplane Operating Weight Empty	21500. lb (gas) 24000. lb (shaft)

19. EQUATIONS OF MOTION

This section presents the principal equations used in the simulation program. Included are summations of aerodynamic and propulsion forces and moments which are generated in other sections of the model. These forces and moments are transformed and integrated as necessary to yield velocities, displacements, angular rates, and angles which are then used elsewhere in the math model.

In the first set of equations, presented in Figure 19-1, all applied torques are first summed to generate the total torques acting on the aircraft (L_B, M_B, N_B). The total torques are then used to compute aircraft angular accelerations ($\dot{p}$, $\dot{q}$, $\dot{r}$) which are then integrated to yield body axes angular rates, p, q, and r. The moments and products of inertia, used in computation of angular accelerations, are defined in Figure 19-2. The computed body angular rates are used in generating the Euler angular rates (Figure 19-3) which are then integrated to provide the aircraft's Euler angles.

The summation of forces in body axes is represented by the last set of equations in Figure 19-3. The forces in body axes are transformed into earth axes by the matrix equation in Figure 19-4. This figure also defines the direction cosines as function of Euler angles.

The aircraft's translational accelerations ($\dot{u}_E$, $\dot{v}_E$, $\dot{w}_E$), velocities (u_E, v_E, w_E), and displacements (x, y, h) are defined in Figure 19-5. This figure also includes the matrix equation which transforms the aircraft inertial velocity components (u_E, v_E, w_E) from earth axes into body axes velocity components (u_B, v_B, w_B) which represent aircraft velocity with respect to the air. That is, the mean wind components (w_x, w_y, w_z) and wind turbulence (u_{BN}, v_{BN}, w_{BN}) are included in the matrix equation defining the body axes velocity components.

Figures 19-6 and 19-7 contain additional equations which are necessary to generate the parameters for pilot's motion and visual cues, and other quantities needed in data reduction. Figure 19-6 also includes equations defining two

FIGURE 19-1

EQUATIONS OF MOTION

SUMMATION OF TORQUES

$$L_B = L_A + L_F + L_{RAM} + L_{LG}$$

$$M_B = M_A + M_F + M_{RAM} + M_{LG}$$

$$N_B = N_A + N_F + N_{RAM} + N_{LG}$$

ANGULAR ACCELERATIONS

$$\dot{p} = \frac{1}{I_1}\left[I_2 pq + I_3 qr + I_{xz} L_B + I_{xz} N_B + (I_{xz} I\Omega_x - I_z I\Omega_z) q\right]$$

$$\dot{q} = \frac{1}{I_Y}\left[(I_z - I_x) pr + I_{xz}(r^2 - p^2) + M_B - I\Omega_x r + I\Omega_z p\right]$$

$$\dot{r} = \frac{1}{I_1}\left[I_4 pq - I_2 qr + I_x N_B + I_{xz} L_B + (I_x I\Omega_x - I_{xz} I\Omega_z) q\right]$$

WHERE:

$$I_1 = I_x I_z - I_{xz}^2$$

$$I_2 = I_{xz}(I_x - I_Y + I_z)$$

$$I_3 = I_z (I_Y - I_z) - I_{xz}^2$$

$$I_4 = I_x (I_x - I_Y) + I_{xz}^2$$

ANGULAR VELOCITIES

$$p = \int_0^t \dot{p}\, dt$$

$$q = \int_0^t \dot{q}\, dt$$

$$r = \int_0^t \dot{r}\, dt$$

FIGURE 19-2

AIRCRAFT MOMENTS OF INERTIA

GAS-COUPLED FANS

$$I_x = 19{,}400. - 0.7538\,(28{,}000. - W)$$
$$I_y = 52{,}400. - 0.2308\,(28{,}000. - W)$$
$$I_z = 67{,}500. - 0.8462\,(28{,}000. - W)$$
$$I_{xz} = 2{,}575. - 0.1192\,(28{,}000. - W)$$

SHAFT-COUPLED FANS

$$I_x = 23{,}000. - 1.2778\,(28{,}500. - W)$$
$$I_y = 54{,}000. - 0.2222\,(28{,}500. - W)$$
$$I_z = 68{,}500. - 1.2222\,(28{,}500. - W)$$
$$I_{xz} = 3{,}050. - 0.2111\,(28{,}500. - W)$$

FIGURE 19-3

EULER ANGLE RATES

$$\dot{\psi} = (r\cos\phi + q\sin\phi)\sec\theta$$

$$\dot{\theta} = q\cos\phi - r\sin\phi$$

$$\dot{\phi} = p + (r\cos\phi + q\sin\phi)\tan\theta$$

EULER ANGLES

$$\phi = \int_0^t \dot{\phi}\, dt$$

$$\theta = \theta_0 + \int_0^t \dot{\theta}\, dt$$

$$\psi = \psi_0 + \int_0^t \dot{\psi}\, dt$$

SUMMATION OF FORCES

$$X_B = X_A + X_F + X_{RAM} + X_{LG}$$

$$Y_B = Y_A + Y_F + Y_{RAM} + Y_{LG}$$

$$Z_B = Z_A + Z_F + Z_{RAM} + Z_{LG}$$

FIGURE 19-4

DIRECTION COSINES

$$l_1 = \cos\theta \cos\psi$$

$$l_2 = \cos\theta \sin\psi$$

$$l_3 = -\sin\theta$$

$$m_1 = -\cos\phi \sin\psi + \sin\phi \sin\theta \cos\psi$$

$$m_2 = \cos\phi \cos\psi + \sin\phi \sin\theta \sin\psi$$

$$m_3 = \sin\phi \cos\theta$$

$$n_1 = \sin\phi \sin\psi + \cos\phi \sin\theta \cos\psi$$

$$n_2 = -\sin\phi \cos\psi + \cos\phi \sin\theta \sin\psi$$

$$n_3 = \cos\theta \cos\phi$$

TRANSFORMATION OF FORCES

$$\begin{bmatrix} X_E \\ Y_E \\ Z_E \end{bmatrix} = \begin{bmatrix} l_1 & m_1 & n_1 \\ l_2 & m_2 & n_2 \\ l_3 & m_3 & n_3 \end{bmatrix} \begin{bmatrix} X_B \\ Y_B \\ Z_B \end{bmatrix}$$

FIGURE 19-5

TRANSLATIONAL ACCELERATIONS

$$\dot{U}_E = \frac{X_E}{m}$$

$$\dot{V}_E = \frac{Y_E}{m}$$

$$\dot{W}_E = \frac{Z_E}{m} + g \qquad \ddot{h} = -\dot{W}_E$$

TRANSLATIONAL VELOCITIES

$$U_E = \int_0^t \dot{U}_E \, dt + U_{E_0}$$

$$V_E = \int_0^t \dot{V}_E \, dt + V_{E_0} \qquad \dot{h} = -W_E$$

$$W_E = \int_0^t \dot{W}_E \, dt \qquad \gamma = \tan^{-1} \frac{\dot{h}}{\sqrt{U_E^2 + V_E^2}}$$

TRANSFORMATION OF VELOCITIES

$$\begin{bmatrix} U_B \\ V_B \\ W_B \end{bmatrix} = \begin{bmatrix} l_1 & l_2 & l_3 \\ m_1 & m_2 & m_3 \\ n_1 & n_2 & n_3 \end{bmatrix} \begin{bmatrix} U_E - W_X \\ V_E - W_Y \\ W_E - W_Z \end{bmatrix} + \begin{bmatrix} U_{BN} \\ V_{BN} \\ W_{BN} \end{bmatrix}$$

AIRCRAFT CG TRAVEL WITH RESPECT TO EARTH

$$x = x_0 + \int_0^t U_E \, dt$$

$$y = y_0 + \int_0^t V_E \, dt$$

$$h = h_0 - \int_0^t W_E \, dt$$

FIGURE 19-6

PILOT MOTION IN EARTH AXES

$$\begin{bmatrix} x_{PE} \\ y_{PE} \\ h_{PE} \end{bmatrix} = \begin{bmatrix} l_1 & m_1 & n_1 \\ l_2 & m_2 & n_2 \\ -l_3 & -m_3 & -n_3 \end{bmatrix} \begin{bmatrix} x_P \\ y_P \\ z_P \end{bmatrix} + \begin{bmatrix} x \\ y \\ h \end{bmatrix}$$

AIRCRAFT CG ACCELERATIONS SENSED ALONG BODY AXES

$$n_x = \frac{X_B}{W} \qquad n_Y = \frac{Y_B}{W} \qquad n_z = \frac{Z_B}{W}$$

ACCELERATION COMPONENTS SENSED AT PILOT STATION

$$n_{xP} = n_x + \left[-x_P (q^2 + r^2) - y_P (\dot{r} - pq) + z_P (\dot{q} + rp) \right] / g$$

$$n_{YP} = n_Y + \left[-y_P (r^2 + p^2) - z_P (\dot{p} - qr) + x_P (\dot{r} + pq) \right] / g$$

$$n_{zP} = n_z + \left[-z_P (p^2 + q^2) - x_P (\dot{q} - rp) + y_P (\dot{p} + qr) \right] / g$$

GYROSCOPIC COUPLING EQUATIONS

$$I\Omega_x = J_E (\omega_1 + \omega_2 + \omega_3) - J_F (\omega_{F1} + \omega_{F2}) - J_F \omega_{F3} \sin 15^\circ$$

$$I\Omega_E = J_F \omega_{F3} \cos 15^\circ$$

gyroscopic coupling parameters, while Figure 19-7 shows the summation of actual angular velocities (p, q, r) and gust disturbance components in angular velocity terms (p_N, q_N, r_N). The total angular rates (p_T, q_T, r_T) relative to ambient air are then used in Section 15 to compute the aerodynamic forces and moments.

Figure 19-8 presents the glideslope and localizer equations and the marker beacon heading equation. Figures 19-8 and 19-9 list the constants used in this section.

FIGURE 19-7

ANGULAR VELOCITY TURBULENCE EFFECTS

$$p_T = p + p_N$$
$$q_T = q + q_N$$
$$r_T = r + r_N$$

BODY AXES INERTIAL VELOCITIES

$$\begin{bmatrix} u_{IB} \\ v_{IB} \\ w_{IB} \end{bmatrix} = \begin{bmatrix} \ell_1 & \ell_2 & \ell_3 \\ m_1 & m_2 & m_3 \\ n_1 & n_2 & n_3 \end{bmatrix} \begin{bmatrix} u_E \\ v_E \\ w_E \end{bmatrix}$$

FIGURE 19-8

GLIDESLOPE AND LOCALIZER EQUATIONS

$$R = \sqrt{(x - x_{LGS})^2 + (y - y_{LGS})^2}$$

$$\varepsilon_{GS} = \tan^{-1} \frac{h}{R} - \gamma_{GS}$$

$$\varepsilon_{LOC} = \tan^{-1} \frac{y - y_{LLOC}}{x_{LLOC} - x}$$

MARKER BEACON HEADING

$$\psi_{ADF} = -\psi - \tan^{-1} \frac{y - y_{LMRK}}{x_{LMRK} - x}$$

NAVIGATION EQUATION PARAMETERS

x_{LGS}	Glideslope Transmitter Location	0.0
y_{LGS}		0.0
x_{LLOC}	Localizer Transmitter Location	0.0
y_{LLOC}		2000. ft
x_{LMRK}	Marker Beacon Location	-11394. ft
y_{LMRK}		0.0

FIGURE 19-9

LOCATION OF PILOT
(Pilot's Eyes)

x_P	x Coordinate of Pilot	11.82 ft
y_P	y Coordinate of Pilot	1.17 ft
z_P	z Coordinate of Pilot	-1.18 ft

ENGINE AND FAN MOMENT OF INERTIA

J_E	Engine Rotor Moment of Inertia	1.73 slug-ft^2 (gas) 1.33 slug-ft^2 (shaft)
J_F	Fan Rotor Moment of Inertia	21.5 slug-ft^2 (gas) 14.40 slug-ft^2 (shaft

20. COCKPIT CONTROLS AND INSTRUMENTS

The cockpit controls and switches used by the pilot are tabulated in Figure 20-1. The simulation symbols used to represent the corresponding pilot's input are tabulated in the column next to the names of input parameters. The total control deflections for the stick and rudder pedals are tabulated in Figure 20-2 together with the associated control breakout forces. The force gradients for the stick and yaw pedals are plotted in Figure 20-3.

The cockpit indicator instruments and the corresponding symbols are tabulated in Figure 20-4. The cockpit indicator lights and associated symbols are tabulated in Figure 20-5. In each of the last two figures the expected minimum and maximum parameter values are listed in a column adjoining the parameter names and symbol designations.

FIGURE 20-1

COCKPIT CONTROLS

1.	Lateral Stick	$\delta_{I\phi}$
2.	Longitudinal Stick	$\delta_{I\theta}$
3.	Rudder Pedals	$\delta_{I\psi}$
4.	Power Lever	δ_{T}
5.	Transition Lever	ζ_{TL}
6.	#1 Engine Throttle	δ_{1}
7.	#2 Engine Throttle	δ_{2}
8.	#3 Engine Throttle	δ_{3}
9.	Side Force Controller	δ_{IY}

COCKPIT SWITCHES

1.	Flap Switch	I_{FLAP}
2.	Lateral Trim	$ITRIM_{\phi}$
3.	Longitudinal Trim	$ITRIM_{\theta}$
4.	Directional Trim	$ITRIM_{\psi}$
5.	Roll CAS	$ICAS_{\phi}$
6.	Pitch CAS	$ICAS_{\theta}$
7.	Yaw CAS	$ICAS_{\psi}$

FIGURE 20-2

COCKPIT CONTROL TRAVEL LIMITS

Lateral Stick	±3.55 Inches
Longitudinal Stick	±4.05 Inches
Rudder Pedals	±2.55 Inches

COCKPIT CONTROL BREAKOUT FORCES

Lateral Stick	±1.25 lb
Longitudinal Stick	±1.25 lb
Rudder Pedals	±5.0 lb

FIGURE 20-3

COCKPIT CONTROL GRADIENTS

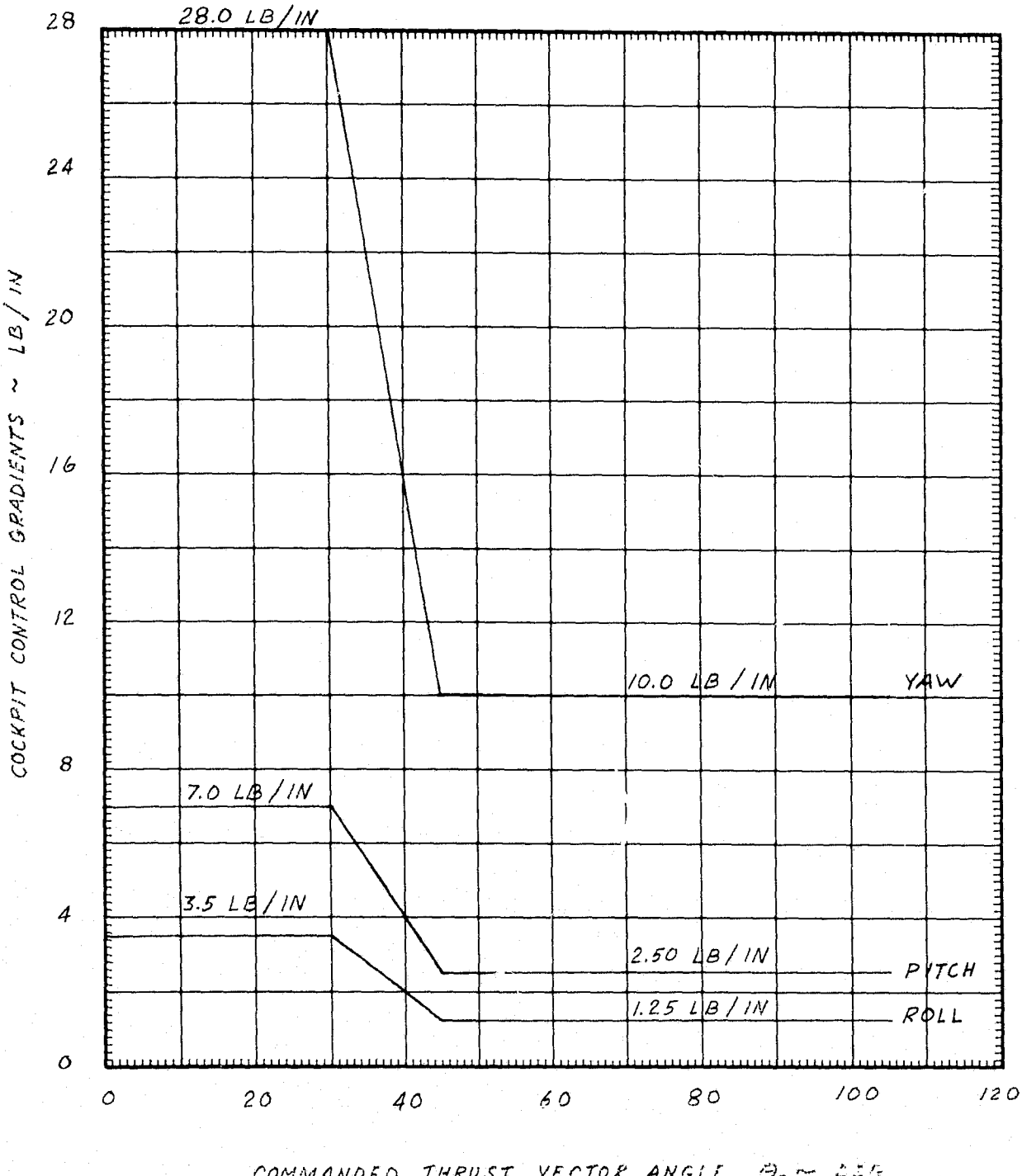

FIGURE 20-4

COCKPIT INSTRUMENTS

1.	Bank Indicator	Attitude Indicator	ϕ	$\pm$180 deg
2.	Pitch Indicator		θ	$\pm$90 deg
3.	Heading Indicator	Horizontal Situation Indicator	ψ	-0, +360 deg
4.	Localizer Error		ε_{LOC}	$\pm$2.5 deg
5.	Glideslope Error		ε_{GS}	$\pm$1.25 deg
6.	Barometric Altitude		h	-0, +10000 ft
7.	Radar Altitude		h	-0, +2500 ft
8.	Vertical Speed		$\dot{h}$	$\pm$6000 ft/min
9.	Airspeed Indicator		u_B	-20, +280 knots
10.	Angle of Attack		α	$\pm$30 deg
11.	Angle of Sideslip		β	$\pm$30 deg
12.	Turn Rate	Turn & Bank	$\dot{\psi}$	$\pm$3 deg/sec
13.	Lateral Acceleration		a_{YP}	$\pm$0.15 g
14.	Vector Angle		θ_J	-0, +105 deg
15.	Pitch Trim		δ_H	$\pm$30 deg
16.	#1 Engine Speed		N_1	-0, +110%
17.	#2 Engine Speed		N_2	-0, + 110%
18.	#3 Engine Speed		N_3	-0, +110%
19.	#1 Fan Speed		N_{F1}	-0, +110%
20.	#2 Fan Speed		N_{F2}	-0, +110%
21.	#3 Fan Speed		N_{F3}	-0, +110%
22.	Flap Position		δ_{FLAP}	-0, +25 deg
23.	Automatic Direction Finder		ψ_{ADF}	-0, +360 deg
24.	Fuel Gauge		W_{GAUGE}	-0, +100%

FIGURE 20-5

COCKPIT INDICATOR LIGHTS

1.	Landing Gear Up	I_{GEARU}	0, 1
2.	Landing Gear Down	I_{GEARD}	0, 1
3.	Fan Doors Closed	I_{DOORC}	0, 1
4.	Fan Doors Open	I_{DOORO}	0, 1
5.	Attitude Command Mode	I_{ATT}	0, 1
6.	Height Damper	I_{DAMP}	0, 1
7.	Roll CAS	$I_{CAS\phi}$	0, 1
8.	Pitch CAS	$I_{CAS\theta}$	0, 1
9.	Yaw CAS	$I_{CAS\psi}$	0, 1

21. DATA REDUCTION

The main simulation parameters were selected to be recorded on three strip charts during the simulation tests. The strip chart data, together with pilot comments, will be needed to document and analyze the simulation results. The signals to be recorded include the analog parameters listed in Figures 21-1 and 21-2 and the discrete data tabulated in Figure 21-3.

A few of the main simulation parameters are labeled with different symbols in the shaft-coupled configuration than in the gas-coupled version even though the parameters are either similar or equivalent in both versions. In such cases a uniform symbol is assigned to these parameters for recording purposes so that the associated recording arrangements and chart labeling remain the same for gas-coupled and shaft-coupled versions. The chosen common symbols are defined in Figure 21-4 and include the parameter N_{GI} which is used only for strip chart recording.

FIGURE 21-1
ANALOG STRIP CHART RECORDER SIGNALS

RECORDER #1

CHANNEL	LONG SIGNAL	SHORT SIGNAL
1	$\delta_{I\phi}$ ($\pm$ 5 in.)	ϕ ($\pm$50°)
2	$\delta_{I\theta}$ ($\pm$ 5 in.)	θ ($\pm$25°)
3	$\delta_{I\psi}$ ($\pm$ 2.5 in.)	ψ (0 → 400°)
4	N_{GI} (90 → 110%)	N_G (90 → 110%)
5	θ_J (0 → 100°)	V (0 → 250 KTS)
6	α ($\pm$25°)	$\dot{h}$ ($\pm$25 fps)
7	β ($\pm$25°)	y ($\pm$250 Ft)
8	h (0 → 250 Ft)	x ($\pm$250 Ft)

RECORDER #2

CHANNEL	LONG SIGNAL	SHORT SIGNAL
9	n_X ($\pm$0.5 g)	ε_{GS} ($\pm$2.5°)
10	n_Y ($\pm$0.5 g)	ε_{LDC} ($\pm$5.0°)
11	$-n_Z$ (0 → 2.5 g)	γ ($\pm$25)
12	δ_ϕ ($\pm$1.0)	p ($\pm$1.0 rad/sec)
13	δ_θ ($\pm$1.0)	q ($\pm$1.0 rad/sec)
14	δ_ψ ($\pm$1.0)	r ($\pm$0.5 rad/sec)
15	δ_A ($\pm$25°)	N_1 (0 → 100%)
16	δ_H ($\pm$25°)	N_2 (0 → 100%)

FIGURE 21-2
ANALOG STRIP CHART RECORDER SIGNALS (CONTINUED)

RECORDER #3

CHANNEL	LONG SIGNAL		SHORT SIGNAL	
17	δ_R	($\pm$25°)	N_3	(0 → 100%)
18	$\dot{p}$	($\pm$1.0 rad/sec^2)	N_{F1}	(0 → 100%)
19	$\dot{q}$	($\pm$1.0 rad/sec^2)	N_{F2}	(0 → 100%)
20	$\dot{r}$	($\pm$0.5 rad/sec^2)	N_{F3}	(0 → 100%)
21	δ_{IY}	($\pm$1.0)	HP_1	(0 → 10,000 HP)
22	h	(0 → 2500 Ft)	HP_2	(0 → 10,000 HP)
23	-x	(0 → 10,000 Ft)	HP_3	(0 → 10,000 HP)
24	W_{FUEL}	(0 → 10,000 Lb)	δ_{FLAP}	(0 → 25°)

FIGURE 21-3

DISCRETE STRIP CHART RECORDER SIGNALS

RECORDER #1

Channel		Values
1	$ITRIM_{\phi}$	(-1, 0, +1)
2	$ITRIM_{\theta}$	(-1, 0, +1)
3	$ITRIM_{\psi}$	(-1, 0, +1)
4	$ICAS_{\phi}$	(0, 1)
5	$ICAS_{\theta}$	(0, 1)
6	$ICAS_{\psi}$	(0, 1)
7	I_{DAMP}	(0, 1)

RECORDER #2

Channel		Values
1	I_{ATT}	(0, 1)
2	I_{WOW}	(0, 1)
3	ICON	(-1, 0, 1)
4	$I\theta_{DUMP}$	(0, 1)
5	$I\theta_{IV}$	(0, 1)
6	--	
7	--	

FIGURE 21-4

STRIP CHART RECORDER COMPUTATIONS

$N_{GI} = N_G + N_{GDAMP}$

$N_{F1} = N_{\%}$

$N_{F2} = N_{\%}$

$N_{F3} = N_{\%} \times V_{CLUTCH}$

} Shaft-Coupled Fans

$N_{F1} = N_{F1}$

$N_{F2} = N_{F2}$

$N_{F3} = N_{F3}$

} Gas-Coupled Fans

$HP_1 = HP_{F1}$

$HP_2 = HP_{F2}$

$HP_3 = HP_{F3}$

} Shaft-Coupled Fans

$HP_1 = HP_1$

$HP_2 = HP_2$

$HP_3 = HP_3$

} Gas-Coupled Fans